0098 OUTOKUMPU EXPLORATION AUSTRALIA PTY LIMITED

Report No: R72.10
File No: 2.72a.9
Filename: 272GM106.RT1

ANNUAL REPORT TO 6 APRIL, 1991
EL 56/89 - CORINNA SOUTH, TASMANIA
Volume 1 of 2

For: Outokumpu Exploration Australia Pty Limited
77 Pacific Highway, NORTH SYDNEY NSW 2060

By: W. Herrmann, RSD 1066, DEVONPORT TAS 7310

Date: 22 May 1991

DISTRIBUTION:

1. OEA Library
2. Department of Resources & Energy

CONTENTS

VOLUME 1

List of Figures

(P) = plan in map pocket.

List of Appendices

VOLUME 2

1. SUMMARY

Mineral exploration under EL 56/89, during Outokumpu's first year of tenure, has been concentrated on the Alpine magnetic anomalies as part of a regional assessment of the copper-gold potential of ironstone bodies within the Arthur Metamorphic Complex. Work undertaken has included a review of previous exploration data, relogging and sampling of previous drillholes, petrographic studies of the ironstones and host rocks intersected in those holes, re-cutting and extension of the Alpine grid, detailed magnetic survey and a four loop TEM survey.

The TEM survey has not indicated any significant conductive zones. However, interpretation based on three dimensional modelling of the magnetic data indicates that the major magnetic anomaly has been only partially tested by a previous drillhole, AP2, which intersected a series of thin ironstone bands which averaged 0.5% Cu over 27.4m and included a couple of 2m intervals @ 1.3% Cu. Other magnetic anomalies in the northern part of the grid remain completely untested.

The known copper mineralisation at Alpine is closely associated with magnetite-pyrite-quartz-carbonate ironstones and can be interpreted as a primary component of stratiform exhalative iron formations with local remobilisation during deformation / metamorphism. It represents one of the most significant occurrences of ironstone associated copper mineralisation yet reported from the Arthur Metamorphic Complex. Possibilities, including drilling, for further investigation of this mineralisation are discussed.

2. INTRODUCTION

Exploration Licence 56/89 lies near the southern end of the Arthur Metamorphic Complex in western Tasmania. It covers an area of 18sq km centred on a cluster of aeromagnetic features collectively termed the "Alpine Anomaly" which were investigated by a Geopeko/CRAE joint venture in the years 1983 to 1985. That programme culminated in two precollared diamond drill holes which intersected a number of narrow bands of magnetite-pyrite-quartz-carbonate ironstone enclosed by phyllitic, psammo-pelitic metasedimentary and semi mafic meta-volcaniclastic? schists; both holes intersected short intervals of low grade copper mineralisation associated with the ironstones.

Outokumpu's objective is to examine the ironstone bodies, as part of a regional exploration programme extending also to adjoining EL's 14/89 and 37/90, for Cu-Au mineralisation, with an exploration model loosely based on the stratiform Starra and Trough Tank deposits of the Mt.Isa Inlier in western Queensland.

This report presents results and discussion of the exploration programme conducted during the first year of Outokumpu tenure of the Alpine area and consisting of:

* a review of previous exploration,
* petrographic studies of core samples from previous drill intersections,
* recutting and infilling of the Alpine grid,
* detailed ground magnetic survey and interpretation,
* a four loop TEM survey.

3. TENURE, LOCATION and ACCESS

EL 56/89 was granted on 6 April 1990 to Outokumpu Exploration Australia which has wholly funded and managed the exploration programme to date.
The licence covers an area of 18sq km straddling the Heemskirk Road just west of the Reece Dam on the lower Pieman River. The Alpine grid covers an area of about 4sq km bisected by the road which is a sealed highway and the prospect is about 30 minutes drive from the township of Zeehan. (Figures 7 and 8)

Topography over the grid area is mostly gently undulating with a few small steep gullies in the eastern part. The country is covered by moderate to thick regrowth vegetation after eucalypt forest which was largely destroyed by wildfire in 1982. Dominant plants include tea tree, Melaleuca, Banksia, Bauera, bracken and cutting grass growing amongst a tangle of fallen, partly burnt, logs. There are some patches of open marshy sedgeland in the northern parts of the grid and areas of surviving Eucalypt forest with an open understorey of dogwood etc. mainly in the central and southwestern parts. Remnants of rainforest vegetation exist in some of the gullies.

4. REGIONAL GEOLOGY

The regional geological setting of the Arthur Metamorphic Complex has been discussed in reasonable detail in a previous report (Herrmann, 1989) from which the following summary has been reproduced.

The Arthur Metamorphic Complex (AMC) is a narrow linear zone of strongly deformed and regionally metamorphosed rocks trending north northeasterly across northwestern Tasmania. It separates two sequences of unmetamorphosed late PreCambrian sediments; the Rocky Cape Group to the west representing a stable continental shelf facies, and the Burnie/Oonah Formation to the east representing deeper water turbidites. The metamorphic rocks within the Complex are divided into two "sequences":
The western most (Timbs Group) consists of quartz-chlorite-mica-albite-carbonate schists, amphibolites and dolomite-magnesite marble of the greenschist to amphibolite facies of regional metamorphism. They are beleived to have compositional similarities, especially in the tholeiitic nature of the amphibolites, to the clastic-carbonate-mafic volcanic sequence of the Ahrberg Group which unconformably overlies the Rocky Cape Group west of the southern part of the AMC.
The eastern metamorphic sequence consists mainly of psammo-pelitic schists and quartzite compositionally similar to the Burnie/Oonah Formations with which they appear to have a transitional eastern boundary.

On the basis of the Timbs-Ahrberg lithological correlation and the similarity of the Ahrberg Group to the EoCambrian ? sequences of the Smithton Trough and western Dundas Trough (which are interpreted to have formed in continental margin rift basins) it is hypothesized that the AMC represents a similar EoCambrian ? rift assemblage which was deformed and metamorphosed after the Middle Cambrian.

The Arthur Metamorphic Complex is host to several large magnetite-pyrite deposits which appear to be stratiform and localized within the eastern most part of the Timbs Group (known as the Bowry Member). Minor copper, zinc and gold mineralization is associated with the ironstones. The ironstone deposits and the hypothetical tectonic setting have some characteristics with similarity to the Starra Cu-Au ironstone deposits of western Queensland and the massive sulphide deposits of Besshi style in Japan.

Although none of the known ironstone deposits contain remotely economic base or precious metal grades the previous exploration for these targets has not been exhaustive and there remains some scope for further exploration based on interpretation and follow up of existing aeromagnetic survey data as well as systematic geological mapping which appears to have been substantially neglected in the past.

5. PREVIOUS EXPLORATION

An airborne magnetic survey flown in 1981, by Geoex for the Tasmanian Department of Mines, indicated a cluster of strong "bullseye" anomalies near the southern end of the Arthur Metamorphic Complex four kilometres southwest of Reece Dam.
The area at that time was part of CRAE's extensive EL 1/77 which was being explored for granitoid associated tin-tungsten deposits by a Geopeko/CRAE joint venture partnership.
The aforementioned aeromagnetic anomalies were collectively designated the "Alpine Anomaly" and were followed up by the joint venturers with apparently three possible exploration models in consideration: (Weir, 1985)

- (i) Skarn type Sn/W similar to St.Dizier and Granville.
- (ii) Stratiform sulphides; shale hosted Pb-Zn or Keith River bedded pyrite type.
- (iii) Gold mineralisation associated with iron formations or stratiform sulphides.

The Alpine area was gridded with N-S lines cut at 200m intervals (the local strike trend is about 060 deg.). An initial programme of geological mapping, C-horizon/bedrock auger geochemical sampling, ground magnetics and Scintrex Genie-EM was carried out during 1983-84 and followed by a two hole drilling programme in early 1985.

Outcrop over the area is poor with extensive superficial cover of Tertiary basalt and associated gravels but surface geological mapping assisted by logging of Jacro auger and Wacker bedrock chip samples indicated that the local basement sequence was dominantly of metasedimentary psammitic and pelitic quartz-mica schists and graphitic phyllite with subordinate chloritic schists (after mafic volcanics?), silicified carbonates and banded siliceous ironstones (with >10% Py, minor Mt,Cpy,Cc).

Bedrock geochemical sampling was carried out along the road by Bombardier mounted Jacro auger and elsewhere by Wacker drill but was only partly effective and partially completed due to the extensive Tertiary basalt and gravel cover. The samples were analysed for Cu Pb Zn Ag Au As Fe Mn Ni Co Sn W and Ba.
No anomalous results were recorded for Pb Ag Sn W or Au; there were some weak and rather scattered bedrock anomalies in Cu Fe and Zn. Iron, copper and to a lesser degree zinc anomalies were in proximity to the major magnetic features but not of perfect co-incidence.

The ground magnetic survey indicated two principal anomalous zones, about 500-800m apart, trending ENE and NE (ie: approximately parallel to the host rock strike and foliation trends).
The northern anomaly was quite narrow and linear, semi-continuous over about 1000m, with an amplitude ranging about 1000-2000nT above background. CRAE interpreted it to have a "lithological" source although their geological mapping

suggested it lay within unexceptional metasedimentary schists with the the western end nearly coincident with an interpreted lense of silicified/pyritised carbonate.
The southern magnetic anomaly had a major high amplitude (2000-5000nT) bullseye centred on line 8700E with a narrow tail extending off in a northeasterly trend. It was recognised as having a magnetite source. The CRAE geological interpretation suggested near co-incidence with a narrow band of pyritic cherty carbonate within metasedimentary quartz-mica schists and graphitic phyllite, partly covered by thin Tertiary basalt and gravel. The (CRAE) map indicates a number of scattered outcrops of limonitic ironstone in the vicinity but none are co-incident with the magnetic anomaly; some were interpreted as Tertiary basalt weathering features.

A Scintrex Genie-EM survey was carried out over the entire grid and although there were some problems with the field procedure the data was considered to be useful. The survey led to the identification of several strongly and moderately conductive anomalies; the three best anomalies were co-incident with the southern magnetic anomaly on lines 8500E, 8700E and 9100E. The latter two were subsequently tested by drillholes AP2 and AP1 respectively.

The drilling results were (briefly) reported by Caithness, 1985:

AP1 of 106.7m was designed to test a co-incident strong Genie-EM and magnetic anomaly associated with weakly anomalous Cu, Zn and Fe bedrock geochemical values on line 9100E. The hole intersected a metasedimentary sequence of psammitic (qtz-musc-carb-chl-alb) schists, graphitic phyllite and marly metapelite with several bands of banded magnetite-pyrite-carbonate-quartz ironstone over a 12.75m interval which averaged 0.24% copper. Gold was apparently not assayed for this interval. The metasedimentary schist immediately uphole of the ironstone interval was found to contain a number of very narrow bands or veins (upto 0.3m thick) of near massive pyrite-carbonate with subordinate quartz,muscovite,sphalerite and traces of chalcopyrite and galena which averaged 0.19% Zn (and 0.04% Cu) over an 8.2m interval.

AP2 of 85.8m was drilled to test the Genie-EM anomaly co-incident with the large magnetic bullseye anomaly on line 8700E; the hole was optimised for the EM anomaly and did not (being collared near the centre of the magnetic bullseye) provide a complete test of the magnetic anomaly. The hole was precollared to 55.5m; coring commenced in banded magnetite-pyrite-quartz-carbonate ironstone and the hole went on to intersect four narrow bands of ironstone over an interval of about 18m within banded felsic to mafic qtz-alb-chl-carbonate schists. The overall mineralised zone (intersected partly by precollar percussion drilling) averaged 0.53% Cu over an interval of 27.4m downhole corresponding to an estimated true thickness of about 18m. A few gold analyses from the upper part of this zone indicated values mostly below detection limit and a maximum of 0.03g/t Au. As in AP1 the ("qtz-mica and qtz-mica-chl") schists immediately uphole of the ironstone bands were found to contain considerable veiny and disseminated pyrite and to be weakly anomalous in zinc with scattered values upto 1600ppm Zn; the 26m interval above the ironstones averaged 500ppm Zn.

Caithness (op cit) concluded that the intersected mineralisation explained the targeted anomalies, that the anomalies had been adequately tested and, in the absence of high base metal and gold values, did not justify further exploration.

6. OUTOKUMPU EXPLORATION PROGRAMME 1990-91

The exploration programme conducted to date by Outokumpu has been focussed entirely on the Alpine prospect.

The work undertaken has consisted of:

* A review of the previous CRAE exploration data.
* Relogging, magnetic susceptibility measurement and selective sampling and assaying of CRAE's drillholes AP1 and AP2.
* Petrographic studies of ironstones and host rocks intersected in AP1 and AP2.
* Recutting, extension and infill cutting of the Alpine exploration grid.
* Ground magnetic survey and geophysical modelling of anomalies.
* A four loop GDP-16 TEM survey to cover the main magnetic anomalies.

The data review, core relogging and selective sampling was undertaken by the writer with the general objective of elucidating the geological setting, type and relative age of the known mineralisation.

The diamond drill cores of holes AP1 and AP2 are at present stored at CRAE's former office and warehouse at Cambridge, Tasmania; it is not known if splits or analytical pulps of percussion chips from the upper parts of the holes or the intervals of half sawn core are extant.

Descriptive geological core logs are presented in Appendix III.

A number of core specimens representative of the ironstones and host rocks were taken for a petrographic study, carried out by Dr. Joe Stolz, of which the results are presented here in Appendix II.

Thirteen, short (10-20cm) segments of quarter sawn core, representatve of the mineralogically variable ironstone intersections in both holes, were sampled for analysis to determine a wider range of elements, particularly gold, than originally reported b CRAE. The list of samples and assay data are presented in Appendix IV. These samples were analysed by Analabs/Burnie for the following elements:

Cu Pb Zn Ag Bi Co Ni Fe Mn Mg Ca Na K As	by AAS methods
Au	by method 309 fusion/AAS
Sb Sn	by method 401 XRF
W Mo Ba Zr Y La Ti Cr	by method 201 ICP/OES

The original (CRAE/Geopeko) Alpine grid was found to be heavily overgrown and necessitated complete recutting and repegging at 25m intervals. In addition, the grid was extended by several lines at both eastern and western ends, infilled by three lines between 8600E and 9000E to provide 100m line spacing and by east-west lines for TEM transmitting wire loops.
The layout of the grid is shown in Figure 8.
Trackcutting amounted to about:

17.0 km recutting of old lines,
13.2 km cutting of new lines,
5.6 km cutting of TEM loop lines,

and was carried out under contract by G.Mallinson and company in December 1990 to January 1991.

A detailed ground magnetic survey, with a station spacing of 5m, was carried out over the entire grid by B.Stedman and the data interpreted by Mitre Geophysics (Appendix I).

The TEM survey was conceived with the objective of identifying conductive zones, which could be attributable to copper mineralisation associated with the magnetite ironstones; CRAE's drill testing of Scintrex Genie (a relatively low powered system) EM anomalies seemed to indicate that the low grade copper mineralization (or the pyrite rich ironstone ?) was significantly conductive. The TEM survey was carried out in late January 1991 by Zonge Engineering using a GDP-16 receiver and the data interpreted by Mitre Geophysics (Appendix I).

7. DISCUSSION

Geological Setting:

As interpreted in Figures 9 and 10, the ironstone bodies intersected by CRAE's AP1 and AP2 occur as a number of thin bands or lenses upto about 4m thick associated with or enclosed by more or less felsic/mafic chl-qtz-alb-(carb) schists. In AP1 the immediate footwall to ironstone consists of graphitic phyllite similar to metasediments in the hanging wall but the contact zone is intensely brecciated and sheared probably representing a fault and it is conceivable that this footwall has been structurally emplaced. In AP2 the rocks sandwiched between bands or lenses of ironstone and in the footwall are of banded, alternately quartzo-feldspathic and chloritic schists which have been petrographically interpreted (Stolz, Appendix II) as probably having sedimentary precursors consisting of interbedded psammitic, quartzo-feldspathic and mafic materials partly derived from mafic, and perhaps also felsic, vulcanism.

Unfortunately the hanging wall was not cored in AP2 but the CRAE chip log refers to quartz-mica-(chlorite) schists which I assume may be akin to the psammitic schists cored in the upper part of AP1. My initial interpretation from the available core was that ironstones in AP1 and AP2 were hosted by very different rocks; however, by faulting off the downhole contact of ironstone in AP1 against metasedimentary phyllite and assuming that the hanging wall in AP2 is similar to that of AP1, it is reasonable to consider the ironstones in both holes to be of similar type and setting.

The ironstones are certainly of similar constitution being composed essentially of rather variable proportions of magnetite, pyrite, quartz and, probably sideritic, carbonate. Dr. Stolz's petrographic work indicates that the phases magnetite, pyrite and chalcopyrite are substantially in synmetamorphic textural equilibrium and although there is some evidence that chalcopyrite has been remobilised into late deformation carb-qtz veins and fractures in pyrite and magnetite, it is generally apparent that magnetite, pyrite and chalcopyrite were co-depositional.

There is, however, considerable evidence for locally pervasive alteration of magnetite to carbonate leaving an essential pyrite-carbonate assemblage and, paradoxically in some instances, of magnetite replacement of carbonate along cleavage planes. Narrow zones of near massive carbonate-pyrite+/-qtz commonly occur at the margins of the ironstone bodies and it is notable that the relatively pyrite rich-magnetite poor ironstones tend to occur near the "outer" parts of the overall ironstone intersections.

Bands and veins of near massive granular pyrite-carbonate are prominent in the immediate hanging wall of ironstones in AP1 and are reported (Caithness, 1985) in AP2; these are associated with minor sphalerite mineralisation and appear to be somewhat less strained.

Micro-textural indications in the ironstones are that they have been deformed, with the high strain which produced mylonitic fabrics in some samples possibly associated with peak prograde metamorphism. The carbonate replacement of magnetite may be a fairly late tectonic phase perhaps associated with retrograde shearing.

Dr. Stolz concluded that the textural evidence suggests that the ironstones were emplaced prior to deformation and metamorphism and considered that their mineralogy is consistent with an origin as iron bearing submarine exhalatives; (eg: AP1 90.5m, Appendix II).

Mineral assemblages in both the metasedimentary and meta-basic volcaniclastic? host rocks indicate that they have been metamorphosed to mid-upper amphibolite facies of regional metamorphism with extensive, perhaps shear localised, partial retrogression to the albite-chlorite greenschist facies. Carbonate is a common phase in the host schists but the absence of calc-silicate phases such as epidote or actinolite is taken as an indication that much of the carbonate was introduced fairly late in the retrogressive stage (or that CO_2 pressure may have been consistently high?).

Geochemistry: The analytical data (Appendix IV) from thirteen short sections of ironstone from both drill holes can be summarized as follows:

Fe	range ~30-60% Fe, the magnetite rich samples tend to be higher in iron but the variation seems more related to amount of quartz gangue rather than Mt:Py ratio.
Mn	range 710-6600ppm with a weak positive correlation to carbonate and perhaps Py content.
Ti	variable in range 30-340ppm, no obvious correlations.
Zr,Y,La	all low, 10ppm or less
Ca and Mg	variable in the range upto 5.5% apparently correlated with carbonate content.
Na and K	very low, essentially below detection except in massive pyrite-carbonate bands/veins.
Ni and Cr	<50ppm

Co	variable in range 85-650ppm, no obvious correlations.
Bi,Sn,W,Mo	all low, <20ppm
As	<20ppm in ironstones, 50-230ppm in py-carb bands and veins.
Ag	<0.5-1g/t in ironstones; upto 3g/t in massive py-carb bands and veins.
Cu	variable 0.2-1.5% in ironstones; Py rich ironstones all have >0.6%Cu, Mt rich ironstones <0.4% with one exception @ 0.75%Cu. Bands and veins of massive Py-carb in AP1 have <0.1%Cu.
Au	generally low <30ppb in ironstones; 80-105ppb in massive py-carb veins and bands in AP1.
Pb	<30ppm in ironstones; upto 400ppm in massive Py-carb veins and bands in AP1.
Zn	range 100-250ppm in ironstones not obviously correlated with Mt:Py ratio. Bands and veins of massive Py-carb in AP1 anomalous @ 300-16500ppm.

It is interesting to make comparisons between this data and the equally scanty trace element analyses available for banded and massive ironstones of the Doctor's Creek - Owen Meredith area further north in EL's 14/89 and 37/90: (Herrmann, 1990 and 1991)
The significant manganese, copper and modal quartz contents and the relatively low and variable iron contents of the Alpine ironstones seem to indicate that they are analogous to the banded siliceous ironstones of the Doctor's Creek - Owen Meredith area albeit generally rather more iron rich and less siliceous than the latter.
Titanium contents of the Alpine ironstones are consistently low in comparison to the highly variable Ti in ironstones from further north but I am doubtful of the significance of the latter which may reflect some contamination by wall rock mafic schists.

The banded felsic/mafic qtz-alb-chl-(carb) schists of AP2 appear to be broadly comparable to similar rocks which enclose the banded siliceous ironstones of the Doctor's Creek - Owen Meredith area. In consideration of the association of the latter with the eastern contact of the Bowry Member mafic schists against psammo-pelitic metasediments not unlike the hanging wall rocks (and faulted footwall ?) in AP1 it is tentatively suggested that the Alpine ironstones could be analogues of the banded siliceous ironstones with structural complexities as yet undefined.

The CRAE Cu, Zn and Au analytical data of mainly 2m downhole samples from AP1 and AP2 have been re-plotted against the geological sections in Figures 9 and 10.
Although the ironstones are mineralogically variable on quite a small scale and the sub-division into pyrite rich and magnetite rich ironstone is rather generalised, it is apparent that:

i) copper grades tend to be higher in the pyrite rich ironstone intervals
ii) copper is erratically distributed within the ironstones (cf: Cu grades from the short segment samples of ironstone [A104622...34] with the CRAE samples of 2m runs).

Both features possibly indicate remobilisation of copper during deformation. Although textural evidence for pyritisation of magnetite is not prominent it seems, to me, that the pyrite rich ironstones represent some form of marginal alteration of pre-existent magnetite rich ironstone (perhaps originally containing no more than 10-20% Py?). The alteration may be dominantly of carbonate replacing magnetite which, as it diminishes, gives the impression of pyrite becoming the principal iron bearing phase even though the carbonate (which tends to recede into the background "gangue" and which I find more difficult to visually estimate in hand specimens) is probably largely sideritic.
However, the copper mobility seems to be on a fairly local scale and in neither hole does copper reach anomalous levels at more than a few metres away from ironstone.

Another interesting feature of the CRAE data is the rough negative correlation between copper and zinc; zinc is essentially at background levels within the copper bearing ironstone intervals but is faintly to distinctly anomalous in the hanging wall metasediments and appears to be particularly associated with the bands and veins of granular/massive pyrite-carbonate there. I would interpret these as being of late tectonic/epigenetic origin but their spatial association in the hanging wall of ironstones is interesting and may be a hint of metallogenic zoning, either syngenetic or epigenetic? In this respect it is of some regret that the hanging wall of AP2 was not core drilled.

The limited gold analyses are not encouraging; it is generally below detection limit in ironstones but ranges upto 30ppb in some of the pyrite rich ironstone. The veins and bands of massive pyrite-carbonate in AP1 are weakly anomalous at upto 100ppb and therefore are weakly correlated with zinc but the CRAE data from percussion chips in AP2 suggest that bulk grades, in intersections to date, are not significant.

Geophysics:

Three dimensional modelling of the magnetic data, with susceptibility parameters determined from measurements on ironstone intersections in AP1 and AP2, has been carried out for line 8700E over the main southern anomaly and for lines 8700 and 9000E over the northern anomaly. (Appendix I)

In both cases the magnetic sources are interpreted to dip steeply to the south-east or south-south-east which is consistent with the dip of the principal foliation and the trend of the gross lithological layering in the rocks of the Arthur Metamorphic Complex here, (N.Turner, pers comm 16/5/91 in preview of the 1:50,000 Corinna sheet).

The southern anomaly, on 8700E which was partially tested by AP2, is interpreted to be attributable to at least five thin parallel, steeply dipping bands or lenses of ironstone of which the western one comes closest to the surface. AP2 appears to have intersected only one of these five bodies (Fig. 4) and the observation that this intersection actually included four thin bands lends support to Dr.Bishop's comment that the source could actually be a greater number of thinner bodies. Whether these represent a stacked sequence of individual layers or transposed slices of one or a few iron formations remains speculative although the petrographic evidence for strong strain and observations of tight isoclinal folding and minor transposition further to the north (Herrmann, 1991) suggests that the latter is a reasonable possibility.

The northern anomaly is interpreted to be due to a single thin tabular body on 9000E which diverges into two bodies at 8700E which appear to further diverge, and perhaps plunge and peter out, to the west. The lateral discontinuity of this northern anomaly, most apparent on the magnetic contour plan, suggests that this also has been structurally dismembered.

The relationship between the northern and southern magnetic anomalies remains obscure because of the poor surface exposure and lack of drilling of the northern anomaly. The convergence of magnetic trends towards the eastern edge of the grid might infer the presence of a fold closure there though there is no "connection" of the trends and there is little symmetry in the CRAE geological interpretation to support such a structure.

An alternative, equally unsupported, interpretation can be based on the "paired" occurrence of massive magnetite rich and banded more siliceous ironstones in the Owen Meredith area where the former type occur close to the western margin of the Bowry Member (loosely defined by the appearance of mafic schist/amphibolite) and the latter at the eastern contact adjacent to structurally overlying psammitic-pelitic metasediments. If, as is geochemically inferred, the southern Alpine anomaly is analogous to the eastern banded siliceous ironstones at Owen Meredith then perhaps the northern Alpine anomaly is due to a discontinuous, structurally attenuated, massive silica poor-magnetite rich ironstone body. Further comparative magnetic modelling of data from both areas, with input of magnetic susceptibility parameters appropriate to the massive type of ironstone might elucidate the interpretation but is unlikely to be definitive in the absence of drilling information.

The TEM survey has apparently not been successful in defining (the optimistically anticipated) significant conductive zones which could be interpreted to represent high copper concentrations and to be worthwhile drilling targets.

However, I am not entirely discouraged by the TEM results. The petrographic indications are that chalcopyrite occurs as fine disseminations, veinlets and fracture fillings within the ironstones and which may not provide good electrical conductivity; there are, so far, no indications of the occurrence of zones of massive chalcopyrite. All the rocks have been extensively recrystallised and even the pyrite rich ironstones and pyrite-carbonate veins often show a granoblastic fabric in which sulphide grains may not be well connected.

The absence of a TEM response over the southern ironstone partly tested by AP2, which intersected two significant intervals averaging greater than 0.6% Cu with 2m sections upto 1.3% Cu, suggests that the known copper mineralisation is not significantly conductive and provides no basis for an assumption that copper grades two or three times greater will be significantly conductive. The reported extensive veiny and disseminated pyrite-(sphalerite?) mineralisation of the hanging wall in this hole likewise appears to be non-conductive. This question of conductivity requires further investigation before it can be confidently concluded that the TEM results rule out the existence of significant copper mineralisation in the areas surveyed; a good start would be to carry out conductivity measurements on core from AP1 and AP2.

In consideration of the tendency for higher copper grades (>0.6% Cu) and to a much lesser degree gold, to be associated with the relatively pyrite rich - magnetite poor ironstones, it may be possible that Induced Polarisation surveys could be applied to the search for economic mineralisation. The IP responses might be blurred by the prescence of disseminated and veiny pyrite in the hanging wall metasediments but (according to the tentative genetic model which envisages copper as a primary component of exhalative iron formations with localised re-mobilisation associated with carbonate alteration late in the retrograde metamorphic stage) any IP responses closely co-incident with magnetic anomalies would probably be good drilling targets. AP1 indicates that the base of sulphide oxidation occurs at about 30m but this can be expected to vary considerably.

Possibilities for further exploration:

a) The magnetic modelling of data from line 8700E confirms that AP2 has not adequately tested the source of the main southern magnetic anomaly. This hole did however intersect some fairly interesting copper mineralisation associated with ironstones - by far the best yet encountered by Outokumpu's sampling and review of ironstones in the Arthur Metamorphic Complex. Dr. Bishop's comments on the limited strike potential and likelihood of discovery of a gold deposit here are valid but do not, I think, infer that AP2 has provided an adequate test of the style, grade and distribution of copper mineralisation there. This magnetic anomaly is exceptional amongst the several on the Alpine grid in its amplitude and complexity which may be due to unknown structural complexity. In consideration of the apparent structural controls on ore in the Starra "model" deposit and the tentatively interpreted links between mineralisation, structurally controlled local remobilisation and late retrograde metamorphic carbonate alteration at Alpine, such a zone of possible structural complexity may represent a favourable target.

Furthermore, the target is accessible and not subject to the logistical problems attendant on drill testing of ironstones on Outokumpu's licences north of the Pieman River.
A 300-350m deep inclined drill hole on 8700E could provide a complete test of the magnetic anomaly and provide useful information on the "sequence" hosting the ironstones and the style and extent of copper mineralisation. Additional holes on adjacent sections 8800E and 8600E or 8500E (where the magnetic source seems to plunge westward?) could provide indications of the lateral extent of mineralisation and partly elucidate the structural setting.

b) The northern magnetic anomaly is an attractive mystery and is likely to remain so in the absence of a drill hole or two. The magnetic feature is not supported by (CRAE) "bedrock/soil" geochemistry but nor is the copper mineralisation in AP2 reflected in soil geochemistry data and there is some doubt about its effectiveness here. The western end of the magnetic anomaly is nearly co-incident with an occurrence (in float) of pyritic chert which has been petrographically interpreted (Weir, 1985) as a recrystallised silicified cherty carbonate and contains traces of chalcopyrite.
A 150-200m inclined diamond drill hole on either 8700E or 9000E would be sufficient to determine the source of the anomaly as well as providing interesting "stratigraphic" information.

c) The failure of the TEM survey to pick up a conductive response attributable to known weak copper mineralisation and bands of fairly pyritic ironstone (intersected in AP1 and AP2) requires resolution. Systematic electrical / petrophysical testing of the AP1 and AP2 drill core would yeild real physical parameters of the observed mineralisation and could be applied in geophysical modelling of the TEM dta to determine if the survey has been effective and if the method is appropriate to exploration in this setting.

d) Consideration should be given to application of IP surveys to identify pyritic zones, closely associated with magnetic ironstones, which may be enriched in copper and, perhaps, gold. Systematic application of IP surveys should probably be dependent on the results of petrophysical testing of ironstones already intersected and assessment of whether the apparent association of copper mineralisation with the pyritic zones of ironstones is substantiated by future drill intersections.

8. REFERENCES

Bishop, J.	1991	A report on EM and Magnetic Surveys, Alpine Grid Corinna South (EL 56/89) Mitre Geophysics for: Outokumpu Exploration
Caithness, S.J.	1985	Rocky Cape EL 1/77, Report on drilling for the period 1/2/85 to 30/11/85. CRAE report no: 13678 TCR 86-2538
Herrmann, W.	1989	Geology of the Arthur Metamorphic Complex, NW Tasmania Outokumpu Exploration Australia Report No: R72.1
Herrmann, W.	1990	EL 14/89 - Corinna, Exploration Progress Report, July 1990. Outokumpu Exploration Australia
Herrmann, W.	1991	Progress report on exploration of the Owen Meredith grid extensions, EL 14/89 - Corinna. Outokumpu Exploration Australia
Turner, N.	(in press)	Corinna 1:50,000 geological atlas sheet; Tas. DMMR Geol. Surv.
Stolz, J.	1991	Report on the petrographic examination of ironstones and associated metamorphic rocks from the Arthur Metamorphic Complex, NW Tasmania. Dept. of Geology, Univ. of Tas. for: Outokumpu Exploration
Weir, J.	1985	Rocky Cape EL 1/77, Progress report on the Alpine prospect for the period 1/2/84 to 31/1/85 CRAE report no: 13135 TCR 85-2335

Appendix I A report on EM and Magnetic Surveys, Alpine Grid Corinna South (EL 56/89)

Dr. J.R.Bishop / Mitre Geophysics

0117

364020

MITRE GEOPHYSICS PTY LTD
MINERAL EXPLORATION AND ENGINEERING CONSULTANTS
BUGGS LANE ELLIOTT TASMANIA 7325 PHONE 004-363143

A REPORT ON EM AND MAGNETIC SURVEYS,

ALPINE GRID, CORINNA SOUTH (E.L. 56/89)

for

Outokumpu Exploration

by

Dr J.R. Bishop

OUT/MG91/04
May, 1991.

0110 364021

CONTENTS

LIST OF TABLES AND FIGURES

SUMMARY

The Alpine grid covers a magnetic anomaly lying within the Arthur Metamorphic Complex in north western Tasmania. Previous mapping and limited drilling has shown the source of the anomaly to be due to ironstones with raised copper values. A fixed loop EM survey has failed to define any responses suggesting a significant body of copper sulphide.

Modelling of the main magnetic anomaly has shown that it has only been partially tested by earlier drilling. However, there is little encouragement to further test this area. Rather, an overview of all of the Complex is suggested with a priority ordering of target areas from an interpretation of aeromagnetics together with regional geochemistry.

INTRODUCTION

Outokumpu has recently taken exploration licences over parts of the PreCambrian Arthur Metamorphic Complex (AMC) in north western Tasmania. This narrow lineament covers a strike length of around 100kms and has known deposits of iron and magnesite (one of the former, Savage River, being mined) and a history of (mostly) alluvial gold production. There are also several old base metal prospects. Previous explorers have tended to concentrate on the old prospects and much of the area remains untouched in any detail (Herrmann, 1989).

Outokumpu has followed up recommendations of a previous explorer, CRAE, and carried out a large fixed loop EM survey over one of the old prospects: the Alpine Prospect (Figure 1). The ground magnetics were also repeated in more detail. This report presents the results of these surveys together with an interpretation and recommendations for further exploration within the area.

EXPLORATION TARGET

Outokumpu's prime target is for an ironstone associated Cu/Au deposit, perhaps similar to Cyprus Gold's Starra (aka Selwyn) Mine which occurs within the Proterozoic Mt Isa Inlier in northern Queensland and where reserves of 5.3 million tonnes grading 5g/t Au and 2% Cu have been identified (Kary and Harley, 1990). Whilst significant differences can be expected between Starra and any deposit found here, it may be relevant to note some of Starra's more salient features and to summarise Cyprus' experiences there with geophysics.

At Starra, the mineralisation occurs over a long strike length (10km) in association with magnetic ironstones (quartz-magnetite-hematite-chalcopyrite-siderite) with the economic deposits in structurally complex zones. Whilst the mineralisation is always associated with magnetite, there is no correlation between gold grade and susceptibility. An extensive zone of adjacent non-magnetic ironstones, apparently a folded arm of the host rocks, are barren. Kary and Harley note that throughout the area, mineralisation occurs adjacent to magnetic amphibolites. Magnetics were used to map the ironstones, but magnetic schists in close proximity to the ironstones were a strong source of 'noise'. EM surveys at Starra defined the massive chalcopyrite mineralisation, but also responded to disseminated chalcopyrite in the footwall schists and particularly strongly to a clayey-hematite-magnetite rock (Collins, 1987).

Herrmann (1989) also lists some of the similarities and differences of the Japanese Besshi Cu-Ag-Au mineralisation to the expected target. The principal difference being that Besshi deposits are sulphides-rich, whereas the AMC is an oxide-rich domain.

The AMC, also referred to as the Arthur Lineament or Arthur Mobile Belt, is a 5-15km wide north east trending linear belt of Late Proterozoic deformed metasedimentary and metavolcanic rocks extending for more than 100kms across north western Tasmania. Turner (1990) summarises the geology of the main lithological association, the Timbs Creek Formation, as consisting of pelitic and carbonate rich schists with subordinate amphibolites and minor quartzose schists and carbonate. The various magnetite-pyrite and magnesite deposits are contained within the Bowry Creek Member of the Timbs Formation and this consists of a pelitic schist with amphibolite and associated pyrite-magnetite lenses, magnesite and dolomite.

Apart from the Savage River deposit, there are a number of other magnetite-pyrite deposits and base metal prospects. The most significant of these have been summarised by Herrmann (1989), who notes that all of the prospects occur within, or are closely associated with, the Bowry Member. Herrmann also discusses the likely genesis of the mineralisation, but concludes that there is insufficient detail "to allow a confident generalisation of the tectonic and metallogenic environment of the AMC."

EXPLORATION HISTORY

Herrmann (1989) states that until recently most of the central section of the AMC was held by IMI/Savage Resources, with the southern and northern parts held by CRAE and Mineral Holdings. Prior to 1980, IMI/Savage Resources limited their exploration to iron deposits. Post 1980, they branched into base metals, relying largely on stream sediment geochemistry with little geological or geophysical follow up. CRAE and Mineral Holdings apparently restricted themselves to investigating old prospects, some stream sediment geochemistry and later, some testing of aeromagnetic anomalies.

The Alpine anomaly was one such followed up by CRAE, who carried out c-horizon soil geochemistry, ground magnetics and Genie EM*. Von Strokirch (1985) identified four significant Genie anomalies and two of these, associated with some geochemistry and/or magnetics were drilled (see figure TASh 2544 in Caithness, 1985). (Von Strokirch suggested that the Genie survey could be usefully followed up by a fixed loop TEM survey "to locate any large bodies at greater depth".) The results of the two short holes, AP1 and AP2 (107m and 86m respectively), were disappointing (Caithness, 1985). Herrmann (1990a) has summarised the results and states that AP1 "intersected a sequence of psammitic quartz schist, graphitic? phyllite and minor dolomitic metasiltstone containing several 'bands' of near massive pyrite and magnetite + pyrite (+/- quartz, carbonate) ironstones over an 11m interval".

---

* Labelling of a VLF conductor coincident with outcropping sulphides on CRAE plan TASh 2544, suggests that some VLF has also been carried out.

AP2 intersected a "different looking sequence of quartz + albite + chlorite + carbonate schist with several zones of magnetite + pyrite ironstones over about a 25m interval". (Coring of AP2 commenced in ironstone at 55m.) Herrmann notes that whilst the host rocks in the two drill holes are different, the ironstones are quite similar and he suggests that they "may represent tectonically dismembered lenses of a formerly continuous body".

The best mineralised intersections for AP1 were 8m of 0.19% Zn and 13m of 0.24% Cu; for AP2, they were 12m of 0.6% Cu and 8m of 0.7% Cu. Both had disappointing gold values. AP2 was sited primarily to test a Genie response and was collared well within the boundaries of the grid's largest magnetic anomaly.

SURVEY DETAILS

The fixed loop EM was carried out by Zonge Engineering using a GDP-16 receiver set at 16Hz (ie, 25 channels monitoring between 0.05 to 12 msecs) measuring the 'X' and 'Z' components. Four 800m x 400m loops were used, with currents of 15 amps. The traverses were up to 600m long and spaced 200m apart, with a station interval of 25m. Each traverse was started inside the loop and strong 'loop edge effects' were recorded on most lines. There was also a power line running across the northern part of the survey and down the western side (see Figure 1). This was turned off for part of the survey and its effect is only local (ie, mostly one station). However the data is generally noisy at amplitudes below about 1 mv/a.

The data was plotted at 1:5,000 scale using a logarithmic mode for the magnitudes. This is not necessarily the best way to identify low amplitude, early to mid-time responses, but any responses not identified would be reflecting very poor conductors ie, not ones due to economic concentrations of chalcopyrite. Copies of the Zonge profiles are included with this report.

The ground magnetic survey was carried out by Highland Exploration using GSM-18 proton precession magnetometers. A station spacing of 5m was used with a line spacing of 100m over most of the grid, but at 200m near the western and eastern edges. This data was processed by Encom Technology who produced a 1:5,000 plan of stacked profiles (Figure 2) and a contour plan (Figure 3) at the same scale.

INTERPRETATION

The survey defined a number of generally weak, and mostly shallow, EM responses. With one significant exception, the responses recorded by CRAE's Genie survey were relocated (with a consistent discrepancy of about 50m) as well as defining three weakly conductive zones. The interpreted responses are shown superimposed on the magnetic contours (Figure 3). None of the TEM anomalous zones coincide with the magnetic responses and one actually cuts across a magnetic trend.

The strongest TEM response was recorded at 8900E/9580N. This is a broad response, indicating a significant depth to the source (~75m). However, the anomaly, which correlates with CRAE's Genie anomaly no.4, has no associated geochemistry (raised Fe & Mn only) or magnetic responses. Von Strokirch (1985) suggests that the Genie response is caused by a "carbonaceous unit".

A clear response was also obtained over CRAE's no.2 Genie anomaly at 9100E/9450N, which was drilled by CRAE with DH AP1. As was mentioned above, this hole intersected several bands of massive pyrite and pyrite-magnetite over a 10m interval, as well as graphitic sequences. Correlating the TEM response with similar ones to the east (see Figure 3) suggests that, although the magnetics and EM are coincident at 9100E/9450N, they have separate sources: the EM possibly responding to a cross-cutting fault (at least two of which were logged by Herrmann (1990b) in AP1).

The 'missing' TEM response is over the Genie anomaly at 8700E/9125N which was given the highest priority by Von Strokirch. This was drilled by CRAE with DH AP2 which, as was mentioned above, intersected several metres of massive pyrite and magnetite and produced some interesting copper values (see above). The lack of a corresponding TEM anomaly suggests that the conductive portion of the mineralisation has limited strike and depth extent; ie, it has poorly coupled to the fixed transmitter loop.

Given the poor TEM responses, no quantitative interpretations have been made on this data.

The repeat magnetic survey has reproduced the broad features of the CRAE work, with the hand contouring of the earlier data (CRAE figure TASh 2365) possibly better reflecting the geology than Encom's computer generated plan. However some of the differences in the latter are supported by the TEM (see Figure 3).

Modelling of the main magnetic anomaly along line 8700E shows that AP2 tested only a small portion of the source of the magnetic anomaly. Figure 4 shows a total of five thin, steeply dipping bodies, however it is quite possible that the source of the anomaly is actually a larger number of thinner bodies.

Herrmann (pers. comm.) has suggested that further north, on the Owen Meredith grid (E.L. 14/89), gold appears to be associated with thin magnetic ironstones near the eastern contact of the Bowry Creek Member, whereas more massive ironstones further to the west are barren. Thus the smaller anomalies at Alpine, although on the 'wrong' (ie, western) side of the larger responses, may be of interest. Two of the responses were modelled: 8700E and 9000E (Figures 5 and 6). A thin belt of discontinuous ironstones is indicated, with a more easterly strike, but a similar steep southerly dip to the more massive ironstones to the south. Two bodies provide a good fit to the data on 8700E and these appear to diverge (and plunge?) to the west. These two bodies were then modified for 9000E.

The modelling has not accounted for the effect of the Tertiary Basalt which is at least 17m thick (weathered?) immediately to the north of the AP2 collar (see CRAE figures TASh 2535 and 2549; Caithness, 1985) and present elsewhere on the grid (though apparently not over the northern ironstones). But this is not expected to significantly alter the models, which indicate two zones of strongly magnetic, north east trending, strike limited (cross faulted?) ironstone 'bands' dipping steeply to the south east. The model parameters are given in Table 1.

CONCLUSIONS AND RECOMMENDATIONS

The TEM survey produced only disappointing results. No significant body of chalcopyrite is indicated within say 100m of the surface. The magnetic modelling has indicated that AP2 has only partially tested the ironstones. However those ironstones that were intersected are only anomalous in copper, not gold. Another hole, sited to thoroughly test the source of this magnetic anomaly (as has been proposed in discussions) might add to the structural and geochemical knowledge of the area, but is unlikely to define a potential orebody, since any deposit would require the gold to be concentrated in strike limited (~350m) ironstones, which have no surface geochemical expression and which lie immediately adjacent to ironstones quite barren in gold. Drill testing of an adjacent and similar(?), but apparently separate, thinner belt of ironstones should be considered and a target can be taken off one of the models.

Given Herrmann's (1990c) conclusion that the AMC is effectively unexplored, it is suggested that an exploration program in which the belt is evaluated as a whole would be worthwhile. Herrmann suggests a program of systematic rock chip and stream sediment sampling. The primary geophysical contribution to such an approach would be identification, via magnetics, of any folded or faulted zones within the AMC which, given the Starra model (and many others), would be high priority targets. The 1981 Mines Dept, with a 500m line spacing and a nominal terrain clearance of 135m is not sufficiently detailed to reveal the most information that the method could give. Nevertheless, an interpretation of this survey, in conjunction with any (smaller) more detailed data sets on open file would identify the larger structures. Much more information could be expected from a new helicopter-borne detailed survey which, assuming a flight line spacing of 150m, would cost about $25,000, to cover E.L.'s 14/89 and 56/89.

J.R. Bishop
May, 1991.

REFERENCES

Caithness, S.J., 1985. Rocky Cape E.L. 1/77 report on drilling for the period 1/2/85 to 30/11/85. CRAE report. Mines Dept file no. 86-2538.

Collins, S., 1987. The geophysics of the Starra gold/copper deposits. Explor. Geophysics 18, 20-22.

Herrmann, W., 1989. Geology of the Arthur Metamorphic Complex. Outokumpu report no. R72.1

Herrmann, W., 1990a. Background notes on the 'Alpine' anomaly, E.L. 56/89 (17/7/90).

Herrmann, W., 1990b. Geological log, AP1 & AP2; Alpine anomaly, E.L. 56/89 (21/6/90).

Herrmann, W., 1990c. Notes on the ironstone occurrences of the Arthur Metamorphic Complex south of Savage River (15/10/90).

Kary, G.L. and Harley, R.A., 1990. Selwyn copper-gold deposits, in Geology of the Mineral Deposits of Australia and Papua New Guinea. AusIMM monograph 14, 955-960.

Turner, N.J., 1990. Late proterozoic of northwest Tasmania - regional geology and mineral deposits, in Geology of the Mineral Deposits of Australia and Papua New Guinea. AusIMM monograph 14, 1169-1174.

Von Strokirch, T., 1985. Alpine prospect: Genie and ground magnetic surveys. Appendix 3 in: Rocky Cape (E.L. 1/77) progress report for period 1/2/84 to 31/1/85. CRAE company report by D.J. Weir (1985). Mines Dept file no. 85-2335.

Table 1

MAGNETIC PROPERTIES AND MODELLING PARAMETERS

1. Magnetic Susceptibilities of Ironstones (cgs).

AP1	
85m	.032 - .037
86m	.010 - .024
88m	.010 - .029
AP2	
66m	.034 - .070
67m	.006 - .054
69m	.048 - .056
70m	.001 - .021

(Measurements by Herrmann in June 1990, on core using a KT-5 'Kappameter' susceptibility meter. Readings converted from 10^-3 SI units.)

2. Modelling Parameters.

(input to 'Toolkit 3Dplus')

Total Field Intensity = 62,000nt
Dip = -72.°
Declination = 12.5°

Tabular bodies with dimensions between 200-350m long x 100-250m deep x 8-15m thick and susceptibilities between 0.03-0.04 cgs and with negligible remanence were used for the model bodies. Demagnetisation was ignored, but note that the bodies' dips are close to parallel to the earth's field.

0128 364031

OUTOKUMPU EXPLORATION

ALPINE GRID (E.L. 56/89)

TEM SURVEY

LOCATION PLAN

SCALE 1:25000

FIG. 1

N.W. Coast Computer Aided Drafting Centre. Phone (004 354315)

10008

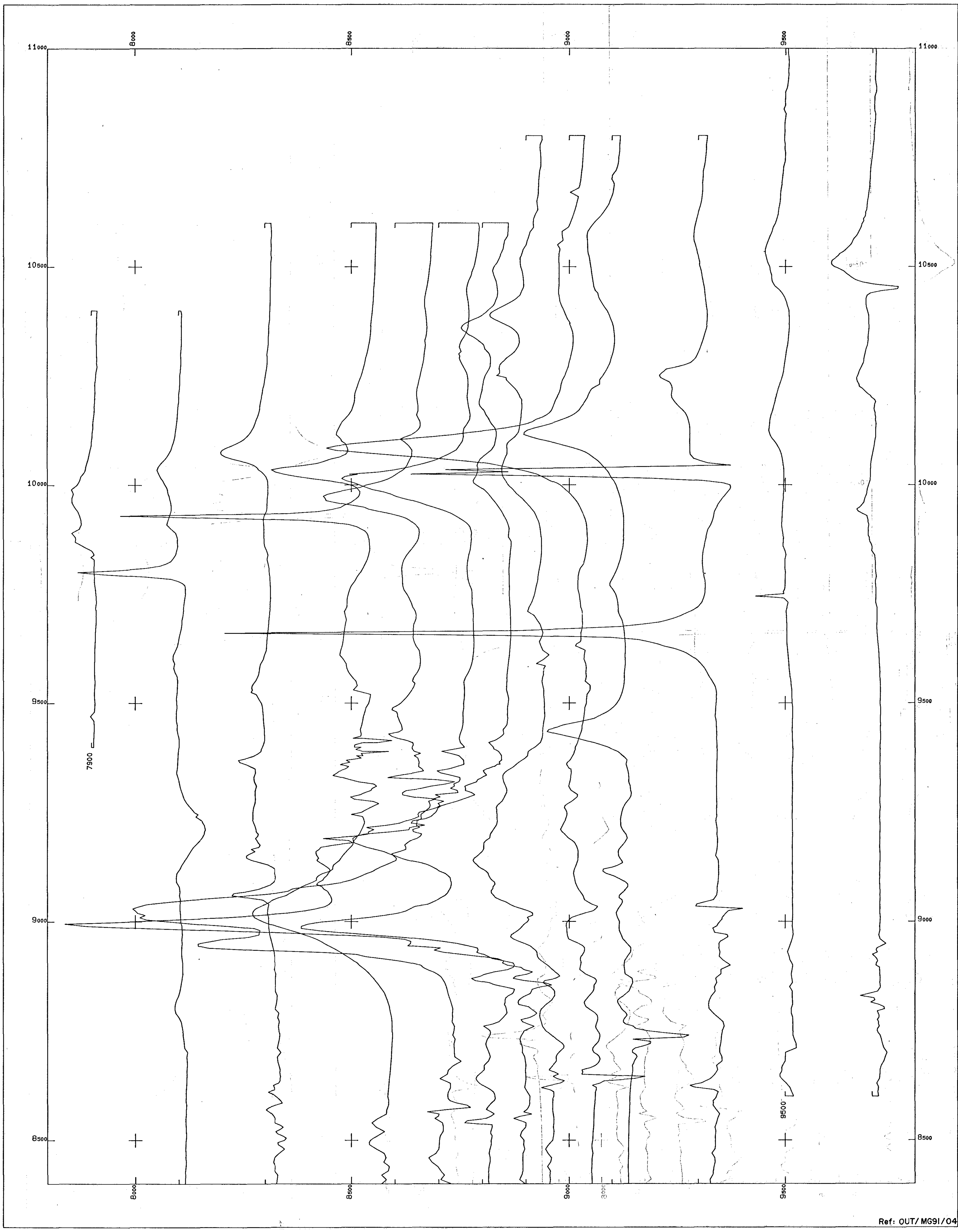

Alpine Grid ground magnetics
Surveyed by Highland Exploration
21/12/1990
Instrumentation GSM-18
Proton Magnetometers

5 metre station spacing along
lines indicated

91-3269.

N

SCALE
364032 1:5000
0 50 100 150 200 250 300 m

5 cm

Outokumpu Exploration

Alpine Grid

Raw Magnetic

Stacked Profile Map

Vertical Scale = 250 nT/cm.

Ref: OUT/MG91/04

Compiled by:	Date: 15 Mar 1991
Drawn by:	Drawing No.: **FIG.2**

10008

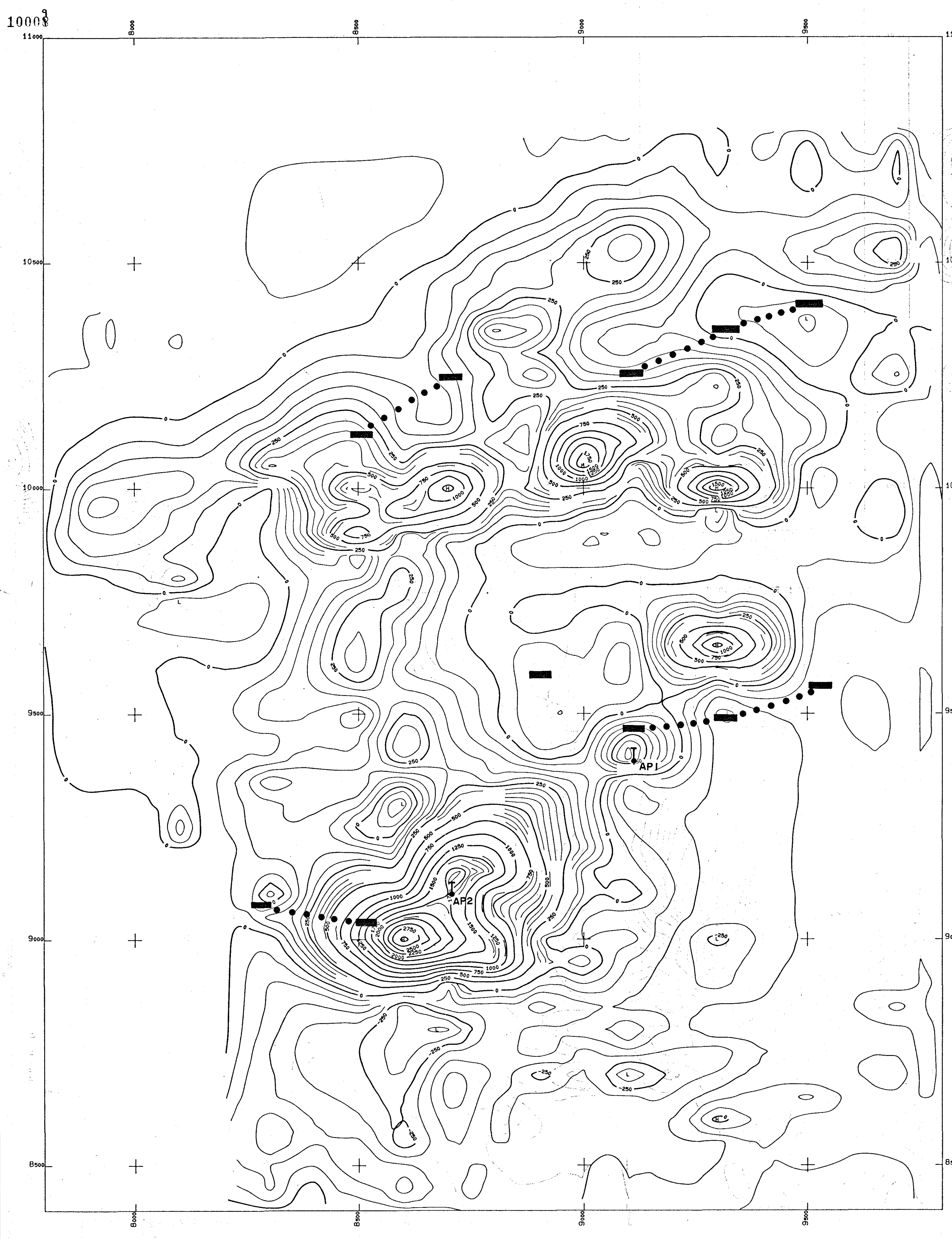

Alpine Grid ground magnetics
Surveyed by Highland Exploration
21/12/1990
Instrumentation GSM-18
Proton Magnetometers

Station spacing = 5 metres
Grid lines

TEM ANOMALY

TEM Survey by: Zonge Engineering
Date: Feb. 1991
Fixed Loop TEM with GDP-16 at 16Hz
X and Z Components

91-3269.

N

364033

SCALE
1: 5000
m 0 50 100 150 200 250 300 m
5 cm

Outokumpu Exploration

Alpine Grid
TEM ANOMALIES
AND
MAGNETIC CONTOURS
Contour Interval = 50 nT

Compiled by:	Date: 15 Mar 1991
Drawn by:	Drawing No.: FIG.3

Ref: OUT/MG91/04

364034

0129

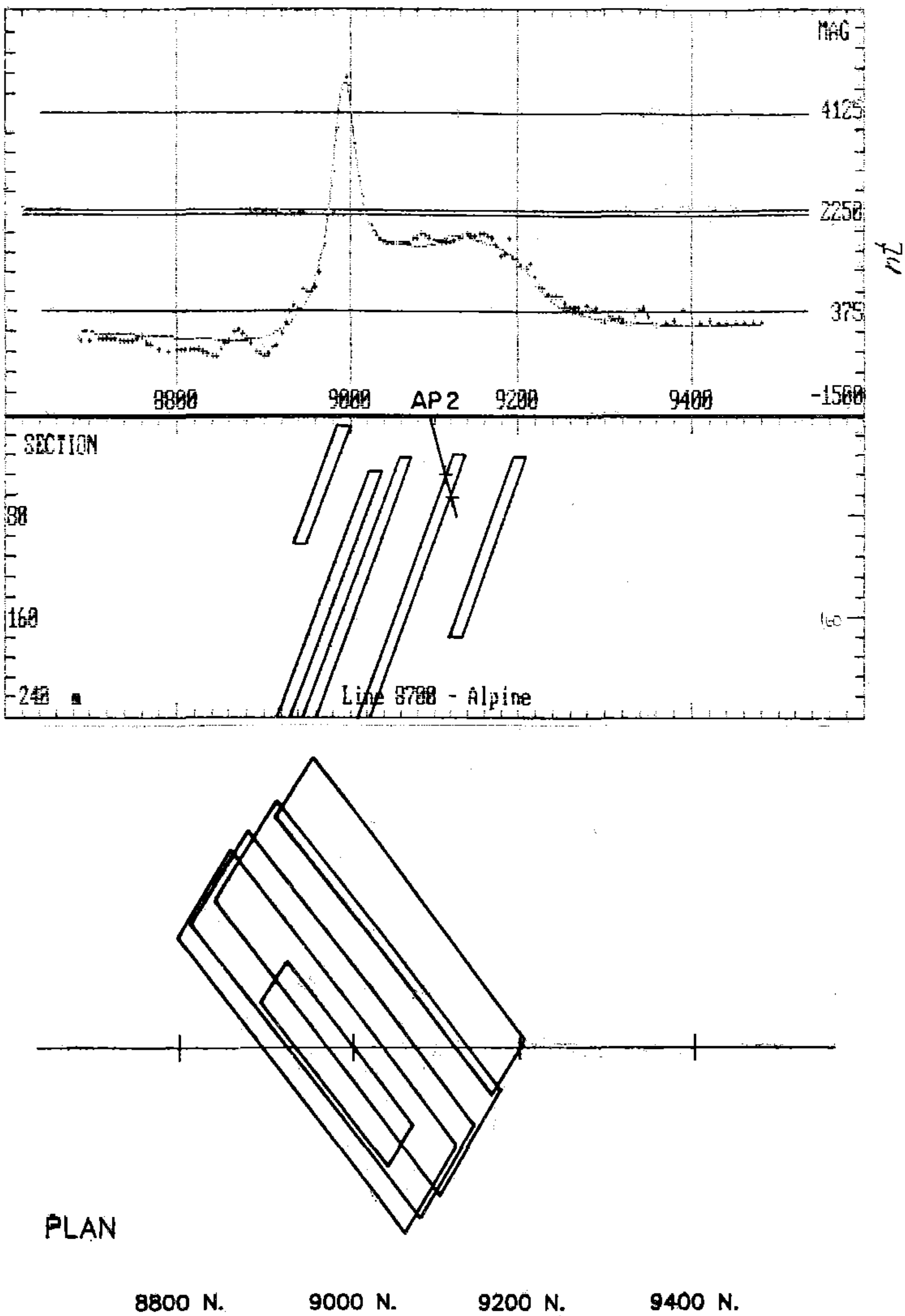

Interpretation by Mitre Geophysics

Ref: OUT/MG91/04

OUTOKUMPU EXPLORATION

ALPINE GRID (E.L. 56/89)
MAGNETIC MODELLING
LINE 8700 E. (South)

FIG. 4

0130

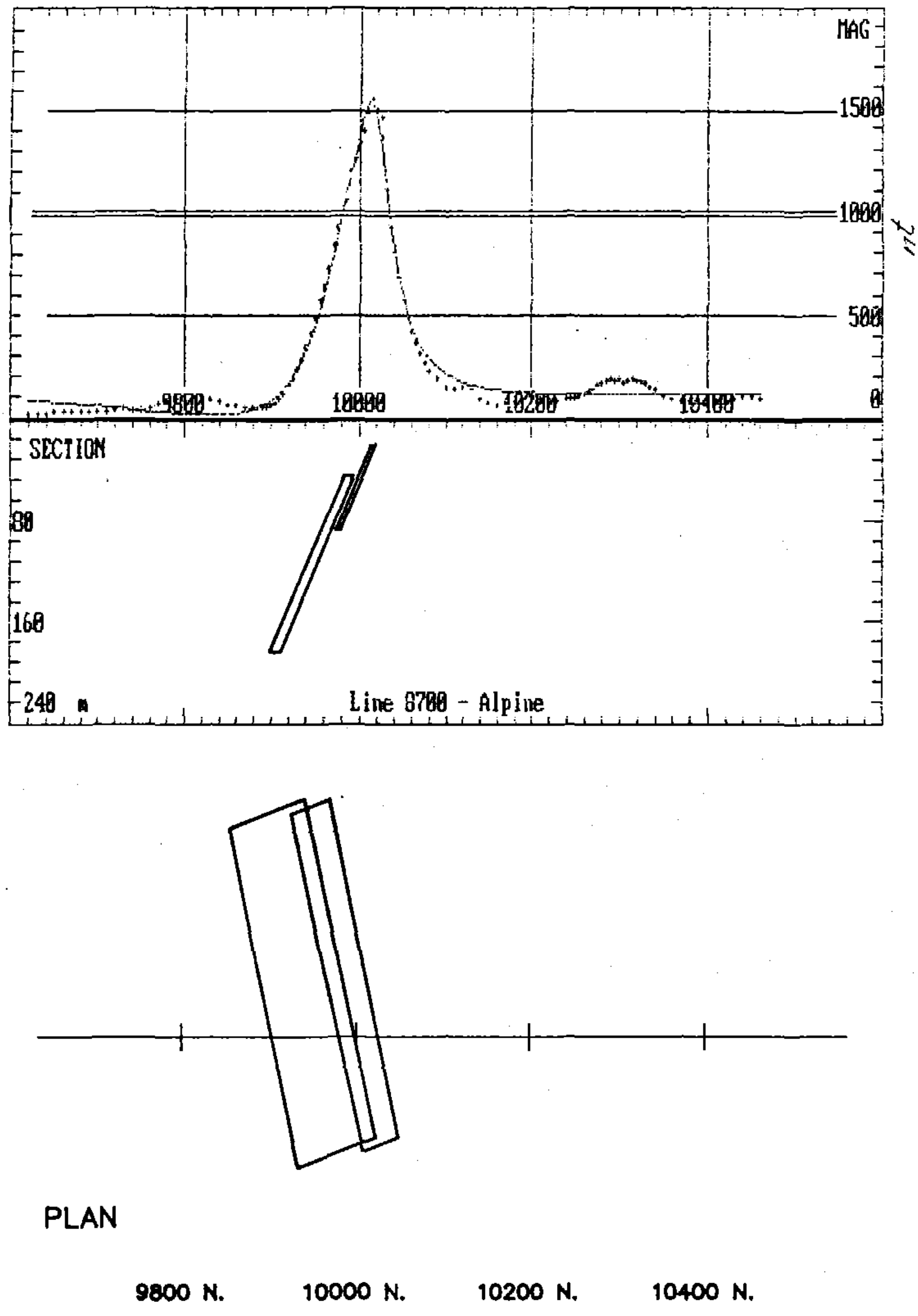

Interpretation by Mitre Geophysics

Ref: OUT/MG91/04

OUTOKUMPU EXPLORATION

ALPINE GRID (E.L. 56/89)

MAGNETIC MODELLING
LINE 8700 E. (North)

FIG. 5

N.W. Coast Computer Aided Drafting Centre. Phone (004 354315)
Fax. (004 354495)

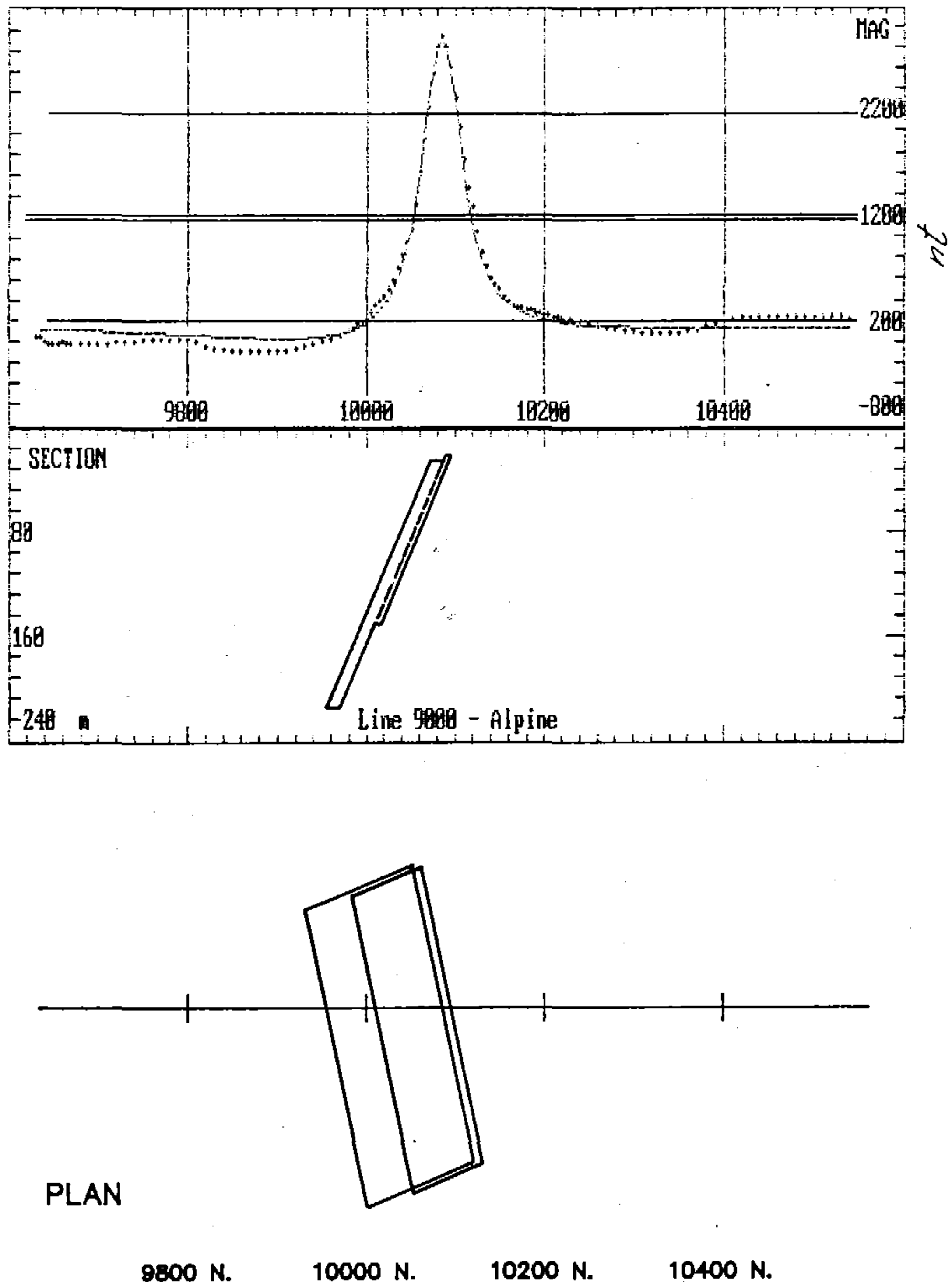

OUTOKUMPU EXPLORATION

ALPINE GRID (E.L. 56/89)

MAGNETIC MODELLING
LINE 9000 E.

FIG. 6

Interpretation by Mitre Geophysics

Ref:OUT/MG91/04

N.W. Coast Computer Aided Drafting Centre. Phone (004 354315)
Fax. (004 354495)

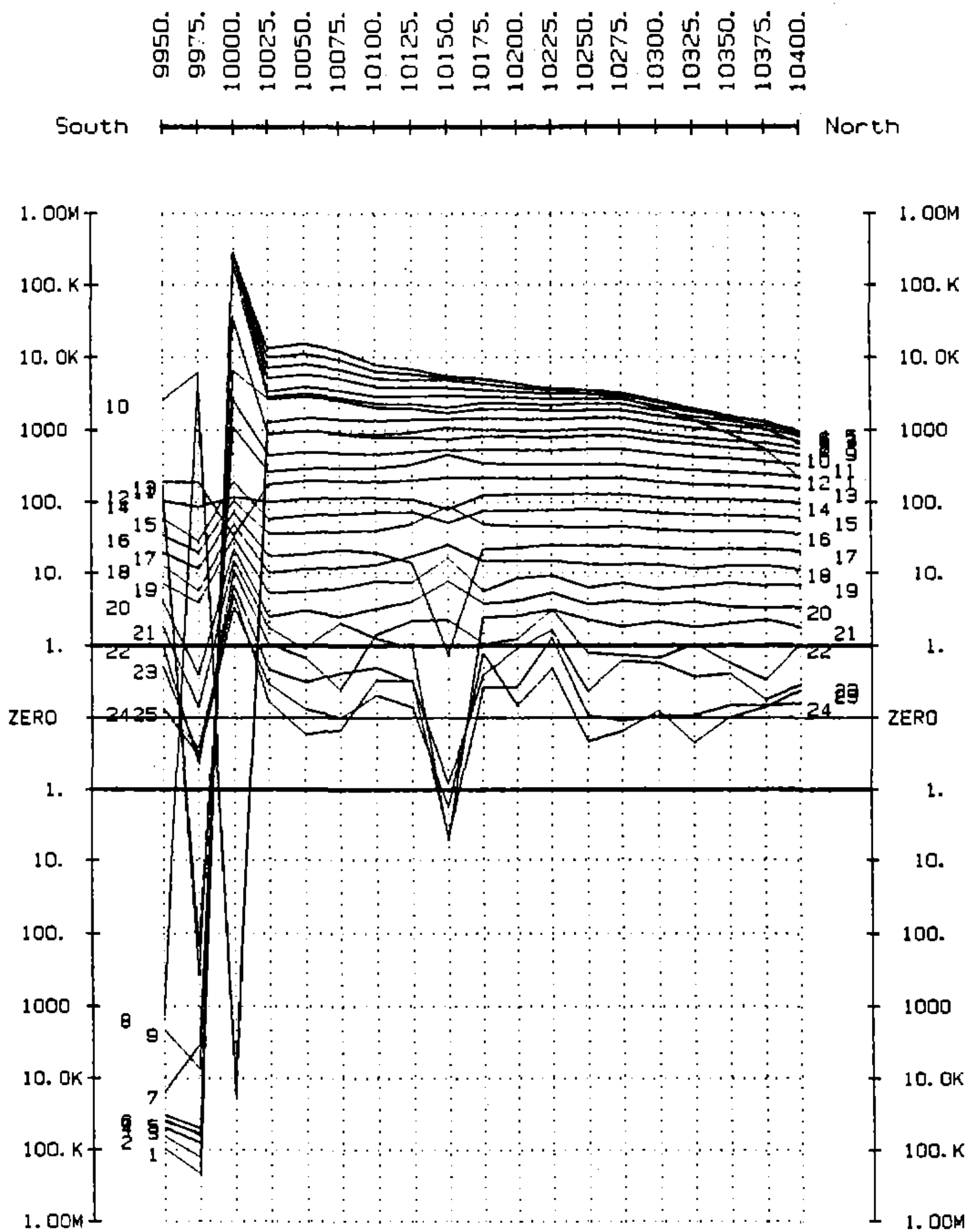

Window MAGNITUDE
values in microV/ampere
Component: CH1 X. Rxna=10000.0
Loop 1: 8900E-9700E
9600N-10000N
15AMPS, 16HZ
Tx Delay 150 uSec

Win	Mag	Win	Mag
1	54.20u	14	1.023m
2	84.60u	15	1.264m
3	115.0u	16	1.580m
4	145.4u	17	1.961m
5	175.8u	18	2.454m
6	206.2u	19	3.106m
7	251.2u	20	3.878m
8	312.2u	21	4.870m
9	373.0u	22	6.114m
10	433.9u	23	7.678m
11	536.8u	24	9.663m
12	675.7u	25	12.16m
13	825.7u		

LINE 8900E
X Component

Field Job 062
Plot by CPLOT 5.71
Plotted 03 Mar 91

0132

364037

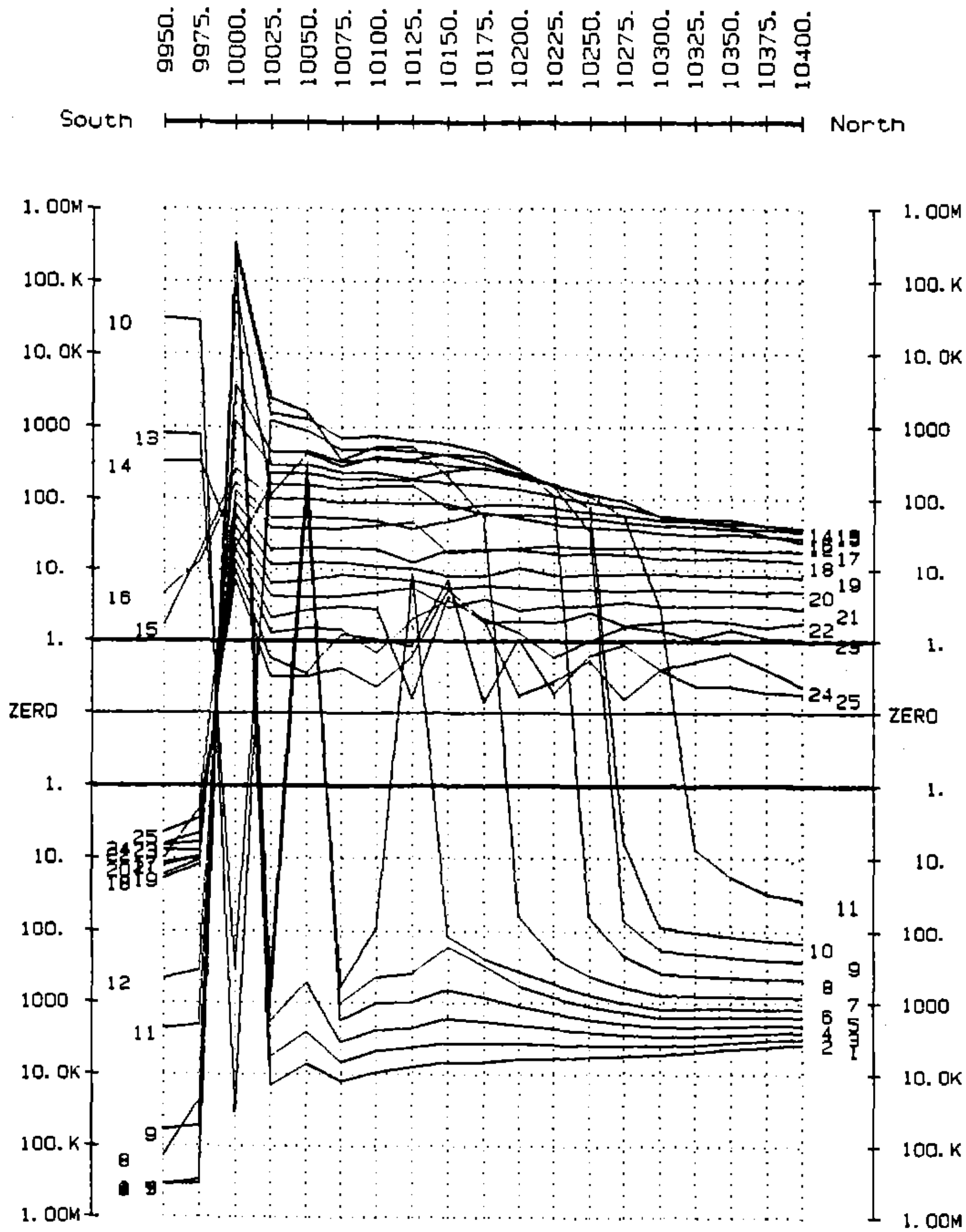

Window MAGNITUDE
values in microV/ampere
Component: CH1 Z. Rxno=10000.0
Loop 1: 8900E-9700E
9600N-10000N
15AMPS. 16HZ
Tx Delay 150 uSec

Win	Mag	Win	Mag
1	54.20u	14	1.023m
2	84.60u	15	1.264m
3	115.0u	16	1.580m
4	145.4u	17	1.961m
5	175.8u	18	2.454m
6	206.2u	19	3.106m
7	251.2u	20	3.878m
8	312.2u	21	4.870m
9	373.0u	22	6.114m
10	433.9u	23	7.678m
11	536.8u	24	9.663m
12	675.7u	25	12.16m
13	825.7u		

LINE 8900 E
Z Component

Field Job 062
Plot by CPLOT 5.71
Plotted 03 Mar 91

0133

364038

0134

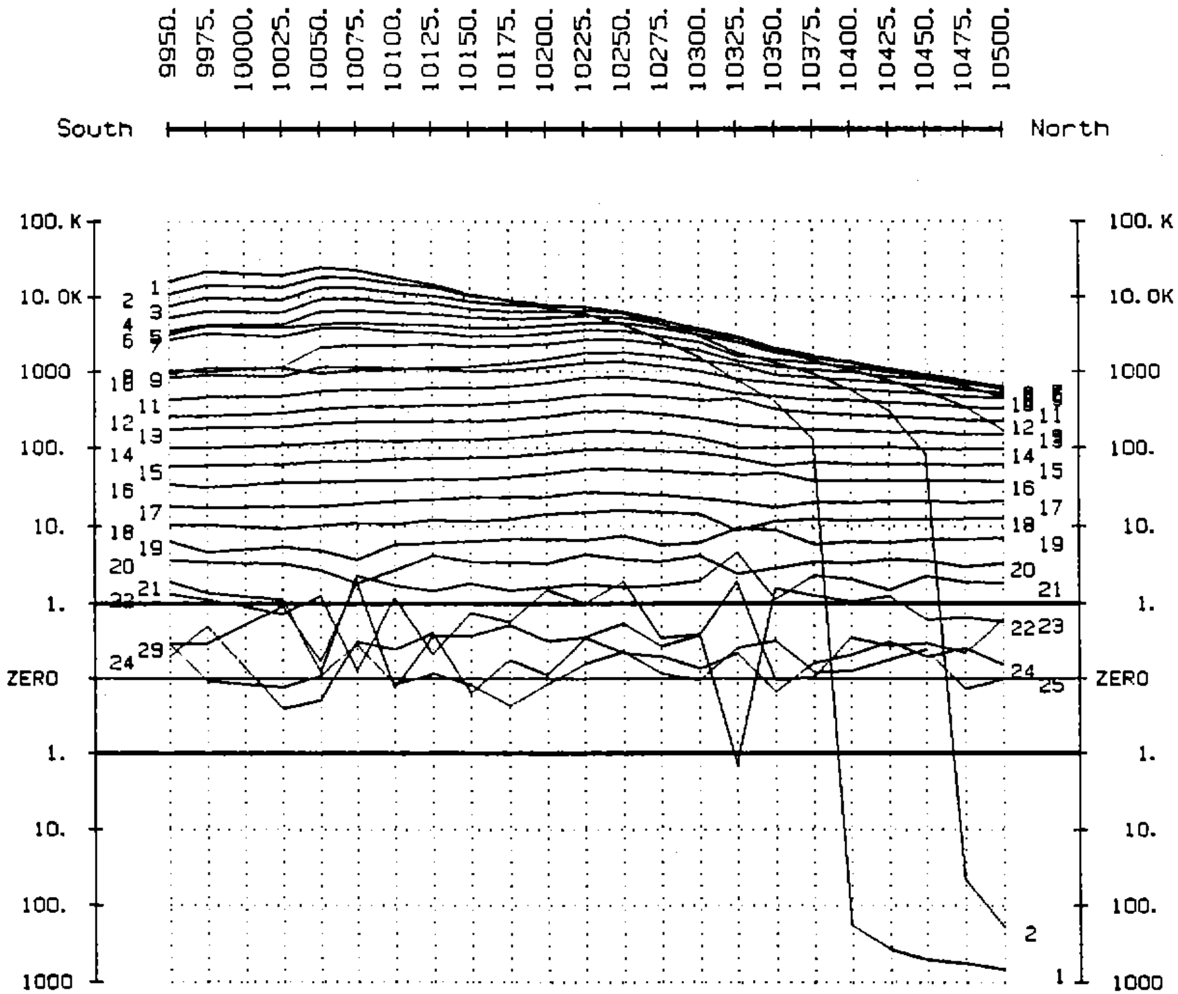

Window MAGNITUDE
values in microV/ampere
Component: CHl X, Rxna=10000.0
Loop 1: 8900E-9700E
9600N-10000N
15AMPS, 16HZ
Tx Delay 150 uSec

Win	Mag	Win	Mag
1	54.20u	14	1.023m
2	84.60u	15	1.264m
3	115.0u	16	1.580m
4	145.4u	17	1.961m
5	175.8u	18	2.454m
6	206.2u	19	3.106m
7	251.2u	20	3.878m
8	312.2u	21	4.870m
9	373.0u	22	6.114m
10	433.9u	23	7.678m
11	536.8u	24	9.663m
12	675.7u	25	12.16m
13	825.7u		

LINE 9100 E
X Component

Field Job 062
Plot by CPLOT 5.71
Plotted 03 Mar 91

364039

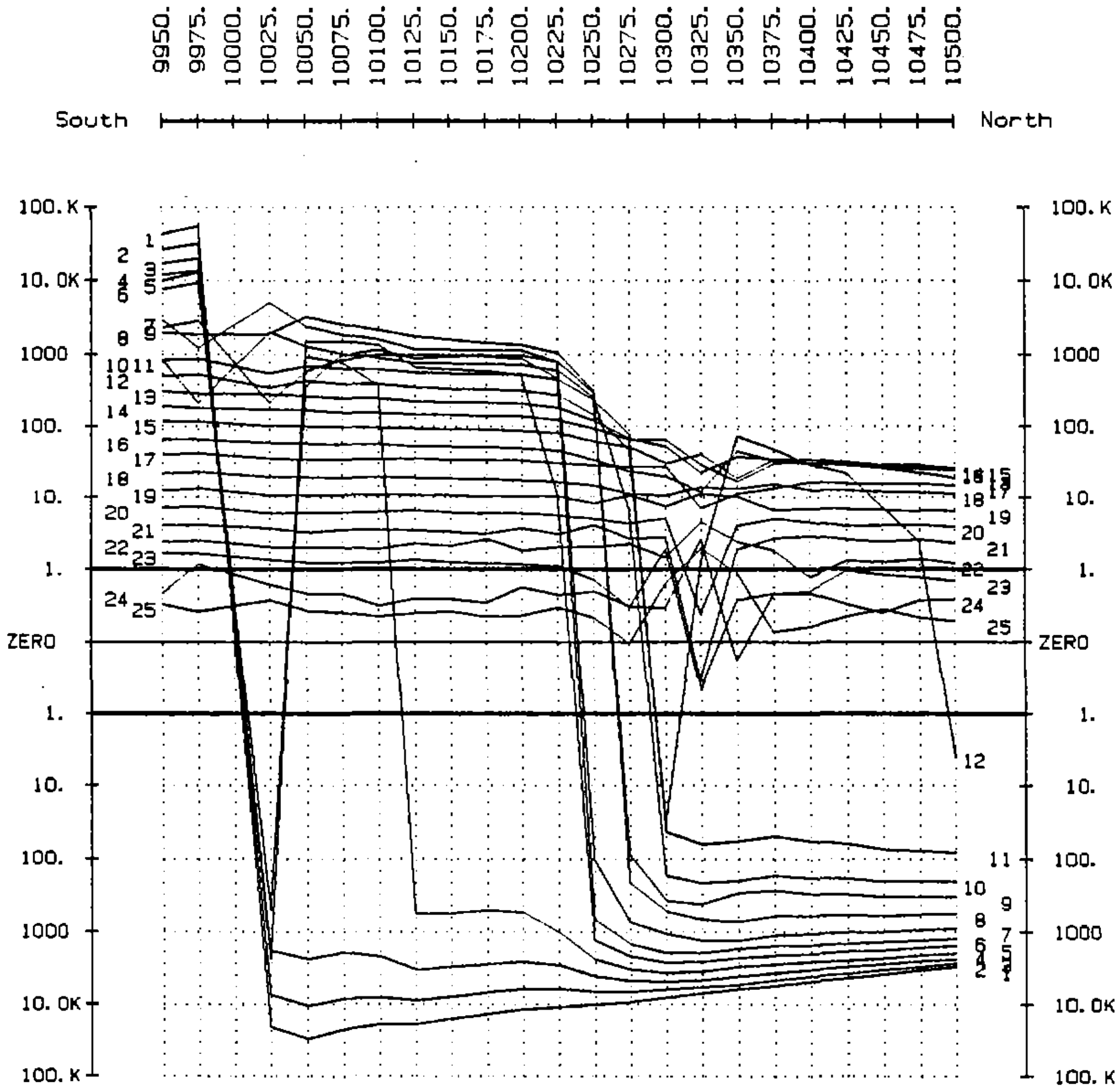

Window MAGNITUDE
values in microV/ampere
Component: CH1 Z. Rxna=10000.0
Loop 1: 8900E-9700E
9600N-10000N
15AMPS. 16HZ
Tx Delay 150 uSec

Win	Mag	Win	Mag
1	54.20u	14	1.023m
2	84.60u	15	1.264m
3	115.0u	16	1.580m
4	145.4u	17	1.961m
5	175.8u	18	2.454m
6	206.2u	19	3.106m
7	251.2u	20	3.878m
8	312.2u	21	4.870m
9	373.0u	22	6.114m
10	433.9u	23	7.678m
11	536.8u	24	9.663m
12	675.7u	25	12.16m
13	825.7u		

LINE 9100 E
Z Component

Field Job 062
Plot by CPLOT 5.71
Plotted 03 Mar 91

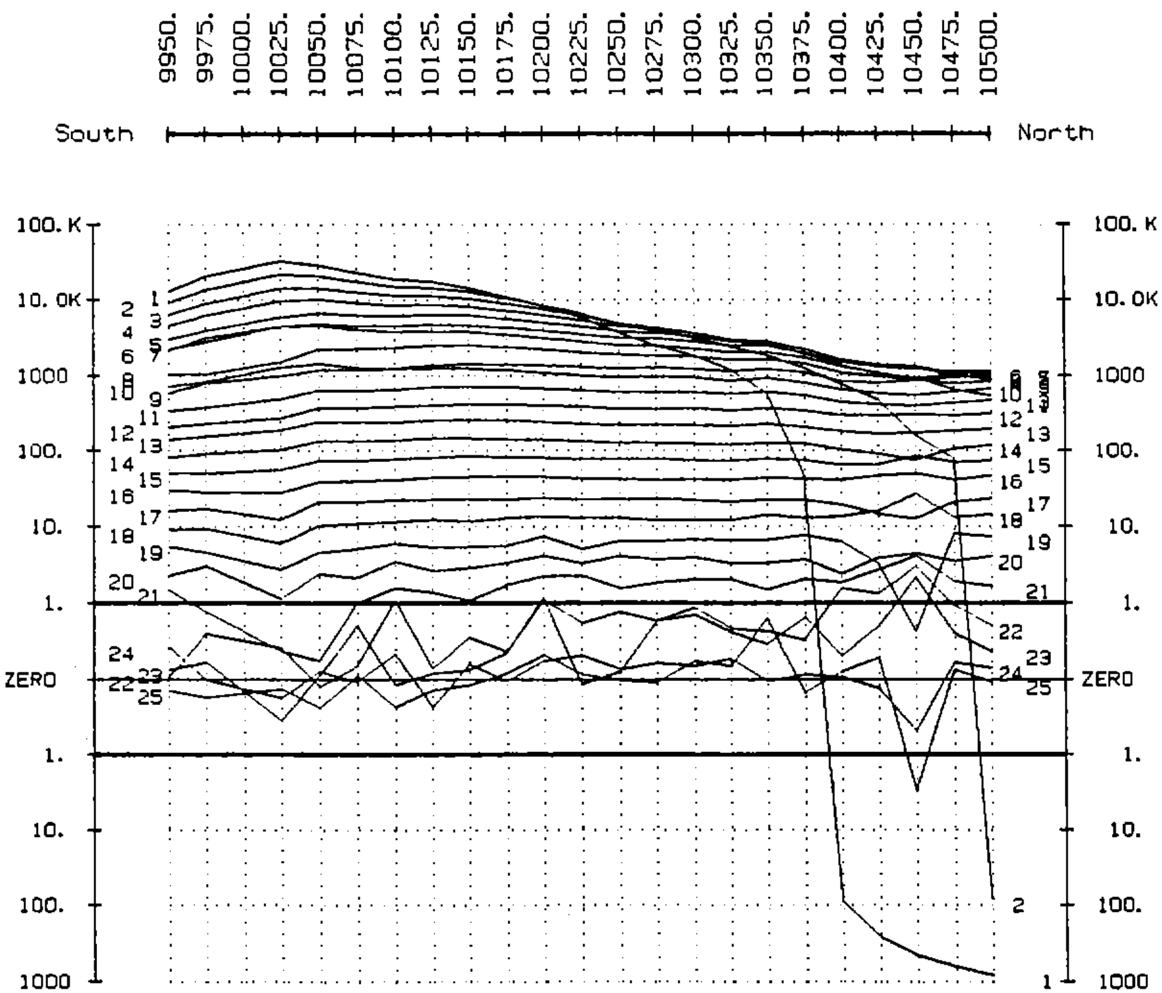

Window MAGNITUDE
values in microV/ampere
Component: CH1 X, Rxna=10000.0
Loop 1: 8900E-9700E
9600N-10000N
15AMPS, 16HZ
Tx Delay 150 uSec

Win	Mag	Win	Mag
1	54.20u	14	1.023m
2	84.60u	15	1.264m
3	115.0u	16	1.580m
4	145.4u	17	1.961m
5	175.8u	18	2.454m
6	206.2u	19	3.106m
7	251.2u	20	3.878m
8	312.2u	21	4.870m
9	373.0u	22	6.114m
10	433.9u	23	7.678m
11	536.8u	24	9.663m
12	675.7u	25	12.16m
13	825.7u		

LINE 9300E
X Component

Field Job 062
Plot by CPLOT 5.71
Plotted 03 Mar 91

013b

364041

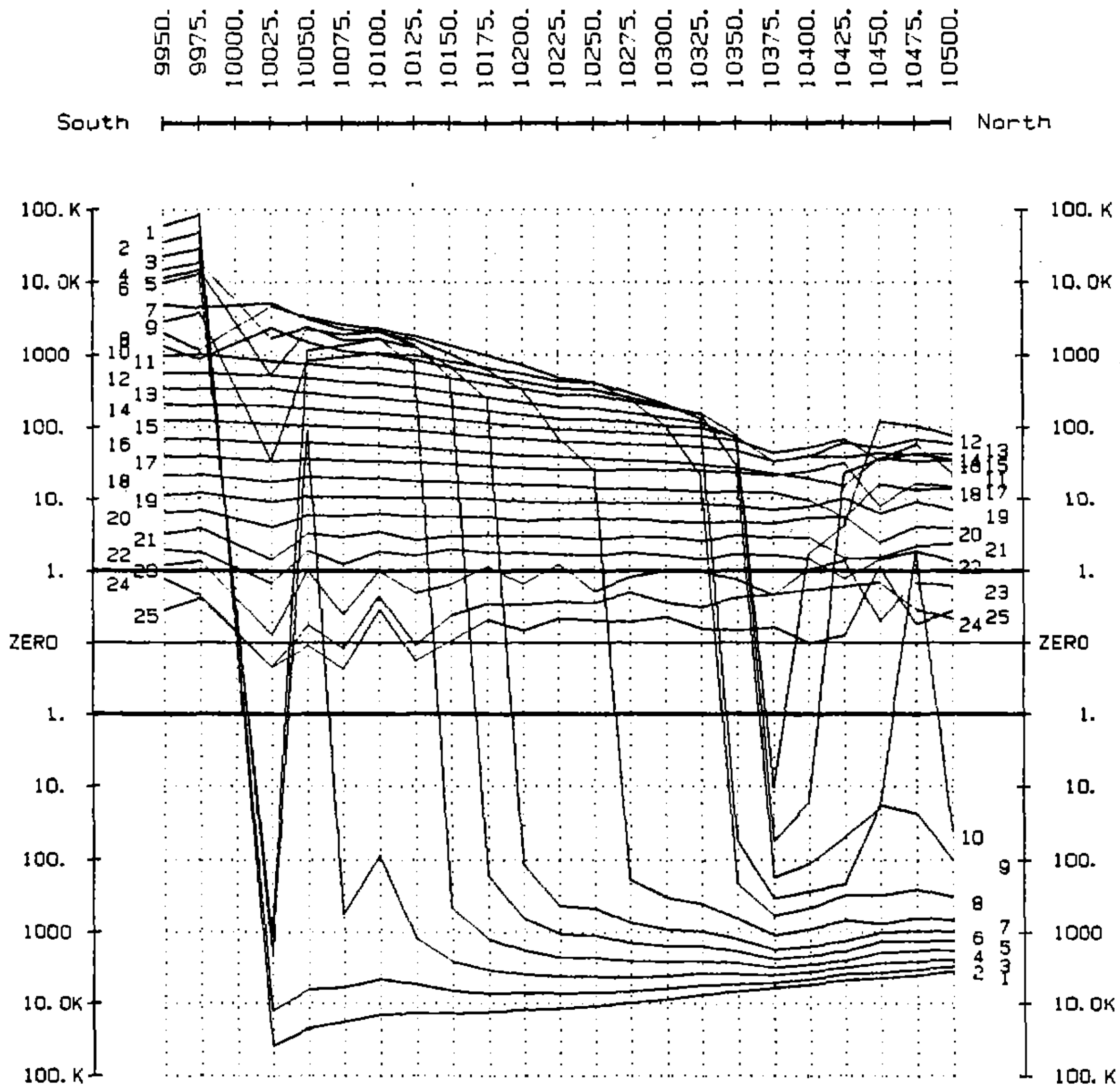

Window MAGNITUDE
values in microV/ampere
Component: CH1 Z, Rxno=10000.0
Loop 1, 8900E-9700E
9600N-10000N
15AMPS, 16HZ
Tx Delay 150 uSec

Win	Mag	Win	Mag
1	54.20u	14	1.023m
2	84.60u	15	1.264m
3	115.0u	16	1.580m
4	145.4u	17	1.961m
5	175.8u	18	2.454m
6	206.2u	19	3.106m
7	251.2u	20	3.878m
8	312.2u	21	4.870m
9	373.0u	22	6.114m
10	433.9u	23	7.678m
11	536.8u	24	9.663m
12	675.7u	25	12.16m
13	825.7u		

LINE 9300 E

Z Component

Field Job 062
Plot by CPLOT 5.71
Plotted 03 Mar 91

0137

364042

0138

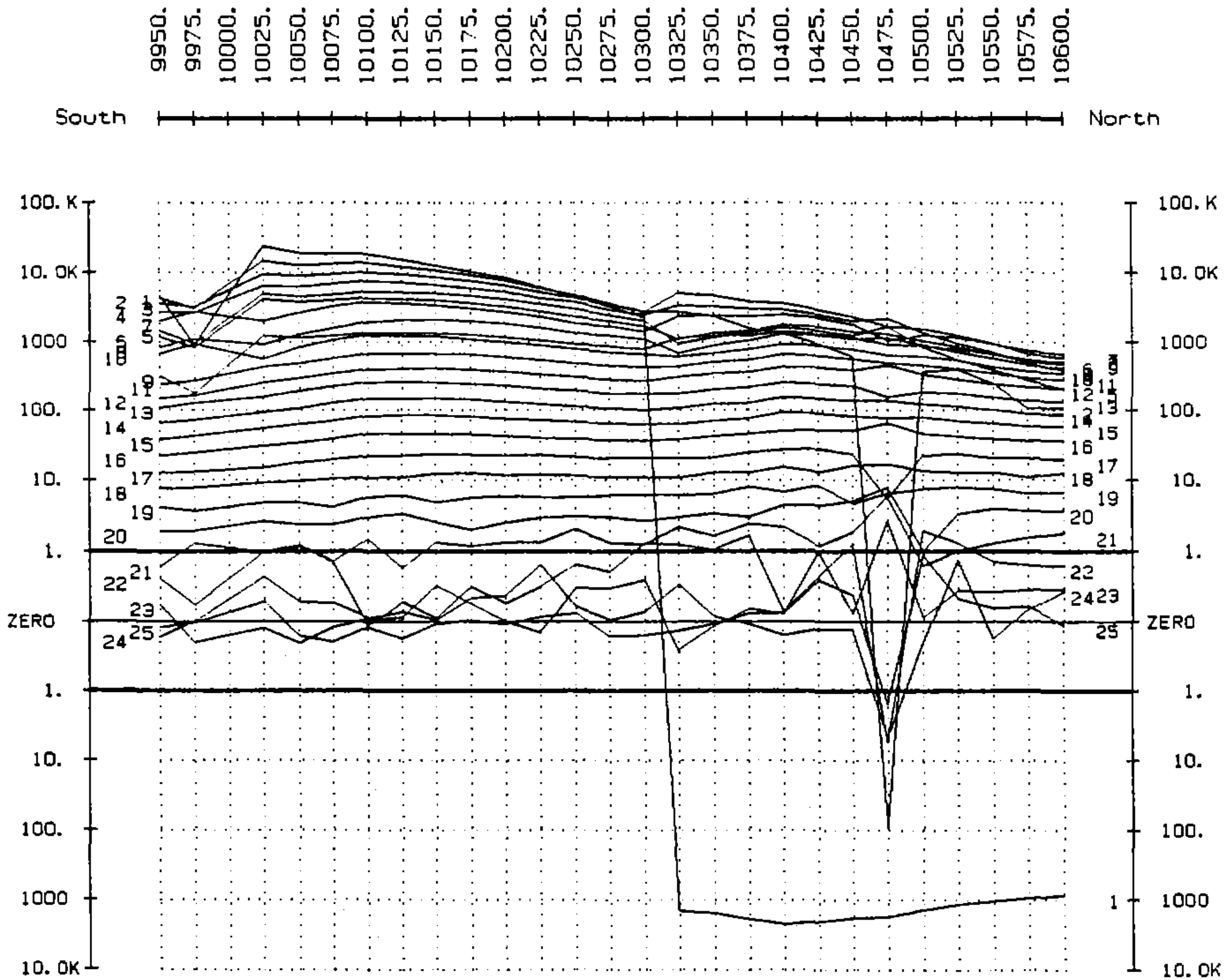

Window MAGNITUDE
values in microV/ampere
Component: CH1 X, Rxna=10000.0
Loop 1: 8900E-9700E
9600N-10000N
15AMPS, 16HZ
Tx Delay 150 uSec

Win	Mag	Win	Mag
1	54.20u	14	1.023m
2	84.60u	15	1.264m
3	115.0u	16	1.590m
4	145.4u	17	1.961m
5	175.8u	18	2.454m
6	206.2u	19	3.106m
7	251.2u	20	3.878m
8	312.2u	21	4.870m
9	373.0u	22	6.114m
10	433.9u	23	7.678m
11	536.8u	24	9.663m
12	675.7u	25	12.16m
13	825.7u		

LINE 9500 E
X Component

36404 3

Field Job 062
Plot by CPLOT 5.71
Plotted 03 Mar 91

0139

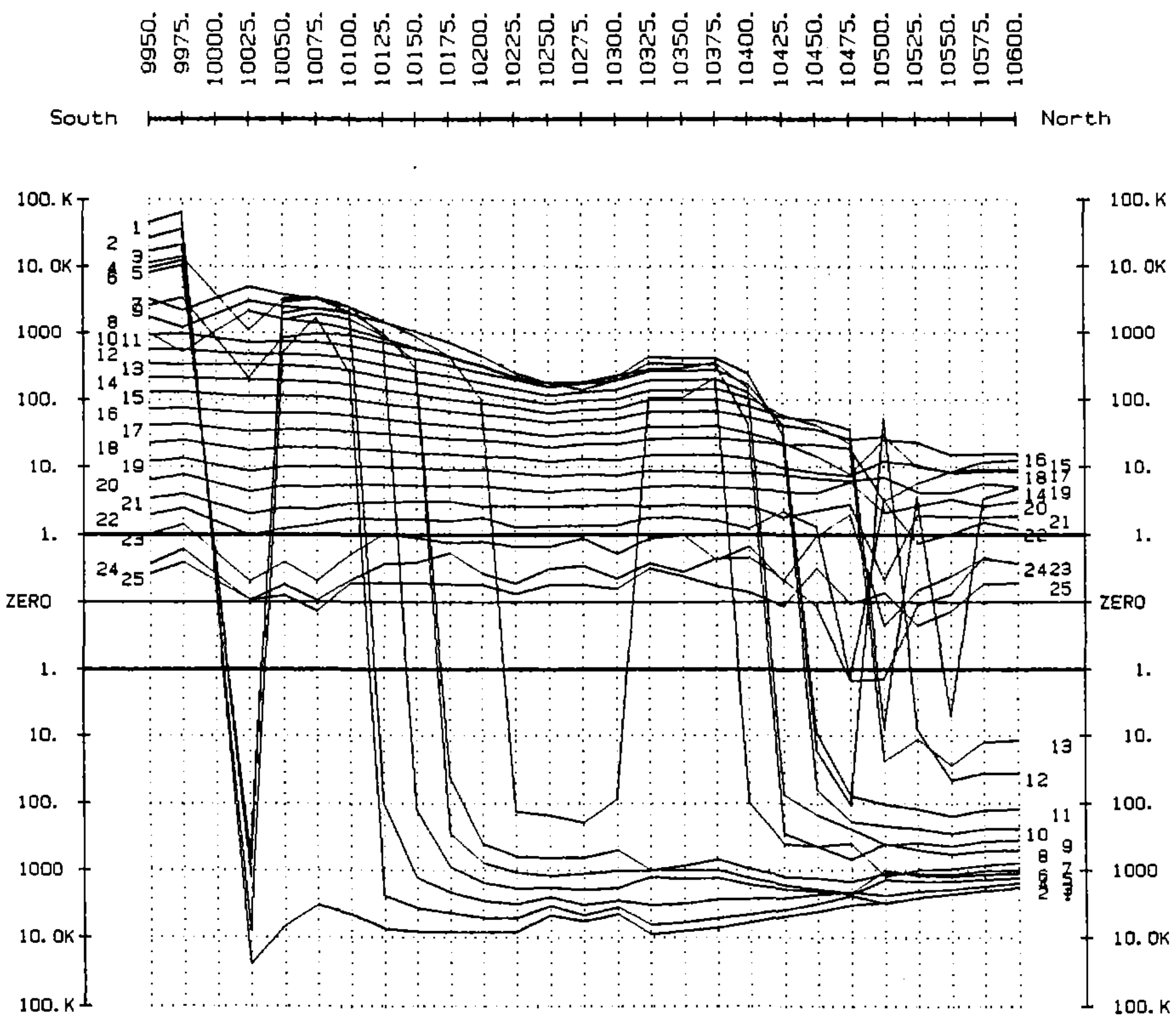

Window MAGNITUDE
values in microV/ampere
Component: CH1 Z. Rxna=10000.0
Loop 1: 8900E-9700E
9600N-10000N
15AMPS, 16HZ
Tx Delay 150 uSec

Win	Mag	Win	Mag
1	54.20u	14	1.023m
2	84.60u	15	1.264m
3	115.0u	16	1.580m
4	145.4u	17	1.961m
5	175.8u	18	2.454m
6	206.2u	19	3.106m
7	251.2u	20	3.878m
8	312.2u	21	4.870m
9	373.0u	22	6.114m
10	433.9u	23	7.678m
11	536.8u	24	9.663m
12	675.7u	25	12.16m
13	825.7u		

LINE 9500 E
Z Component

364044

Field Job 062
Plot by CPLOT 5.71
Plotted 03 Mar 91

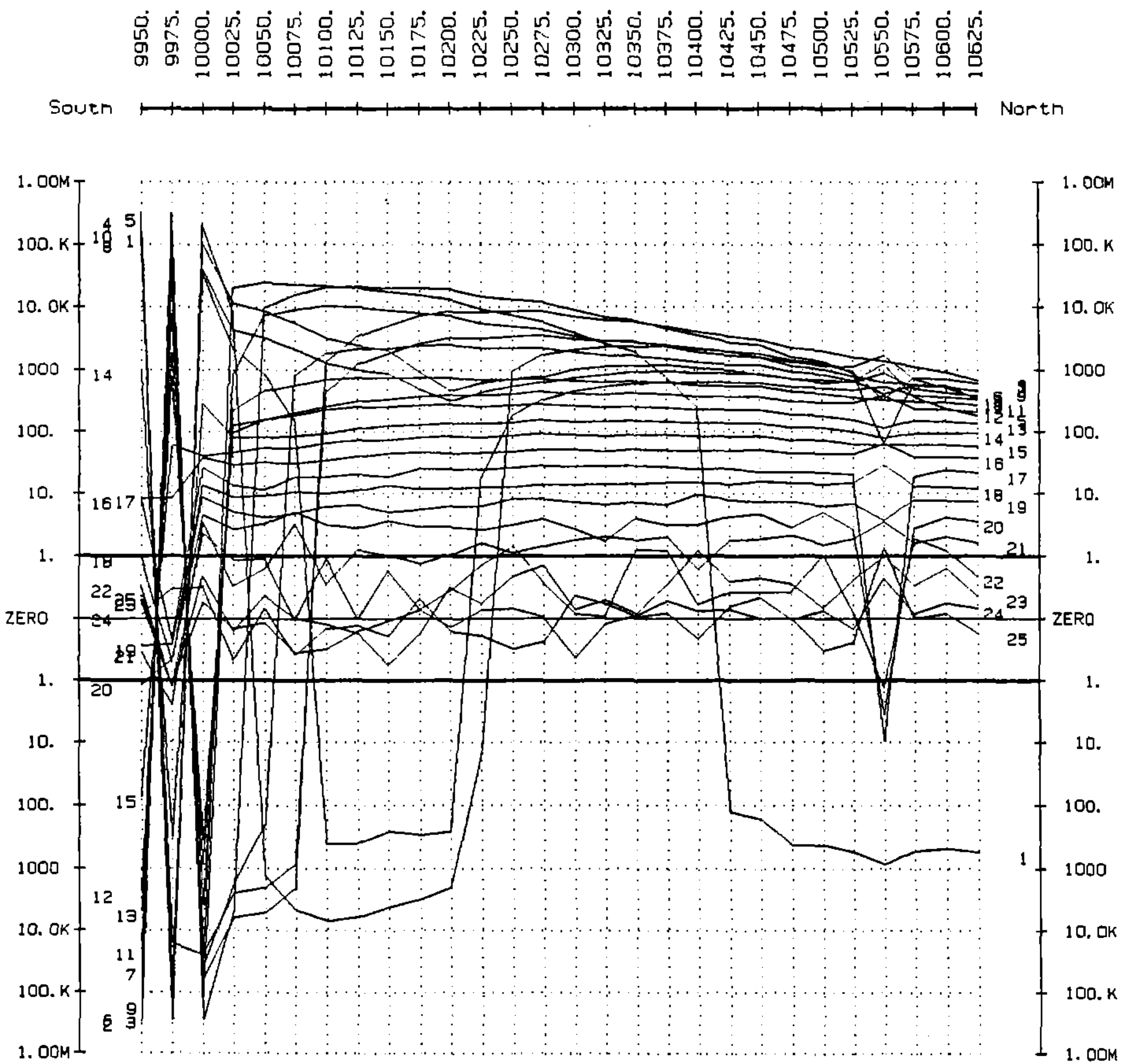

0140

Window MAGNITUDE
values in microV/ampere
Component: CHI X, Rxna=10000.0
Loop 1: 8900E-9700E
9600N-10000N
15AMPS, 16HZ
Tx Delay 150 uSec

Win	Mag	Win	Mag
1	54.20u	14	1.023m
2	84.60u	15	1.264m
3	115.0u	16	1.580m
4	145.4u	17	1.961m
5	175.8u	18	2.454m
6	206.2u	19	3.106m
7	251.2u	20	3.878m
8	312.2u	21	4.870m
9	373.0u	22	6.114m
10	433.9u	23	7.678m
11	536.8u	24	9.663m
12	675.7u	25	12.16m
13	825.7u		

LINE 9700 E
x Component

364045

Field Job 062
Plot by CPLOT 5.71
Plotted 03 Mar 91

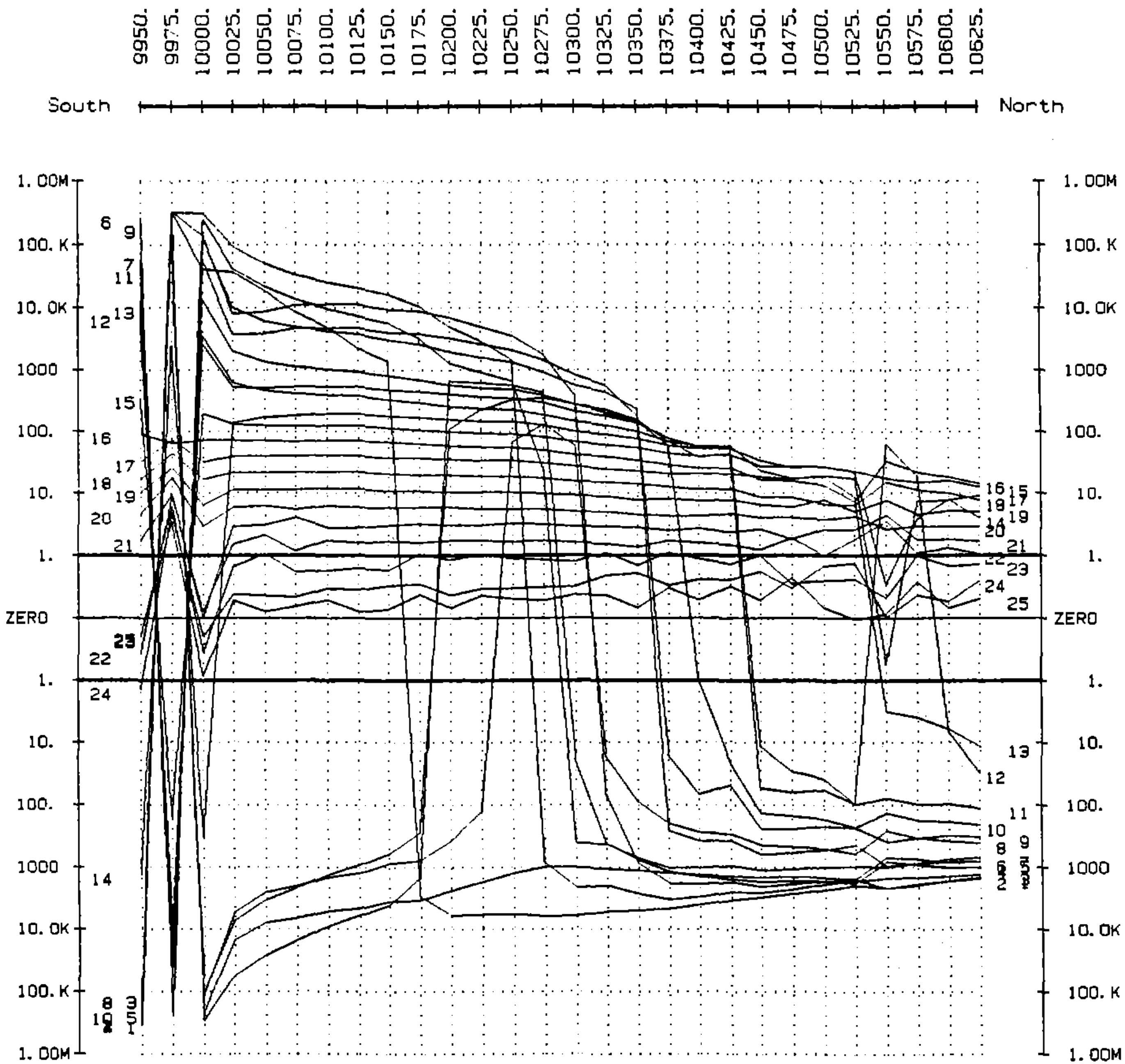

Window MAGNITUDE
values in microV/ampere
Component: CH1 Z, Rxng=10000.0
Loop 1: 8900E-9700E
9600N-10000N
15AMPS, 16HZ
Tx Delay 150 uSec

Win	Mag	Win	Mag
1	54.20u	14	1.023m
2	84.60u	15	1.264m
3	115.0u	16	1.580m
4	145.4u	17	1.961m
5	175.8u	18	2.454m
6	206.2u	19	3.106m
7	251.2u	20	3.878m
8	312.2u	21	4.870m
9	373.0u	22	6.114m
10	433.9u	23	7.678m
11	536.8u	24	9.663m
12	675.7u	25	12.16m
13	825.7u		

LINE 9700 E

Z Component

364046

Field Job 062
Plot by CPLOT 5.71
Plotted 03 Mar 91

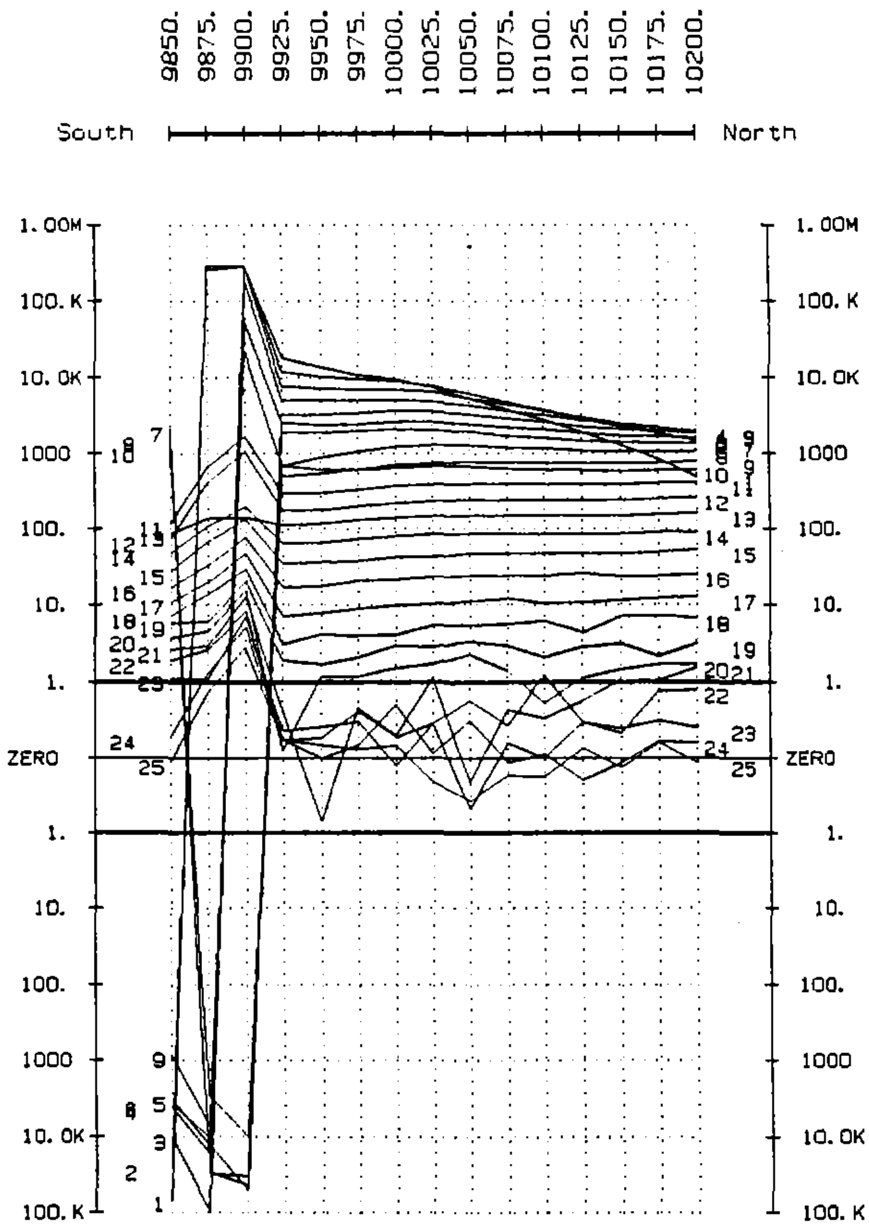

Window MAGNITUDE
values in microV/ampere
Component: CH1 X, Rxna=10000.0
Loop 2: 8100E-8900E
9500N-9900N
15AMPS, 16HZ
Tx Delay 150 uSec

Win	Mag	Win	Mag
1	54.20u	14	1.023m
2	84.60u	15	1.264m
3	115.0u	16	1.580m
4	145.4u	17	1.961m
5	175.8u	18	2.454m
6	206.2u	19	3.106m
7	251.2u	20	3.878m
8	312.2u	21	4.870m
9	373.0u	22	6.114m
10	433.9u	23	7.678m
11	536.8u	24	9.663m
12	675.7u	25	12.16m
13	825.7u		

LINE 8100E

X Component

Field Job 062
Plot by CPLOT 5.71
Plotted 03 Mar 91

SURVEY L
Line Or
A - Spc

Date of

0142

264047

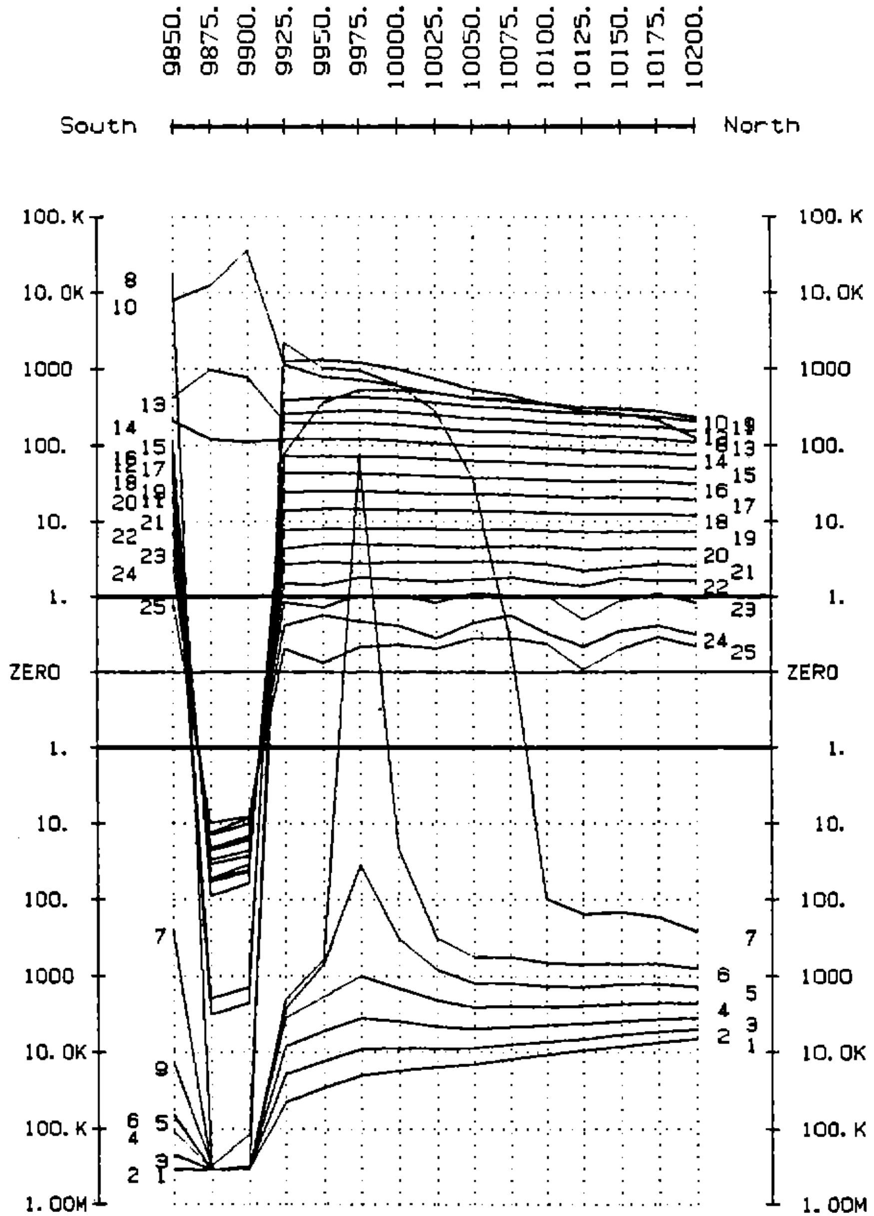

Window MAGNITUDE
values in microV/ampere
Component: CH1 Z, Rxna=10000.0
Loop 2: 8100E-8900E
9500N-9900N
15AMPS, 16HZ
Tx Delay 150 uSec

Win	Mag	Win	Mag
1	54.20u	14	1.023m
2	84.60u	15	1.264m
3	115.0u	16	1.580m
4	145.4u	17	1.961m
5	175.8u	18	2.454m
6	206.2u	19	3.106m
7	251.2u	20	3.878m
8	312.2u	21	4.870m
9	373.0u	22	6.114m
10	433.9u	23	7.678m
11	536.8u	24	9.663m
12	675.7u	25	12.16m
13	825.7u		

LINE 8100 E
Z Component

Field Job 062
Plot by CPLOT 5.71
Plotted 03 Mar 91

SURVEY L
Line Or
A - Sp

Date of

0143

364048

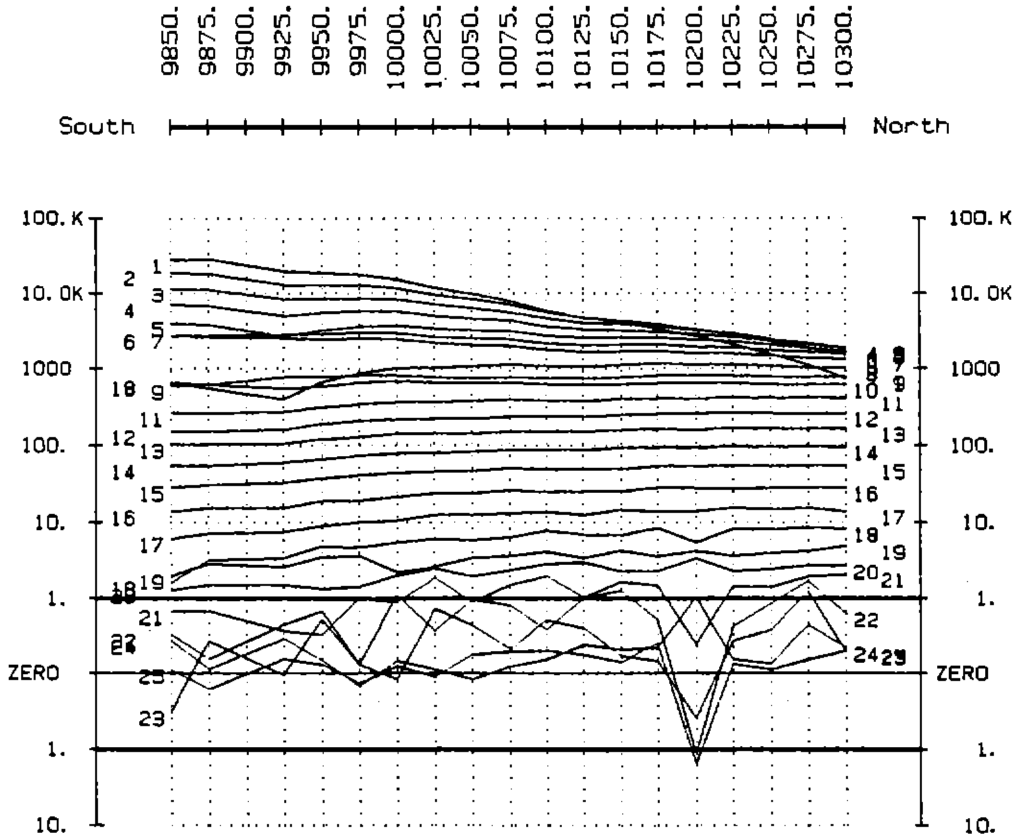

Window MAGNITUDE
values in microV/ampere
Component: CH1 X, Rxna=10000.0
Loop 2: 8100E-8900E
9500N-9900N
15AMPS, 16HZ
Tx Delay 150 uSec

Win	Mag	Win	Mag
1	54.20u	14	1.023m
2	84.60u	15	1.264m
3	115.0u	16	1.580m
4	145.4u	17	1.961m
5	175.8u	18	2.454m
6	206.2u	19	3.106m
7	251.2u	20	3.878m
8	312.2u	21	4.870m
9	373.0u	22	6.114m
10	433.9u	23	7.678m
11	536.8u	24	9.663m
12	675.7u	25	12.16m
13	825.7u		

LINE 8300 E
X Component

Field Job 062
Plot by CPLOT 5.71
Plotted 03 Mar 91

364049

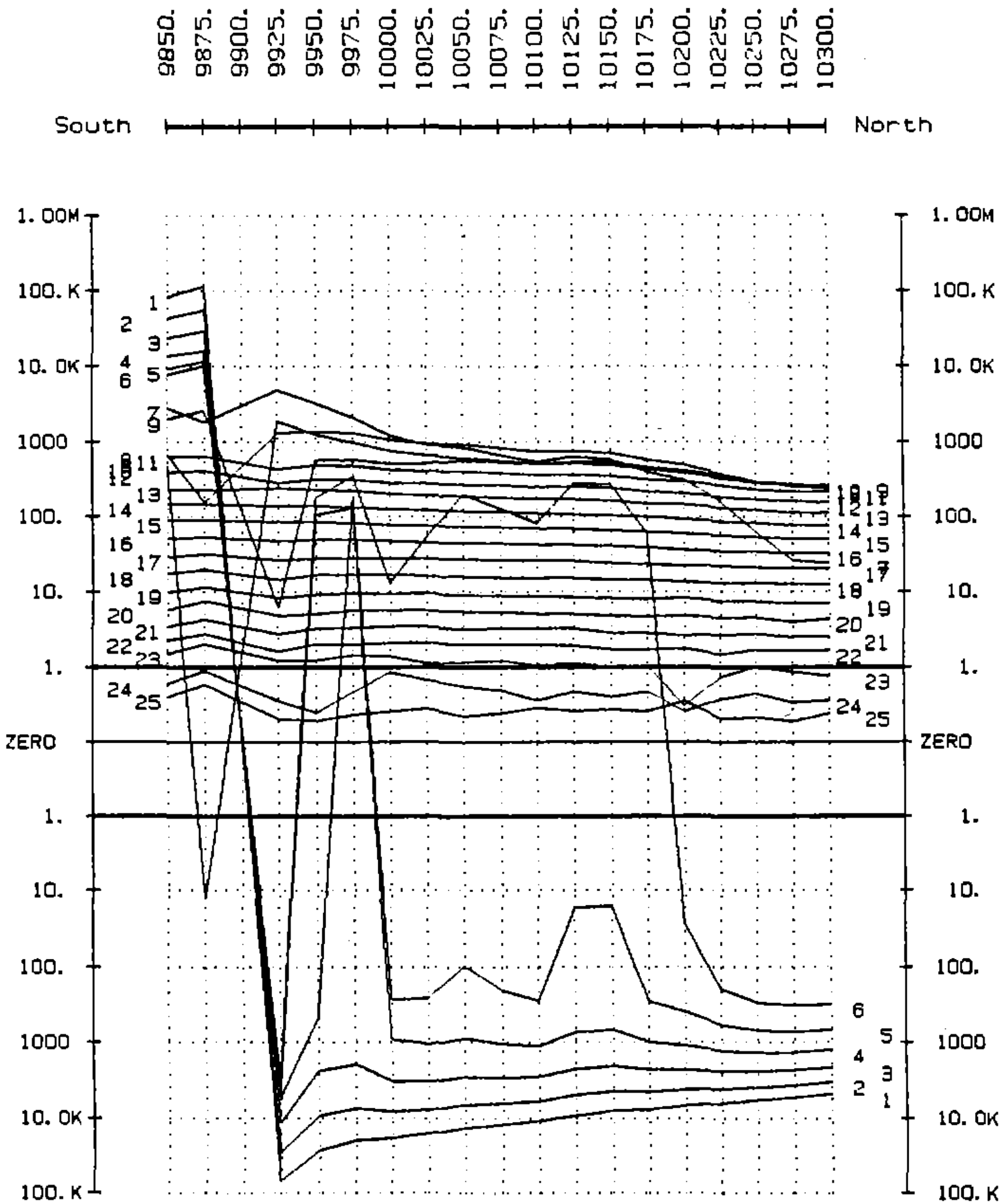

Window MAGNITUDE
values in microV/ampere
Component: CH1 Z, Rxna=10000.0
Loop 2: 8100E-8900E
9500N-9900N
15AMPS, 16HZ
Tx Delay 150 uSec

Win	Mag	Win	Mag
1	54.20u	14	1.023m
2	84.60u	15	1.264m
3	115.0u	16	1.580m
4	145.4u	17	1.961m
5	175.8u	18	2.454m
6	206.2u	19	3.106m
7	251.2u	20	3.878m
8	312.2u	21	4.870m
9	373.0u	22	6.114m
10	433.9u	23	7.678m
11	536.8u	24	9.663m
12	675.7u	25	12.16m
13	825.7u		

LINE 8300E
Z Component

Field Job 062
Plot by CPLOT 5.71
Plotted 03 Mar 91

0145

364050

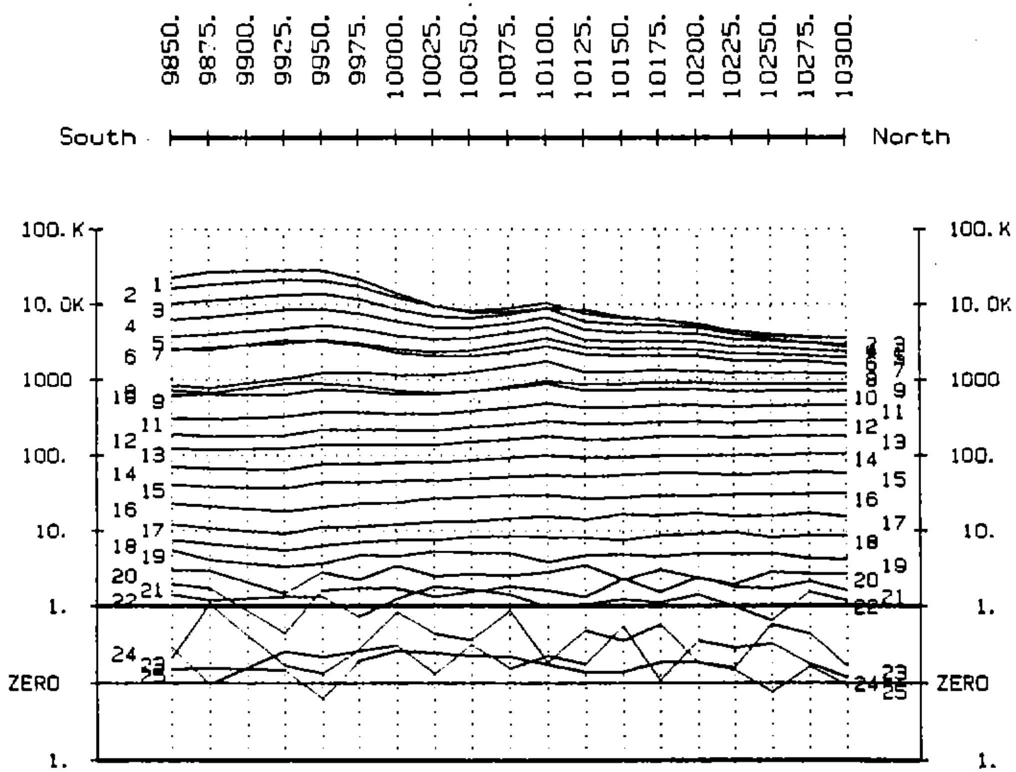

Window MAGNITUDE
values in microV/ampere
Component: CH1 X, Rxno=10000.0
Loop 2: 8100E-8900E
9500N-9900N
15AMPS, 16HZ
Tx Delay 150 uSec

Win	Mag	Win	Mag
1	54.20u	14	1.023m
2	84.60u	15	1.264m
3	115.0u	16	1.580m
4	145.4u	17	1.961m
5	175.8u	18	2.454m
6	206.2u	19	3.106m
7	251.2u	20	3.878m
8	312.2u	21	4.870m
9	373.0u	22	6.114m
10	433.9u	23	7.678m
11	536.8u	24	9.663m
12	675.7u	25	12.16m
13	825.7u		

LINE 8500 E

X Component

Field Job 062
Plot by CPLOT 5.71
Plotted 03 Mar 91

0146

364051

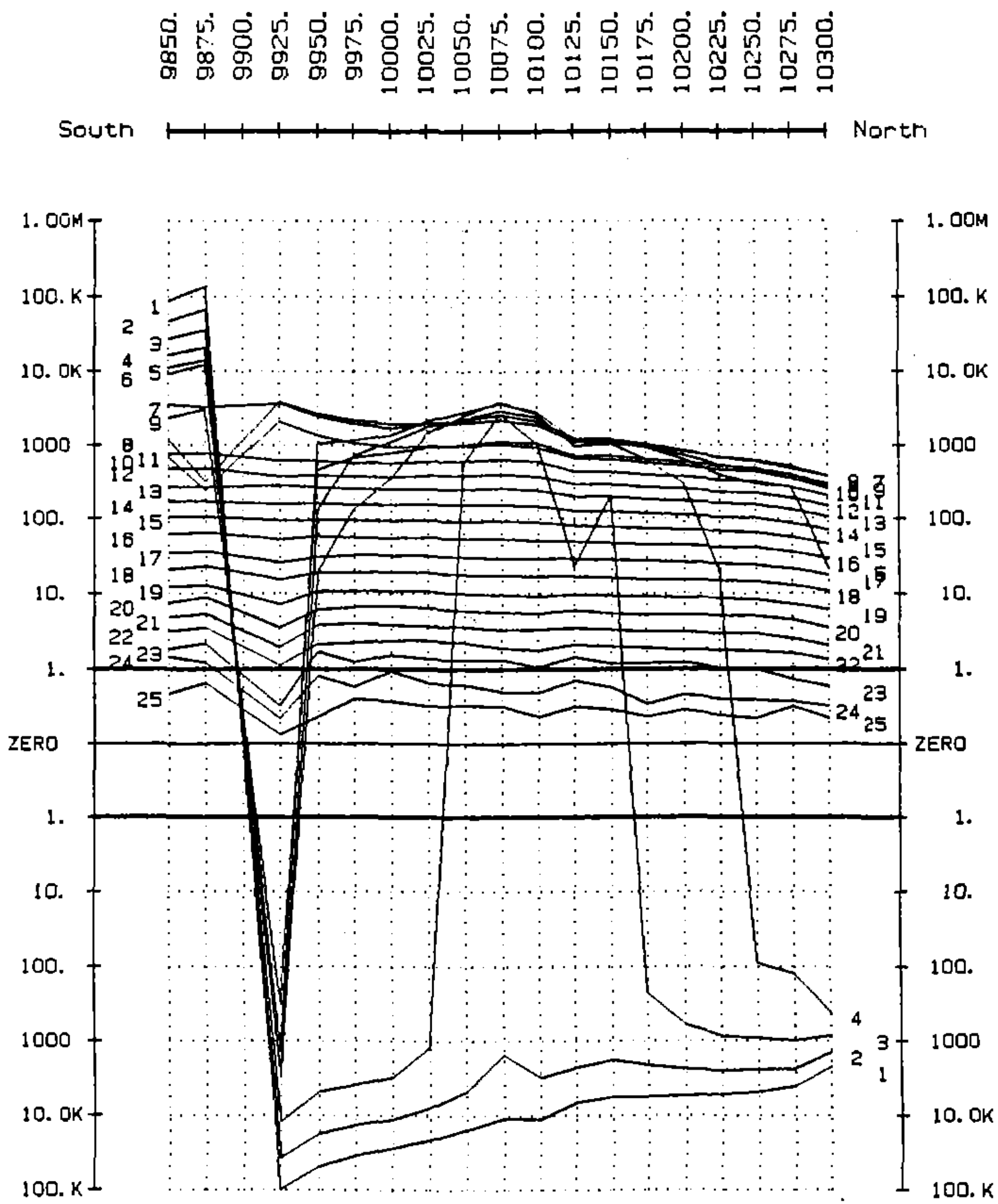

Window MAGNITUDE
values in microV/ampere
Component: CH1 Z. Rxna=10000.0
Loop 2: 8100E-8900E
9500N-9900N
15AMPS. 16HZ
Tx Delay 150 uSec

Win	Mag	Win	Mag
1	54.20u	14	1.023m
2	84.60u	15	1.264m
3	115.0u	16	1.580m
4	145.4u	17	1.961m
5	175.8u	18	2.454m
6	206.2u	19	3.106m
7	251.2u	20	3.878m
8	312.2u	21	4.870m
9	373.0u	22	6.114m
10	433.9u	23	7.678m
11	536.8u	24	9.663m
12	675.7u	25	12.16m
13	825.7u		

LINE 8500 E
Z Component

Field Job 062
Plot by CPLOT 5.71
Plotted 03 Mar 91

0147

364052

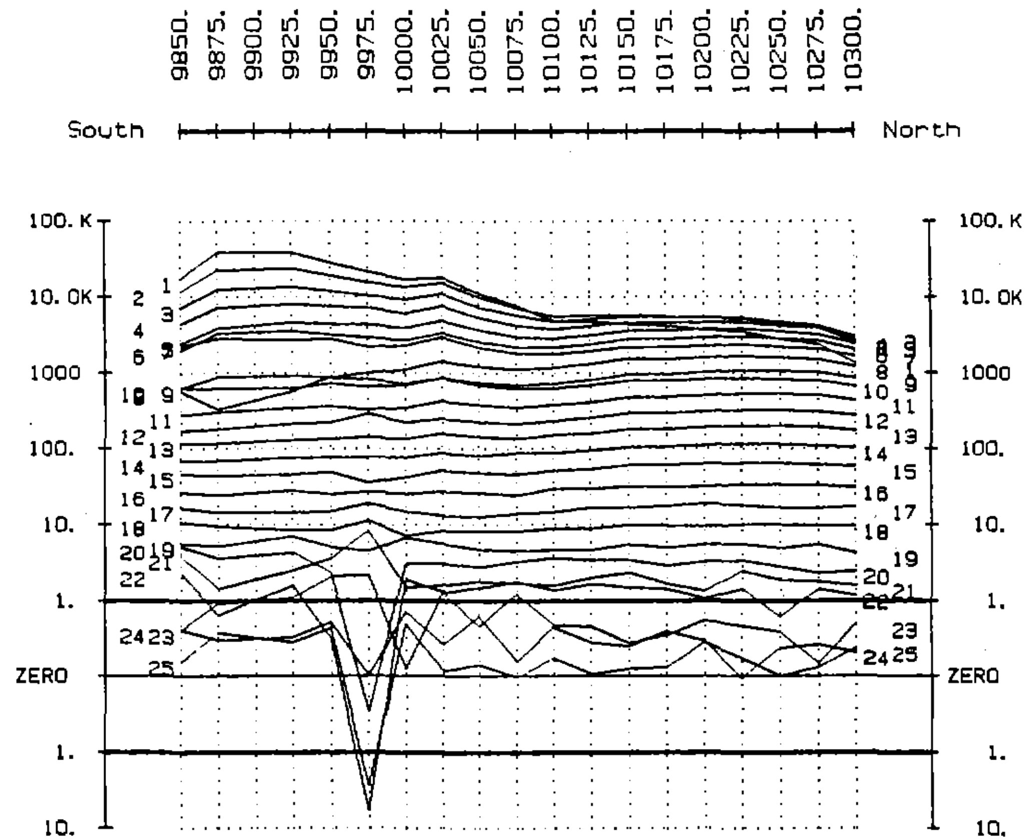

Window MAGNITUDE
values in microV/ampere
Component: CH1 X. Rxna=10000.0
Loop 2: 8100E-8900E
9500N-9900N
15AMPS. 18HZ
Tx Delay 150 uSec

Win	Mag	Win	Mag
1	54.20u	14	1.023m
2	84.60u	15	1.264m
3	115.0u	16	1.580m
4	145.4u	17	1.961m
5	175.8u	18	2.454m
6	206.2u	19	3.106m
7	251.2u	20	3.878m
8	312.2u	21	4.870m
9	373.0u	22	6.114m
10	433.9u	23	7.678m
11	536.8u	24	9.663m
12	675.7u	25	12.16m
13	825.7u		

LINE 8700E
X Component

Field Job 062
Plot by CPLOT 5.71
Plotted 03 Mar 91

0148

364053

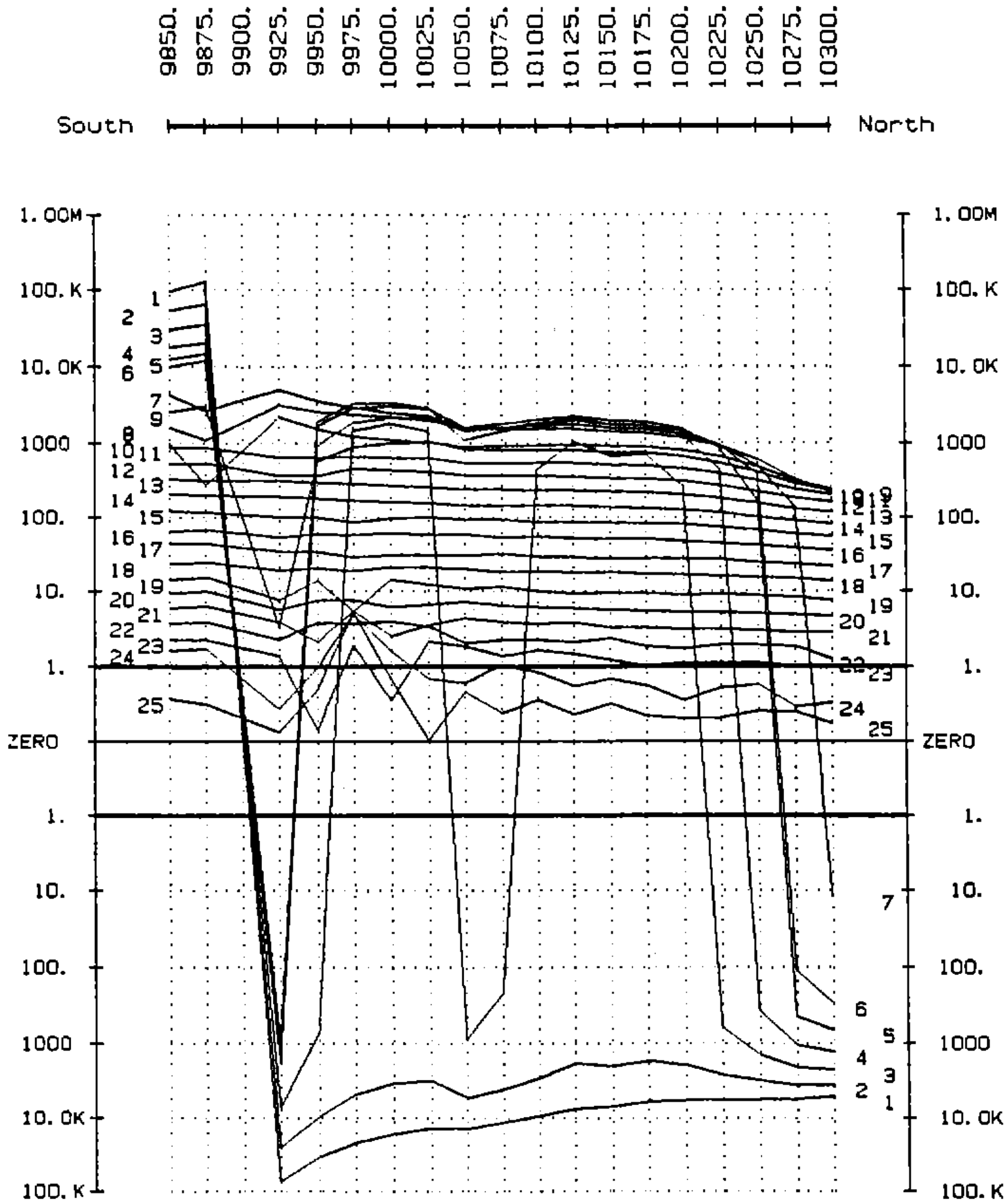

Window MAGNITUDE
values in microV/ampere
Component: CH1 Z. Rxng=10000.0
Loop 2: 8100E-8900E
9500N-9900N
15AMPS. 16HZ
Tx Delay 150 uSec

Win	Mag	Win	Mag
1	54.20u	14	1.023m
2	84.60u	15	1.264m
3	115.0u	16	1.580m
4	145.4u	17	1.961m
5	175.8u	18	2.454m
6	206.2u	19	3.106m
7	251.2u	20	3.878m
8	312.2u	21	4.870m
9	373.0u	22	6.114m
10	433.9u	23	7.678m
11	536.8u	24	9.663m
12	675.7u	25	12.16m
13	825.7u		

LINE 8700 E
Z Component

Field Job 062
Plot by CPLOT 5.71
Plotted 03 Mar 91

0149

364054

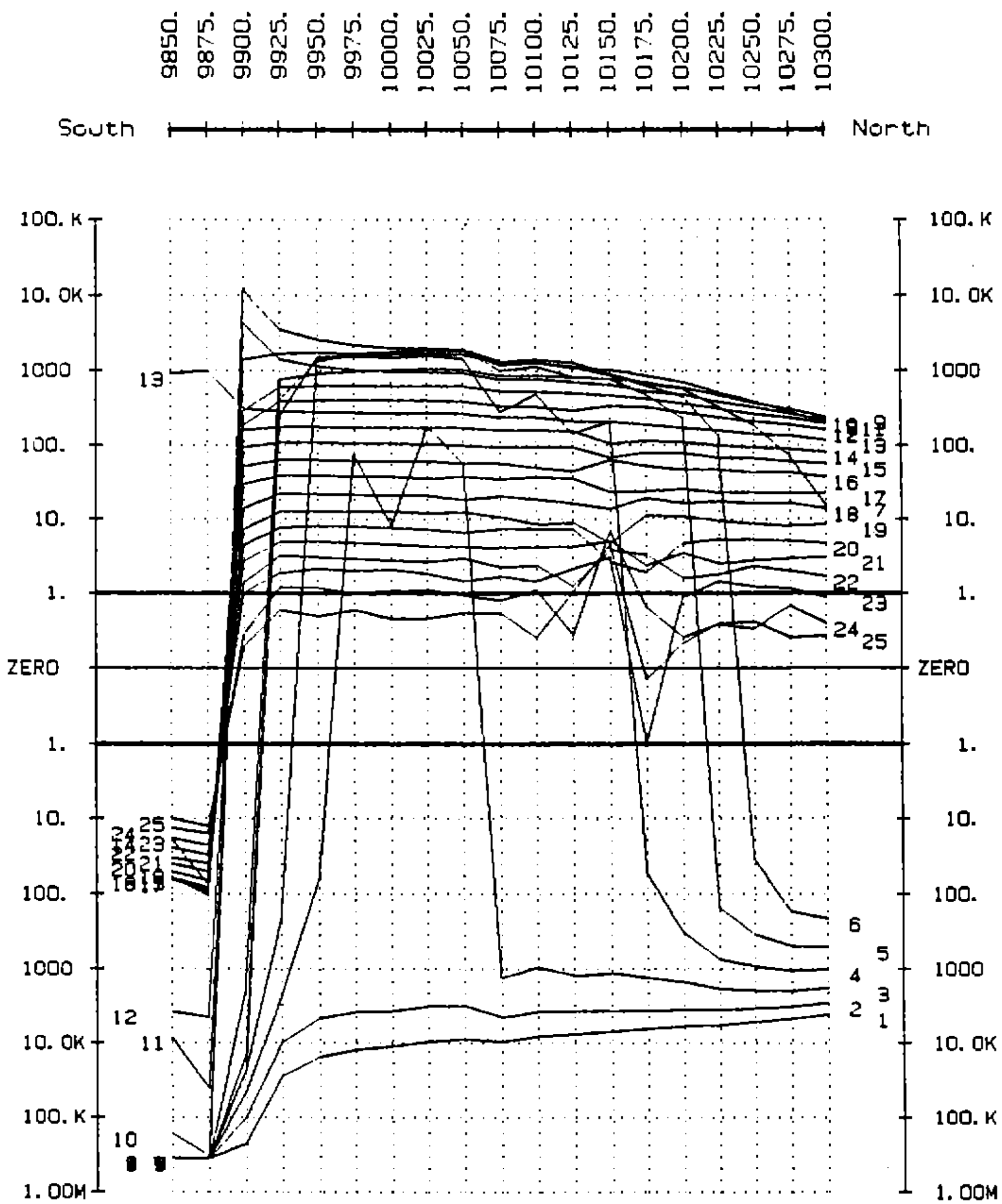

Window MAGNITUDE
values in microV/ampere
Component: CH1 X, Rxno=10000.0
Loop 2: 8100E-8900E
9500N-9900N
15AMPS, 16HZ
Tx Delay 150 uSec

Win	Mag	Win	Mag
1	54.20u	14	1.023m
2	84.60u	15	1.264m
3	115.0u	16	1.580m
4	145.4u	17	1.961m
5	175.8u	18	2.454m
6	206.2u	19	3.106m
7	251.2u	20	3.878m
8	312.2u	21	4.870m
9	373.0u	22	6.114m
10	433.9u	23	7.678m
11	536.8u	24	9.663m
12	675.7u	25	12.16m
13	825.7u		

LINE 8900 E
X Component

Field Job 062
Plot by CPLOT 5.71
Plotted 03 Mar 91

0150

364055

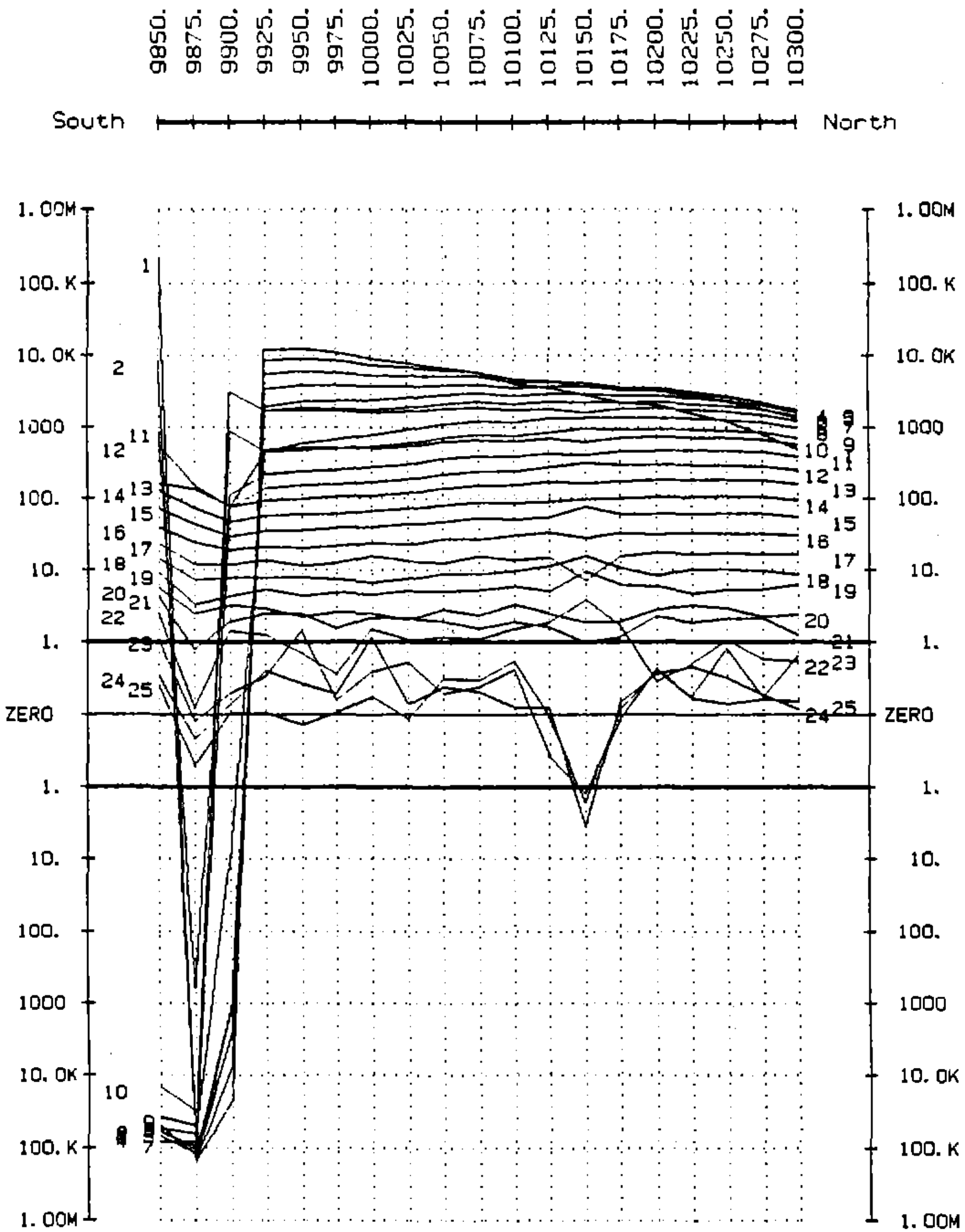

Window MAGNITUDE
values in microV/ampere
Component: CH1 Z, Rxna=10000.0
Loop 2: 8100E-8900E
9500N-9900N
15AMPS, 16HZ
Tx Delay 150 uSec

Win	Mag	Win	Mag
1	54.20u	14	1.023m
2	84.60u	15	1.264m
3	115.0u	16	1.580m
4	145.4u	17	1.961m
5	175.8u	18	2.454m
6	206.2u	19	3.106m
7	251.2u	20	3.878m
8	312.2u	21	4.870m
9	373.0u	22	6.114m
10	433.9u	23	7.678m
11	536.8u	24	9.663m
12	675.7u	25	12.16m
13	825.7u		

LINE 8900 E
Z Component

Field Job 062
Plot by CPLOT 5.71
Plotted 03 Mar 91

0151

364056

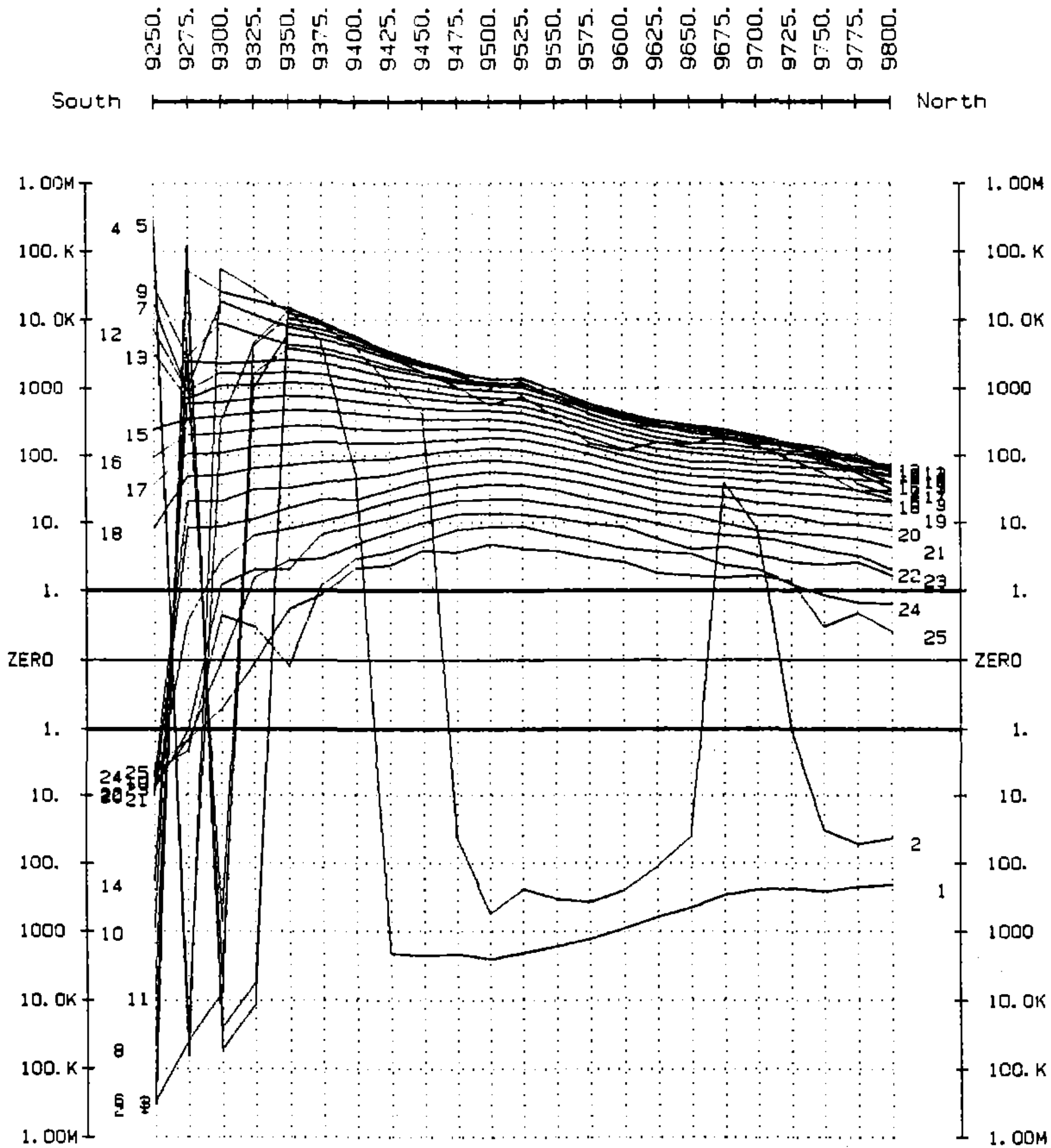

Window MAGNITUDE
values in microV/ampere
Component: CH1 X, Rxna=10000.0
Loop 3: 8900E-9700E
8900N-9300N
15AMPS, 16HZ
Tx Delay 150 uSec

Win	Mag	Win	Mag
1	54.20u	14	1.023m
2	84.60u	15	1.264m
3	115.0u	16	1.580m
4	145.4u	17	1.961m
5	175.8u	18	2.454m
6	206.2u	19	3.106m
7	251.2u	20	3.878m
8	312.2u	21	4.870m
9	373.0u	22	6.114m
10	433.9u	23	7.678m
11	536.8u	24	9.663m
12	675.7u	25	12.16m
13	825.7u		

LINE 8900 E
X Component

Field Job 062
Plot by CPLOT 5.71
Plotted 03 Mar 91

0152

364057

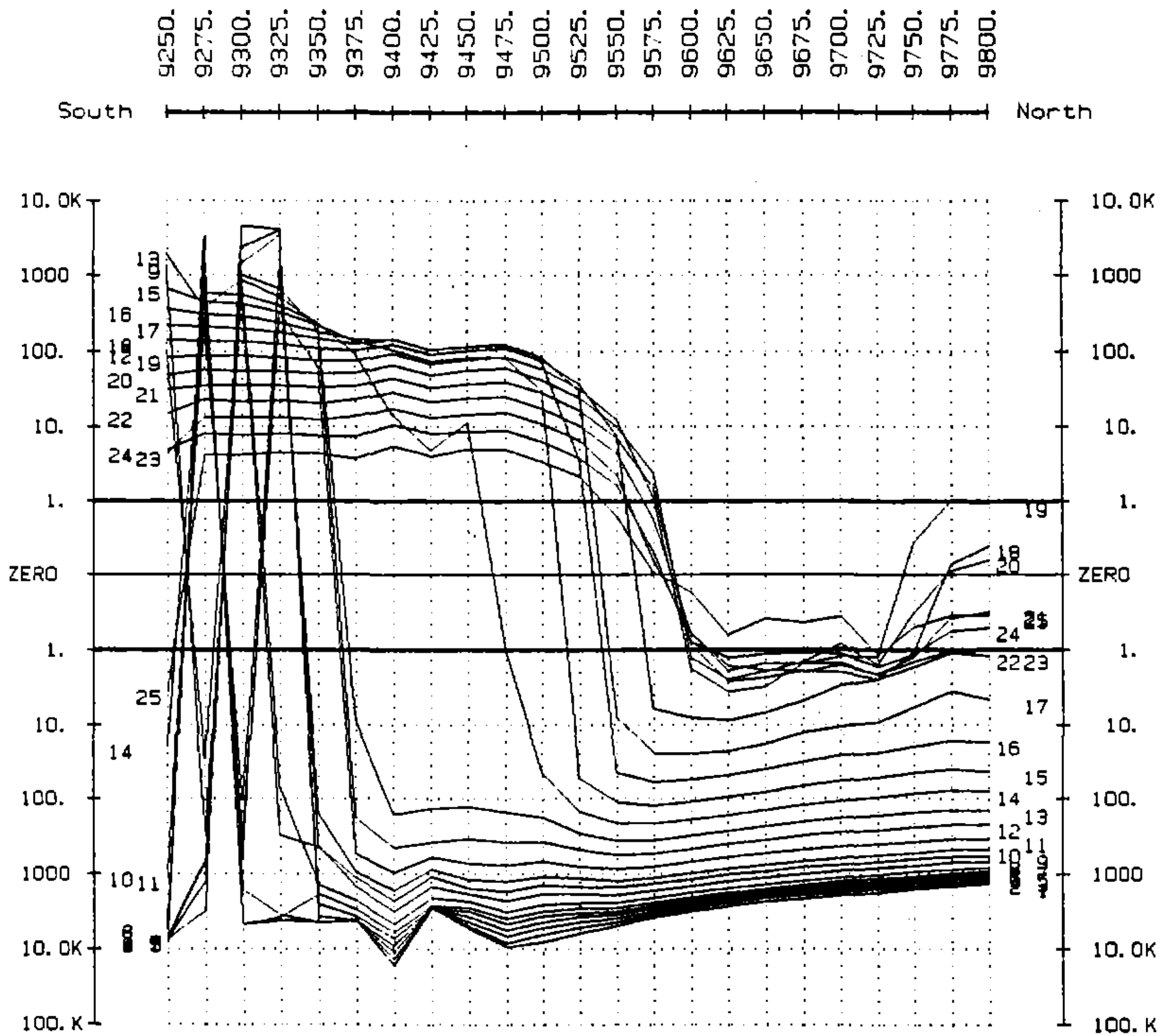

Window MAGNITUDE
values in microV/ampere
Component: CH1 Z. Rxna=10000.0
Loop 3: 8900E-9700E
8900N-9300N
15AMPS, 16HZ
Tx Delay 150 uSec

Win	Mag	Win	Mag
1	54.20u	14	1.023m
2	84.60u	15	1.264m
3	115.0u	16	1.580m
4	145.4u	17	1.961m
5	175.8u	18	2.454m
6	206.2u	19	3.106m
7	251.2u	20	3.878m
8	312.2u	21	4.870m
9	373.0u	22	6.114m
10	433.9u	23	7.678m
11	536.8u	24	9.663m
12	675.7u	25	12.16m
13	825.7u		

LINE 8900 E
Z Component

Field Job 062
Plot by CPLOT 5.71
Plotted 03 Mar 91

0153

364058

0154

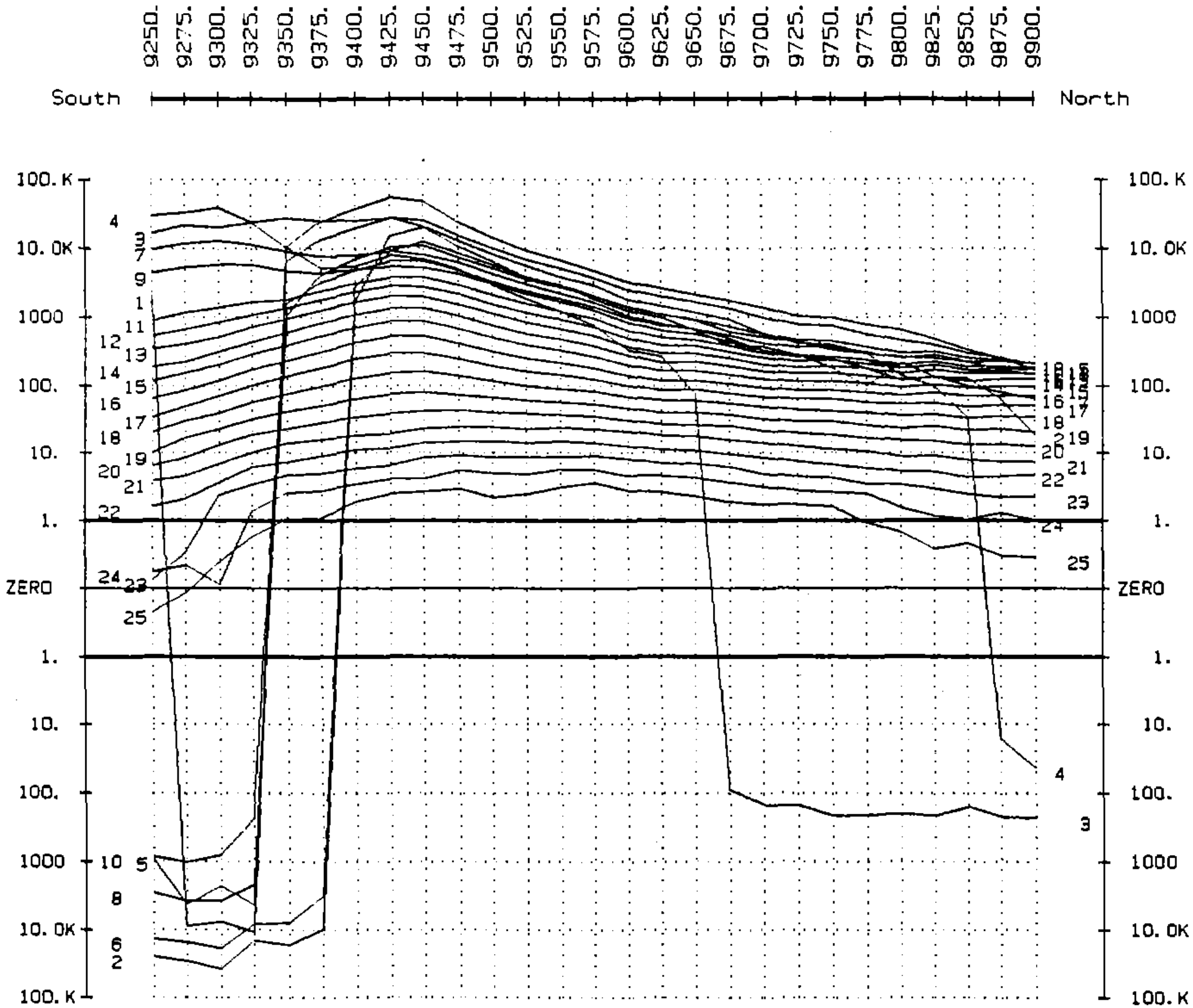

Window MAGNITUDE
values in microV/ampere
Component: CH1 X, Rxno=10000.0
Loop 3: 8900E-9700E
8900N-9300N
15AMPS, 16HZ
Tx Delay 150 uSec

Win	Mag	Win	Mag
1	54.20u	14	1.023m
2	84.60u	15	1.264m
3	115.0u	16	1.580m
4	145.4u	17	1.961m
5	175.8u	18	2.454m
6	206.2u	19	3.106m
7	251.2u	20	3.878m
8	312.2u	21	4.870m
9	373.0u	22	6.114m
10	433.9u	23	7.678m
11	536.8u	24	9.663m
12	675.7u	25	12.16m
13	825.7u		

LINE 9100 E
X Component

364059

Field Job 062
Plot by CPLOT 5.71
Plotted 03 Mar 91

0155

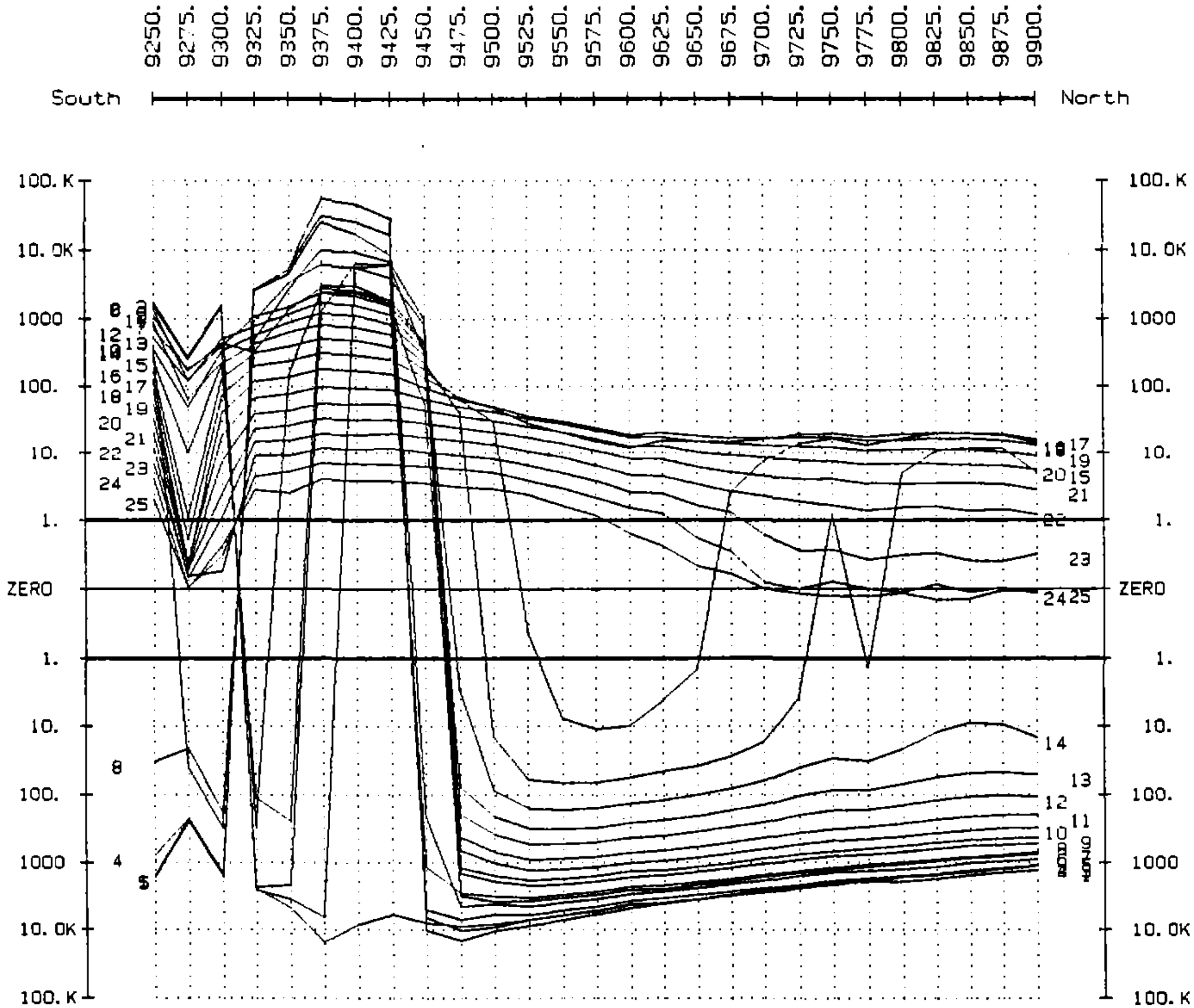

Window MAGNITUDE
values in microV/ampere
Component: CH1 Z, Rxna=10000.0
Loop 3: 8900E-9700E
8900N-9300N
15AMPS, 16HZ
Tx Delay 150 uSec

Win	Mag	Win	Mag
1	54.20u	14	1.023m
2	84.60u	15	1.264m
3	115.0u	16	1.580m
4	145.4u	17	1.961m
5	175.8u	18	2.454m
6	206.2u	19	3.106m
7	251.2u	20	3.878m
8	312.2u	21	4.870m
9	373.0u	22	6.114m
10	433.9u	23	7.678m
11	536.8u	24	9.663m
12	675.7u	25	12.16m
13	825.7u		

LINE 9100 E
Z Component

364060

Field Job 062
Plot by CPLOT 5.71
Plotted 03 Mar 91

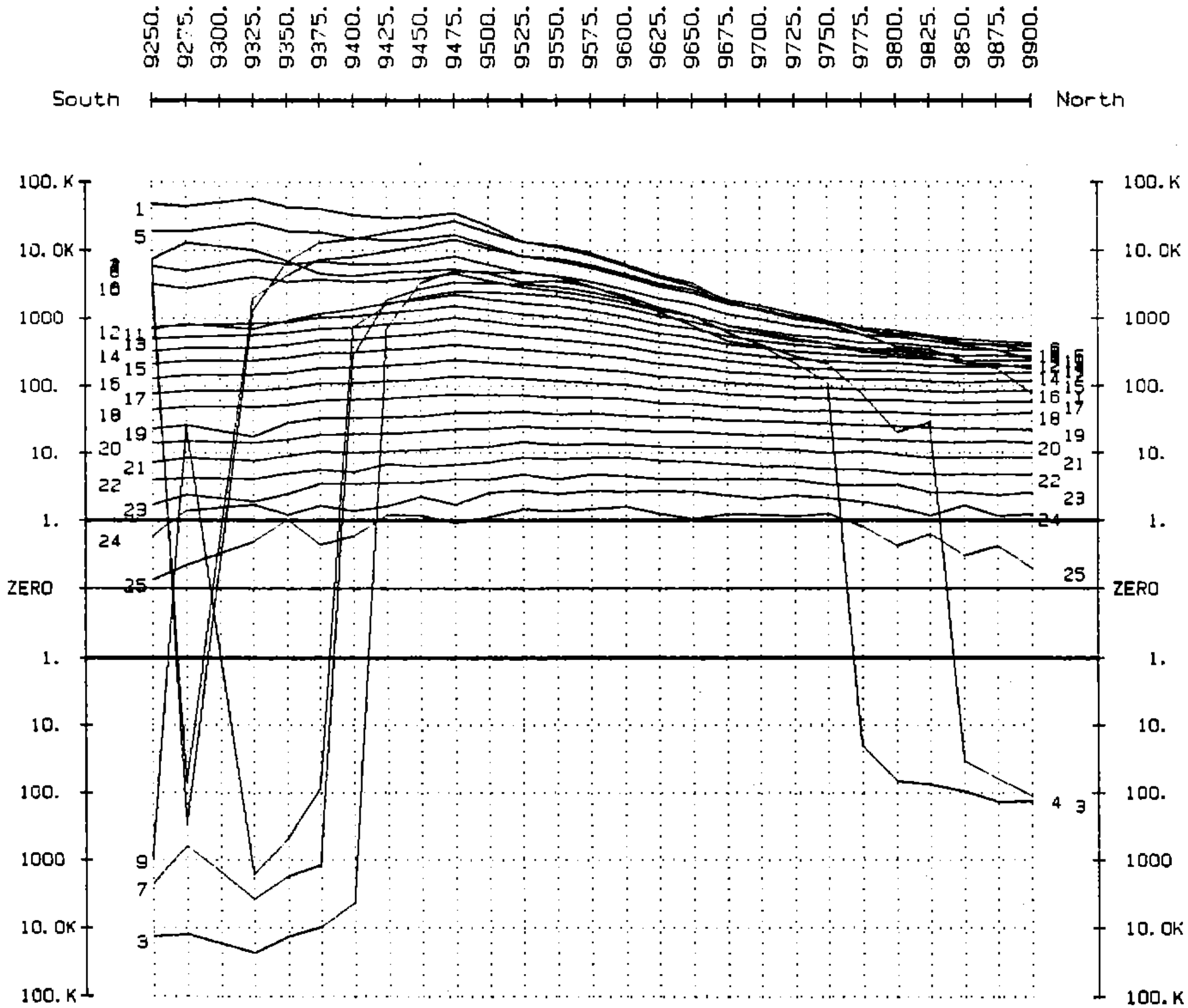

0156

Window MAGNITUDE
values in microV/ampere
Component: CH1 X, Rxna=10000.0
Loop 3, 8900E-9700E
8900N-9300N
15AMPS, 16HZ
Tx Delay 150 uSec

Win	Mag	Win	Mag
1	54.20u	14	1.023m
2	84.60u	15	1.264m
3	115.0u	16	1.580m
4	145.4u	17	1.961m
5	175.8u	18	2.454m
6	206.2u	19	3.106m
7	251.2u	20	3.878m
8	312.2u	21	4.870m
9	373.0u	22	6.114m
10	433.9u	23	7.678m
11	536.8u	24	9.663m
12	675.7u	25	12.16m
13	825.7u		

LINE 9300 E
X Component

364061

Field Job 062
Plot by CPLOT 5.71
Plotted 03 Mar 91

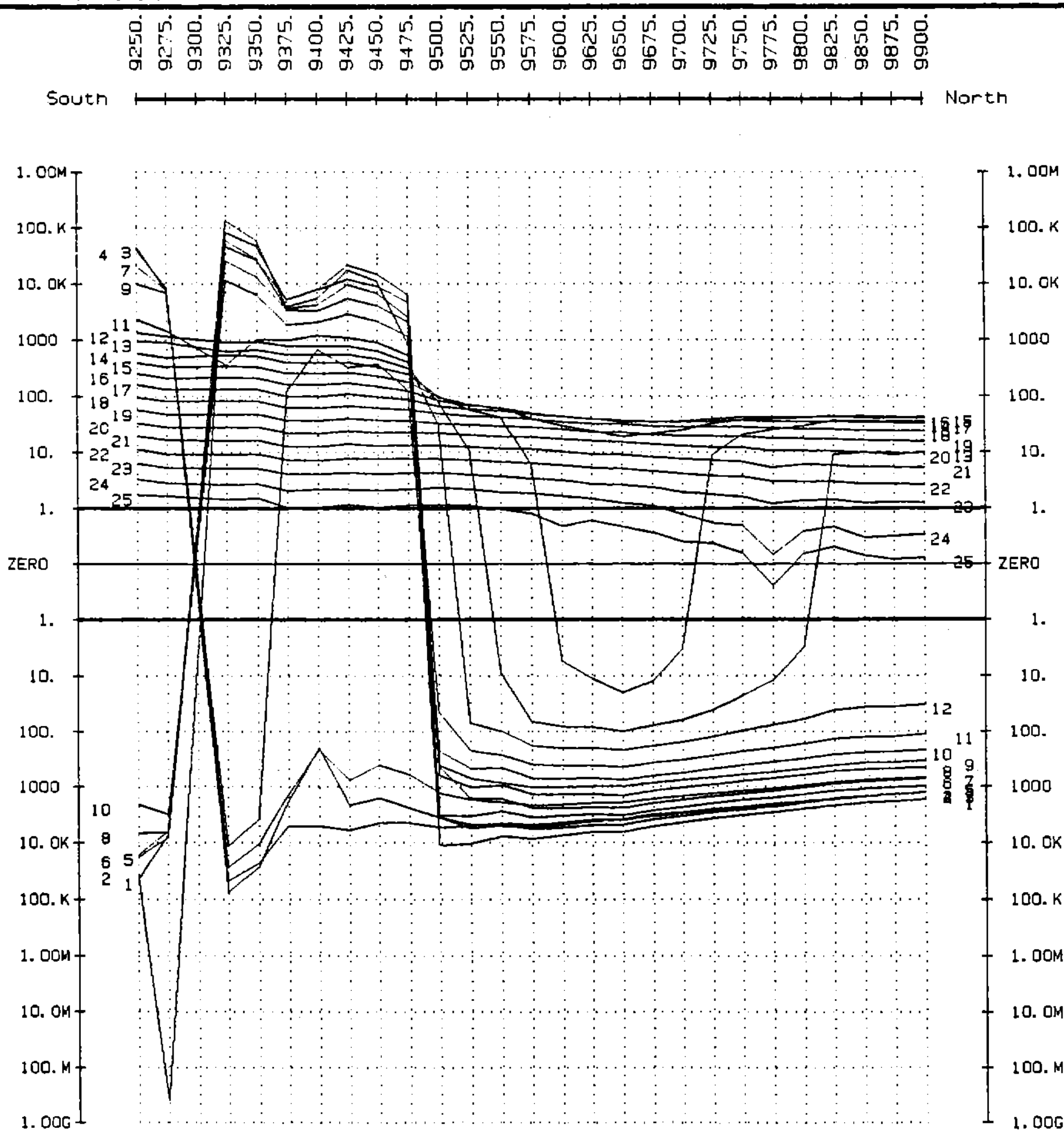

Window MAGNITUDE
values in microV/ampere
Component: CH1 Z, Rxna=10000.0
Loop 3: 8900E-9700E
8900N-9300N
15AMPS, 16HZ
Tx Delay 150 uSec

Win	Mag	Win	Mag
1	54.20u	14	1.023m
2	84.60u	15	1.264m
3	115.0u	16	1.580m
4	145.4u	17	1.961m
5	175.8u	18	2.454m
6	206.2u	19	3.106m
7	251.2u	20	3.878m
8	312.2u	21	4.870m
9	373.0u	22	6.114m
10	433.9u	23	7.678m
11	536.8u	24	9.663m
12	675.7u	25	12.16m
13	825.7u		

0157

LINE 9300 E
Z Component

364062

Field Job 062
Plot by CPLOT 5.71
Plotted 03 Mar 91

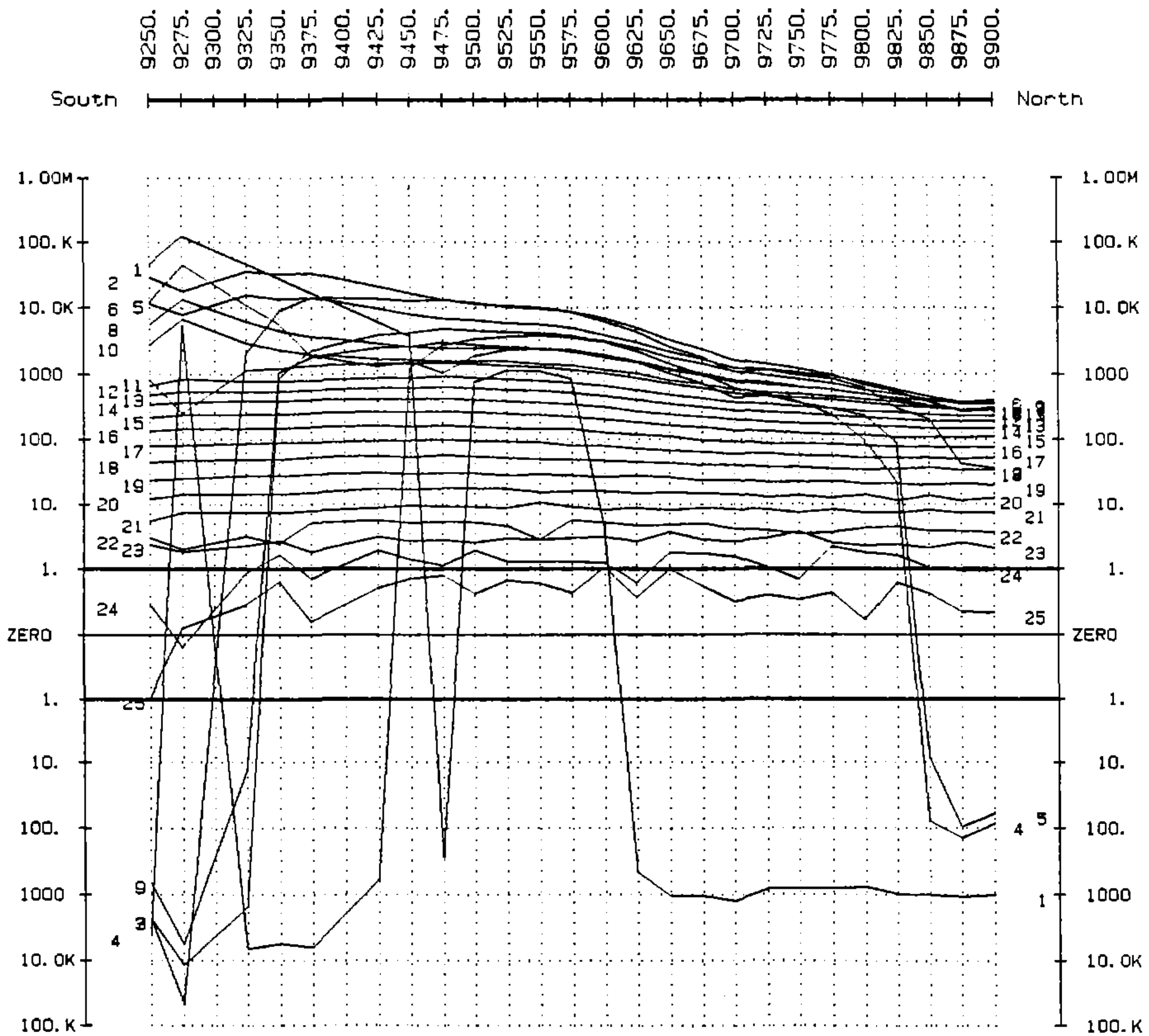

Window MAGNITUDE
values in microV/ampere
Component: CH1 X, Rxna=10000.0
Loop 3: 8900E-9700E
8900N-9300N
15AMPS, 16HZ
Tx Delay 150 uSec

Win	Mag	Win	Mag
1	54.20u	14	1.023m
2	84.60u	15	1.264m
3	115.0u	16	1.580m
4	145.4u	17	1.961m
5	175.8u	18	2.454m
6	206.2u	19	3.106m
7	251.2u	20	3.878m
8	312.2u	21	4.870m
9	373.0u	22	6.114m
10	433.9u	23	7.678m
11	536.8u	24	9.663m
12	675.7u	25	12.16m
13	825.7u		

LINE 9500 E
X Component

Field Job 062
Plot by CPLOT 5.71
Plotted 03 Mar 91

0158

364063

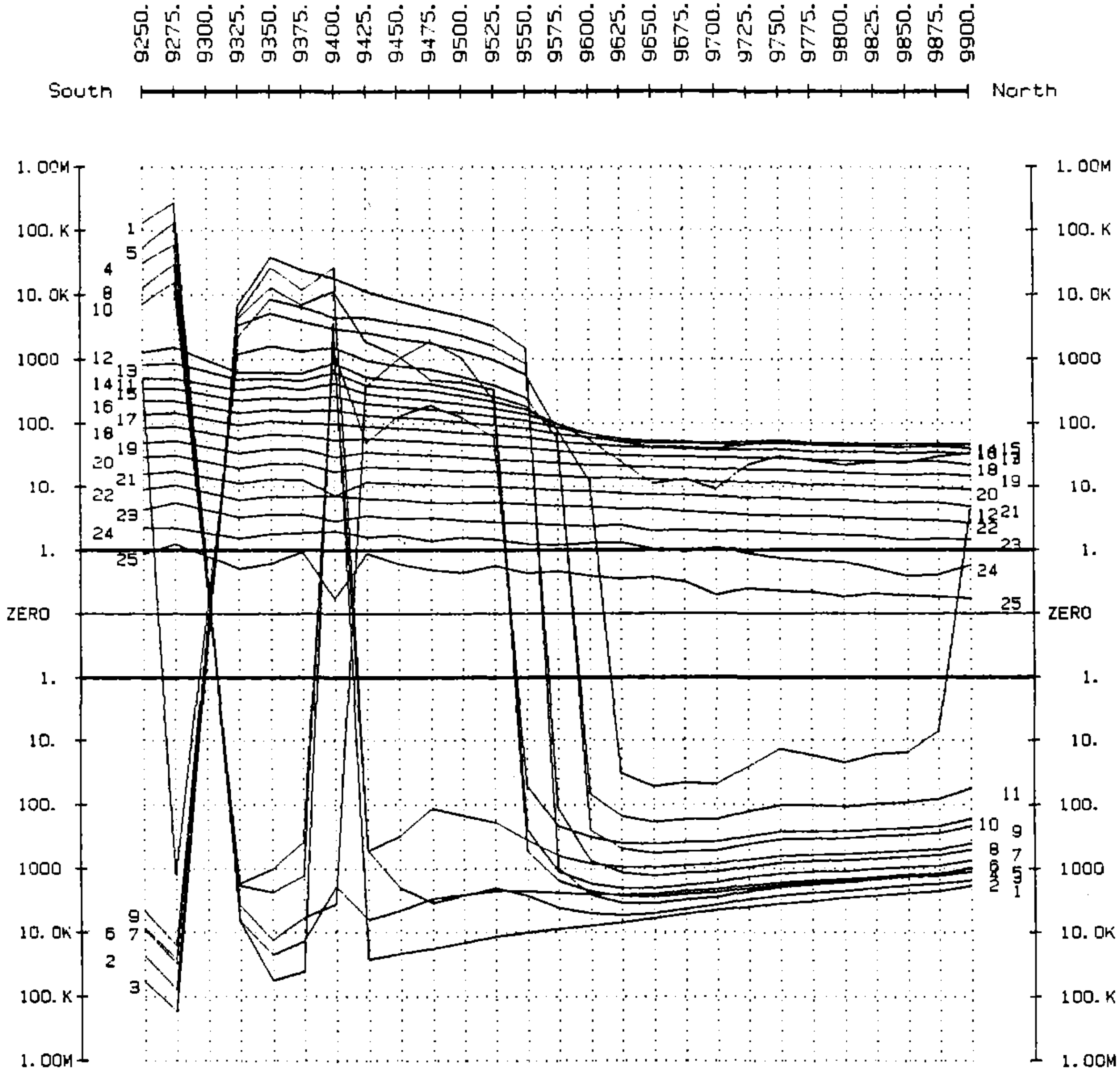

Window MAGNITUDE
values in microV/ampere
Component: CH1 Z. Rxnd=10000.0
Loop 3: 8900E-9700E
8900N-9300N
15AMPS, 16HZ
Tx Delay 150 uSec

Win	Mag	Win	Mag
1	54.20u	14	1.023m
2	84.60u	15	1.264m
3	115.0u	16	1.580m
4	145.4u	17	1.961m
5	175.8u	18	2.454m
6	206.2u	19	3.106m
7	251.2u	20	3.878m
8	312.2u	21	4.870m
9	373.0u	22	6.114m
10	433.9u	23	7.678m
11	536.8u	24	9.663m
12	675.7u	25	12.16m
13	825.7u		

LINE 9500E
Z Component

Field Job 062
Plot by CPLOT 5.71
Plotted 03 Mar 91

0159

364064

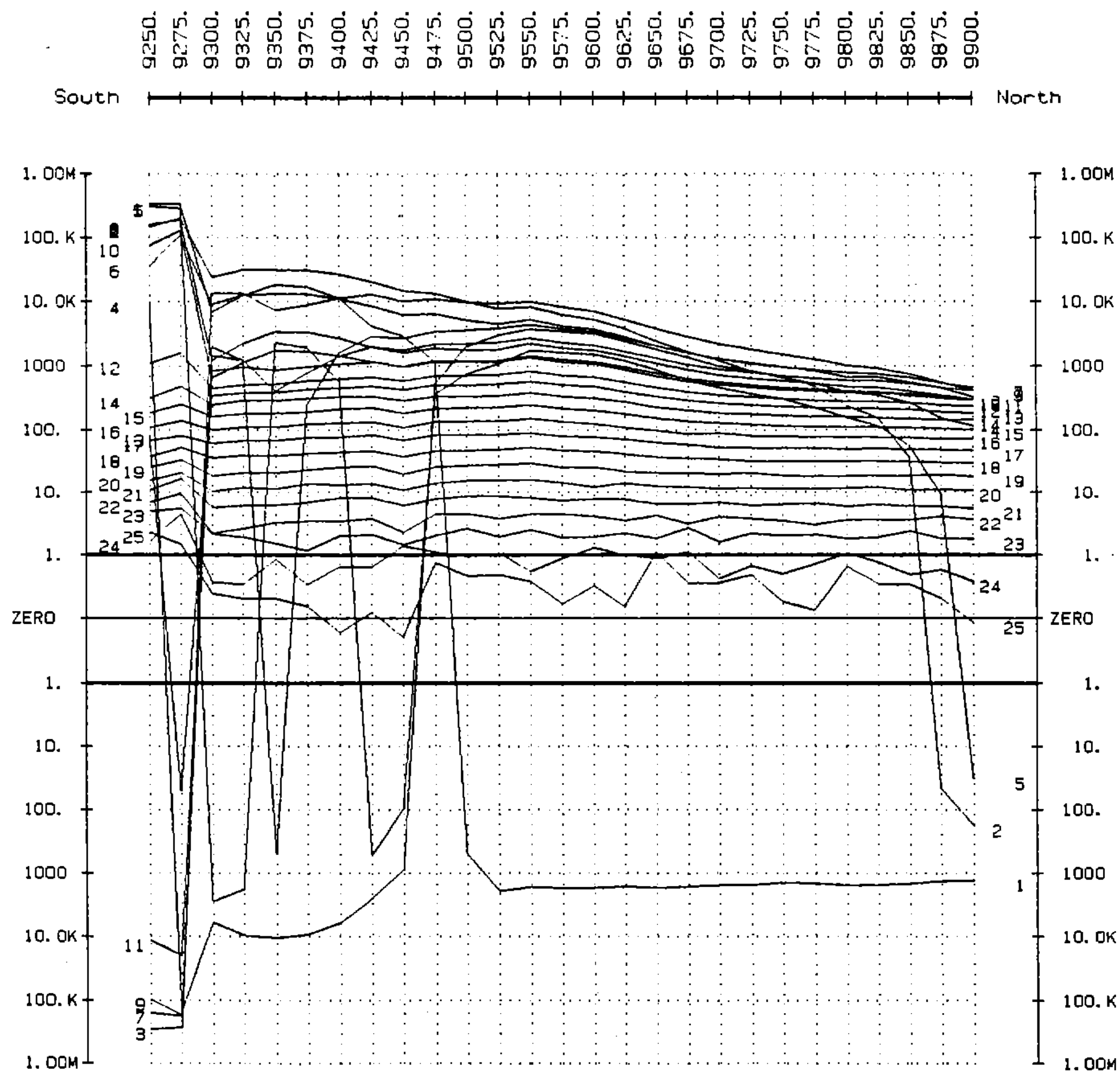

Window MAGNITUDE
values in microV/ampere
Component: CH1 X, Rxna=10000.0
Loop 3: 8900E-9700E
8900N-9300N
15AMPS, 16HZ
Tx Delay 150 uSec

Win	Mag	Win	Mag
1	54.20u	14	1.023m
2	84.60u	15	1.264m
3	115.0u	16	1.580m
4	145.4u	17	1.961m
5	175.8u	18	2.454m
6	206.2u	19	3.106m
7	251.2u	20	3.878m
8	312.2u	21	4.870m
9	373.0u	22	6.114m
10	433.9u	23	7.678m
11	536.8u	24	9.663m
12	675.7u	25	12.16m
13	825.7u		

LINE 9700 E
X Component

Field Job 062
Plot by CPLOT 5.71
Plotted 03 Mar 91

0160

364065

0161

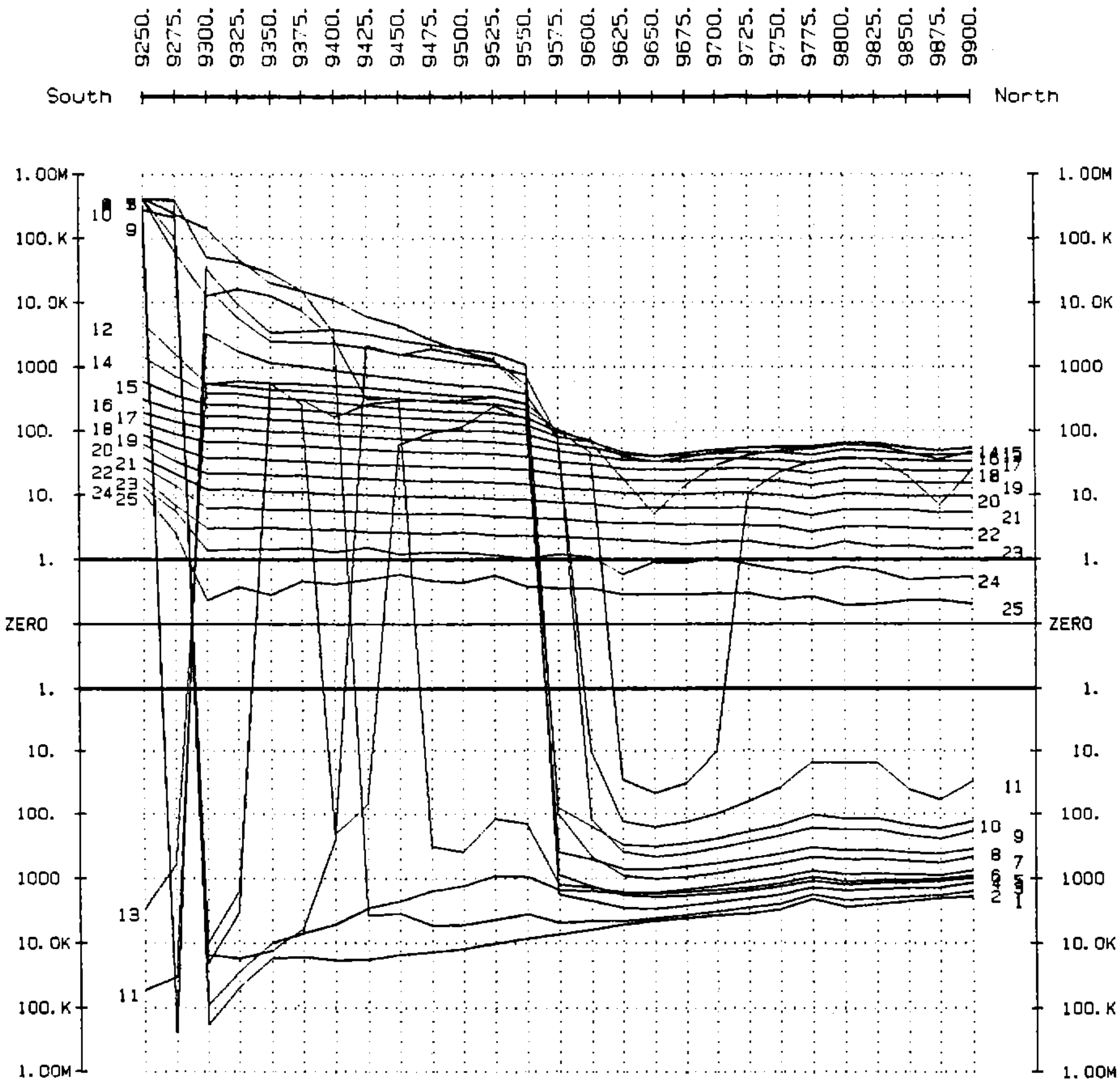

Window MAGNITUDE
values in microV/ampere
Component: CH1 Z, Rxna=10000.0
Loop 3: 8900E-9700E
8900N-9300N
15AMPS, 16HZ
Tx Delay 150 uSec

Win	Mag	Win	Mag
1	54.20u	14	1.023m
2	84.60u	15	1.264m
3	115.0u	16	1.580m
4	145.4u	17	1.961m
5	175.8u	18	2.454m
6	206.2u	19	3.106m
7	251.2u	20	3.878m
8	312.2u	21	4.870m
9	373.0u	22	6.114m
10	433.9u	23	7.678m
11	536.8u	24	9.663m
12	675.7u	25	12.16m
13	825.7u		

LINE 9700 E
Z Component

364066

Field Job 062
Plot by CPLOT 5.71
Plotted 03 Mar 91

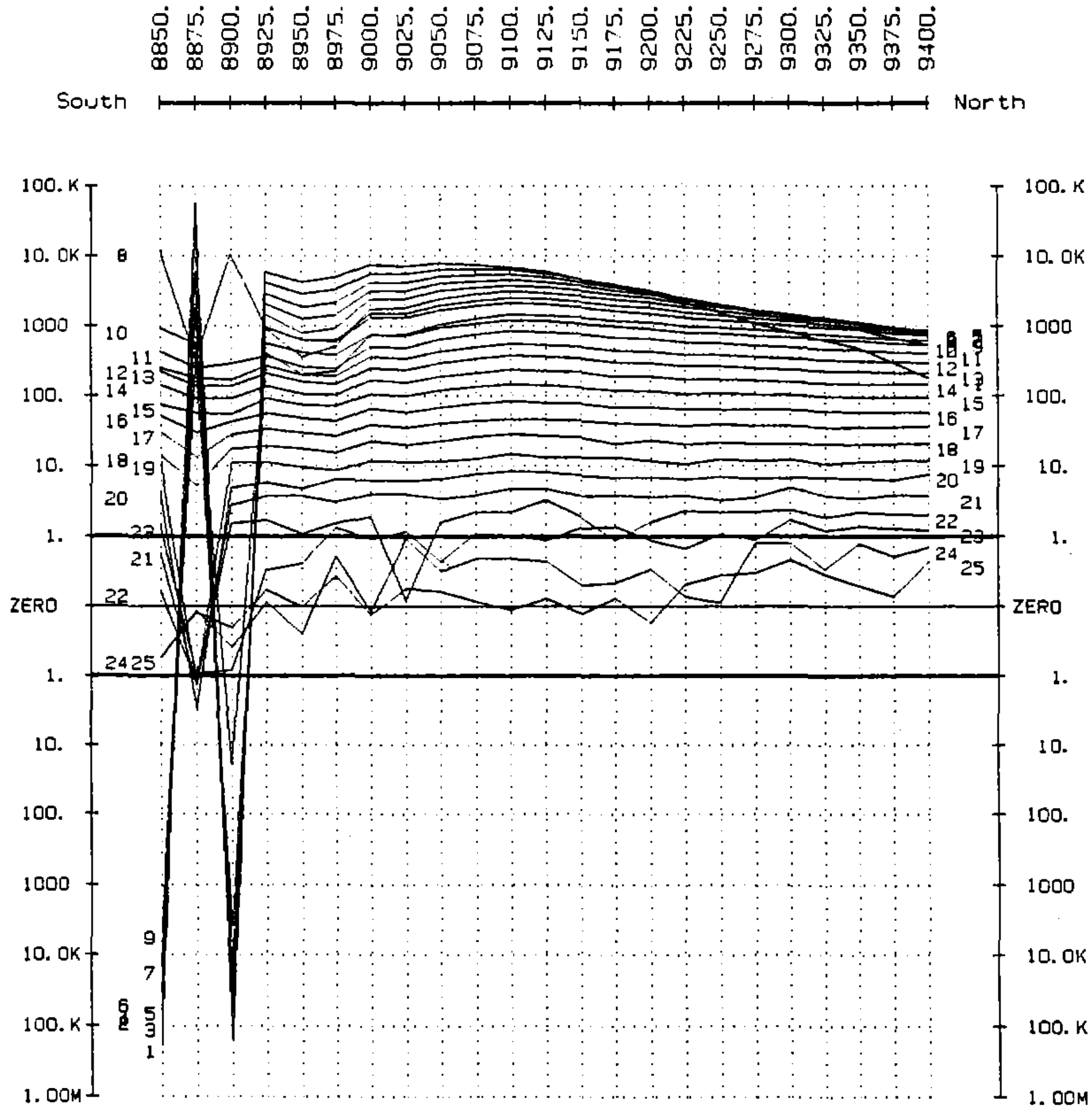

Window MAGNITUDE
values in microV/ampere
Component: CH1 X, Rxna=10000.0
Loop 4: 8100E-8900E
8500N-8900N
15AMPS, 16HZ
Tx Delay 150 uSec

Win	Mag	Win	Mag
1	54.20u	14	1.023m
2	84.60u	15	1.264m
3	115.0u	16	1.580m
4	145.4u	17	1.961m
5	175.8u	18	2.454m
6	206.2u	19	3.106m
7	251.2u	20	3.878m
8	312.2u	21	4.870m
9	373.0u	22	6.114m
10	433.9u	23	7.678m
11	536.8u	24	9.663m
12	675.7u	25	12.16m
13	825.7u		

LINE 8100 E
X Component

Field Job 062
Plot by CPLOT 5.71
Plotted 09 Feb 91

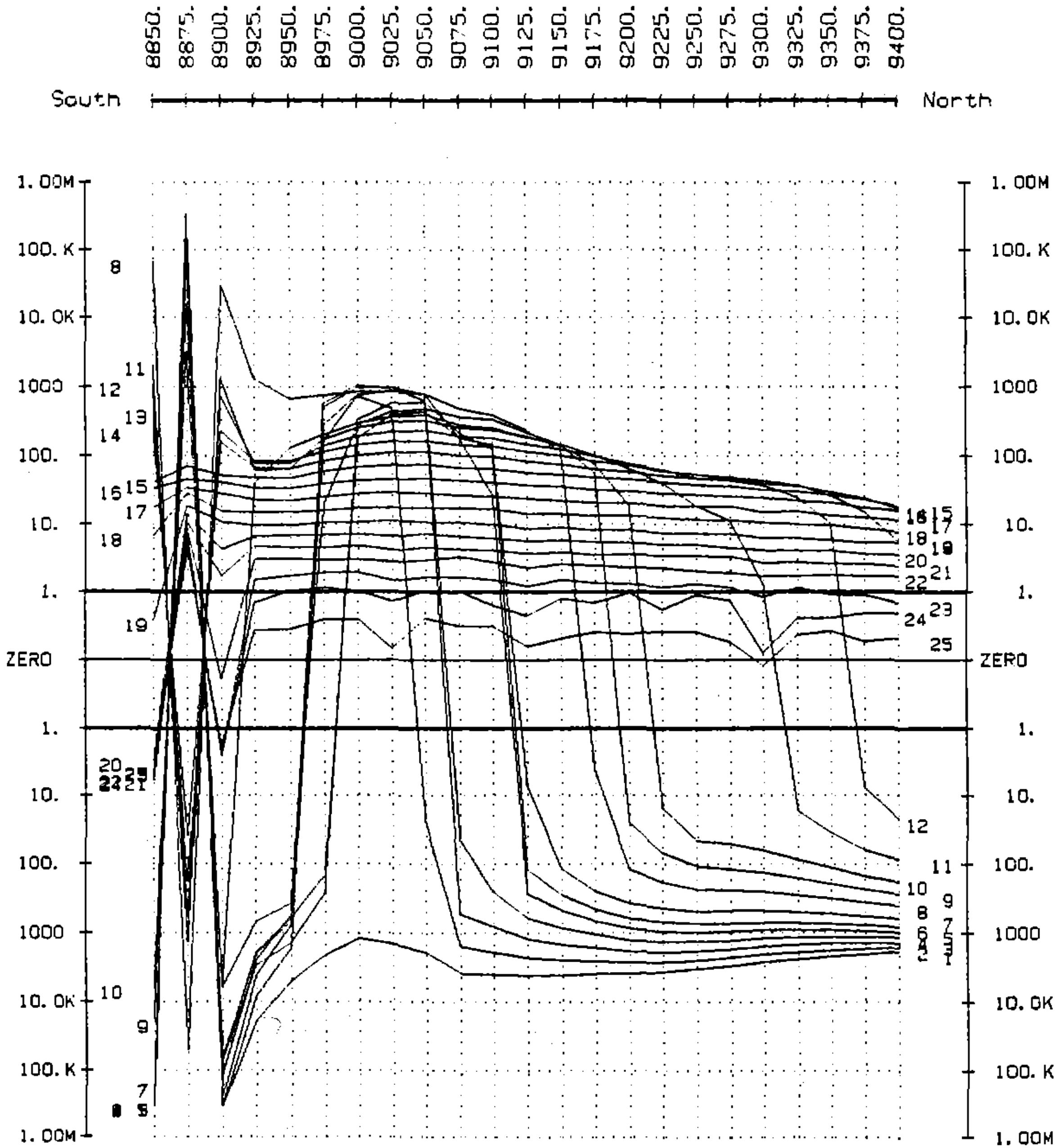

Window MAGNITUDE
values in microV/ampere
Component: CH1 Z. Rxna=10000.0
Loop 4: 8100E-8900E
8500N-8900N
15AMPS. 16HZ
Tx Delay 150 uSec

Win	Mag	Win	Mag
1	54.20u	14	1.023m
2	84.60u	15	1.264m
3	115.0u	16	1.580m
4	145.4u	17	1.961m
5	175.8u	18	2.454m
6	206.2u	19	3.106m
7	251.2u	20	3.878m
8	312.2u	21	4.870m
9	373.0u	22	6.114m
10	433.9u	23	7.678m
11	536.8u	24	9.663m
12	675.7u	25	12.16m
13	825.7u		

LINE 8100 E
Z Component

Field Job 062
Plot by CPLOT 5.71
Plotted 09 Feb 91

0163

364068

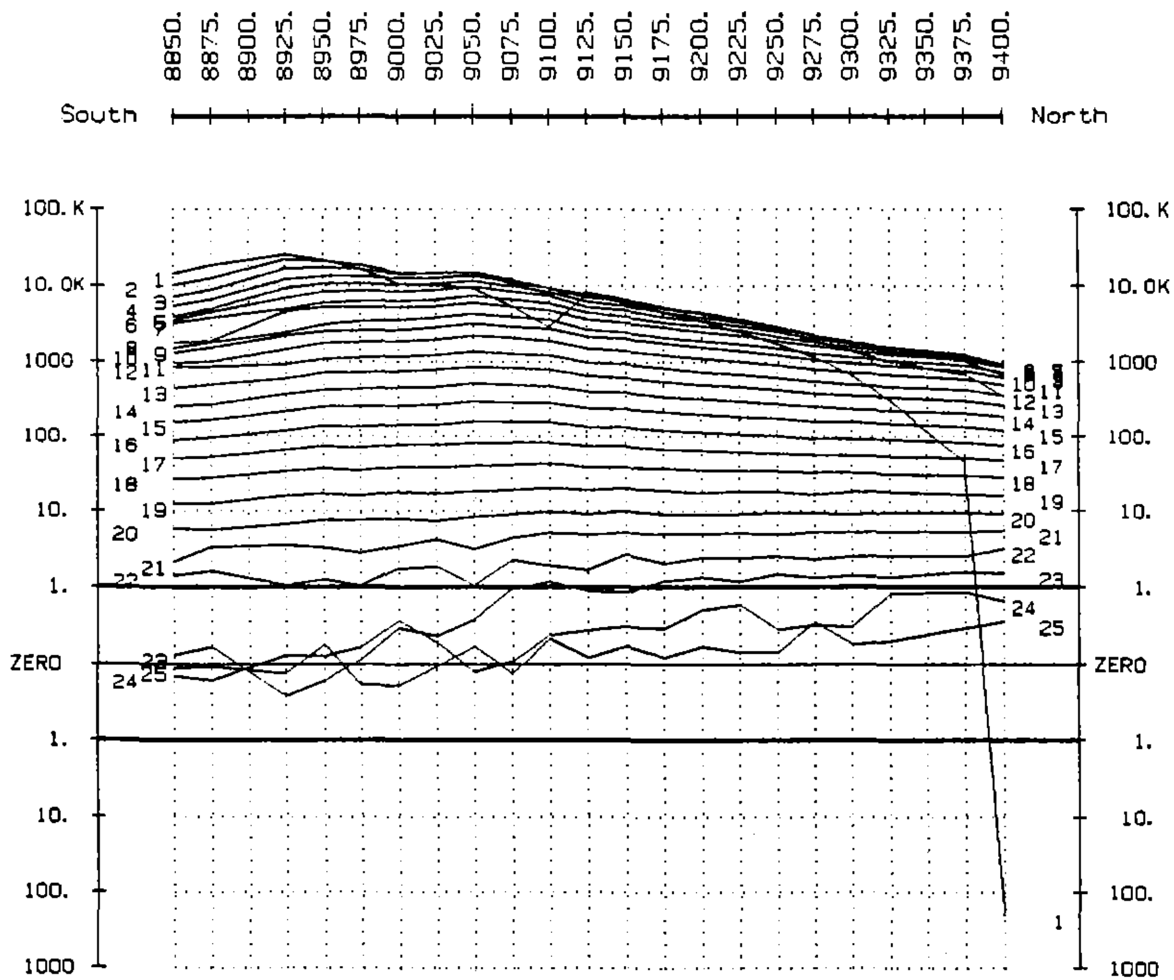

Window MAGNITUDE
values in microV/ampere
Component: CH1 X. Rxno=10000.0
Loop 4: 8100E-8900E
8500N-8900N
15AMPS. 16HZ
Tx Delay 150 uSec

Win	Mag	Win	Mag
1	54.20u	14	1.023m
2	84.60u	15	1.264m
3	115.0u	16	1.580m
4	145.4u	17	1.961m
5	175.8u	18	2.454m
6	206.2u	19	3.106m
7	251.2u	20	3.878m
8	312.2u	21	4.870m
9	373.0u	22	6.114m
10	433.9u	23	7.678m
11	536.8u	24	9.663m
12	675.7u	25	12.16m
13	825.7u		

LINE 8300E
X Component

Field Job 062
Plot by CPLOT 5.71
Plotted 03 Mar 91

0164

364069

0165

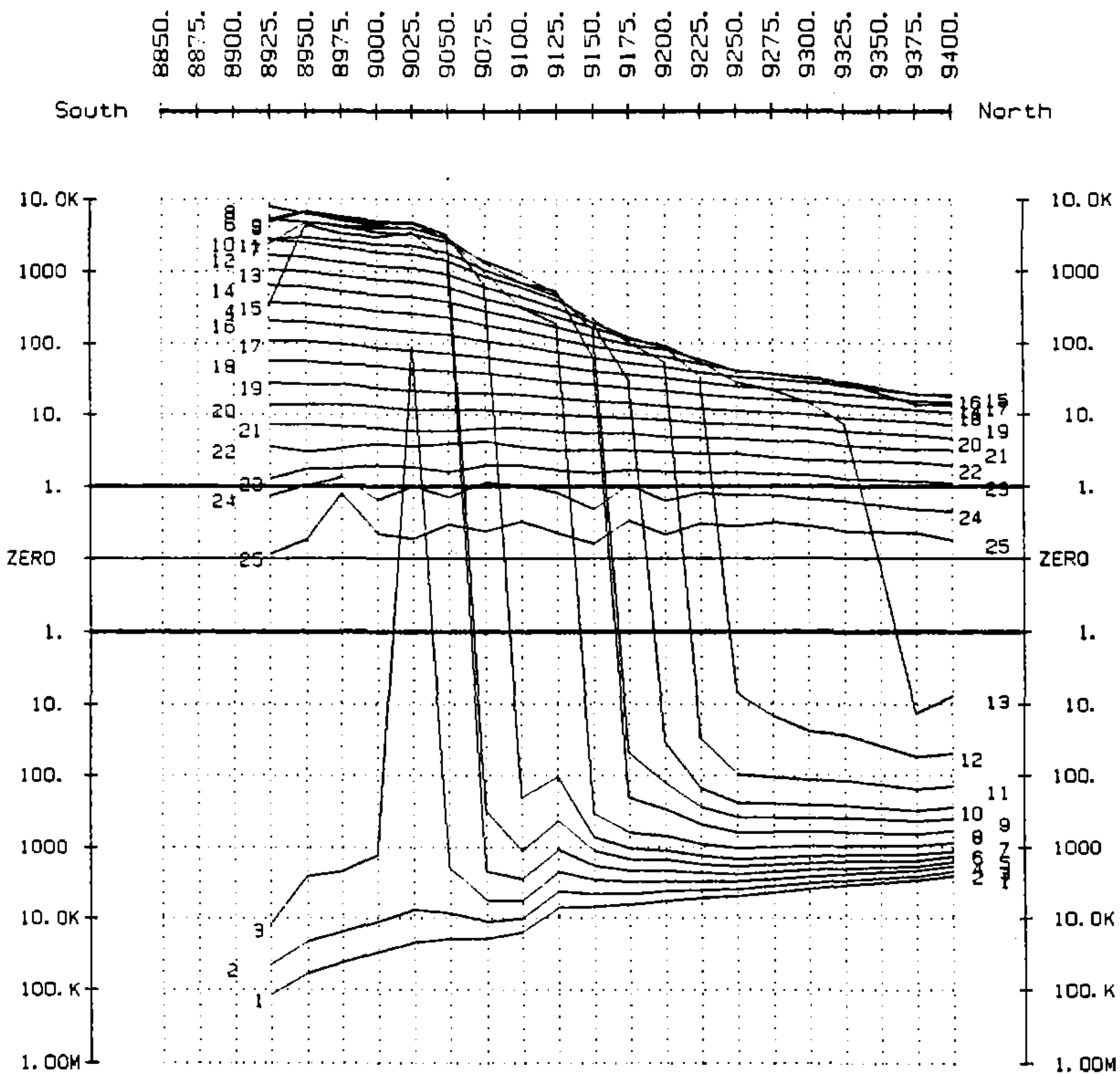

Window MAGNITUDE
values in microV/ampere
Component: CH1 Z, Rxna=10000.0
Loop 4: 8100E-8900E
8500N-8900N
15AMPS, 16HZ
Tx Delay 150 uSec

Win	Mag	Win	Mag
1	54.20u	14	1.023m
2	84.60u	15	1.264m
3	115.0u	16	1.580m
4	145.4u	17	1.961m
5	175.8u	18	2.454m
6	206.2u	19	3.106m
7	251.2u	20	3.878m
8	312.2u	21	4.870m
9	373.0u	22	6.114m
10	433.9u	23	7.678m
11	536.8u	24	9.663m
12	675.7u	25	12.16m
13	825.7u		

LINE 8300 E
Z Component

364070

Field Job 062
Plot by CPLOT 5.71
Plotted 03 Mar 91

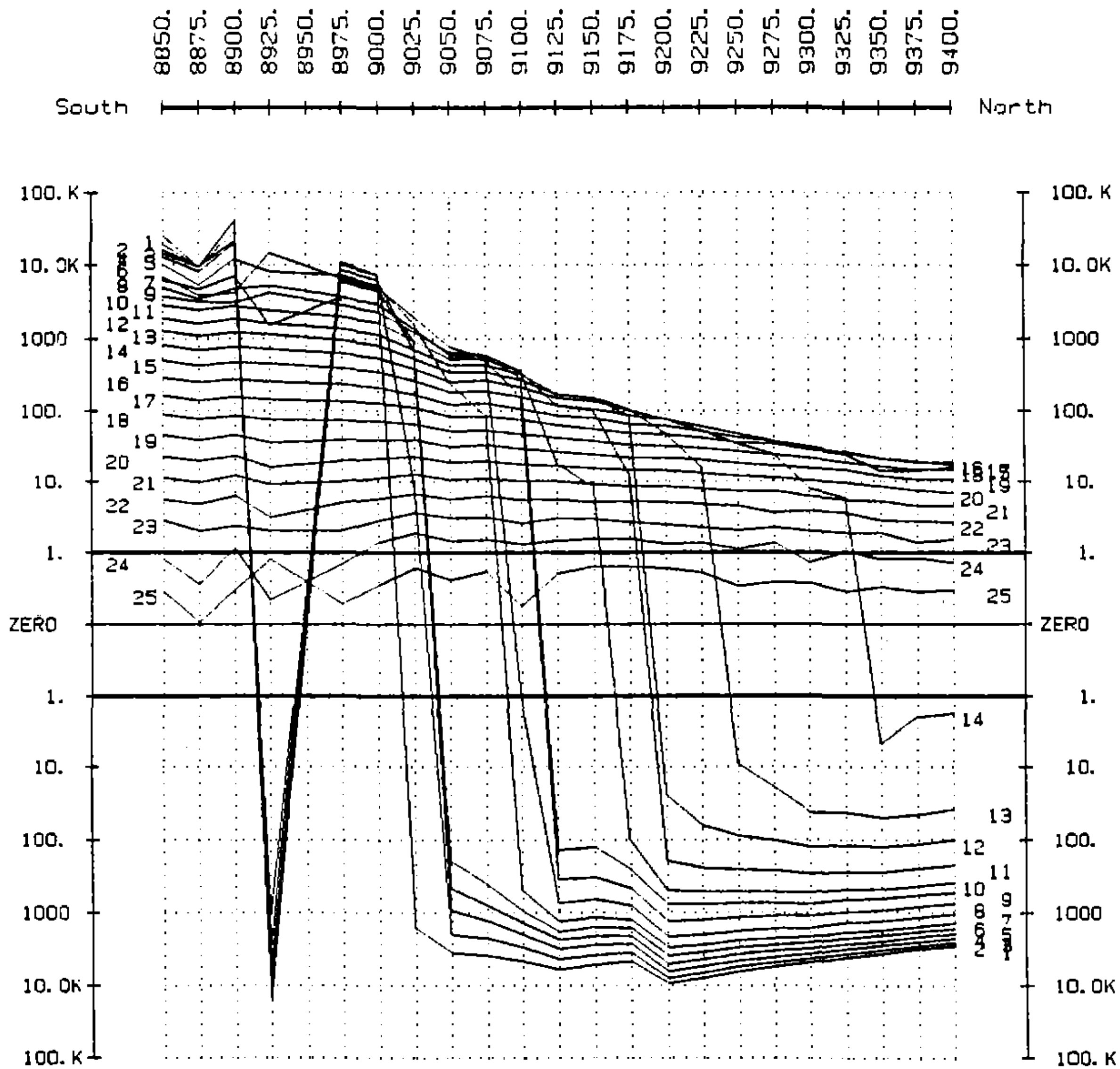

Window MAGNITUDE
values in microV/ampere
Component: CH1 Z, Rxno=10000.0
Loop 4: 8100E-8900E
8500N-8900N
15AMPS, 16HZ
Tx Delay 150 uSec

Win	Mag	Win	Mag
1	54.20u	14	1.023m
2	84.60u	15	1.264m
3	115.0u	16	1.580m
4	145.4u	17	1.961m
5	175.8u	18	2.454m
6	206.2u	19	3.106m
7	251.2u	20	3.878m
8	312.2u	21	4.870m
9	373.0u	22	6.114m
10	433.9u	23	7.678m
11	536.8u	24	9.663m
12	675.7u	25	12.16m
13	825.7u		

LINE 8500 E
Z Component

Field Job 062
Plot by CPLOT 5.71
Plotted 09 Feb 91

0166

364071

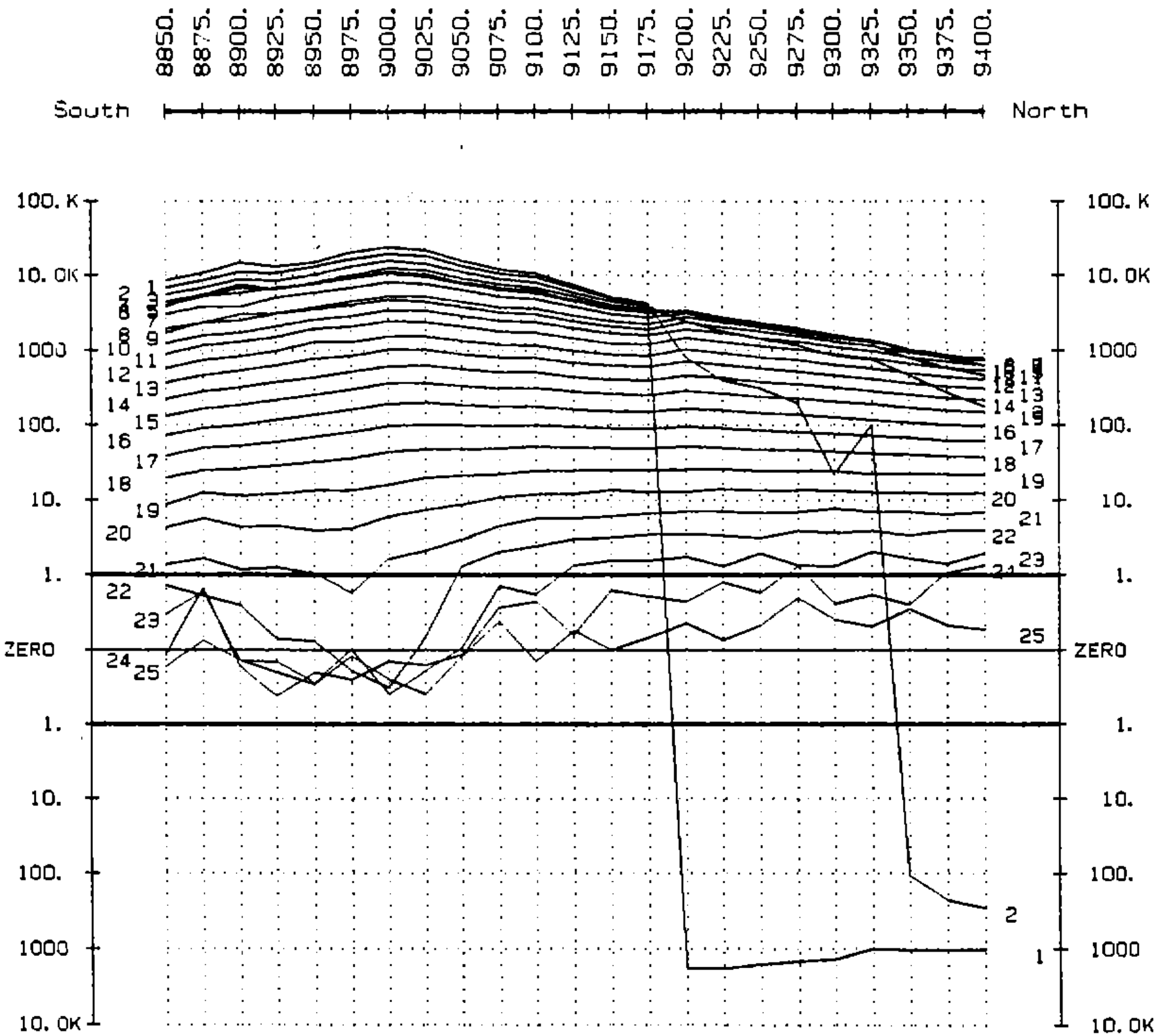

Window MAGNITUDE
values in microV/ampere
Component: CH1 X. Rxna=10000.0
Loop 4: 8100E-8900E
8500N-8900N
15AMPS. 16HZ
Tx Delay 150 uSec

Win	Mag	Win	Mag
1	54.20u	14	1.023m
2	84.60u	15	1.264m
3	115.0u	16	1.580m
4	145.4u	17	1.961m
5	175.8u	18	2.454m
6	206.2u	19	3.106m
7	251.2u	20	3.878m
8	312.2u	21	4.870m
9	373.0u	22	6.114m
10	433.9u	23	7.678m
11	536.8u	24	9.663m
12	675.7u	25	12.16m
13	825.7u		

LINE 8500 E
X Component

Field Job 062
Plot by CPLOT 5.71
Plotted 09 Feb 91

0167

364072

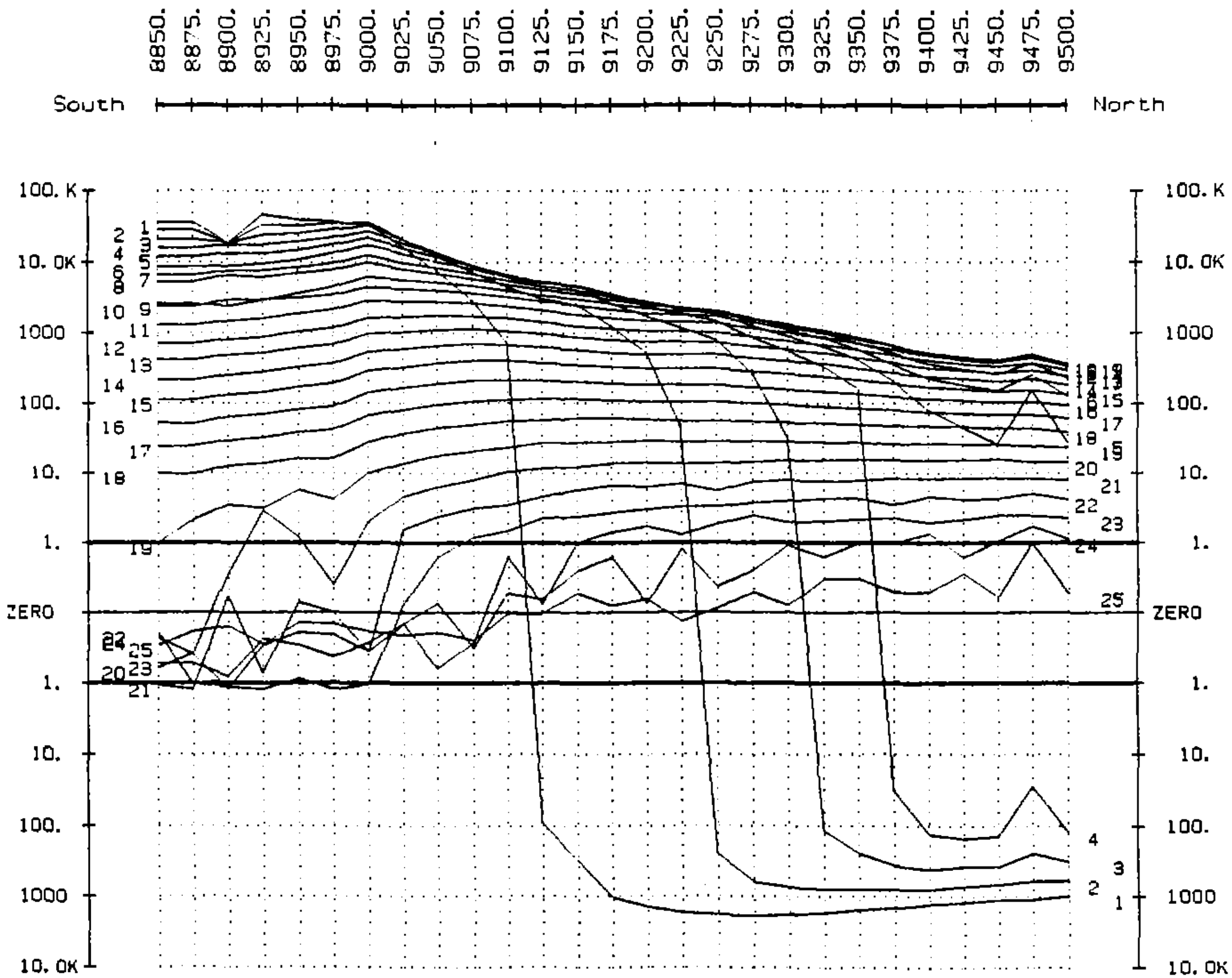

Window MAGNITUDE
values in microV/ampere
Component: CH1 X, Rxno=10000.0
Loop 4: 8100E-8900E
8500N-8900N
15AMPS, 16HZ
Tx Delay 150 uSec

Win	Mag	Win	Mag
1	54.20u	14	1.023m
2	84.60u	15	1.264m
3	115.0u	16	1.580m
4	145.4u	17	1.961m
5	175.8u	18	2.454m
6	206.2u	19	3.106m
7	251.2u	20	3.878m
8	312.2u	21	4.870m
9	373.0u	22	6.114m
10	433.9u	23	7.678m
11	536.8u	24	9.663m
12	675.7u	25	12.16m
13	825.7u		

LINE 8700 E
X Component

Field Job 062
Plot by CPLOT 5.71
Plotted 09 Feb 91

0168

364073

0169

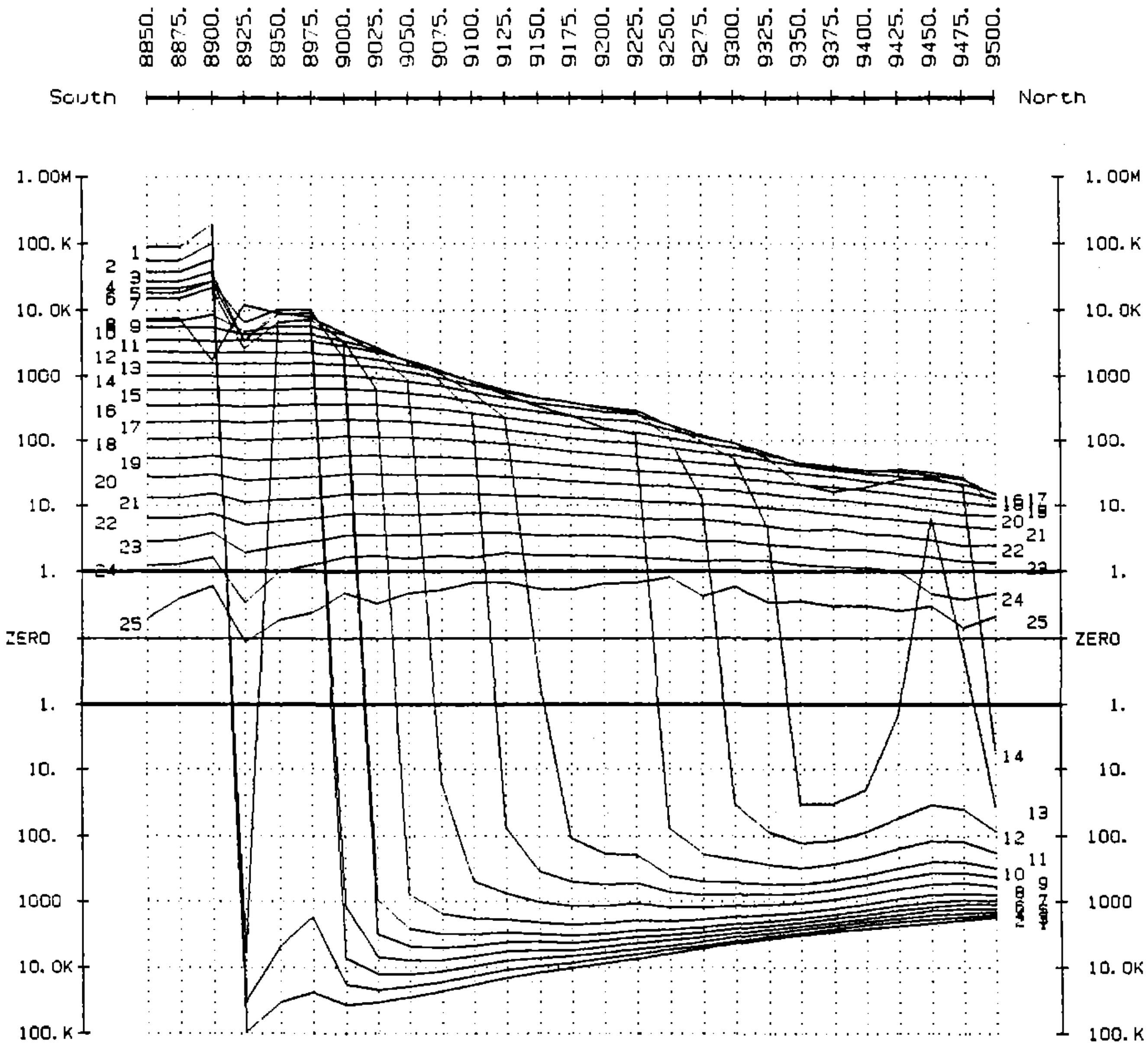

Window MAGNITUDE
values in microV/ampere
Component: CH1 Z, Rxna=10000.0
Loop 4: 8100E-8900E
8500N-8900N
15AMPS, 16HZ
Tx Delay 150 uSec

Win	Mag	Win	Mag
1	54.20u	14	1.023m
2	84.60u	15	1.264m
3	115.0u	16	1.580m
4	145.4u	17	1.961m
5	175.8u	18	2.454m
6	206.2u	19	3.106m
7	251.2u	20	3.878m
8	312.2u	21	4.870m
9	373.0u	22	6.114m
10	433.9u	23	7.678m
11	536.8u	24	9.663m
12	675.7u	25	12.16m
13	825.7u		

LINE 8700 E
Z Component

364074

Field Job 062
Plot by CPLOT 5.71
Plotted 09 Feb 91

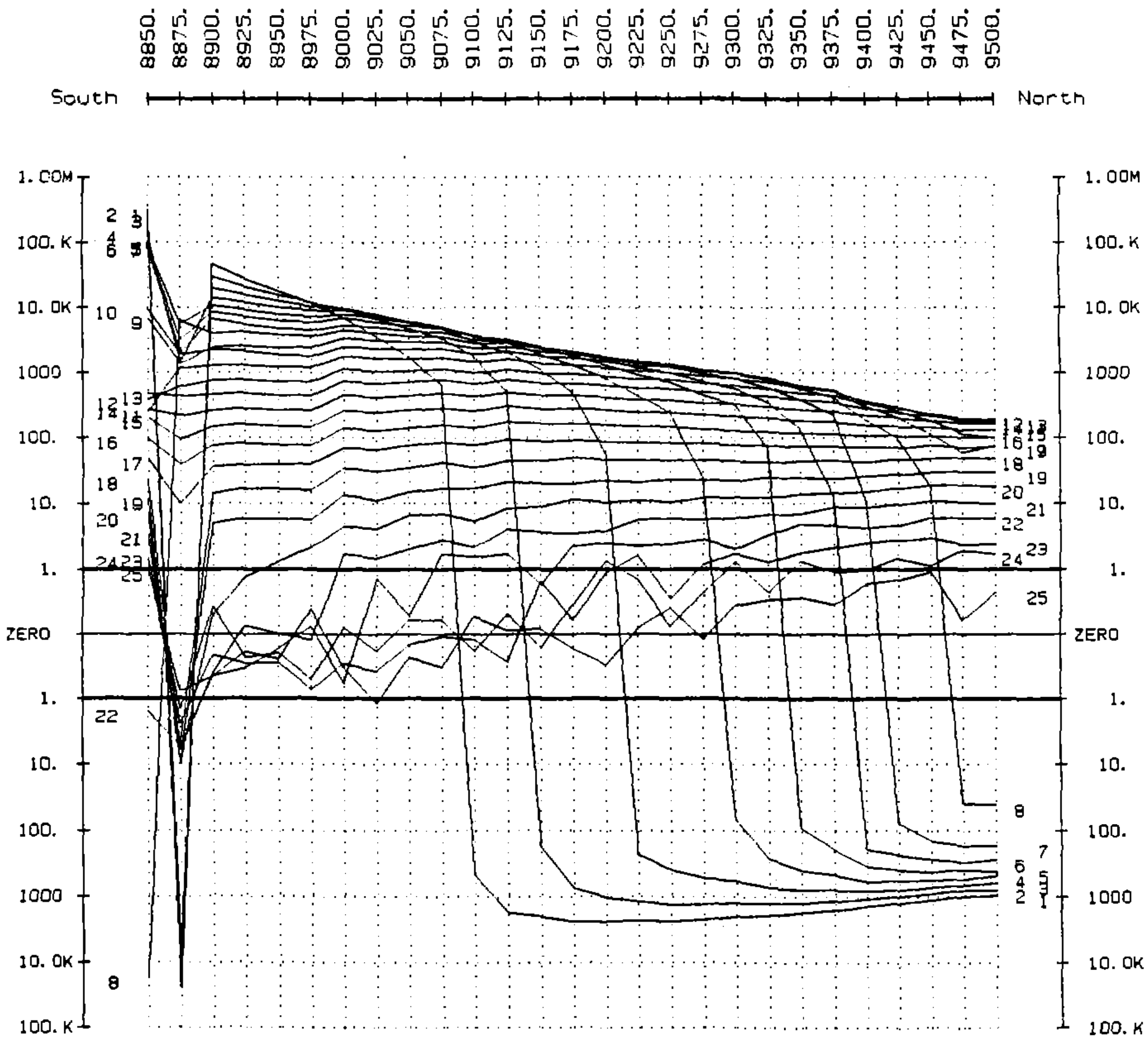

Window MAGNITUDE
values in microV/ampere
Component: CH1 X, Rxna=10000.0
Loop 4: 8100E-8900E
8500N-8900N
15AMPS, 16HZ
Tx Delay 150 uSec

Win	Mag	Win	Mag
1	54.20u	14	1.023m
2	84.60u	15	1.264m
3	115.0u	16	1.580m
4	145.4u	17	1.961m
5	175.8u	18	2.454m
6	206.2u	19	3.106m
7	251.2u	20	3.876m
8	312.2u	21	4.870m
9	373.0u	22	6.114m
10	433.9u	23	7.678m
11	536.8u	24	9.663m
12	675.7u	25	12.16m
13	825.7u		

LINE 8900 E
X Component

Field Job 062
Plot by CPLOT 5.71
Plotted 03 Mar 91

0170

364075

0171

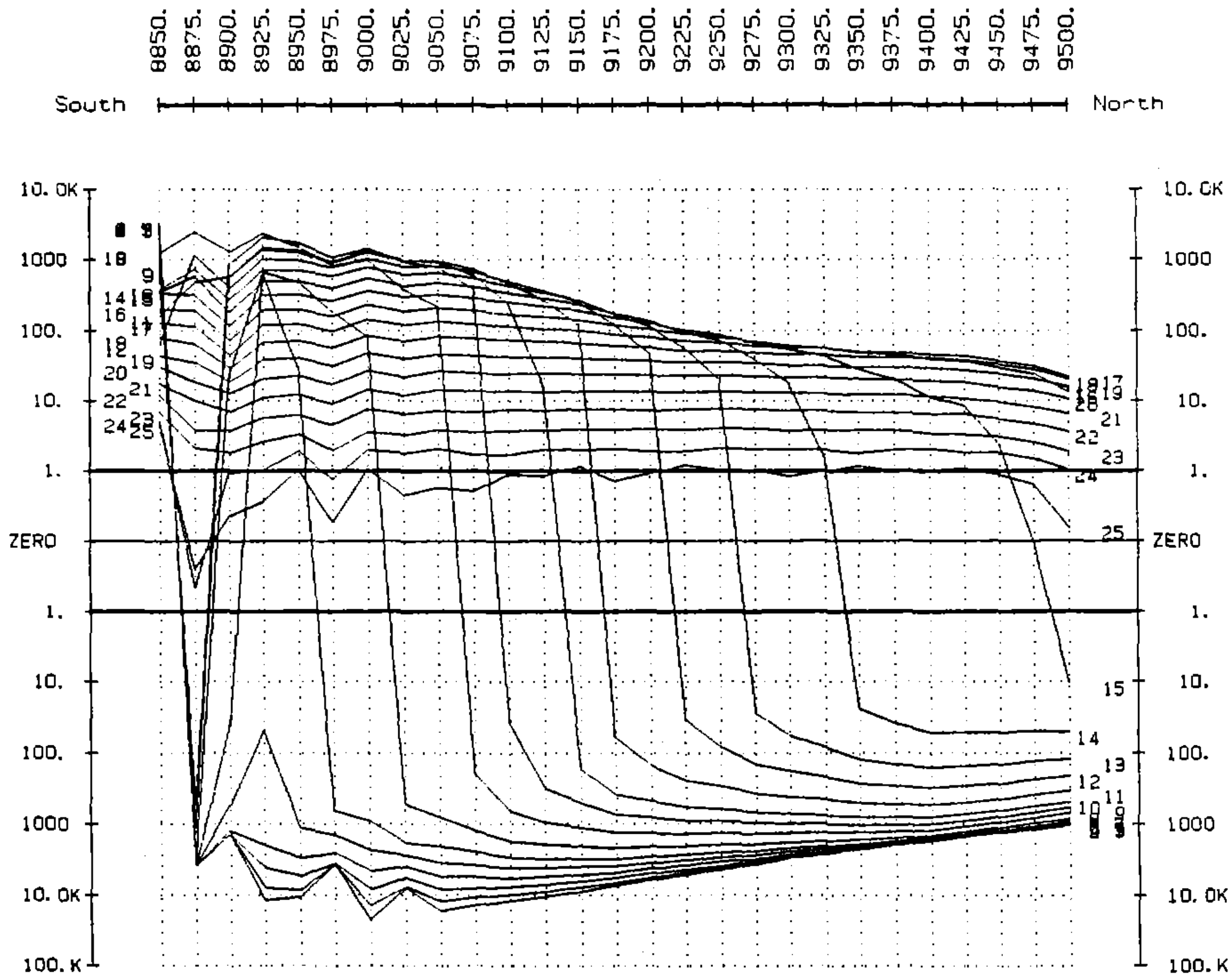

Window MAGNITUDE
values in microV/ampere
Component: CHI Z. Rxna=10000.0
Loop 4: 8100E-8900E
8500N-8900N
15AMPS, 16HZ
Tx Delay 150 uSec

Win	Mag	Win	Mag
1	54.20u	14	1.023m
2	84.60u	15	1.264m
3	115.0u	16	1.580m
4	145.4u	17	1.961m
5	175.8u	18	2.454m
6	206.2u	19	3.106m
7	251.2u	20	3.878m
8	312.2u	21	4.870m
9	373.0u	22	6.114m
10	433.9u	23	7.678m
11	536.8u	24	9.663m
12	675.7u	25	12.16m
13	825.7u		

LINE 8900 E
Z Component

364076

Field Job 062
Plot by CPLOT 5.71
Plotted 03 Mar 91

0172

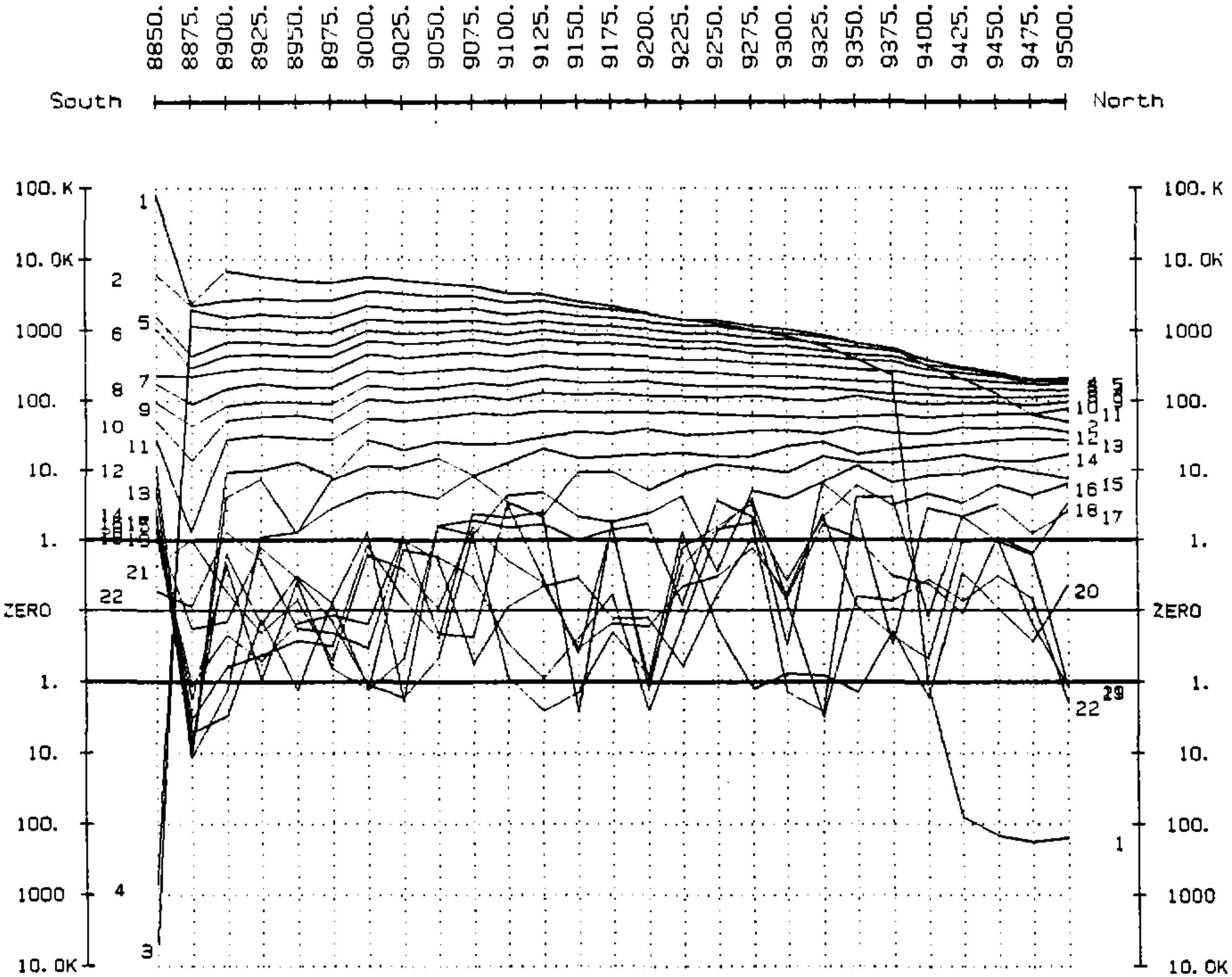

Window MAGNITUDE
values in microV/ampere
Component: CH1 X. Rxno=10000.0
Loop 4: 8100E-8900E
8500N-8900N
15AMPS. 8HZ
Tx Delay 150 uSec

Win	Mag	Win	Mag
1	227.4u	14	4.101m
2	349.0u	15	5.067m
3	470.6u	16	6.332m
4	592.2u	17	7.853m
5	713.8u	18	9.825m
6	835.4u	19	12.44m
7	1.015m	20	15.52m
8	1.259m	21	19.49m
9	1.503m	22	24.47m
10	1.746m		
11	2.158m		
12	2.714m		
13	3.313m		

LINE 8900 E
X Component
(8 Hz)

364077

Field Job 062
Plot by CPLOT 5.71
Plotted 03 Mar 91

0173

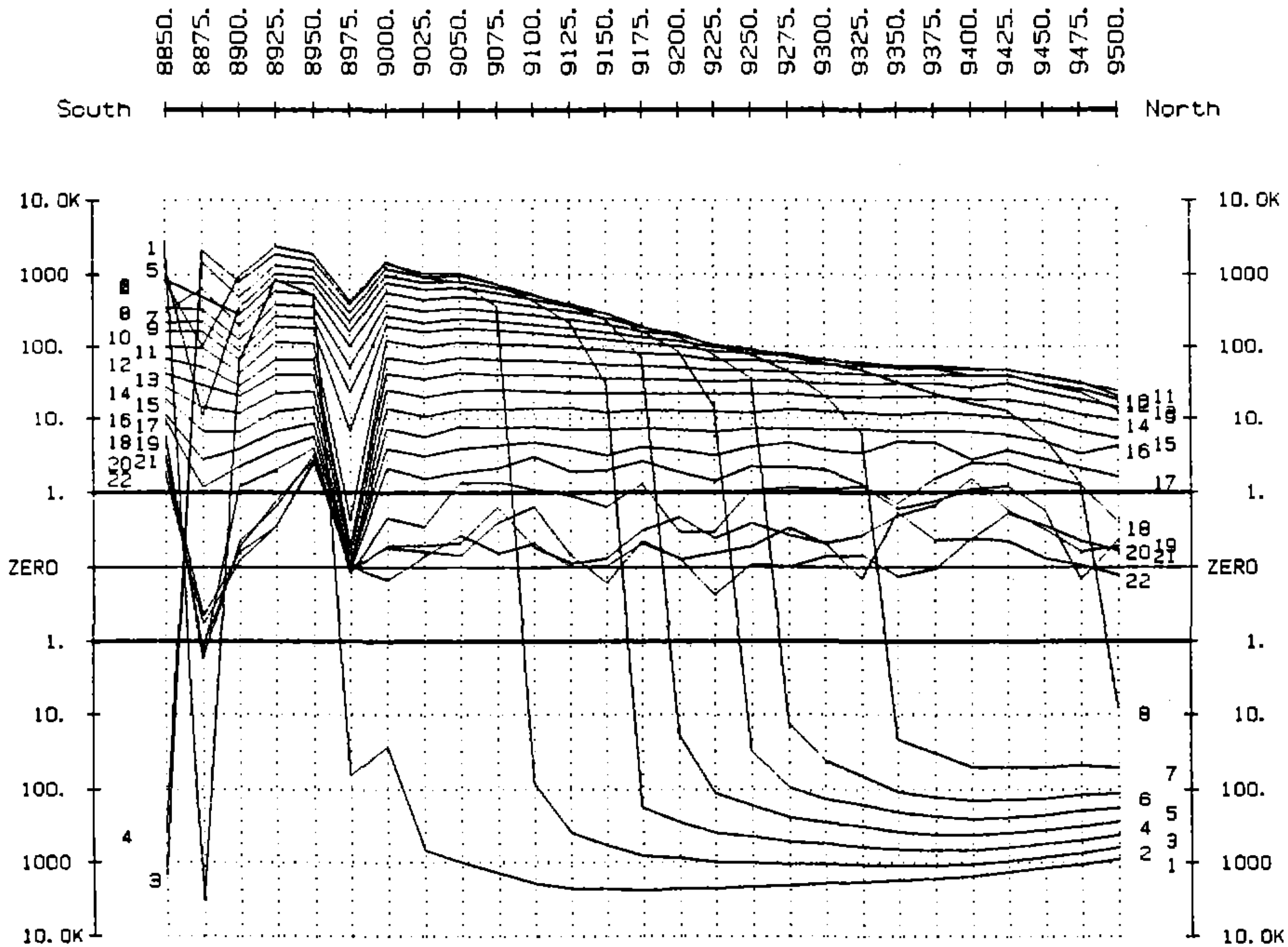

Window MAGNITUDE
values in microV/ampere
Component: CH1 Z. Rxna=10000.0
Loop 4: 8100E-8900E
8500N-8900N
15AMPS. 8HZ
Tx Delay 150 uSec

Win	Mag	Win	Mag
1	227.4u	14	4.101m
2	349.0u	15	5.067m
3	470.6u	16	6.332m
4	592.2u	17	7.853m
5	713.8u	18	9.825m
6	835.4u	19	12.44m
7	1.015m	20	15.52m
8	1.259m	21	19.49m
9	1.503m	22	24.47m
10	1.746m		
11	2.158m		
12	2.714m		
13	3.313m		

LINE 8900E
Z Component
(8Hz)

364078

Field Job 062
Plot by CPLOT 5.71
Plotted 03 Mar 91

0175

TASMANIA 1:100 000
TOPOGRAPHIC SURVEY

PIEMAN

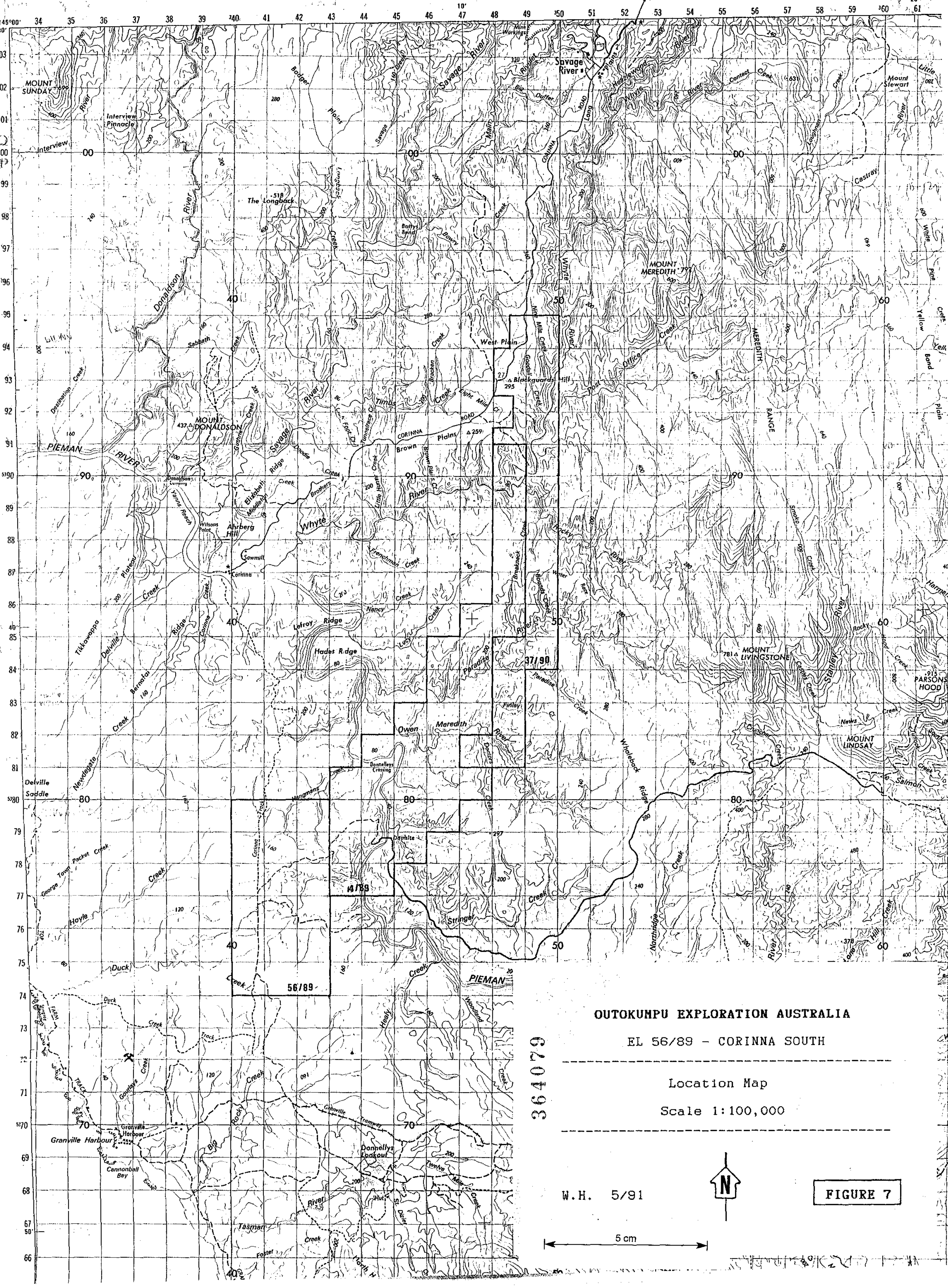

OUTOKUMPU EXPLORATION AUSTRALIA

EL 56/89 - CORINNA SOUTH

Location Map

Scale 1:100,000

W.H. 5/91

N

FIGURE 7

5 cm

364079

0174

TASMANIA 1:25 000 SERIES

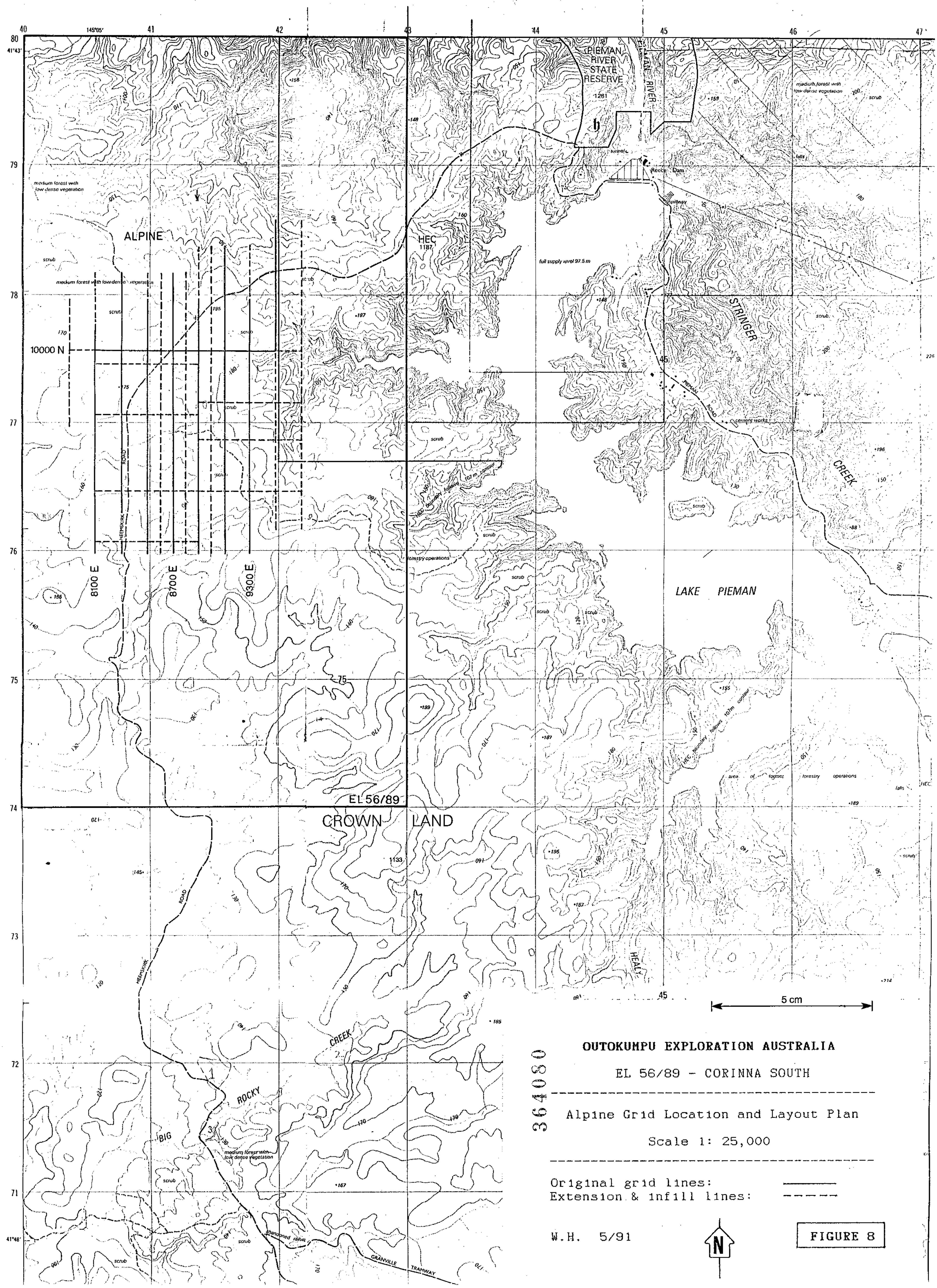

0176

OUTOKUMPU EXPLORATION AUSTRALIA

EL 56/89 - CORINNA SOUTH

ALPINE Geological/Assay Section

Drillhole AP1, 9100E

Scale 1: 250

W.H. 5/91 364081 **FIGURE 9**

91-3269.

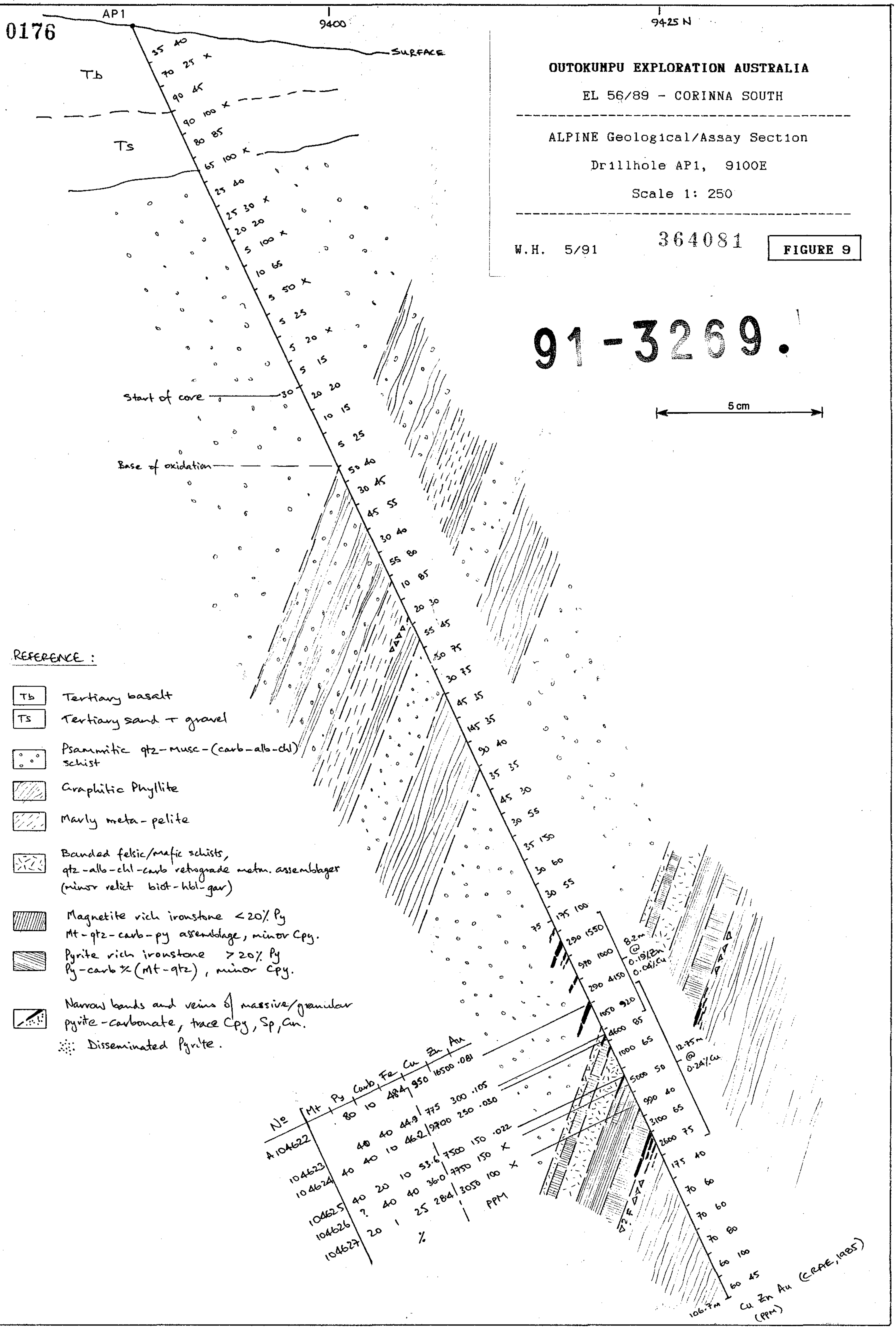

0177

OUTOKUMPU EXPLORATION AUSTRALIA

EL 56/89 - CORINNA SOUTH

ALPINE Geological/Assay Section

Drillhole AP2, 8700E

Scale 1: 250

W.H. 5/91

364082

FIGURE 10

91-3269.

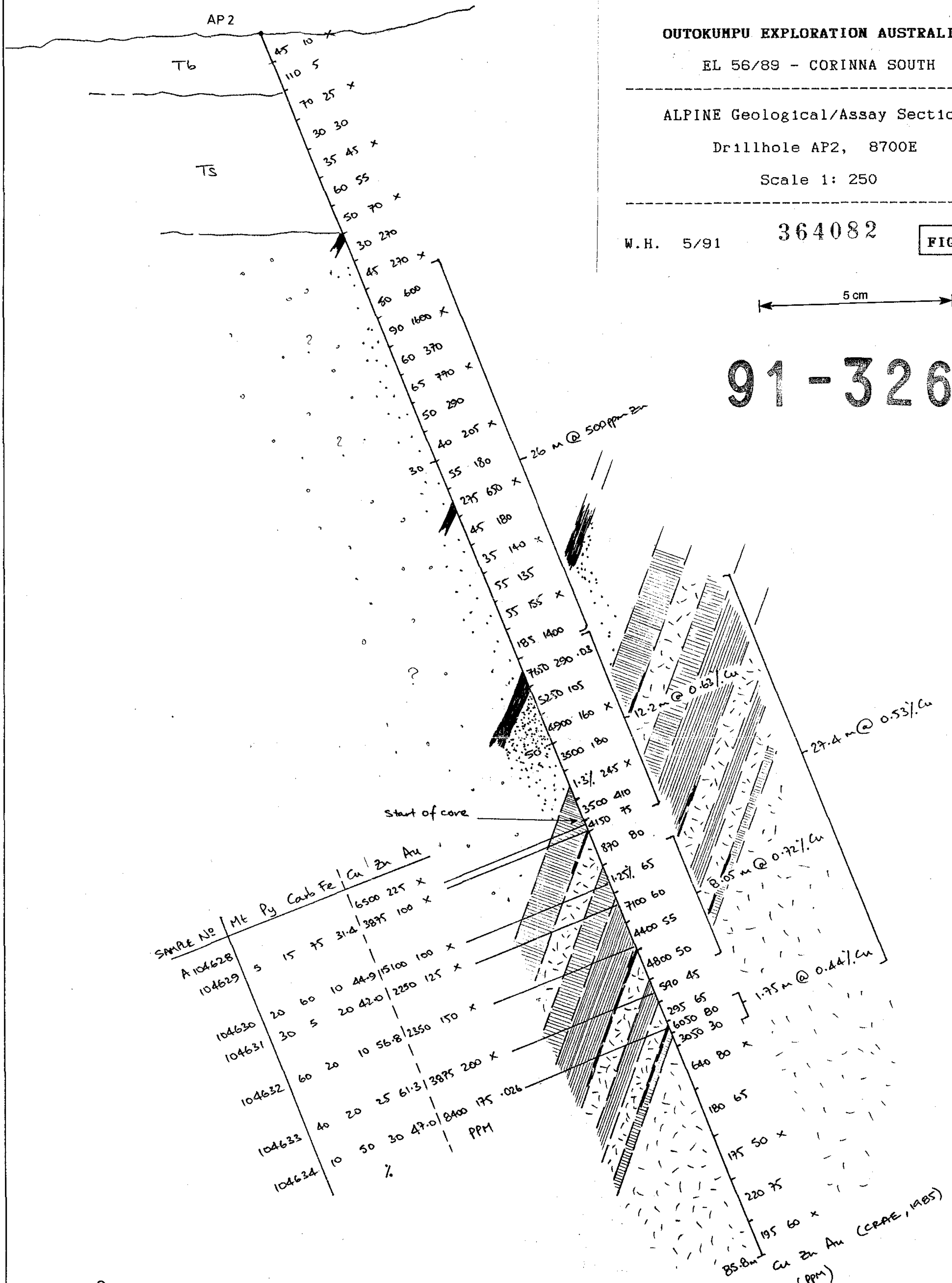

REFERENCE :
as for Figure 9

364083

0000

OUTOKUMPU EXPLORATION AUSTRALIA PTY LIMITED

Report No: R72.10
File No: 2.72a.9
Filename: 272GM106.RT1

ANNUAL REPORT TO 6 APRIL, 1991
EL 56/89 - CORINNA SOUTH, TASMANIA
Volume 2 of 2

For: Outokumpu Exploration Australia Pty Limited
77 Pacific Highway, NORTH SYDNEY NSW 2060

By: W. Herrmann, RSD 1066, DEVONPORT TAS 7310

Date: 22 May 1991

DISTRIBUTION:

1. OEA Library
2. Department of Resources & Energy

CONTENTS

VOLUME 1

List of Figures

(P) = plan in map pocket.

List of Appendices

VOLUME 2

Appendix II Report on the petrographic examination of ironstones and associated metamorphic rocks from the Arthur Metamorphic Complex, NW Tasmania.

Dr. J.Stolz / Dept. of Geology, Univ. of Tas.

0003

364086

REPORT ON THE PETROGRAPHIC EXAMINATION OF IRONSTONES AND ASSOCIATED METAMORPHIC ROCKS FROM THE ARTHUR METAMORPHIC COMPLEX, NW TASMANIA

: Including material from the Alpine and Owen Meredith Projects.

For: Outokumpu Exploration Australia Pty Ltd
77 Pacific Highway, North Sydney NSW 2060.

By: Joe Stolz

Department of Geology
University of Tasmania
GPO Box 252C,
Hobart Tas 7001.

November 26th 1990.

The Owen-Meredith Area

OBJECTIVES

The specific aims of this study are to determine;

1. the nature of the amphibolites and their likely precursors; comparison with interpretations given by Minpet Services' previous petrographic report

2. the nature of the 'sodic granitoids', for example; is there any evidence for pre-, syn- or post-metamorphic origin? Does the tourmaline (in vein) have affinities with that of samples 104617, 104574?

3. the nature of the ironstones and the style of mineralisation, ie., pre-, syn- or post-metamorphism? Comparison with ironstones from the Alpine area

4. the nature of the tourmaline/actinolite schorls, and in particular, do these have any chemical/mineralogical association with the amphibolites, 'sodic granitoids' or banded/massive ironstones? Is there any textural evidence for a pre-, syn- or post-metamorphic origin?

RESULTS

Detailed petrographic analyses are presented in the following section for the samples previously described by Minpet Services, and an additional 7 samples from the Owen Meredith area provided by W. Herrmann. The mineralogical and textural relationships gleaned from examination of these specimens provide the basis for the following discussion of the problems listed above.

1. Nature of the Amphibolites.

A number of rocks examined by Minpet Services (including 104569, 104593 and 104594) were interpreted as metamorphosed calc-silicate assemblages. However, I would argue on the basis of their mineralogical and chemical characteristics that these rocks (together with 104587, 104580, 104591 and 104595) are regionally metamorphosed mafic volcanics.

The majority of these rocks exhibit similar mineralogical assemblages and proportions of phases. They are dominantly composed of albitic plagioclase, chlorite, amphibole, epidote, magnetite and sphene. Although broadly similar assemblages could be produced by metamorphism of impure limestones, the predominance of albitic plagioclase coupled with low whole-rock CaO in at least one specimen (eg. 104569 CaO = 0.21%) does not support a calcareous sedimentary precursor. The mineralogy of 104569 does not differ significantly from the other rocks considered by Minpet Services to be meta-sedimentary (eg. 104592 -

104594), and although no chemical data are available for those specimens, low CaO would be predicted.

Relatively high Na_2O and low CaO contents are consistent with seafloor alteration of a basalt prior to metamorphism, although some variation in the degree of alteration will result in a range of Ca/Na ratios.

The major elements (particularly Na_2O, K_2O, CaO and MgO) are susceptible to modification during metamorphism, hydrothermal alteration and weathering and hence can be misleading when interpreting precursor compositions. However, Ti and Zr are relatively immobile, except perhaps during intense hydrothermal alteration, and can provide a useful means of identifying precursor lithologies. A plot of Ti versus Zr for the Owen-Meredith host rocks (Fig. 1) indicates a fairly consistent Ti/Zr ratio which is in the range for typical basaltic rocks (ie. Ti/Zr > 60). Even if calc-silicate assemblages with similar Ti/Zr values exist, it is unlikely that a heterogeneous sedimentary sequence would have such consistent Ti/Zr values.

The compositions of tholeiites from the Smithton-Trowutta area (Griffin, 1974), and data for Cambrian Mt Read mafic rocks are plotted for comparison with the Timbs Group Metabasalts. The similarity of the Smithton-Trowutta basalts and those from the Bowry Member is striking, and both are clearly different from the Mt Read basalts. The latter were formed in a convergent margin setting whereas the Smithton and Bowry mafic rocks have compositions typical of continental tholeiites. Their similar compositions indicate they are likely to have formed in a similar tectonic setting, and provides tacit support for the idea that they represent the same sequence (Herrmann, 1989).

2. *Nature of the 'Sodic Granitoids'.*

The sodic granitoids (eg. 104566, 104596, 104598, 104638) consist dominantly of medium-grained aggregates of albite and quartz. All samples show evidence of moderate dislocation metamorphism. Plagioclase twin lamellae are invariably bent, whereas quartz exhibits undulose extinction and has undergone significant subgrain development. The latter feature has resulted in relatively large plagioclase porphyroclasts being set in a finer recrystallised quartz-rich matrix. Sample 104596 has experienced the most intense deformation, whereas 104598 retains the best textural evidence that these were originally even-grained and medium-grained intrusive rocks. Narrow, very localised zones of more intense cataclasis are evident in 104566 and these contain minor sericite which has grown in random orientations, thereby suggesting they represented a pathway for post-deformation K-bearing fluids.

The textural evidence indicates that the sodic granitoids were emplaced at least prior to the latest deformation, and some (eg. 104598) probably after the most intense phase of deformation which produced the amphibolite facies assemblages. More intense granulation of plagioclase (particularly in 104598) would be expected if it had experienced comparable levels of strain to these rocks. Nevertheless, 104596 contains some blue-green hornblende which is a prograde phase in the

0006

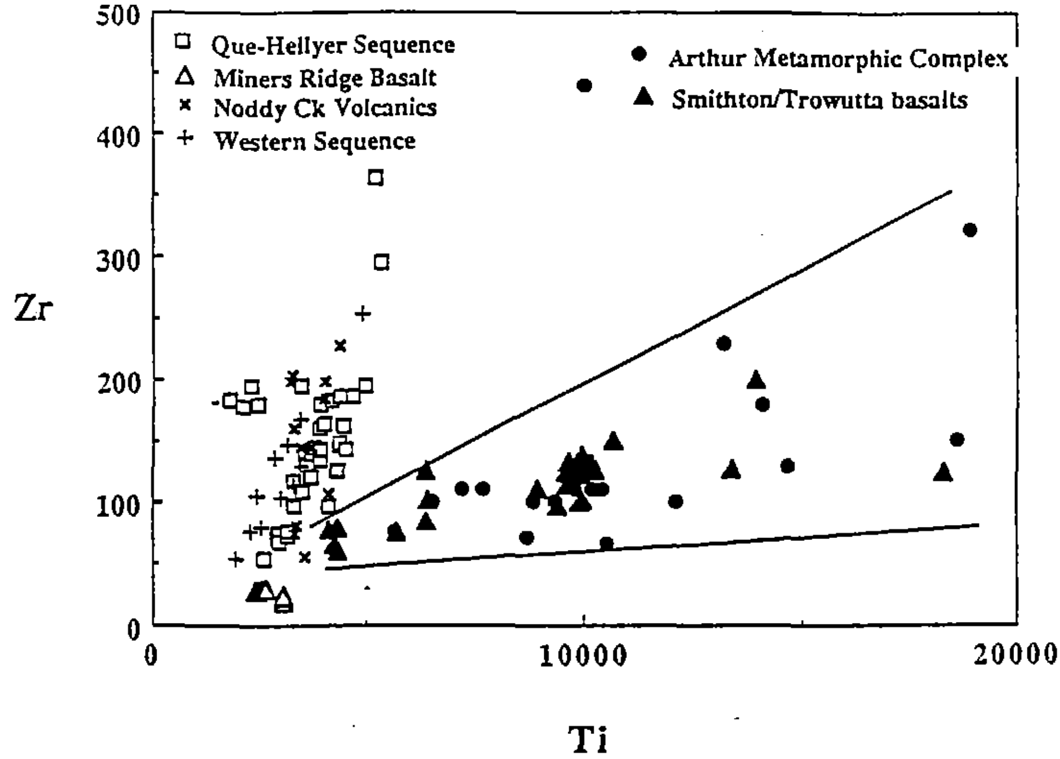

Fig. 1. Plot of Ti versus Zr for metabasaltic rocks from the Arthur Metamorphic Complex and the Smithton-Trowutta area showing their close similarity. Some Cambrian subduction-related volcanics from the Mt Read Volcanic Belt are plotted for comparison.

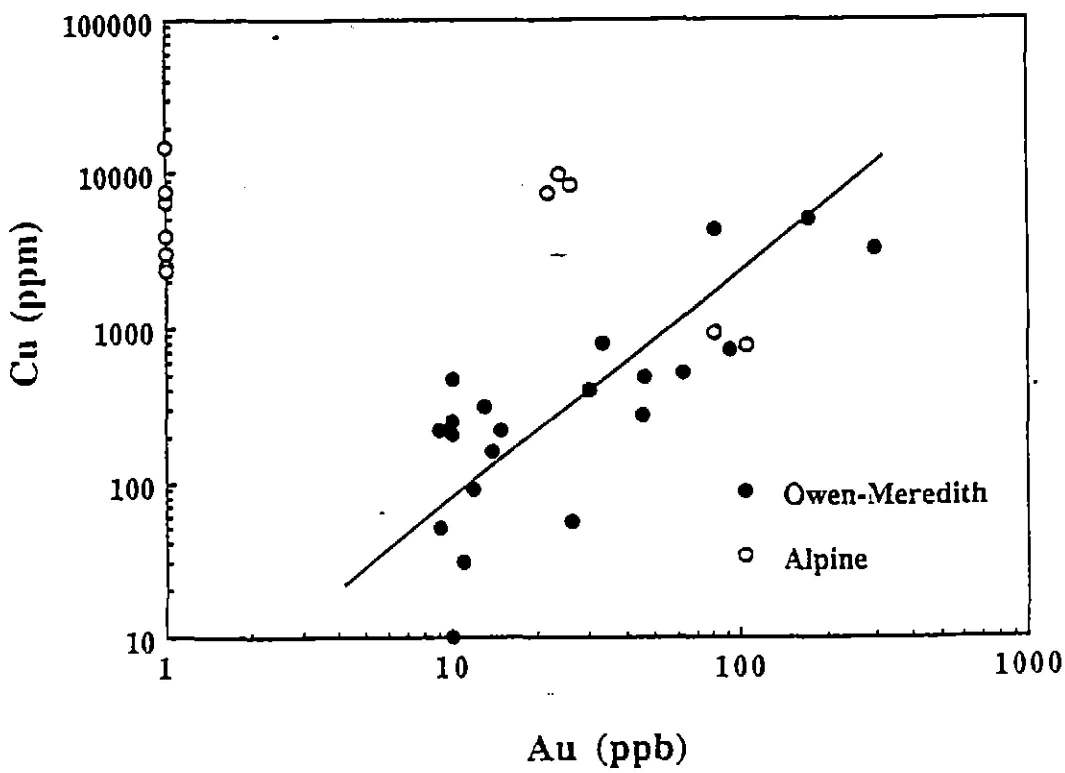

Fig. 2. Plot of Au (ppb) versus Cu (ppm) for ironstones from the Owen-Meredith and Alpine areas. There is a good positive correlation for the Owen-Meredith data, and a very poor correlation for the Alpine ironstones.

amphibolites, therefore suggesting that it was emplaced prior to the peak of metamorphism.

The vein tourmaline in sample 104638 has a very dark blue-green to tan coloured pleochroism which is consistent with iron-rich schorls associated with granitic rocks and pegmatites. On the other hand, the tourmaline in samples 104574 and 104617 has a pale green to yellowish pleochroism which is typical of relatively magnesian or dravitic tourmalines. This is consistent with the higher whole-rock MgO contents (eg. 104574, MgO = 6.2%) and the presence of co-existing tremolitic amphibole.

3. *Nature of the Ironstones*

The three ironstone samples examined from the Owen-Meredith area (ie, 104581, 104586 and 105609) consist of interlayered quartz and magnetite-pyrite bands of varying thickness. The broader scale banding in these rocks probably reflects original bedding although in such highly deformed rocks it is difficult to be certain of this. For example, sample 104586 has essentially a mylonitic fabric with strongly recrystallised quartz occurring as elongate crystals, and very fine milled magnetite grains. The segregation of quartz and magnetite could therefore be partly due to differential shear and recrystallisation within the rock.

Pyrite occurs mainly in discrete bands associated with magnetite, and chalcopyrite is closely associated with the pyrite, sometimes occupying cracks and fractures in the pyrite and magnetite. The pyrite and magnetite generally appear to be in textural equilibrium and no evidence was found of pyrite replacing magnetite.

All phases in these rocks have experienced deformation, as evidenced by quartz deformation around annealed pyrite and by cracking in magnetite. Therefore the chalcopyrite-pyrite mineralisation was clearly present before the deformation. Although there is evidence in the host rocks for several episodes of deformation, the absolute timing of which is poorly constrained, the bulk of the textural evidence suggests that the mineralisation occurred prior to the peak of metamorphism and deformation.

The banded ironstones from the Owen-Meredith area are more siliceous than the massive magnetite-pyrite ironstones of the Alpine area. Massive ironstones apparently also occur in the Owen-Meredith area (Herrmann, 1990) but were not included in this study. The most significant differences between the ironstones from these two prospects relate to the nature of the host sequences, and the relative abundance of carbonate. The host sequence to the Alpine ironstones is a mixed psammitic-pelitic sedimentary sequence with some associated interbedded mafic volcaniclastics. In contrast, mafic volcanics (now amphibolites or the retrogressed greenschist equivalents) appear to be more common in the host sequence to the Owen-Meredith ironstones.

Carbonate is a relatively minor phase associated with both the ironstones and the host rocks in the Owen-Meredith area. However, the Alpine ironstones and host rocks are characterised by an abundance of carbonate. In the host rocks it replaces plagioclase, chlorite and magnetite, whereas in the ironstones it extensively replaces magnetite and vice versa.

A discussion of the style of mineralisation is included with the discussion of the Alpine ironstones.

4. Nature of the Tourmaline/Actinolite Schorls.

The two tourmaline-tremolite/actinolite-rich samples (104574 and 104617) have similar petrographic features and undoubtedly formed in a similar manner. The major differences between the two samples relate to the evidence for some cataclasis and post-deformation recrystallisation in 104574 which is not apparent in 104617. Textural evidence suggests that tremolite/actinolite and magnetite in these rocks crystallised under low strain, contact metamorphic conditions, and this was followed by substantial replacement of the amphibole and magnetite by tourmaline. There is evidence in 104574 that it was affected by mild cataclasis resulting in some granulation of tourmaline and recrystallisation of amphibole. Coarse tremolite-rich veins (free of tourmaline) appear to be due to open space filling by dolomite and quartz followed by contact metamorphism. The inferred reaction for the development of tremolite is as follows;

$$\underset{\text{dolomite}}{5\,CaMg(CO_3)_2} + \underset{\text{quartz}}{8\,SiO_2} + H_2O \rightleftharpoons \underset{\text{tremolite}}{Ca_2Mg_5Si_8O_{22}(OH)_2} + \underset{\text{calcite}}{3\,CaCO_3} + 7\,CO_2$$

The above sequence of events implied by the textural relationships suggests that the crystallisation of tourmaline was due to the metasomatic addition of Fe- and B-rich fluids, probably from a granitic source.

The composition of the precursor material is more difficult to ascertain. Limited chemical data supplied by Wally Herrmann indicates that 104574 has Ti and Zr concentrations (and a Ti/Zr value) similar to many of the metabasalts from the Bowry Member of the Timbs Group. This suggests a basaltic precursor. However, the mineralogy seems difficult to reconcile with this unless the basalt experienced significant carbonate alteration prior to metamorphism. There is considerable evidence for late widespread carbonate alteration in the Alpine area but this is not a feature of the samples examined from the Owen-Meredith area.

The bulk of the evidence favours the interpretation that these tourmaline-tremolite rocks are metasomatically altered carbonate-rich assemblages, and that they formed after the regional metamorphism. Some localised shearing, possibly associated with the emplacement of the Meredith Granite, may be responsible for the cataclastic textures in sample 104574.

The Meredith Granite itself may well be responsible for the contact metamorphic effects, and also have been the source for the metasomatic fluids which caused tourmalinisation. Greisens consisting of quartz-tourmaline-cassiterite occur along north-south zones in the Meredith granite and commonly show evidence of strained quartz (Stockley, 1972).

Tourmaline also occurs as fine veinlets in the sodic granitoid 104638 and is observed replacing plagioclase in 104590, and replacing epidote and magnetite in 104594. All these samples have tourmaline with a blue-green to brownish pleochroism consistent with a relatively Fe-rich schorl composition. The paler colours in the tourmaline from the tourmaline-tremolite rocks may indicate slightly more magnesian compositions due to reaction with a relatively Mg-rich host.

The tourmaline in all samples appears to have formed subsequent to the regional metamorphism and is interpreted to be from a common granitic source (ie, the Meredith Granite).

The Alpine Prospect

1. *Nature of the Host Sequence.*

As noted earlier the host sequence to the Alpine ironstones appears to contain a greater sedimentary component than the host of the Owen-Meredith ironstones which appear to be predominantly mafic volcanics. The pre-metamorphic sedimentary sequence comprised interbedded quartzo-feldspathic rocks, pelites, and possibly volcaniclastics derived from basaltic volcanism.

These rocks underwent regional metamorphism to mid-upper amphibolite facies with prograde assemblages of garnet-biotite-quartz in the quartzo-feldspathic rocks and garnet-amphibole-plagioclase in the basic volcanic compositions (eg AP2 82). Both assemblages have undergone partial retrogression involving breakdown of garnet, biotite and amphibole to chlorite. Some samples (eg. AP2 82) contain chlorite-rich bands several centimetres thick with albite porphyroblasts. These appear to represent zones of complete retrogression of the prograde assemblage, possibly facilitated by localised shearing.

The relict snowball structures in pseudomorphed garnet porphyroblasts from sample AP1 85.4 provide good evidence for the syntectonic growth of garnet in a medium undergoing simple shear or laminar flow along the foliation. Plagioclase porphyroblasts in several samples exhibit a similar feature, and there is widespread evidence of high strain which caused the granulation of feldspar and recrystallisation of quartz. This is best developed in thin mylonite zones.

2. *Paragenetic Sequence in the Ironstones.*

Pyrite and magnetite are mainly in textural equilibrium, and at the petrographic scale there is no evidence to support theories of sulfidation involving the replacement of magnetite by pyrite. Sphalerite and galena are only present in some sections from AP1, either as inclusions in pyrite (in textural equilibrium), or as larger grains in which euhedral pyrite has itself been included.

Chalcopyrite is the most obviously remobilised component having migrated into veinlets and fractures within magnetite and pyrite (eg. AP1 92.5). However, this is not surprising for such a ductile phase and does not provide good evidence for an epigenetic origin.

Unfortunately the low Au concentrations of the ironstones resulted in the absence of any observable free Au in the sections, so it is difficult to assess its association with the sulphide or oxide phases. However, a plot of Cu vs Au (Fig. 2) for the Alpine ironstones and Owen Meredith ironstones plus host rocks provides an interesting contrast.

There is a reasonable correlation between Cu and Au in the Owen-Meredith samples suggesting an association of chalcopyrite and Au in the ironstones. on the other hand, the correlation between Cu and Au is poor for the Alpine ironstones. Some of the Cu-enriched samples have relatively high Au, yet Au is below the detection level in the most Cu-rich sample (A104630, 1.5% Cu).

3. *Timing of the Mineralisation.*

A very strong tectonic overprint has affected all of the ironstones and the petrographic evidence from this study supports earlier work which argued that the mineralisation was in place at least prior to the most recent deformation event. This does not preclude the possibility that the mineralisation was emplaced during or following the main regional metamorphic event, and that a subsequent event produced the cataclastic textures.

Unfortunately the simple mineralogy of the ironstones does not result in any useful information about the maximum grade of metamorphism which they experienced. However, the high strain characteristics (mylonitic fabrics) in some of the ironstones would appear to have been generated during the main phase of deformation and prograde metamorphism which characterises the host sequence. Evidence for subsequent folding of this 'S_1' foliation is present in a number of samples in the form of small scale assymetric folds with a crenulation cleavage which is often only weakly developed.

In summary, the textural evidence suggests that the ironstones were emplaced prior to peak metamorphism.

4. *Style of Mineralisation*

The general occurrence of the ironstones, their lateral continuity and strong stratigraphic control within the Bowry Member of the Timbs group provides strong evidence for a syngenetic origin. The conclusion from the textural relationships that the ironstones existed prior to the main phase of deformation and metamorphism also supports this interpretation.

There is no evidence of tourmaline or other phases closely associated with the ironstones which would be considered reliable indicators of the involvement of granitic fluids in the formation of the mineralisation. Further, the petrographic evidence indicates that the tourmalinisation is a very late (Devonian) feature associated with the Meredith Granite, and consequently much later than the pyrite-sphalerite-chalcopyrite mineralisation.

The best available analogue for this type of deposit appears to be the Starra exhalative BIF-Cu/Au deposit. Although the Alpine and

Owen-Meredith ironstones do not have anomalous Sn and W (as is the case at Starra), many do show anomalous Au (i.e. considerably higher values than normal background rock values of 2-5 ppb) which is a feature of the footwall alteration at Starra.

The nature of the footwall alteration, and specific enrichment and depletion characteristics appear to differ between different deposits of this style. For example, Trough Tank does not show the enrichment in Sn and W evident at Starra, but instead shows footwall enrichment in Ni, P, Mo and Co (Davidson, 1989).

Clearly, because of the intense deformation of the ironstones and their hosts, evidence for assymetric footwall alteration would be difficult to identify. It is conceivable that because of their different competency the ironstones may have been tectonically relocated relative to their original stratigraphic hangingwall and footwall sequences.

The observations that regional metal enrichment seems to be typical of exhalatives is probably the most useful attribute from an exploration viewpoint. At Starra, W, Y and Sn extend beyond Au in any given ironstone (Davidson, 1989). Although these elements do not appear to be useful in the north-west Tasmanian ironstones, a more detailed geochemical study may help to identify other trace elements which are closely associated with the transport of Cu and Au in this particular system. This may help to focus exploration for the high-grade zones of mineralisation (if they exist) in these ironstones.

References

Davidson G.J. 1989. Starra and Trough Tank: Iron-Formation Hosted Gold-Copper Deposits of North-West Queensland, Australia. Unpubl. PhD thesis, University of Tasmania.

Griffin B.J. 1974. Cambrian Tectonism and Volcanism in the Smithton Basin. Unpubl. BSc. Hons. thesis, University of Tasmania, 164 pp.

Herrmann W. 1989. Geology of the Arthur Metamorphic Complex, NW Tasmania. Report to Outokumpu Exploration Australia, Report No. R72.1, 26 pp.

Herrmann W. 1990. Exploration Progress Report EL 14/89 - Corinna. July 1990.

Stockley J.L. 1972. The Meredith Granite. Unpubl. BSc. Hons. thesis, University of Tasmania, 75 pp.

PETROGRAPHIC DESCRIPTIONS OF SAMPLES FROM THE OWEN-MEREDITH GRID.

Sample locations are shown on Plate 3 in TCR 91-3256

SAMPLE 104566 om 126m N

Hand-specimen: medium to coarse grained weathered 'granitic' rock.

Thin-section:

Mineral	Percentage abundance (%)
plagioclase	70
quartz	30
zircon	<1
sphene	<1
limonite	<1
tourmaline	trace
muscovite	trace

Mineralogy: plagioclase occurs as intergrown xenoblastic to tabular crystals (0.5 - 3 mm) characterised by abundant lamellar twinning of both albite and pericline. The twin lamellae are invariably bent and display strained extinction. Quartz often occurs as finer recrystallised grains (0.1 - 0.2 mm) intergranular to the feldspars due to subgrain development and recrystallisation of larger xenoblastic crystals.

There are several large euhedral crystals of zircon (0.3 - 1 mm) and some smaller fractured grains, as well as fine granular aggregates of sphene.

The rock has experienced moderate levels of strain resulting in the recrystallisation of quartz and deformation of plagioclase lattices. There are at least two parallel well-defined crush zones which traverse the section. Quartz and feldspar have been extensively granulated and recrystallised in these narrow (0.2 mm) shear zones, and some fine variably oriented muscovite plus a trace of tourmaline also occurs. the lack of preferred orientation of the muscovite suggests that it is post-deformation in origin.

Genetic interpretation: the rock appears to be a sodic granitoid or trondhjemite. The chemical data (K_2O = 0.10% and Na_2O = 5.63%) reflects the absence of alkali feldspar and together with the very low CaO (0.05%) indicates almost pure albite plagioclase.

SAMPLE 104569

Hand-specimen: fine-grained metabasic rock rich in chlorite and amphibole with a moderate foliation.

Thin-section:

Mineral	Percentage abundance (%)
plagioclase	57
chlorite	30
amphibole	5
quartz	3
magnetite	2
pyrite	2
sphene	1
tourmaline	?

Mineralogy: xenoblastic to tabular albite porphyroclasts (some with simple twinning) occur in a matrix dominated by chlorite and blue-green amphibole. These mafic phases define a strong foliation which has experienced a second phase of folding resulting in small-scale assymetric folds with a crenulation cleavage. The distinctive blue-green amphibole occurs as prismatic crystals and has a low birefringence and a very low negative 2V (probably <10°). These optical characteristics are most consistent with a relatively sodic high-pressure amphibole of the glaucophane-riebeckite series. Unfortunately this could not be checked by microprobe as the machine was not functioning during the time of the study. However, by elimination, there are no obvious alternatives to this conclusion. The whole-rock chemistry (CaO = 0.21%) supports the notion of a Ca-poor amphibole, and the optical characteristics are not consistent with it being one of the orthorhombic amphiboles.

Occasional crystals of biotite and muscovite are associated with elongate pods of recrystallised quartz and minor biotite occurs intergrown with chlorite in the matrix.

Magnetite occurs as elongate laths and as xenoblastic grains and aggregates. The former could be pseudomorphs after primary hematite, but it is more likely original magnetite octahedra have been broken up and strung out during deformation and recrystallisation. Pyrite occurs as discrete rounded or cubic grains, and although pyrite and magnetite are adjacent in several instances, there is no evidence for replacement of magnetite by pyrite.

Genetic interpretation: the rock appears to have been a porphyritic mafic rock with phenocrysts of plagioclase which has experienced very high strain during recrystallisation producing a strong foliation. A subsequent deformation resulted in small scale folding and cleavage development perpendicular to the original foliation.

SAMPLE 104574

Hand-specimen: very heterogeneous amphibole-tourmaline-rich rock with large (cm size) layers of tourmaline showing a somewhat brecciated or strained appearance.

Thin-section:

Mineral	Percentage abundance (%)
tourmaline	55
tremolite/actinolite	35
sphene	5
carbonate	2
magnetite	3

Mineralogy: The rock consists of some relatively large (2 mm) xenoblastic aggregates of elongate to stumpy tourmaline crystals. These larger aggregates of tourmaline may have replaced some primary phase such as feldspar, although there is no clear evidence for a precursor phase. There is some elongation of the tourmaline aggregates due to cataclasis, and narrow stringers (1 - 2 mm long) of carbonate and minor magnetite occur along grain boundaries.

This contrasts with coarse-grained idioblastic elongate crystals of tremolite which appear to infill fractures within the rock (Fig. 3). There is also a significant amount of carbonate (previously called sphene) associated with the tremolite which appears to be in textural equilibrium.

There are several shear zones through the tourmaline without tremolite which have resulted in some recrystallisation and there is a concentration of granular sphene and granulated magnetite along these zones (Fig. 3).

A fine-grained part of the section is dominated by finer-grained tremolite (0.1 mm) and magnetite porphyroblasts, in textural equilibrium with associated subordinate carbonate. Relatively large subidioblastic to xenoblastic porphyroblasts of tourmaline appear to be replacing this fine tremolite-carbonate matrix and magnetite porphyroblasts.

Occasional inclusions of tremolite in tourmaline are very rare, although some fine carbonate inclusions are observed.

Genetic interpretation: The fine grained tremolitic matrix appears to have formed by contact metamorphism in view of the lack of preferred orientation of elongate amphibole crystals. This matrix then appears to have been partly replaced by tourmaline. Mild deformation of the rock produced some cataclastic textures in the tourmaline and granulation of the tourmaline and magnetite. This appears to have been followed by introduction of dolomitic carbonate plus quartz as an open space filling. Subsequent contact metamorphism has resulted in the recrystallisation of the carbonate to produce tremolite and probably also some recrystallisation of tourmaline.

The fine tremolite in the groundmass appears to represent carbonate replacement of some pre-existing material such as a mafic tuff perhaps, which may have had phenocrysts that had been tourmalinised. The reaction for the formation of tremolite is as follows;

$$\underset{\text{dolomite}}{5\,CaMg(CO_3)_2} + \underset{\text{quartz}}{8\,SiO_2} + H_2O \rightleftharpoons \underset{\text{tremolite}}{Ca_2Mg_5Si_8O_{22}(OH)_2} + \underset{\text{calcite}}{3\,CaCO_3} + 7\,CO_2$$

Figure 3. Shearing of tourmaline-rich layers in tourmaline-tremolite rock (104574) with trails of sphene, adjacent to an unstrained vein of tremolite with a magnetite porphyroblast. Magnification X50, PPL.

SAMPLE 104581 Posky River

Hand-specimen: thin-banded (0.5 - 1 mm) quartz-magnetite-rich rock with dominant pyrite throughout.

Thin-section:

Mineral	Percentage abundance (%)
quartz	75
magnetite	20
pyrite	3
hematite	2
sericite	trace

Mineralogy: alternating relatively quartz-rich and magnetite-rich bands (0.5 - 1 mm wide). The quartz occurs as slightly elongate xenoblastic grains with extensively sutured margins. The larger grains (0.5 - 0.8 mm) exhibit undulose extinction and substantial subgrain development.

Relatively large octahedra (0.1 - 0.5 mm) of magnetite and pyrite are disseminated throughout the quartz-rich layers, occurring as single crystals and aggregates. The magnetite- and pyrite-rich layers appear to represent merely a greater concentration of similar shaped and size grains, although there may be a greater proportion of finer-grained magnetite in these layers. Minor oxidation of magnetite has resulted in minor replacement by hematite.

Genetic interpretation: This rock most likely represents an exhalative chemical sediment which has experienced regional metamorphism. The previous interpretation that it represents an original sandstone on the basis of cross-bedding seems doubtful. The rock has been subjected to considerable strain as evidenced by the nature of the recrystallised quartz and it seems unlikely that primary sedimentary structures would survive such intense recrystallisation.

SAMPLE 104586 Rocky River

Hand-specimen: Very finely-banded quartz-magnetite rock, banding on the scale of 0.08 mm.

Thin-section:

Mineral	Percentage abundance (%)
quartz	80
magnetite	15
hematite	5

Mineralogy: there is moderate variation in grain size in this rock. Some relatively coarse-grained quartz-rich layers (1 - 1.2 mm long) occur with interstitial hematite and minor magnetite. These alternate with very fine-grained bands which consist of small elongate quartz grains (0.1 - 0.2 mm) with very finely disseminated octahedra or cubes of magnetite (0.005 - 0.01 mm) and some larger grains (0.3 mm). These fine-grained zones represent zones of more intense cataclasis in which the magnetite grains have been severely milled (Fig. 4), and the quartz grains more strongly recrystallised.

Genetic interpretation: this rock has experienced very high strain and the cataclasis is mylonitic in character with significant evidence of rotation (Fig. 5). Although the broader banding depicted by alternating quartz and magnetite-rich layers could reflect original bedding, the intense nature of the dislocation metamorphism which has affected this rock suggests that much of the banding may be tectonic in origin.

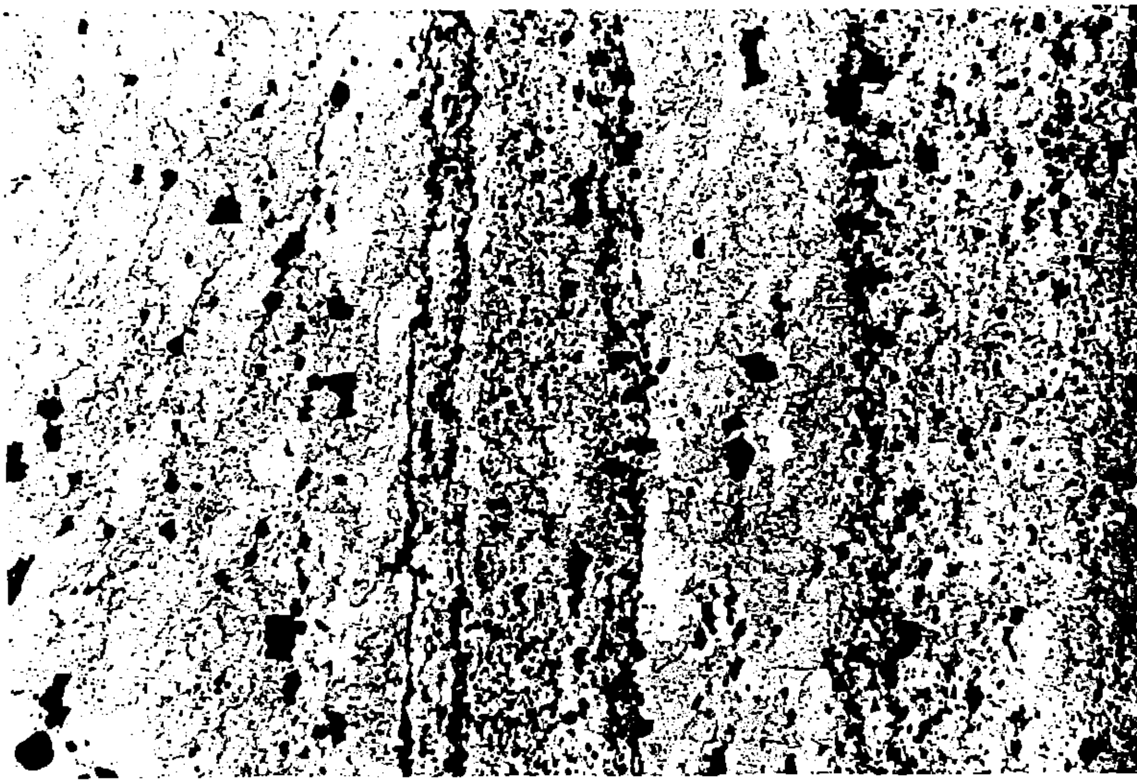

Fig. 4. Banded siliceous ironstone (104586) showing the finer magnetite and recrystallised quartz in the more deformed layers. Magnification x50, PPL.

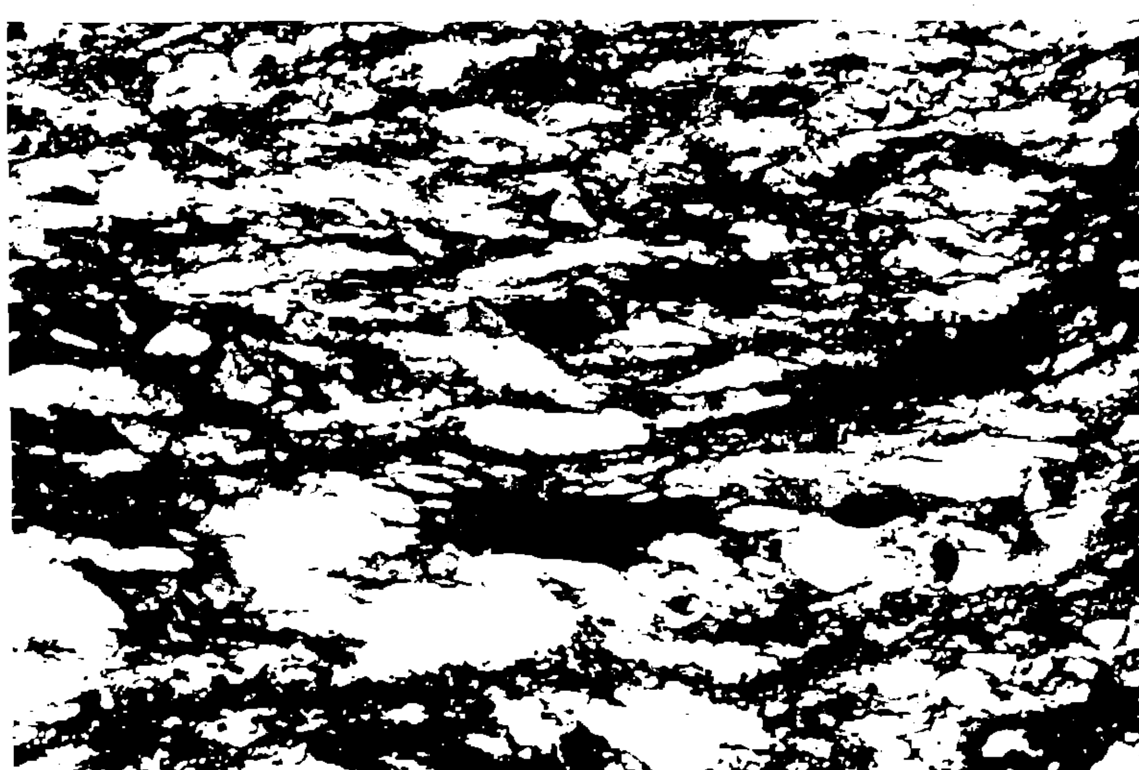

Fig. 5. Banded siliceous ironstone (104586) showing the highly sheared and recrystallised quartz. Magnification x50, PPL.

SAMPLE 104587

Hand-specimen: metamorphic rock rich in chlorite, amphibole and feldspar, which exhibits a contact between a relatively dark coarser-grained zone and fine-grained zone. The contact shows some irregularity and may represent a bedding contact.

Thin-section:

Mineral	Percentage abundance (%)
albite	35
amphibole	50
quartz	5
chlorite	5
sphene	2
pyrite	1
apatite	1
biotite	1

Mineralogy: the section traverses a relatively coarse-grained zone and a finer-grained part which probably reflect original bedding in the rock. The finer-grained portion (0.02 - 0.05 mm) is dominated by granoblastic quartz, albite and amphibole. The latter also occurs as prismatic grains (0.5 mm long). Fine pyrite cubes and aggregates of fine granular sphene are scattered throughout. Minor sheaths of pale green chlorite occur sporadically. Within the fine grained zone there is some variability in the ratio of felsic to mafic components, probably also representing compositional variations in the original bedding.

There is a fairly sharp but irregular boundary between the fine and coarse bands. The relatively coarse material (0.1 - 0.3 mm long prismatic crystals) of albite, quartz and amphibole show granoblastic polygonal textures with individual or aggregate pyrite cubes within aggregates of granular sphene and chlorite patches. This is similar mineralogy and textures to the finer-grained layers, except that there is very little quartz in the finer-grained layers. Most of the colourless material is twinned or untwinned albite.

There are also some very coarse veins cross-cutting the coarse material. They are 2 - 3 mm wide veins rich in recrystallised twinned albite (0.5 mm) with coarse radial aggregates of chlorite and some green biotite (largely replaced by chlorite), interstitial quartz, minor apatite and pyrite cubes up to 0.4 mm (Fig. 6). Textures within the veins are also dominantly granoblastic polygonal, particularly the boundaries between quartz and albite.

Genetic interpretation: The polygonal equi-dimensional textures suggest contact metamorphic recrystallisation. The presence of actinolite suggests a relatively calcic composition which is silica-oversaturated. However, the presence of sodic plagioclase and the paucity of silica throughout the bulk of the rock suggests a mafic volcanic composition which has been contact metamorphosed. The vein material is largely introduced and the veins are where most of the silica is concentrated. The fluid which introduced the silica probably also added the sulphides although this is difficult to prove. One very fine quartz-chlorite-rich vein cross-cuts the coarse material.

Introduction of the vein material appears to have been pre- or syn-contact metamorphism because of the observed textures. The fluids produced dominantly quartz-albite-biotite-chlorite assemblages.

Fig. 6. A coarse vein of chlorite, albite, magnetite and biotite cross-cutting a metamorphosed mafic volcanic (104587). Magnification x50, PPL.

Fig. 7. Tourmaline (dark blue) replacing plagioclase porphyroclasts in a sheared mafic volcanic (104590). Magnification x 50, PPL.

SAMPLE 104588

Hand-specimen: banded rock with alternating layers rich in quartz, feldspar and amphibole. The mafic layers exhibit a boudin structure.

Thin-section:

Mineral	Percentage abundance (%)
albite	80
actinolite	10
quartz	6
Fe oxide	2
pyrite	1
sphene	1

Mineralogy: the rock is composed of alternating layers rich in quartz and feldspar and layers relatively enriched in actinolite with subordinate quartz and feldspar. The fine-grained matrix (0.02 - 0.05 mm) is dominated by albitic feldspar (both twinned and untwinned) which has broadly granoblastic textures. The quartz shows undulose extinction, some sutured margins and a partial elongation which imparts a weak foliation to the rock.

The twin lamellae on the twinned albite grains are often slightly bent and do not show uniform extinction. Small prismatic crystals of actinolite (0.05 - 0.15 mm) are scattered throughout the quartz-feldspar-rich layers together with anhedral granules of sphene, sparse disseminated cubes of pyrite (0.08 mm) and occasional rounded zircon grains. The actinolite needles display a very weak sub-parallelism with the foliation but it is certainly not well defined as there are many grains which appear to be oriented at a high angle to the foliation.

The relatively mafic-rich layers have an increased amount of actinolite, sphene and pyrite with lesser amounts of quartz and feldspar. The amphibole tends to occur in elongate pods or stringers. Fine-grained actinolite occurs as a variably oriented to sub-parallel aligned prismatic crystals of similar size to the grains in the feldspar-rich parts.

There is also a relatively coarse pod (which may be part of a vein) dominated by chlorite, quartz, albite, pyrite (up to 0.5 mm), sphene and with minor subordinate actinolite.

Some quite strongly aligned and narrow bands rich in actinolite, sphene, chlorite and pyrite seem to be related to shearing. These seem to be fracture zones along which some recrystallisation of amphibole and sphene has occurred and along which fluids have been introduced producing chlorite. These features are also often coated with limonite due to the breakdown of pyrite, and some pyrites show limonitic rims.

Some similarly oriented fractures have undergone open space filling of quartz, albite and actinolite needles. The latter two have grown with their long axes perpendicular to the walls of the fractures. There are also some oblique fractures running at a high angle to the general cleavage/lineation indicated by the finer actinolite. These oblique fractures (which may be perpendicular to the cleavage) are dominated by sphene and actinolite which has grown with its c-axis parallel to the fracture and uncontrolled by stress. Some of these are also filled with chlorite.

Genetic interpretation: the rock appears to have been contact metamorphosed and subsequently subjected to moderate stress probably for a short time interval as many of the contact metamorphic textures are only partly modified. This rock appears to be more quartz-rich and generally more felsic compared to the previous sample (104587), which suggests a more felsic volcanic or volcanoclastic precursor. The predominance of sodic plagioclase (albite) does not favour a calcareous-siliceous sedimentary precursor. A Ca-rich dolomitic or calcareous sediment would typically have a high Ca/Na and hence plagioclase would be relatively calcic. Evaporitic sequences may be relatively Na-rich but these are usually also Cl-rich and scapolite is a common part of the metamorphic assemblage.

The Na-rich volcanics would presumably be produced by seafloor alteration if it was a sub-marine basalt. there is clearly some Ca in the rock though as actinolite and sphene are present, thus this process could not have been complete.

The presence of coarse pyrite in the quartz-albite-chlorite bands suggests introduction of the pyrite during the chloritic alteration. this appears to have been prior to the last deformation as chlorite is bent and the pyrite partly broken up. The quartz in these veins has sutured margins and does not retain evidence of contact metamorphism. Consequently the veins could have been introduced after the contact metamorphism but before the last deformation. The tension fractures filled with albite and fibrous actinolite appear to have formed last and possibly post-deformation as they cut across and disturb the foliation and shear-controlled actinolite foliation.

The coarse porphyroblasts of actinolite were also prior to the last deformation as they show some evidence of deformation and they are variably oriented i.e. not always in the general foliation some are perpendicular to this feature.

Regionally metamorphosed quartzite ?

0025

SAMPLE 104589 OR1 Grid : Hoseley Creek (Silicified Carbonate)

Hand-specimen: quartzite with some bands 2 - 3 mm wide relatively enriched in limonite.

Thin-section:

Mineral	Percentage abundance (%)
quartz	97
limonite	2
muscovite	1

Mineralogy: the rock is essentially a quartzite with a weak fabric due to the elongate crystals of quartz (0.2 - 0.3 mm) which have recrystallised in a moderate stress field. The quartz grains exhibit sutured margins and undulose extinction due to the stress. One patch of relatively fine-grained quartz (0.03 - 0.05 mm) has minor associated crystals of muscovite (1 - 2 mm long). These are bent and kinked indicating relatively low temperature deformation without significant recrystallisation.

There is a variability in the quartz textures which suggests that the deformation again was of limited extent and time. In some areas the quartz has a granoblastic polygonal form without sutured margins or undulose extinction and is only weakly deformed. This is consistent with recrystallisation under a pressure load that was equivalent in all directions as opposed to directed stress ie. contact metamorphism.

The last deformation does not appear to have been responsible for crystallisation of muscovite as the stress has caused translation of the cleavage in the muscovite at an angle of about 60° to the cleavage orientation. The muscovite shows minor staining by limonite around its margins and Fe-oxides have penetrated along quartz boundaries tending to occur in zones which represent fluid paths, These patches are unlikely to represent carbonate pseudomorphs.

Genetic interpretation: The rock was probably a quartz-rich sandstone which experienced moderate- to low-grade regional metamorphism resulting in the elongate quartz fabric and crystallisation of muscovite. Subsequent minor shear at low temperature has resulted in cleavage translation in muscovite and some recrystallisation of quartz.

SAMPLE 104590 [illegible]

Hand-specimen: a strongly banded metabasic rock with alternating layers relatively rich in chlorite or quartz. The quartz appears to form stringers and lenses due to dislocation and dynamic metamorphism.

Thin-section:

Mineral	Percentage abundance (%)
chlorite	40
plagioclase	30
quartz	20
magnetite	1
tourmaline	<1
hematite	<1
muscovite	<1

Mineralogy: this is a very chlorite-rich rock. The chlorite-rich matrix consists of intergrown platy chlorite which has a strong foliation that has been partly disrupted by deformation subsequent to the major recrystallisation. Within the chlorite matrix some subhedral to rounded albitised plagioclase phenocrysts have been retained due to the differential shear characteristics of the two phases. Feldspar generally seems to survive deformation reasonably well. In one part of the section along a layer parallel to the shear direction, some of the plagioclase phenocrysts have been replaced completely by tourmaline or tourmaline and quartz (Fig. 7). The tourmaline is a deep blue-green colour typical of Fe-rich schorls associated with granites.

Other chloritic layers include variable amounts of elongate angular pods of recrystallised quartz. The angular character of the quartz aggregates appears to be due to a later deformation which has caused partial break up of the quartz aggregates and recrystallisation of some chlorite oblique to the main stress direction (Fig.8). There is also some micro folding which appears to support this evidence. Relatively large magnetite octahedra/euhedra are also present within the chlorite-rich layers.

There is also some muscovite which appears to have been produced before the second deformation event as it is intergrown with the chlorite and deformed within it. Some of the muscovite has also recrystallised in the fractured quartz aggregates with chlorite. The potassic metasomatism which has produced the muscovite was probably related to a granite and the same fluids which produced the tourmaline. The hand-specimen texture of the rock is due to the differential weathering and hardness of the quartz-rich pods in the soft chloritic matrix.

Genetic interpretation: the abundance of chlorite in this rock is more consistent with a mafic precursor unless some pre-metamorphic hydrothermal alteration has occurred. This rock would have experienced some seafloor alteration producing the sodic plagioclase. It may also have been somewhat silicified accounting for the abundance of quartz. This may have occurred at the same time as tourmalinisation of the feldspar and sericitisation (as indicated by the association of quartz and tourmaline).

The elongate prismatic Fe-oxides are hematite or magnetite after primary hematite. These appear to have crystallised during the major deformation as they are quite strongly aligned in the primary cleavage.

Fig. 8. Growth of chlorite oblique to the principal cleavage in fractured quartz following a second deformation. Sample 104590. Magnification x100, PPL.

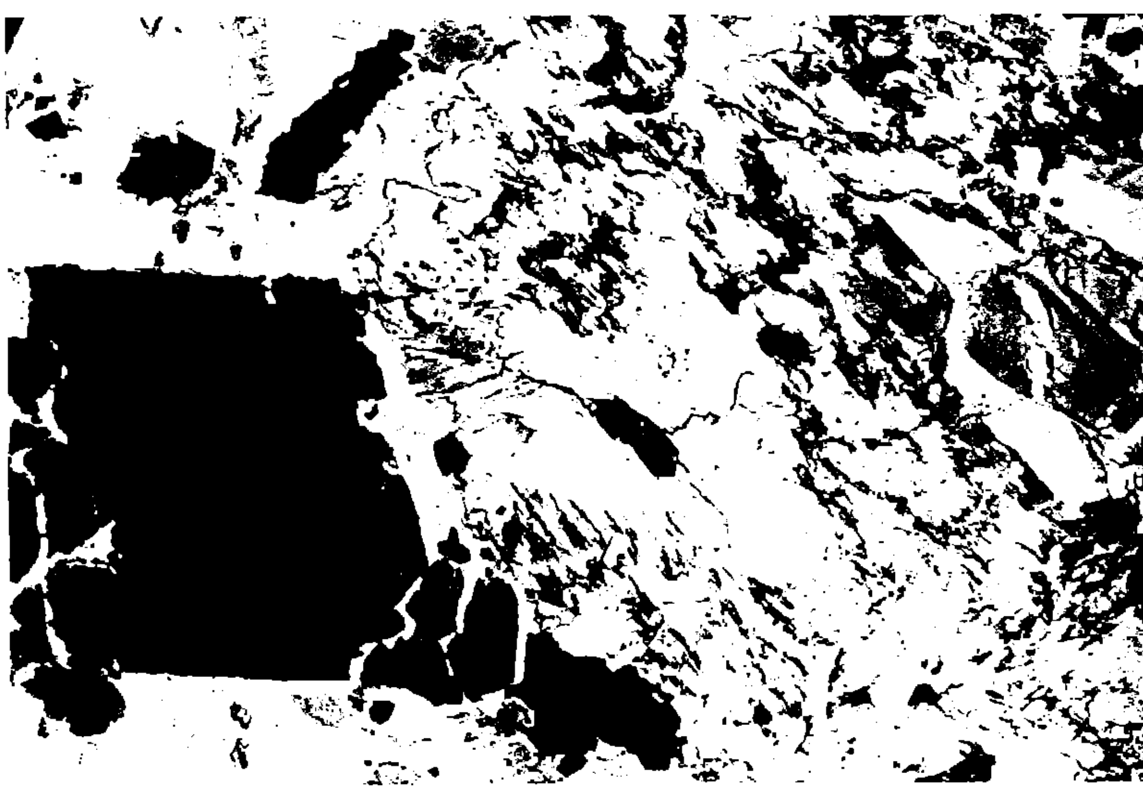

Fig. 9. Tourmaline replacing epidote and magnetite porphyroblasts in amphibole 104594. Magnification x200, PPL.

SAMPLE 104591

Hand-specimen: a weakly foliated metabasic rock with plagioclase and chlorite cut by a vein of feldspar and magnetite.

Thin-section:

Mineral	Percentage abundance (%)
plagioclase	55
chlorite	32
actinolitic amphibole	8
magnetite	4
tourmaline	<1

Mineralogy: tabular to equant crystals of plagioclase (0.1 mm) which often exhibit polygonal granoblastic texture are abundant, but with slightly sutured margins suggesting some stress. They may show simple, multiple or no twinning and twin lamellae are typically not bent. Plagioclase is sometimes intergrown in the groundmass with decussate chlorite aggregates but chlorite dominantly occurs in larger decussate clots (1 - 2 mm) which probably represent pseudomorphs after pyroxene. Most of these have ragged cores of blue-green amphibole which is partially chloritised resulting in some exsolution of fine magnetite.

A small amount of tourmaline euhedra occur throughout the rock but do not obviously replace other phases.

The rock does have a weak fabric defined by a slight flattening of the chlorite/amphibole aggregates, although individual crystals within the aggregates are not strongly aligned with this cleavage.

Xenoblastic patches of brown translucent material (possibly leucoxene), also exhibit a slight elongation (0.1 - 0.5 mm long) and these include relatively abundant magnetite octahedra or cubes.(0.05 - 0.1 mm).

The euhedral, prismatic crystals of tourmaline show zoning from dark bluish-green cores to pale rims. They occur intergrown with chlorite and feldspar and do not appear to be replacing either of these phases.

The section is cut by several veins of relatively coarse albite which has grown as tabular crystals with their long axes perpendicular to the vein walls.

Genetic interpretation: this originally basic volcanic rock may have recrystallised initially under contact metamorphic conditions and was subsequently subjected to relatively minor dislocation metamorphism.

SAMPLE 104592

Hand-specimen: a weakly foliated metabasic rock rich in chlorite, epidote and plagioclase with disseminated euhedral magnetite porphyroblasts and subordinate disseminated pyrite cubes.

Thin-section:

Mineral	Percentage abundance (%)
albite	60
chlorite	14
blue-green amphibole	10
epidote	8
magnetite	4
sphene	2
calcite	1
biotite	<1
tourmaline	trace

Mineralogy: the rock has a moderately strong cleavage defined by intergrown subparallel chlorite and blue-green amphibole crystals. These are moulded around rounded xenoblastic albite crystals (typically 0.1 - 0.3 mm across). Trails of aligned chlorite, amphibole or sphene inclusions within albite phenocrysts occasionally show evidence of rotation. Relatively large porphyroblasts or aggregates of epidote (typically 1 - 2 mm) show a yellowish-green to pale green pleochroism in grain margins and an unusual pale pink pleochroism in the crystal interiors which suggests a significant piemontite (Mn) component. Some epidote porphyroblasts appear to be aligned with the cleavage whereas others appear to be cross-cutting and may be associated with coarse crystals of calcite.

Magnetite occurs as octahedral crystals (0.3 - 1 mm) which may be partially enclosing feldspar, epidote or chlorite. Sphene occurs in well defined trails parallel to cleavage and closely associated with chlorite and amphibole. The magnetite porphyroblasts appear to have been preenrt prior to metamorphism as the relatively large grains of chlorite have grown in adjacent pressure shadows, and the foliation often appears to wrap around them.

There is also a trace of deep blue-green (schorlite) tourmaline occurring in prismatic crystals which cross-cut the cleavage.

Genetic interpretation: the mineralogical and textural evidence suggests that this rock was a metabasalt which experienced strong dynamic metamorphism with consequent recrystallisation of albite, chlorite, amphibole and possibly some epidote.

The tourmaline appears to be due to metasomatic introduction of Fe- and B-rich fluids.

SAMPLE 104593

Hand-specimen: a fine-grained metabasic rock with abundant chlorite, plagioclase, epidote, magnetite porphyroblasts and minor disseminated pyrite.

Thin-section:

Mineral	Percentage abundance (%)
albite	65
chlorite	10
amphibole	10
epidote	8
magnetite	4
sphene	2
limonite	1

Mineralogy: this sample has essentially identical mineralogy to 104592, but is finer-grained. Texturally, this rock exhibits a less well defined foliation. Intergrowths of chlorite and prismatic amphibole crystals only show a very weak preferred orientation and many crystals cross-cut this general direction, as do elongate porphyroblasts of epidote (in aggregates). The boundaries of the feldspar with each other are sutured and while they may have been polygonal or porphyroblastic, subsequent recrystallisation in a weak stress field has modified these.

Euhedral porphyroblasts of magnetite (0.1 - 0.2 mm) appear to be late and cross-cutting. They rarely include epidote only. Albite is generally fine-grained (0.03 - 0.08 mm), whereas amphibole is typically larger (0.05 - 0.2 mm) and epidote porphyroblasts range up to 0.2 - 0.7 mm long. Sphene tends to occur as granular aggregates disseminated throughout the rock.

The specimen has been substantially fractured and veined. One particular vein is characterised by an abundance of relatively coarse epidote (0.1 - 0.5 mm) which is very similar to the epidote porphyroblasts. The vein also includes several small and larger (0.5 mm) magnetite euhedra which partially enclose epidote and albite. These appear to have grown across the vein and wall-rock. The vein has had some recent movement and fracturing which has resulted in a limonite filling, which has also fractured the epidote and magnetite. Another vein is dominated by relatively coarse chlorite, albite and magnetite. Again some late movement has fractured the magnetite with minor limonitic alteration.

Genetic interpretation: this does not appear to be as highly strained as 104592. The presence of epidote in the veins implies that some may have been introduced during metasomatism.

SAMPLE 104594

Hand-specimen: foliated amphibolite with magnetite porphyroblasts.

Thin-section:

Mineral	Percentage abundance (%)
albite	50
amphibole	27
chlorite	8
epidote	5
magnetite	4
sphene	4
tourmaline	2

Mineralogy: this specimen has similar mineralogy to 104592 and 104593. However it shows some quite different and variable textures. The bulk of the rock has a fairly unstrained appearance similar to 104593, although it is slightly finer-grained. Albite grains are typically 0.02 - 0.05 mm across and display a weak elongation. The mafic minerals appear to be slightly more abundant in this rock than 104593. The blue-green amphibole typically has actinolite overgrowths however the epidote does not exhibit the zoning that is apparent in 104592.

Subparallel alignment of intergrown amphibole and chlorite, with some trails of sphene define a weak metamorphic foliation. The rock also exhibits several narrow zones of high strain (1 mm to several mm wide). these zones are parallel to the cleavage and display several different features. One has abundant chlorite and magnetite, the latter appears to have been partially hematised and granulated and there is evidence for growth of sphene on these broken magnetite fragments. Several other bands have abundant chlorite and zoned crystals of tourmaline (0.3 mm long). Any magnetite in these zones exhibit reaction rims of hematite. Epidote occasionally grows in these rims and may be locally concentrated along the margins, although chlorite and tourmaline are generally dominant.

A wider zone shows evidence of higher strain with strongly aligned amphibole and chlorite and trails of sphene. The latter trace out a second deformation of small scale assymetric folds with a crenulation cleavage. The amphibole and chlorite (0.05 - 0.1 mm long) host large porphyroblasts of epidote, tourmaline (0.5 - 1 mm) and magnetite. The latter appear somewhat more rounded and broken than those in the less strained portion of the rock.

Tourmaline is clearly replacing epidote porphyroblasts in places and possibly replacing magnetite although this is more equivocal (Fig. 9).

Genetic interpretation: the epidote and magnetite porphyroblasts appear to have been present in this metabasic rock during a high strain event. The magnetite shows less wrapping around by chlorite and amphibole than the epidote but may have survived due to its strength in a relatively soft deforming matrix (as feldspar does). The tourmaline definitely appears to be later, probably post-deformation.

Epidote and amphibole in this rock are also zoned. The amphibole varies from blue-green cores to actinolite rims and the epidote has yellow-green rims to more colourless cores. This is in the opposite sense to 104592.

SAMPLE 104595

Hand-specimen: foliated amphibolite with minor disseminated pyrite.

Thin-section:

Mineral	Percentage abundance (%)
amphibole	63
albite	20
epidote	8
sphene	6
magnetite	3
chlorite	<1

Mineralogy: this rock is relatively coarse-grained and enriched in mafic minerals compared with 104592 and 104594, and has experienced moderate to high strain. The amphibole in the rock is essentially all blue-green amphibole without the actinolitic rims present in the preceding samples. Chlorite is also only present in trace amounts indicating that there has been minimal retrogression of the higher grade assemblages.

Untwinned albite is intergrown with amphibole but is in relatively low abundance compared with the previous samples, and it typically occurs as slightly elongate grains with sutured margins. The elongate, prismatic amphibole crystals are generally strongly aligned depicting a moderate cleavage/lineation. However, there has been some refolding of the original cleavage into small scale folds.

Relatively large (1 - 2 mm long) stringers of sphene aggregates occur parallel to the foliation but also exhibit this refolding. These often have ragged cores of opaque material within them (probably ilmenite) which acted as nuclei for the crystallisation of sphene.

Xenoblastic aggregates of epidote (including grains 0.1 - 0.5 mm long) tend to be concentrated in feldspar-rich pods or bands, whereas the more mafic (amphibole-rich) layers contain the sphene. There are a few relatively large (1 mm long) porphyroblasts of amphibole which occasionally cut across the foliation direction. Porphyroblasts of magnetite (0.05 - 0.1 mm) are typically euhedral where not in contact with sphene aggregates. The magnetite seems to be finer-grained, more irregular and broken up in the highest strain portions of the rock.

The rock is cut by a vein of albite and amphibole. The albite has grown with the long axes perpendicular to the walls and the vein runs at a high angle to the foliation. Fibrous amphibole has grown across the vein from the walls, indicating that the vein may have been pre-deformation.

Genetic interpretation: The feldspar-poor nature of the rock indicates a very mafic basaltic composition, more so than samples 104593 and 104594.

SAMPLE 104596

Hand-specimen: banded quartzo-feldspathic with some relatively large plagioclase crystals in a finer matrix, and with minor chlorite.

Thin-section:

Mineral	Percentage abundance (%)
plagioclase	70
quartz	12
carbonate	5
epidote	4
chlorite	3
magnetite	3
amphibole	2
sphene	1
pyrite	trace

Mineralogy: this rock has experienced moderate to high strain. Relatively coarse (1 - 2 mm) xenoblastic crystals of sodic plagioclase (albite) with sutured margins occur in a matrix of finer (0.2 - 0.3 mm) xenoblastic to tabular plagioclase and extensively recrystallised quartz aggregates. The quartz occurs in elongate grains (0.1 - 0.2 mm long) with strongly sutured margins and shows strain extinction. The plagioclase often exhibits albite twinning and occasionally also carlsbad twinning. The twin lamellae are generally bent and display variable extinction.

Elongate quartz crystals are strongly aligned depicting a foliation which has been refolded in small scale folds. The quartz aggregates are often wrapped around larger plagioclase crystals which are regarded as porphyroclasts that have preferentially survived the granulation and recrystallisation under high strain.

Carbonate is a relatively abundant phase in this feldspathic rock and appears to be replacing plagioclase in part. Ferromagnesian phases include prismatic crystals of blue-green hornblende (0.1 - 0.4 mm long) and epidote (0.1 - 0.5 mm long), some of which are fractured and broken. Both these phases are aligned in the foliation direction and together with some retrogressive chlorite and trails of sphene help define secondary fold patterns.

Magnetite octahedra (0.1 - 0.2 mm) and aggregates of grains are scattered throughout the rock but in the higher strain zones the magnetite occurs as stringers and highly irregular elongate grains.

Genetic interpretation: this rock appears to have been some sort of sodic granitoid or trondjemite with no K-feldspar, abundant plagioclase and quartz and minor ferromagnesian phases. It has experienced moderate to quite high strain conditions during dislocation metamorphism that has resulted in a significant decrease in the grain size of some plagioclase and most of the quartz. However some relatively large plagioclase porphyroclasts have survived.

0035

SAMPLE 104597

Hand-specimen: banded quartzo-feldspathic rock with a foliation defined by chlorite-rich bands.

Thin-section:

Mineral	Percentage abundance (%)
plagioclase	70
quartz	15
chlorite	8
magnetite	3
carbonate	2
epidote	1
tourmaline	<1
muscovite	<1
zircon	<1
sphene	<1

Mineralogy: this sample is very similar in mineralogy and texture to 104596. It differs in the absence of amphibole and has lesser amounts of epidote. However, the textural features and grain size characteristics are closely comparable. Relatively large (1 - 2 mm) plagioclase porphyroclasts are preserved in a fine-grained matrix of plagioclase and extensively recrystallised quartz. Plagioclase twin lamellae are invariably bent with variable extinction (Fig. 10).

Chlorite is the dominant mafic mineral. It occurs as subparallel plates often wrapped around the larger plagioclase grains but still defining a foliation through the rock together with elongate aggregates of quartz. Epidote is a relatively minor phase which occurs partly replaced by chlorite and sphene aggregates and occasionally with minor muscovite.

Several euhedral crystals of zircon (0.1 mm) and zoned schorl-rich tourmaline (deep blue-green to brown pleochroism) are scattered throughout the rock, and sphene occurs in granular aggregates with chlorite and epidote. Magnetite octahedra are disseminated throughout but a considerable amount of the magnetite occurs as irregular elongate stringers due to granulation during dislocation metamorphism. Some show weak marginal alteration to hematite. Carbonate is abundant through the groundmass and is found partially replacing plagioclase.

Genetic interpretation: this rock appears to be closely related to 104596 and 104598. They appear to be oversaturated sodic intrusives with minor mafic minerals which were emplaced prior to the major deformational event. This deformation has resulted in significant granulation and grain-size reduction, plus development of a foliation in the rock.

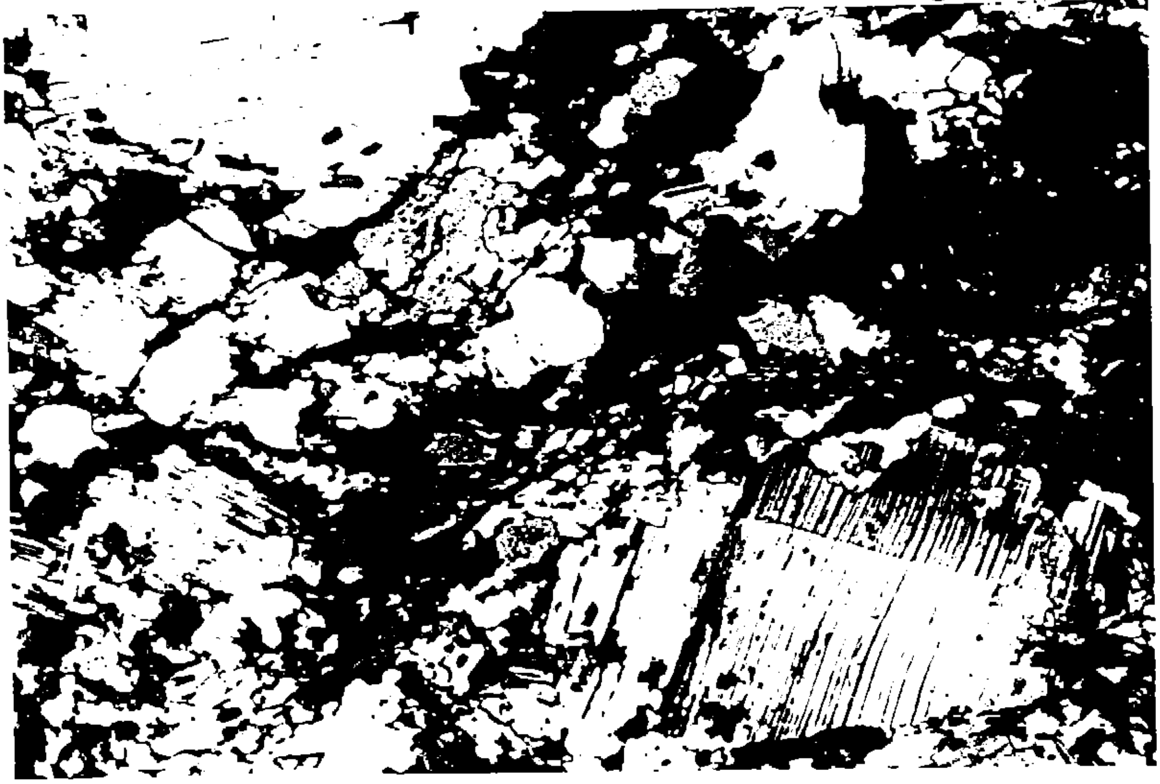

Fig. 10. Bent twin lamellae in plagioclase porphyroclasts, and fine recrystallised matrix quartz in deformed sodic granitoid 104597. Magnification x50, PPL.

Fig. 11. Albite, chlorite and apatite (pigmented with Fe-oxide) vein in metabasalt 104620. Magnification x50, PPL.

SAMPLE 104598

Hand-specimen: a medium-grained quartzo-feldspathic rock with a weak foliation.

Thin-section:

Mineral	Percentage abundance (%)
plagioclase	76
quartz	12
chlorite	5
biotite	2
hematite	2
sphene	2
zircon	<1

Mineralogy: this sample has similar mineralogical and textural characteristics to 104596 and 104597. However it appears to have experienced less intense granulation and a greater proportion of coarse plagioclase porphyroclasts have survived the deformation. Nevertheless, both the coarse and fine plagioclase and the matrix quartz have extensively sutured margins and display strain extinction. The plagioclase twin lamellae are invariably bent. In addition, elongate quartz grains in the matrix, together with platy chlorite, define a moderately strong foliation. Chlorite occurs in bands intergrown with biotite and granular aggregates of sphene, often wrapped around the larger plagioclase porphyroclasts.

A few prismatic crystals of zircon and tourmaline (0.1 - 0.2 mm) are scattered throughout the matrix. The tourmaline is zoned from blue-green cores to darker grey-green rims and appears to be a schorl-rich type. Hematite pseudomorphs after magnetite octahedra are disseminated throughout.

Genetic interpretation: this rock has had a similar history to the previous two samples and probably represents a related intrusive if not part of the same intrusive. Granulation has been less intense, hence the coarse and even-grained character of the precursor intrusive is more apparent in this sample.

EXTRA OWEN-MEREDITH SAMPLES

SAMPLE 104609

Thin-section:

Mineral	Percentage abundance (%)	Size (μm)
Quartz	70	500
Magnetite	20	40
Pyrite	3	150
Chalcopyrite	<0.5	150
Carbonate	trace	50
Goethite	5	
Covellite	<0.5	

Host-rock: a highly deformed rock consisting of interlayered quartz and magnetite-pyrite bands, up to 1 cm thick. The thicker of these have planar contacts which may well constitute bedding, whereas most of the thin (<1 mm wide) magnetite layers are interlaced and irregular, suggestive of syn-tectonic magnetite growth. Euhedral to subhedral pyrite particularly concentrates in the thicker magnetite bands, but is also present in disseminated form throughout the quartz bands. Chalcopyrite is confined to the thicker magnetite bands where it is disseminated within pyrite, but more commonly occupies cracks and fractures in pyrite and magnetite.

Deformation is mainly expressed via quartz. Quartz displays strong elongation, with new growth of fine polygonal quartz on the sutured contacts of larger quartz grains approaching a sub-mylonitic texture. Magnetite and pyrite have both experienced the deformation, as evidenced by quartz deformation around annealed pyrite and by cracking in magnetite.

Significant supergene oxidation has occurred concentrating on fine fractures. Limonite and goethite fill fractures adopting a mammillary form, and concentrically altering pyrite, magnetite and chalcopyrite. Covellite is distinctly replacing chalcopyrite in most instances. Cuprite may also be present, intergrown with limonite adjacent to chalcopyrite; this is difficult to verify because the two phases share similar petrographic features.

Genetic interpretation: All components have experienced the dynamic metamorphism. Some magnetite was precipitated and recrystallised in fractures during tectonism. The layered nature of quartz and magnetite is evidence that the rock developed as a sedimentary iron formation containing some pyrite and chalcopyrite, although this needs to be viewed in the context of the outcrop pattern. Oxidation of magnetite and sulphides is evidence of proximity to meteoric waters in the present day, or close to the bedrock water table.

SAMPLE 104617

Hand-specimen: a tourmaline-rich rock with no distinctive fabric.

Thin-section:

Mineral	Percentage abundance (%)
tourmaline	70
tremolite	30
magnetite	<1

Mineralogy: interlocking prismatic crystals of tremolite (0.3 - 0.5 mm long) which often exhibit simple twinning occur in the interstitial areas between large (1 - 2 mm) xenoblastic aggregates of tourmaline. The latter comprise aggregates of prismatic crystals which commonly display colour zoning from pale buff to blue-green cores to pale brown to dark brown rims. Sometimes the complete aggregate shows a rim of the darker brown pleochroic variety. Fine randomly oriented trails of granular sphene (0.1 - 0.2 mm) occur as inclusions within the tourmaline and also as slightly coarse aggregates with the interstitial tremolite.

The rock is largely devoid of opaques except for a few angular fractured grains of magnetite (0.1 mm).

Genetic interpretation: this rock has close mineralogical affinities with 106574, and although they have the mineralogical characteristics of skarn rocks, 104574 has a Ti/Zr ratio and concentrations of Ti and Zr (immobile elements) which suggest it had a basaltic precursor. Both rocks appear to have experienced extensive alteration by granitic fluids. the zoning in the tourmaline appears to be from a more magnesian core to a more Fe-rich composition. This change in composition possiblyoccurred in response to dilution of Mg in the original rock by relatively Fe-rich fluids.

SAMPLE 104620

Hand-specimen: amphibolite cut by a coarse vein of chlorite and albite.

Thin-section:

Mineral	Percentage abundance (%)
plagioclase	50
amphibole	45
sphene	3
magnetite	2
Vein	
albite	70
chlorite	25
apatite	4
biotite	1

Mineralogy: a very weak foliation is indicated by the preferred orientation of intergrown prismatic amphibole crystals (0.1 - 0.2 mm long) although there is some evidence of a second foliation direction perpendicular to the first. The amphibole is pleochroic from a deep blue-green to a buff colour, occasionally with narrow pale-green actinolitic rims.

Plagioclase is usually untwinned or rarely albite twinned, and occurs as small (0.05 - 0.1 mm) xenoblastic grains with slightly sutured margins. Sphene occurs in granular aggregates which are not significantly strung out or aligned. Euhedral octahedra of magnetite (0.03 - 0.1 mm) are disseminated throughout the rock.

The section is traversed by several coarse-grained veins rich in albite, chlorite and quartz with subordinate apatite and magnetite.

The plagioclase occurs as tabular crystals (0.3 - 1 mm) with albite twinning which is commonly bent indicating mild deformation since their emplacement. Chlorite occurs as decussate aggregates interstitial to the feldspars or in pods with minor associated green-brown biotite. Apatite occurs as large (0.5 - 2 mm) individual crystals with the feldspar but is distinguished by an unusual cloudy alteration (Fig. 11). This is the only occurrence of apatite observed in any of the rocks studied, and although uncommon, does occur as large hydrothermal crystals in the Mt Lyell ore body.

One of the veins also contains elongate quartz crystals with sutured margins that are oriented perpendicular to the vein walls. The veins are clearly cross-cutting the host amphibolite and the lower apparent strain levels they have experienced suggest a late-deformational timing for their emplacement.

A few porphyroblasts of magnetite occur within the veins and several straddle the boundary between the vein and the host minerals, suggesting that this coarse magnetite crystallised very late.

Genetic interpretation: this sample appears to be a metamorphosed mafic volcanic that has experienced several episodes of deformation and metamorphism to amphibolite facies grade. There seems to be minor evidence of retrogression in the form of actinolitic rims on some of the higher pressure-temperature amphiboles. This rock has not experienced the very high strain which characterises many of the other metamorphosed mafic rocks.

SAMPLE 104635

Hand-specimen: banded amphibolite with alternating amphibole and plagioclase-rich bands.

Thin-section:

Mineral	Percentage abundance (%)
albite	65
chlorite	20
quartz	15
epidote	5
magnetite	3
sphene	2

Mineralogy: tabular to xenoblastic porphyroclasts of plagioclase (0.1 - 0.3 mm) display subparallel alignment and are wrapped around by thin layers of intergrown chlorite which define a strong foliation. Elongate pods or aggregates of strongly recrystallised quartz grains also occur between layers relatively rich in chlorite which have associated prismatic crystals of epidote.

Magnetite occurs disseminated throughout the rock as elongate irregular grains and only rarely with octahedral outlines.

Genetic interpretation:this rock may have been a relatively evolved intermediate to mafic volcanic with a greater proportion of felsics to mafics than 104620. This specimen has also been subjected to much greater strain resulting in the substantial granulation of feldspar and magnetite and recrystallisation of quartz. Original higher grade phases (eg. amphibole) appear to have been completely retrogressed to chlorite and epidote.

SAMPLE 104636 Reece Power Stn. (? [illegible] Island)

Hand-specimen: quartz-feldspar-chlorite-muscovite schist.

Thin-section:

Mineral	Percentage abundance (%)
quartz	55
plagioclase	30
muscovite	10
chlorite	5
sphene	<1
zircon	<1

Mineralogy: untwinned or simply twinned albite occurs in augen shaped aggregates which are draped by thin continuous bands (0.1 - 0.2 mm wide) of intergrown chlorite and muscovite. These bands are separated by layers of elongate quartz aggregates which have intricately sutured margins and undulose extinction. Individual feldspar grains in the aggregates often have aligned or curved rows of inclusions which indicate substantial rotation of the porphyroclasts during shearing.

Genetic interpretation: this rock could have been a quartzo-feldspathic sedimentary rock with interlayered pelitic bands or a granitic intrusive. The presence of relict plagioclase porphyroclasts is not definitive, however the relative abundance of muscovite would suggest a more potassic precursor than the sodic trondhjemite intrusives such as 104596, 104597 and 104598. This rock has been subjected to very high strain and is very sheared. This is consistent with the field observations. However, the quartz- muscovite-rich mineralogy is more consistent with a sheared psammo-pelitic schist than a sheared mafic volcanic rock.

SAMPLE 104637

Hand-specimen: unfoliated amphibolite rich in amphibole and plagioclase.

Thin-section:

Mineral	Percentage abundance (%)
amphibole	55
plagioclase	25
epidote	10
chlorite	5
carbonate	3
garnet	2

Mineralogy: this rock does not display a foliation or any preferred mineral orientation. It consists of felted masses of prismatic amphibole crystals (0.1 - 0.5 mm and up to 3 mm long). The amphibole is pleochroic from deep blue to a buff colour with an intermediate pale lilac colour. Narrow rims of pale-green actinolitic amphibole represent a retrogressive phase. The blue-green amphibole in this case is probably a ferro-actinolite in view of its relatively high 2V (~70°), and high birefringence compared with the blue-green amphiboles from some other mafic schists which have optical characteristics transitional to glaucophane. The amphibole-rich aggregates also contain clots of decussate green chlorite, aggregates of pale brown idioblastic garnet and sphene (Fig. 12).

The remaining areas are dominated by untwinned plagioclase feldspar and abundant prismatic or granular epidote plus minor amounts of garnet. The plagioclase occurs as relatively large (0.3 - 0.5 mm) xenoblastic grains including the epidote and garnet, as well as some strongly zoned amphibole crystals. The epidote is also typically zoned having cores with a pink to pale brown pleochroism rimmed by narrow zones of more typical pale green to yellow pleochroic epidote. The cores are likely to be Mn-rich piemontites which would suggest that the garnets are also Mn-rich.

Genetic interpretation: the rock has experienced very little strain compared with 104636. In view of the close proximity of the samples in the field, their different textural features would suggest that 104637 was emplaced after the main deformation events. Alternatively it may represent a kernel of material that escaped the high strain which was preferentially taken up by the enclosing rocks.

It is difficult to determine from the mineralogy alone whether the precursor of this rock was a mafic volcanic or intrusive or some sort of calcareous metasediment. Some geochemical data (eg. Ti/Zr values) would help resolve this problem. However, the presence of Mn-rich epidotes and probably Mn-rich garnets would suggest some metasomatic modification of the rock, as these are both common skarn-related phases.

0045 SAMPLE 104638

Hand-specimen: leucocratic medium grained silicic intrusive rock with minor disseminated magnetite, pyrite and tourmaline veins.

Thin-section:

Mineral	Percentage abundance (%)
plagioclase	65
quartz	30
magnetite	1
chlorite	1
sphene	1
zircon	<1
Vein	
tourmaline	2

Mineralogy: this sample consists of xenoblastic to tabular plagioclase crystals (0.3 - 1 mm long) which have albite twin lamellae that are bent and hence exhibit variable extinction. The plagioclase crystals often have sutured margins and if not intergrown are typically separated by fine aggregates of recrystallised quartz. The quartz exhibits strain extinction and tends to occur in elongate aggregates with a consistent preferred orientation.

Other intergranular phases include minor prismatic crystals of blue-green amphibole (0.1 - 0.2 mm long), aggregates of chlorite and sphene and idioblastic zircon crystals. Octahedral crystals of magnetite (0.1 - 0.2 mm) are also disseminated throughout.

The section is also transected by two veins of tourmaline (0.1 - 0.3 mm wide). The tourmaline shows concentric colour zoning in sections normal to the c-axis from greenish brown margins to almost black in the core. The pleochroism is from dark greenish-brown to a reddish-brown. Introduction of the tourmaline has caused some oxidation of the magnetite porphyroblasts to hematite. Several prismatic tourmaline crystals appear bent and have therefore probably experienced some dislocation metamorphism. The bulk of the rock has experienced moderate levels of strain resulting in the recrystallisation of quartz and destruction of any primary igneous textures.

Genetic interpretation: This particular sample is very similar to the other 'sodic granitoid' samples described by Minpet Services (and again in this report) ie. 104566, 104596 - 104598.

The tourmaline in this sample is similar to that occurring in veins within 104598, however the different pleochroism in samples 104617 and 104574 suggest a different composition, probably more magnesian. This would be consistent with the reaction of the introduced fluids with a moderately Mg-rich basaltic precursor, in contrast to the Mg-poor sodic granitoid host. The inferred Fe-rich schorl composition of the tourmaline from the granitoids would reflect the Fe-rich nature of the introduced fluids. This is the most common type of tourmaline developed around granitic intrusives, and these veins may in fact be derived from late-stage fluids evolved from unsolidified parts of the same intrusive.

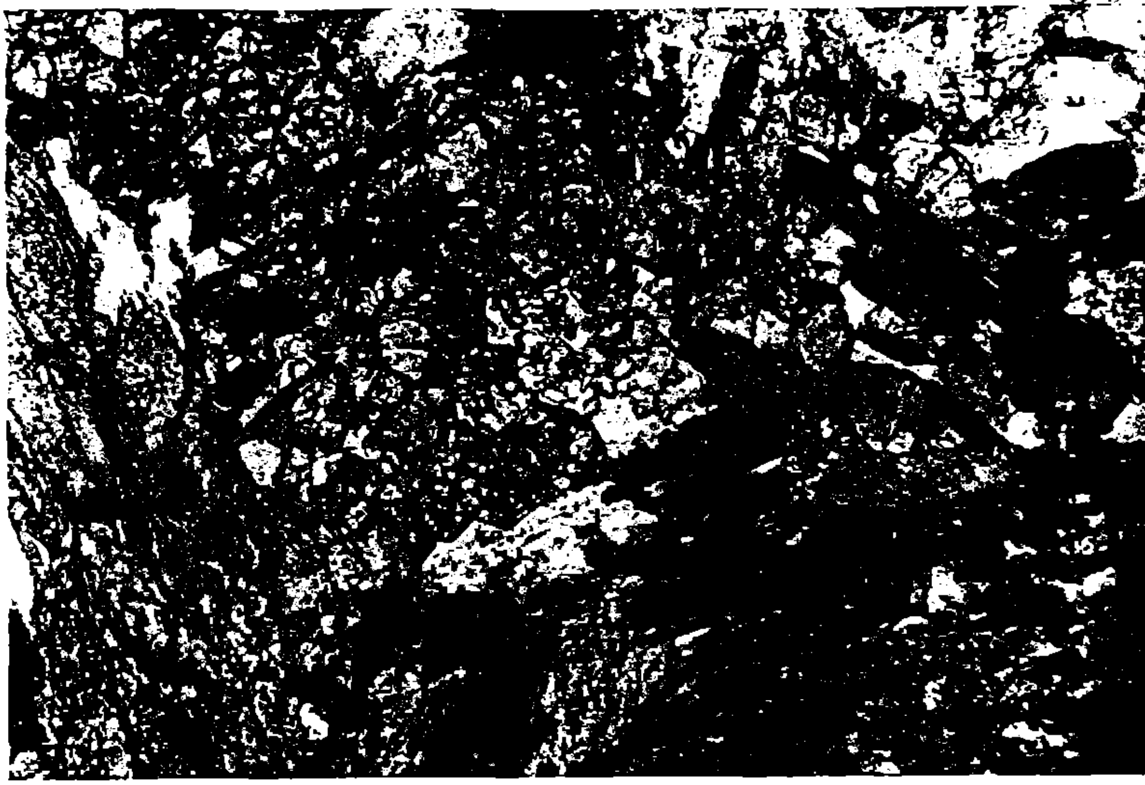

Fig. 12. Aggregate of idioblastic garnet crystals with blue-green amphibole, epidote and chlorite. Sample 104637. Magnification x100, PPL.

Fig. 13. Transposition of an early cleavage by the horizontal cleavage, delineated by the parallel platy muscovite and chlorite. Sample AP1 70.7. Magnification x100, CPL.

PETROGRAPHIC DESCRIPTIONS OF IRONSTONES AND HOST ROCKS FROM THE ALPINE AREA.

SAMPLE AP1 70.7 m

Hand-specimen: quartz-muscovite-chlorite schist.

Thin-section:

Mineral	Percentage abundance (%)
quartz	40
muscovite	35
carbonate	15
plagioclase	5
chlorite	5
pyrite	<1
zircon	trace
tourmaline	trace

Mineralogy: this is a strongly foliated rock consisting of layers relatively enriched in muscovite which alternate with relatively quartz- and carbonate-rich layers. Untwinned or simply twinned xenoblastic to tabular grains of plagioclase exhibit evidence of rotation and are wrapped by intergrown crystals of muscovite and chlorite. The muscovite-rich layers vary in thickness (up to 2.5 mm) and exhibit a strong preferred orientation or crenulation cleavage. They are separated by relatively quartz-rich layers in which the muscovite and chlorite are oblique to the dominant S_2 foliation and depict the refolded S_1 foliation (Fig. 13).

The presence of small scale kink folds in the muscovite-chlorite-rich layers which depict S_2 suggest the presence of a third minor deformation event.

The quartz-, feldspar- and carbonate-rich layers have abundant quartz occurring as slightly elongate and sutured grains with ubiquitious strain extinction. Some of the carbonate occurs as similarly elongate grains with strain extinction, however there are also some larger xenoblastic pods which exhibit no evidence of strain. These may have crystallised late-syn or post-deformation. Some unstrained carbonate appears to have been remobilised into late fractures which are oriented approximately perpendicular to the implied stress direction of the youngest deformation event. A few ring grains of tourmaline and zircon are scattered throughout the rock.

Genetic interpretation: the precursor to this specimen was probably a thin bedded mudstone/siltstone with alternating layers relatively enriched in quartz, feldspar and clays. The present banding is unlikely to reflect the original bedding, considering the rock has been subjected to quite high strain and multiple deformation and recrystallisation events.

SAMPLE AP1	77.0 m	Pyrite-filled vein , shear or band.	GJD

Hand-specimen: A pyrite-filled vein or shear 1.5 cm wide containing small slivers of wallrock (with a sinistral shear sense to their shapes) hosted within a plagioclase-quartz-muscovite schist containing a moderately well-developed differentiation cleavage. Thin (2 mm wide) carbonate ± pyrite veins anastomose at a high angle to the foliation. They do not cross-cut the pyrite zone.

Thin-section:

Mineral	Percentage abundance (%)	Size (μm)
Pyrite	80	150
Carbonate	20	80
Chalcopyrite	<0.5	<5
Sphalerite	~0.5	20-25
Pyrrhotite	<0.5	5-10
Galena	<0.5	10-15

Host-rock: The host-rock is a plagioclase-muscovite-quartz ± K-spar ±chlorite ± pyrite ± sphalerite schist, with minor tourmaline, magnetite and carbonate. It is severely strained, exhibiting an early slaty cleavage overprinted strongly at a high angle by muscovite and highly preferred orientations of quartz. A uniform sinistral movement sense is suggested by the S-C relationships associated with the second cleavage, particularly around knots of quartz feldspar and clots of pyrite. Sphalerite occurs as fine (10-15 μm) disseminated grains throughout the host.

Pyrite Vein/Shear: This feature is notable for the absence of magnetite, and the presence of fine sphalerite as rounded inclusions in pyrite. Such sphalerite is dotted with fine chalcopyrite inclusions (chalcopyrite 'disease'). Galena and sphalerite have a similar included form, and all are in syn-metamorphic equilibrium with coarse pyrite. Pyrite itself occurs as coarse primary fragments which exist as larger kernels amongst finer fractured pyrite embayed by carbonate, quartz, and minor sphalerite. At the edge of the sulphide zone, pyrite forms thin slivers and trains around lenses of strongly reshaped muscovite. An important observation is that massive muscovite occurrences are confined to the interior of the pyrite zone, or to 1 cm of one margin of this zone, which may therefore have constituted a former sericitic alteration selvedge which has been recrystallised.

The younger vein which transects host-rock, but not sulphide, contains carbonate ± pyrite, with ubiquitous and comparatively coarse sphalerite (with inclusions of chalcopyrite). This vein seems likely to predate the main pyrite-sphalerite zone, because pyrite would commonly fracture brittly, as it has elsewhere in the collection. This relationship, and the parallelism of the major pyrite vein with the cleavage, is the best evidence for its epigenetic origin, but in detail the grain-textures are ambiguously syn-tectonic.

SAMPLE AP1	81.7m	Massive pyrite	GJD

Hand-specimen: Massive granular pyrite containing uncommon quartz-filled fractures.

Thin-section:

Mineral	Percentage abundance (%)	Size (μm)
Carbonate	10	120
Quartz	2	120
Muscovite	2	30
Sphalerite	3-5	100
Pyrrhotite	tr	10
Galena	tr	10
Chalcopyrite	<0.5	10
Tourmaline	tr	4

Mineralogy: This is a relatively less-deformed rock compared to others within the examined suite.

Pyrite takes two forms: (1) very coarse zones 0.5 - 2cm across with obvious carbonate-filled extension fractures, and (2) fine recrystallised pyrite in a carbonate-sphalerite-quartz matrix, where pyrite forms euhedral cubes averaging 150 μm across, surrounded by splinters of finer sphalerite (Fig. 15). The contact between the two is relatively sharp, with few gradational fragment sizes, but in places there is clear evidence of separation of small pieces away from the main pyrite nucleus, as of icebergs calving from a stable icesheet (not intended to be an analogous process!).

Sphalerite is mainly confined to the second textural association, of which it comprises ~20%, and may have facilitated the recrystallisation of the pyrite. Minor sphalerite, galena, pyrrhotite and chalcopyrite occur as rounded inclusions in coarse pyrite in syn-metamorphic equilibrium.

There is no evidence at the slide scale of the growth of this pyrite by replacement of magnetite, because no relict magnetite is anywhere evident.

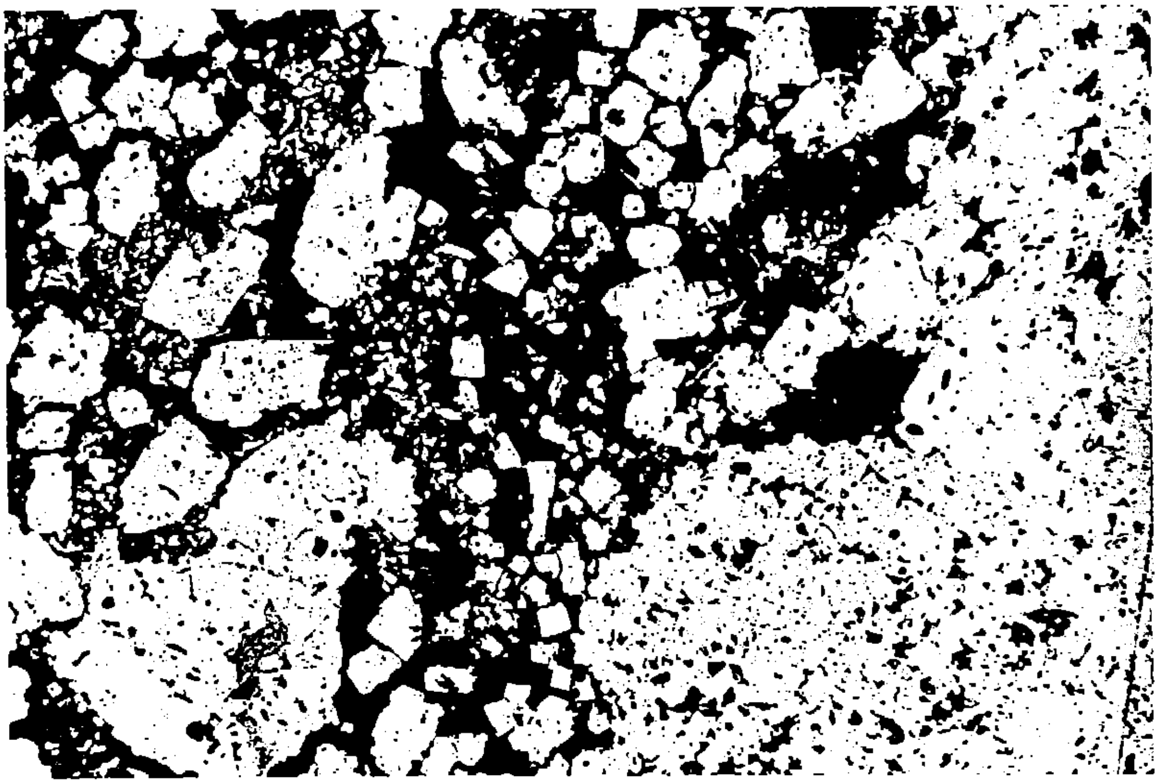

Fig. 15. Granulation of pyrite and recrystallisation as idioblastic porphyroblasts in a matrix of sphalerite (light grey) and carbonate (dark grey). Sample AP1 81.7. Magnification x100, RL.

Fig. 16. A vein zoned from carbonate at the margins to quartz and chalcopyrite in the centre. The vein transects pyrite and magnetite but there is no evidence of sulfidation of magnetite or alteration of pyrite by chalcopyrite. Sample AP1 85.0. Magnification x100, RL.

SAMPLE AP1 85.0 m Strongly foliated pyrite-magnetite ± chalcopyrite GJD

Hand-specimen: A strongly foliated rock in which crudely defined bands of pyrite are distinctively separate from these rich in chalcopyrite-quartz, and a single which (2cm) pyrite-magnetite layer.

Thin-section:

Mineral	Percentage abundance (%)	Size (µm)
Pyrite	40	100
Magnetite	40	120
Carbonate	8	100
Quartz	10	80
Chalcopyrite	2	50
Muscovite	tr.	120
Barite	tr.	250

Mineralogy: Pyrite and magnetite are closely intergrown in this slide, although this was not apparent in the hand-specimen. The extent of deformation is strong, but not as severe as found in AP2 sections.

Chalcopyrite, as noted in hand-specimen, is confined either to more siliceous zones between pyrite layers, or to discrete, late-tectonic, cross-cutting veins (~2mm wide) zoned inward from carbonate to polygonal quartz + coarse chalcopyrite (Fig. 16). This vein-type transects pyrite, but adjacent chalcopyrite shows no tendency to react or replace this pyrite. Chalcopyrite confined to more siliceous bands forms intricate networks defining quartz grain boundaries; these arrays have a broad linear concentration at ~ 50° C to the main foliation. No evidence was found of replacive relationships between pyrite and magnetite. Either pyrite formed subhedral crystal in a magnetite matrix, or the two were inextricably intergrown. Within the thickest band, pyrite forms irregularly shaped fractured aggregates with distinct magnetite cusps.

In several areas, carbonate displays uncharacteristically matchstick-like morphology, suggestive of replacement of deformed muscovite during tectonism.

SAMPLE AP1 85.4m

Hand-specimen: strongly foliated psammo-pelitic schist.

Thin-section:

Mineral	Percentage abundance (%)
chlorite	20
quartz	60
plagioclase	10
sphene	6
biotite	2
magnetite	2

Mineralogy: this section contains superb examples of chloritic pseudomorphs after classic snowball garnet porphyroblasts (typically 0.5 - 1 mm). The evidence for rotation (about 95°) is retained by curved inclusion trails of quartz. The pseudomorphed porphyroblasts are wrapped by chlorite (and minor relict biotite) which define the strong foliation; together with trails of sphene and elongate magnetite grains. The latter are likely to be a residue from the retrogression of prograde biotite to chlorite. Elongate quartz crystals are the other major phase and they exhibit preferred directional orientation due to plastic deformation and recrystallisation.

Genetic interpretation: The prograde assemblage for this specimen was probably a garnet-biotite-quartz schist, suggesting amphibolite facies regional metamorphism. Subsequent retrogression has produced a greenschist assemblage. the precursor for this specimen was most likely a quartzo-feldspathic sediment.

SAMPLE AP1	88.1m	Well-banded pyrite-magnetite rock	GJD

Hand-specimen: A well-banded sulphide-oxide dominated rock, in which individual undulating bands 1 to 2 mm thick are alternatively pyrite-rich and poor. Pyrite mobilisation into fine cross-fractures and some possible boudinage is evident.

Thin-section:

Mineral	Percentage abundance (%)	Size (μm)
Magnetite	40	40
Quartz	38	100
Pyrite	20	80
Carbonate	10	120
Chalcopyrite	0.5	60
Chlorite	tr.	60
Hematite	tr.	25
Tourmaline	tr.	40

Mineralogy: Textural relationships are for the most part not diagnostic of the formative processes in this rock because of substantial tectonic and metamorphic overprint. What appeared to be layering at hand-specimen scale resolves to networks of pyrite and chalcopyrite parallel and perpendicular to the foliation. Most components are subhedral, related in part to moderate degrees of recrystallisation, and in part to crystal fragmentation during deformation, suggesting tensile fracturing perpendicular to compression. Quartz is markedly undulose, with polygonal subgrain development. Some carbonate-magnetite fractures have subsequently been folded. 1% of the magnetite is present as porphyroblasts, which can contain complex trails of fine inclusions.

Moderately well-defined compositional bands are nevertheless present for all components, e.g., carbonate-dominated bands contain no quartz, less magnetite, and more pyrite than elsewhere. Chalcopyrite is disseminated throughout the rock, but displays no particular exclusion to other phases, for instance carbonate zones are not enriched or depleted in chalcopyrite, and all phases make contact with chalcopyrite somewhere in the slide.

Of greatest interest is the relationship between pyrite and magnetite, and between pyrite and chalcopyrite. Within the slide isolated instances of replacement between these phases exist, but mainly ambiguous or metamorphic equilibrium textures dominate (Fig. 17).

Overall the rock is interpreted as a tectonised and recrystallised but pre-existing ore.

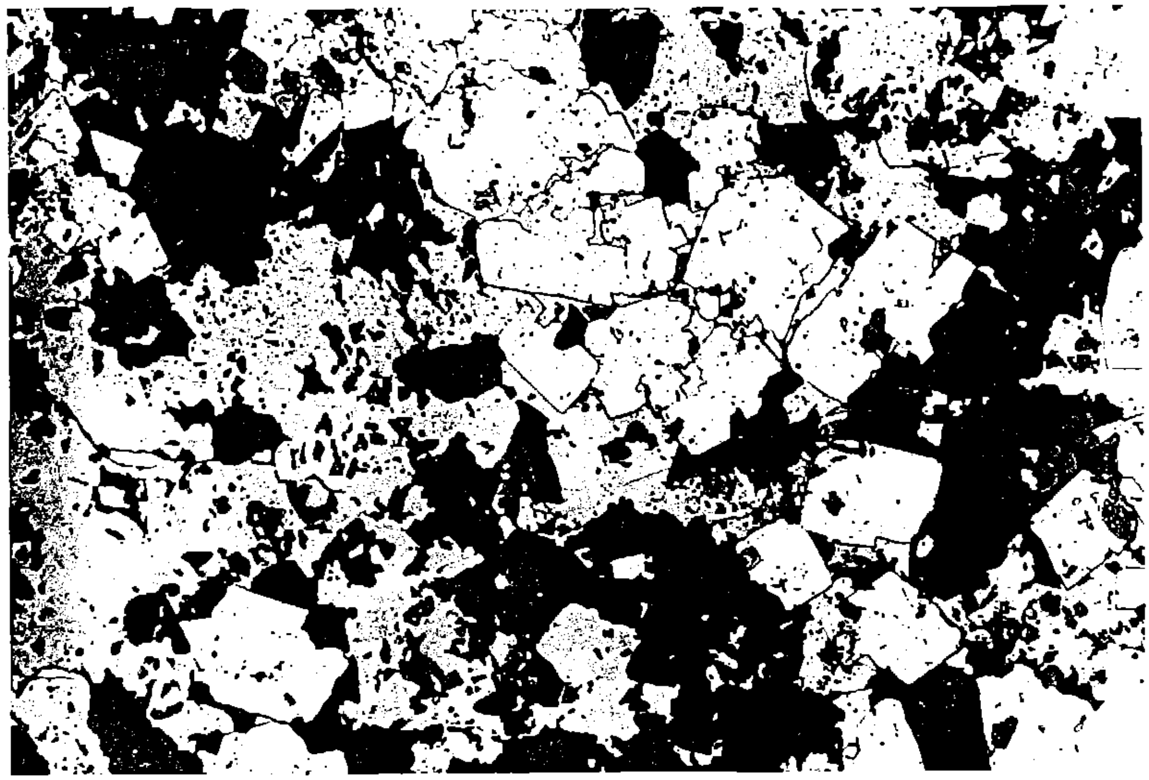

Fig. 17. Typical late syn-deformational intergrown texture showing metamorphic equilibrium between pyrite, magnetite and chalcopyrite. Sample AP1 88.1. Magnification x50, RL.

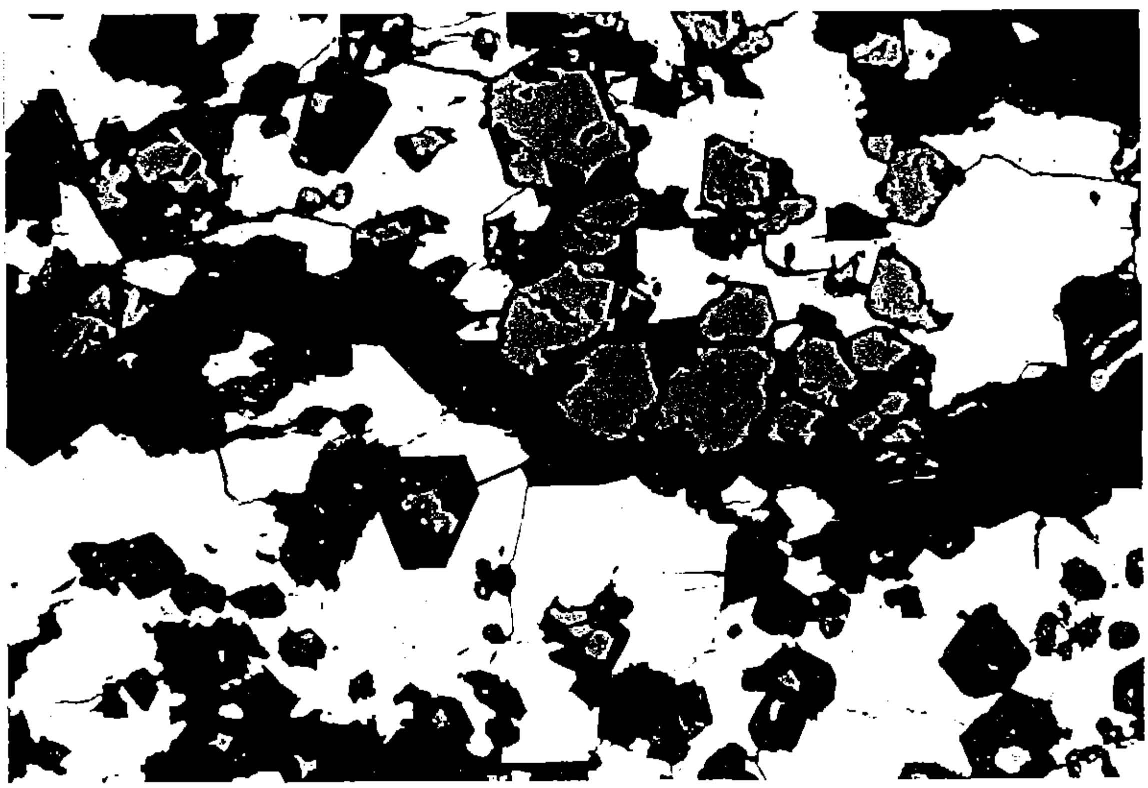

Fig. 18. Replacement of idioblastic magnetite by carbonate post-peak metamorphism. Sample AP1 92.5. Magnification x200, RL.

SAMPLE AP1 90.5m

Hand-specimen: banded quartz-magnetite-carbonate rock.

Thin-section:

Mineral	Percentage abundance (%)
quartz	52
carbonate	25
magnetite	20
biotite	2
pyrite	1
chlorite	<1

Mineralogy: this sample displays a weak banding of alternating relatively quartz-rich and magnetite-rich bands. The quartz-rich bands are composed of xenoblastic aggregates of quartz (0.1 - 0.3 mm) which display strained extinction and sutured margins but which are not particularly elongate or aligned. Sporadic biotite crystals do not show a preferred orientation. Carbonate is abundant and occurs in irregular patches and as veins cutting across the weak banding.

The magnetite-rich layers consist of an increased abundance of idioblastic magnetite crystals (0.03 - 0.1 mm) and fractured grains, together with quartz, carbonate and minor biotite. Idioblastic cubes of pyrite (0.1 - 0.3 mm) and minor xenoblastic grains of chalcopyrite are concentrated in several of the magnetite-rich layers.

Genetic interpretation: the mineralogy of this sample is consistent with an origin as an iron-bearing siliceous submarine exhalative. The carbonate appears to be a relatively late alteration feature. The pyrite and chalcopyrite appear to be in textural equilibrium with magnetite and there is no evidence that they are associated specifically with the carbonate or that they are replacing magnetite.

SAMPLE AP1	92.5 m	Complex massive pyrite and vein quartz	GJD

Hand-specimen: A complex zone of massive pyrite, deformed vein quartz, vein pyrite, and two distinct magnetite bands 0.5 and 2cm wide, with probable zones of pyrite replacement.

Thin-section:

Mineral	**Percentage abundance (%)**	**Size (μm)**
Pyrite	35	100
Magnetite	20	60
Carbonate	30	130
Quartz	15	50
Chlorite/biotite	tr.	50
Chalcopyrite	<0.5	80

Mineralogy: Surprisingly, this slide contains good evidence of equilibrium metamorphism of pyrite in contact with magnetite, and also the best available evidence of the replacement of euhedral magnetite, in the presence of pyrite, by carbonate (Fig. 18).

In general, textures are deformed, but less so than in other slides, on the basis of the preferred elongation of quartz. Much of the opaque matrix consists of interlocked recrystallised quartz and carbonate, with rare flecks of green biotite retrogressed to chlorite. In one small portion of the slide, this forms a thin monomineralic discontinuous band.

Euhedral magnetite is commonly intergrown with anhedral pyrite, a relatively unusual texture in the collection provided. This relationship is destroyed when carbonate has infiltrated and preferentially replaced magnetite leaving unaltered pyrite, a carbonate magnetite pseudomorph, and anhedral wisps of magnetite relicts. At its most extreme, only a sieved pyrite-carbonate aggregate remains. Splinter-like trains of carbonate within quartz are also likely to indicate replacement of a sheet silicate.

Pyrite is commonly fractured sub-perpendicularly to the predominant fabric, with infiltration of carbonate into fractures. Minor chalcopyrite also occurs in these sites (Fig. 19). A final event in the rock history was the development of fine continuous brittle fractures which have locally channelled carbonate and quartz deposition through the magnetite zone, and are sites of millimetric displacement. These are the only sites in the rock which contain coarse chalcopyrite, although this is not common.

Genetic interpretation: In summary, there is evidence that pyrite and magnetite recrystallised in equilibrium throughout the metamorphic history, whereas some carbonate infiltration replaced magnetite after peak-metamorphism, and prior to brittle fracture development.

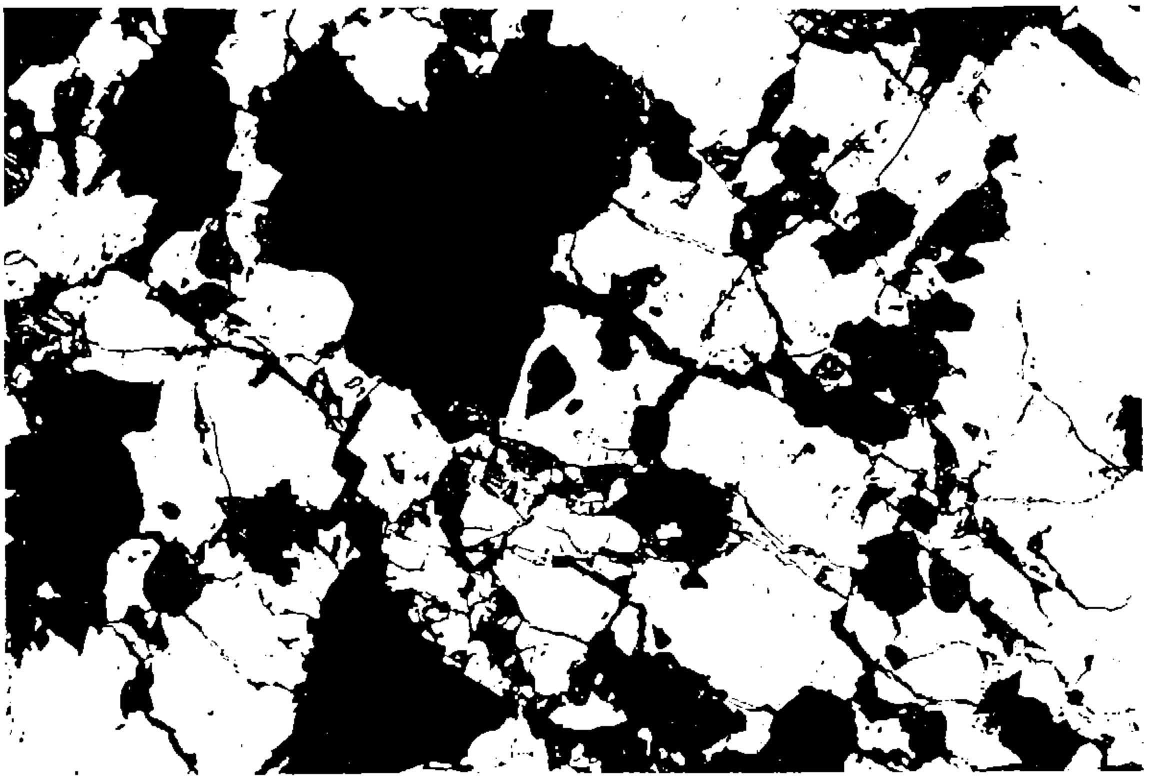

Fig. 19. Typical cataclastic texture with chalcopyrite along grain boundaries and filling fractures in pyrite. Magnetite is also being replaced by carbonate. Sample AP1 92.5. Magnification x100, RL.

Fig. 20. Magnetite replacing carbonate along twin planes (?). Sample AP2 56.1. Magnification x100, RL.

SAMPLE AP1 96m

Hand-specimen: graphitic-quartz-sericite phyllite.

Thin-section:

Mineral	Percentage abundance (%)
muscovite	43
quartz	40
carbonate	12
chlorite	2
graphite	2
magnetite	1
sphene	<1

Mineralogy: This sample has a strong foliation defined by parallel bundles of muscovite/sericite which have associated fine graphite. This imparts a dark colour to the sericite-rich bands in hand specimen. Intervening quartz-rich bands (or elongate pods) consist of elongate quartz crystals (0.1 - 0.2 mm long) with sutured margins, undulose extinction and a strong preferred directional orientation. The quartz in the matrix is somewhat finer-grained (0.01 - 0.02 mm). Carbonate appears to have completely replaced plagioclase porphyroblasts which were wrapped by the muscovite foliation.

There is abundant evidence in the section for a second deformation which has produced small scale assymetric folds of S_1 with localised development of a crenulation cleavage. The initial phase of deformation involved high strain as evidenced by the strong foliation and plastic deformation of the quartz. The subsequent folding of this foliation seems to have been short-lived and characterised by lower strain.

Genetic interpretation: the precursor to this rock was probably a mixed psammitic-pelitic sedimentary rock ie. interbedded thin quartzo-feldspathic and mudstone layers.

SAMPLE AP2 56.1m	Complex pyrite-carbonate veins in a dark matrix	GJD

Hand-specimen: A complex of pyrite, pyrite-carbonate veins, and pervasive pyrite alteration imposed on a dark fine-grained lithology.

Thin-section:

Mineral	Percentage abundance (%)	Size (µm)
Carbonate	75	10
Pyrite	~16	300
Magnetite	~7	100
Quartz	~7	100
Chalcopyrite	~0.25	30
Carbonaceous matter		<5

Mineralogy: This rock is dominated by alteration-related carbonate and pyrite, which has experienced strong brittle-ductile deformation.

Deformation is reflected as a strong preferred fabric in the original rock, affecting all hydrothermal components. The fabric is partitioned into zones of severe foliation (1 to 3 mm wide) in which pre-existing textures in carbonate are pervasively flattened, between more granoblastic fabrics. Pyrite and magnetite have mainly been brittly fractured and brecciated, with the fracture-filling by carbonate. Carbonate surrounding larger relict pyrite has recrystallised to polygonal grains. It is evident from the varying degrees of internal deformation, that the obvious cross-cutting carbonate veins (1 - 4 mm wide) developed at different stages during the deformational history, but none are wholly devoid of the effects of tectonism.

Genetic interpretation: A broad paragenetic sequence is suggested from relict textures. The most likely precursor was a silicified carbonaceous sediment, still preserved as disoriented kernels resulting from brecciation. Silicification may therefore have been the earliest hydrothermal event to affect the rock. Initially minor carbonate-chalcopyrite developed, followed by major carbonate-pyrite alteration and magnetite replacement of carbonate (Fig. 20). The latter has resulted in well-developed fan-fabrics in which magnetite has replaced the cleavage of sprays of carbonate. As a late stage or metamorphic process, most pyrite was embayed by carbonate, as was recrystallised quartz. Chalcopyrite locally replaces pyrite along fractures.

SAMPLE AP2	61.3 m	A strongly foliated jasper-pyrite-mag rock	GJD

Hand-specimen: A strongly foliated rock consisting of discontinuous 1 to 5 mm thick bands of red jasper, pyrite and mag-qtz. Some layers are clearly tightly folded, with transposition evident parallel to layering. At this scale it the rock has been severely tectonised with a strong sense of simple shear.

Thin-section:

Mineral	Percentage abundance (%)	Size (μm)
Quartz	50	120
Magnetite	15	80
Pyrite	5	160
Carbonate	25	100
Goethite	2-5	20
Chalcopyrite	<1	50
Hematite	1-3	30
Chlorite	<1	40
Plagioclase	<1	120

Mineralogy: The section is dominated by severely deformed sub-mylonitic microtextures in which phases are ambiguously related to one another paragenetically. Red chert-like bands in hand-specimen are here resolved as discrete layers of deformed carbonate containing a multitude of ultra-fine hematite inclusions, most of which cannot be seen at 400 X, but which are inferred to be hematite from the constellations of strong red internal reflections. Thin mylonites (0.2 - 0.4 mm wide) probably represent local transposition zones, with a dextral shear sense.

Throughout the slide quartz exhibits marked grain-size reduction, common severe undulose extinction with new grain growth at ~ 45° to the foliation, and lobate to serrated grain-boundaries. Carbonate has recrystallised to a greater degree, and in places "splinters" of carbonate are interpreted as carbonate twins which have separated and continued to individually deform.

Magnetite occurs as euhedra along quartz-carb grain boundaries, but is more common within the carbonate. Pyrite and cpy are more domainal within the fabric, in zones in which qtz is more common than carbonate. Chalcopyrite is found mainly at the edges and within cracks in pyrite, with very local evidence of replacement.

Genetic interpretation: No paragenetic importance is attached to the grain-scale replacement textures because of the clear dominance of the tectonic overprint; there is no strong evidence favouring a late tectonic introduction of metals or carbonate. Notably, these textures are far more strained than those of AP1, and also do not contain signs of brittle fragmentation.

SAMPLE AP2	67.7 m	Finely foliated/banded mag-py-siderite	GJD

Hand-specimen: A foliated magnetite-pyrite-siderite-silicate rock in which the constituents occur in fine ragged bands (1 to 10 mm thick), continuous at the core-width scale. Some reddish carbonate bands have pyrite bands symmetrically disposed at either contact, suggestive of vein and selvedge relationships. A prominent magnetite porphyroblast or fragment 1.5 cm X 2.5 cm has deformed brittly, and is wrapped plastically by sulphide and carbonate bands.

Thin-section:

Mineral	Percentage abundance (%)	Size (µm)
Magnetite	30	150
Carbonate	25	60
Quartz	25	80
Pyrite	20	100
Chalcopyrite	<5	40

Mineralogy: Compositional bands which were relatively discrete in hand-specimen seem less so in thin-section; nevertheless, some thick compositional bands seem to represent an original layering despite a strong tectonic textural overprint. On a finer scale it is evident that this banding is also close to the plane of deformational flattening. In places an earlier foliation is defined by folded and recrystallised mag-carb layers, in panels bounded by the later dominant foliation, which is sub-mylonitic.

Original fragments or metamorphic porphyroblasts of magnetite developed prior to the main foliation, subsequently behaving brittly while sulphides and carbonates flowed around them. A dextral shear sense is indicated.

For the most part py, cpy, mag and carb are in syn-tectonic equilibrium. However, there were several clear examples of millimetre-scale replacement of magnetite by pyrite, and magnetite by carbonate, associated with the brittle extension of magnetite during shearing. Some pyrite has clearly replaced magnetite in ribbons parallel to the foliation (Fig. 21). More clearly, pyrite is only present in mag porphyroblasts/fragments, within tensile quartz-filled fractures and clustered around grain margins(Fig. 22), evidencing some mobility during tectonism. Lastly, tendrils of siderite have replaced magnetite around tensile fractures in isolated instances, and there is evidence of carbonate filling a flexural slip dilation zone.

It is vital to see that these are only instances, whereas most of the fabric is in syn-tectonic textural equilibrium.

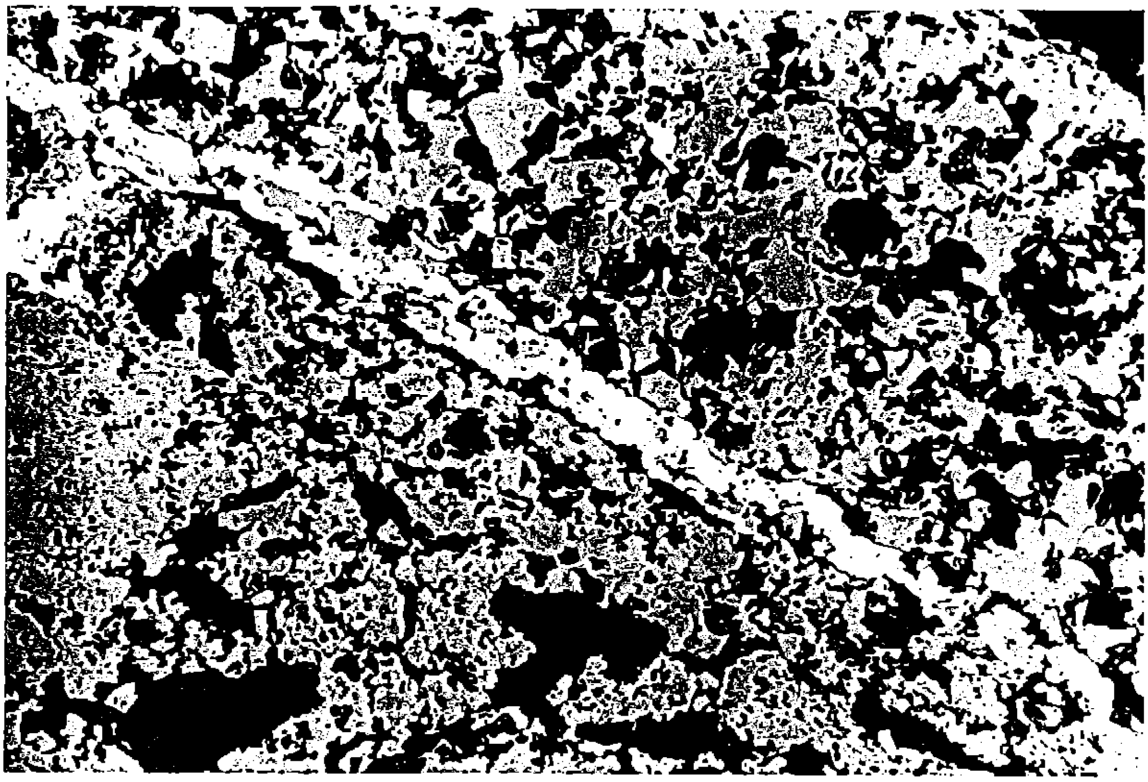

Fig. 21. Minor sulfidation of magnetite along fractures, late syn-deformational. Sample AP2 67.7. magnification x200, RL.

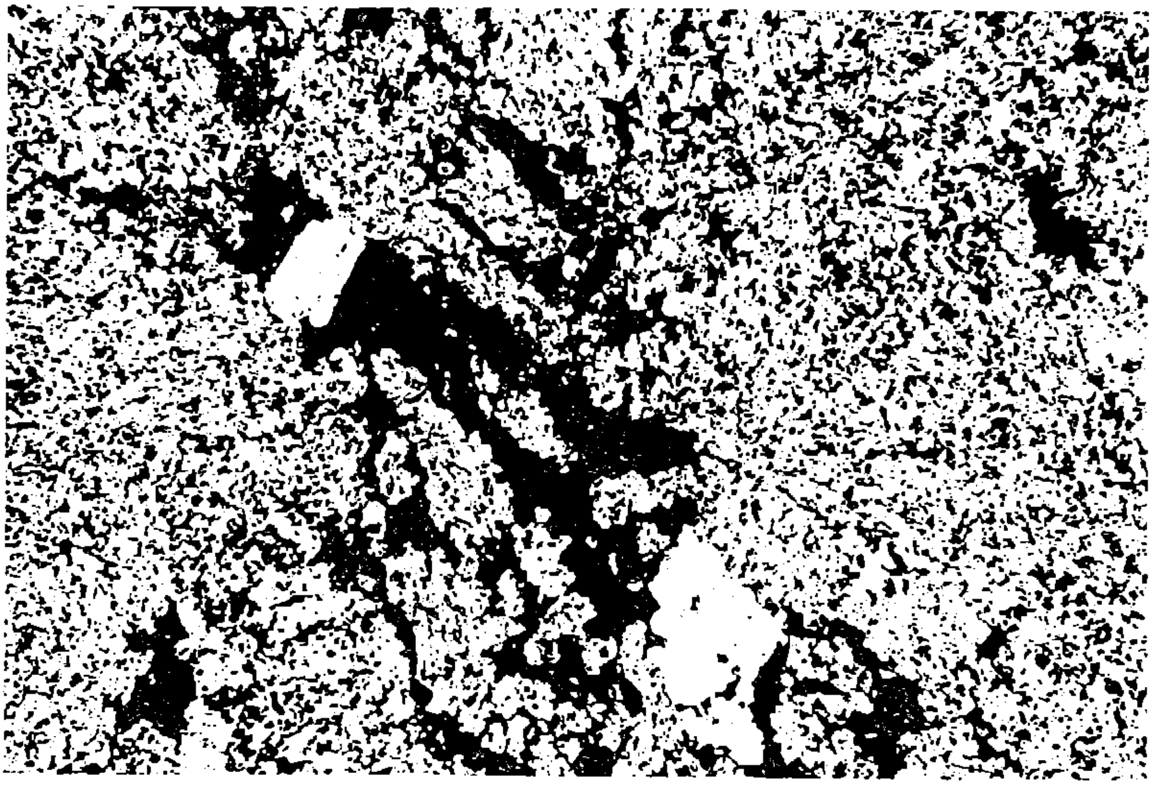

Fig. 22. A magnetite clot with tension gashes from fracturing, into which there has been some remobilisation, or sulfidation by pyrite. Sample AP2 67.7. Magnification x100, RL.

SAMPLE AP2 68.4 m

Hand-specimen: moderately foliated psammo-pelitic schist.

Thin-section:

Mineral	Percentage abundance (%)
quartz	73
feldspar	15
chlorite	5
carbonate	5
magnetite	2
sericite	<1

Mineralogy: intergrown elongate crystals of quartz (0.3 - 0.7 mm long) which show strain extinction and extensively sutured grain margins are abundant and in some cases are recrystallised into finer grained aggregates (0.01 - 0.03 mm).

Dispersed plates of chlorite are aligned subparallel to the elongate quartz crystals and define a foliation which has been folded on the scale of the thin section. Xenoblastic to tabular porphyroclasts of feldspar have been occasionally replaced by carbonate aggregates. The orientation of the tabular plagioclase grains suggests some rotation during deformation. Carbonate aggregates are also disseminated throughout the rock which are not obviously related to pre-existing feldspar grains.

A thin layer (0.2 - 2 mm) of carbonate plus magnetite and minor sericite occurs within the quartz-rich matrix which is parallel to the general foliation and has been folded. The magnetite and carbonate both occur as xenoblastic grains and this layer may have originally represented a vein which has subsequently been recrystallised. There is very little disseminated magnetite through the rest of the rock.

Genetic interpretation: the precursor to this sample was probably a quartzo-feldspathic sedimentary rock which may have been derived from a silicic volcaniclastic, or a weathered sodic granitoid. The rock has experienced quite high strain resulting in the granulation and recrystallisation of feldspar, quartz and chlorite. Subsequent deformation has caused moderately open folding of the initial foliation.

SAMPLE AP2	70.0 m	Semi-massive pyrite and mag-qtz-siderite	GJD

Hand-specimen: Semi-massive pyrite kernels 1 - 4 cm across separated by cuspate magnetite-quartz-siderite zones, broadly parallel and defining a preferred fabric.

Thin-section:

Mineral	Percentage abundance (%)	Size (µm)
Pyrite	50	150
Carbonate	30	80
Quartz	10	100
Magnetite	10	80
Chlorite	1-2	60
Chalcopyrite	<1	100
Covellite		"

Mineralogy: The orientation of the slide has selectively intersected a 2 cm wide higher strain zone in addition to the dominant lower strain texture of the semi-massive pyrite. High strain is reflected in a very strong preferred orientation, marked sub-grain development and sutured boundaries of quartz and carbonate orientations in pressure shadows. Quartz predominates in the non-pyrite zones. In the high strain zone pyrite and magnetite occurs in 0.5 to 2cm long trains parallel to the foliation, in detail consisting of fragmented and separated grains in a quartz-carb matrix.

The more massive pyrite aggregates are in detail highly sieved and cracked, with widespread evidence of replacement by carbonate and quartz inwards from cracks. At its most extreme, this process has resulted in the isolation of small sutured and embayed pyrites in a matrix of carbonate, quartz and magnetite.

There is evidence that some magnetite has replaced deformed sprays of recrystallised carbonate in this area.

Chalcopyrite has an interesting occurrence. Whilst some occurs on fractures and as inclusions in the massive pyrite, most is found in the carbonate-qtz matrix, both in the sheared and less-sheared portions of the slide. Approximately half of any cpy grain has been replaced about its margins by covellite and some chalcocite, which given a lack of similar replacement in cpy at higher levels in the drillhole, may be evidence of a discontinuity or fault, open to surface waters nearby.

SAMPLE AP2 70.9 m

Hand-specimen: moderately banded quartzo-feldspathic rock containing a significant amount of sideritic? carbonate. The carbonate occurs partly parallel to banding but is also transgressive and is cut by later quartz veins.

Thin-section:

Mineral	Percentage abundance (%)
albite	45
quartz	30
carbonate	15
chlorite	8
sphene	2
muscovite	<1
pyrite	<1

Mineralogy: the section traverses a contact between a relatively carbonate-rich recrystallised quartzo-feldspathic assemblage and a carbonate-poor equivalent. The carbonate-poor layer is characterised by recrystallised aggregates of quartz and plagioclase (0.05 - 0.2 mm) with randomly oriented crystals of chlorite (0.2 - 0.3 mm), minor aggregates of carbonate, and accessory sphene, magnetite and pyrite. The quartz shows slightly sutured margins and undulose extinction, the plagioclase is untwinned or exhibits albite twinning.

In the carbonate-rich layer, the matrix plagioclase and quartz is slightly finer-grained (0.02 - 1 mm) and the texture more granoblastic polygonal. The carbonate occurs in coarse aggregates (0.3 - 1 mm) closely associated with fine (0.05 mm) aggregates of sphene. A narrow vein (0.15 mm) cutting this part of the section is characterised by muscovite, magnetite, chlorite and sphene, and a relatively wide cross-cutting vein is rich in quartz and carbonate.

Genetic interpretation: the equigranular polygonal texture of this sample and the random orientation of the platy minerals (eg. chlorite) indicate recrystallisation occurred under low strain conditions compared with many of the samples from this area. Carbonate is abundant, but there is a distinct paucity of Ca-bearing metamorphic phases such as actinolite or epidote, even though the rock has experienced metamorphic recrystallisation probably under lower greenschist facies. This suggests that much of the carbonate is very late and has been introduced subsequent to peak metamorphic conditions.

SAMPLE AP2 78.1 m

Hand-specimen:alternating relatively chlorite-rich and quartz-feldspar-rich banded sediment with some small scale folding evident in core.

Thin-section:

Mineral	Percentage abundance (%)
chlorite-rich layers	
chlorite	50
plagioclase	39
carbonate	10
sphene	1
pyrite	<1
felsic layers	
quartz	42
plagioclase	30
carbonate	15
chlorite	10
sphene	3

Mineralogy: this sample includes folded alternating bands which are rich in quartz and feldspar and chlorite and feldspar respectively. The sharp nature of the boundaries between these layers and the absence of very high strain features suggests that these may represent original compositional banding in a sedimentary rock.

The felsic-rich layers consist of recrystallised xenoblastic to weakly polygonal quartz and feldspar aggregates (0.1 - 0.3 mm). Poorly aligned plates of chlorite (0.2 - 1 mm) define a weak foliation and xenoblastic carbonate appears to have replaced the other phases intially along the grain boundaries and subsequently along cleavage planes in plagioclase. Quartz displays undulose extinction and weakly sutured boundaries but does not display a strong directional preferred orientation that is a feature of the higher strain rocks. Minor aggregates of sphene are typically associated with carbonate.

The chlorite-plagioclase-rich layers consist of tabular to slightly rounded plagioclase porphyroblasts (0.5 - 1 mm) set in a chloritic matrix which displays a weak foliation. However, many bundles of chlorite crystals are oriented oblique to this foliation suggesting fairly low strain conditions during metamorphism. Carbonate is relatively abundant replacing chlorite along the cleavage direction and replacing plagioclase around grain boundaries and along cleavages. Euhedral crystals of sphene occur throughout the chlorite matrix.

Genetic interpretation: the precursor to this specimen was probably a sedimentary rock comprising alternating layers of quartzo-feldspathic material and tuffaceous material derived from mafic volcanism. The carbonate appears to have been introduced post-deformation at relatively low temperatures.

SAMPLE AP2 81.5m

Hand-specimen: moderately foliated interbedded psammitic and mafic schists.

Thin-section:

Mineral	Percentage abundance (%)
chlorite-rich layers	
chlorite	80
plagioclase	15
carbonate	3
magnetite	2
felsic layers	
quartz	65
plagioclase	15
biotite	10
carbonate	7
chlorite	3
pyrite	<1
epidote	trace

Mineralogy: the section traverses a chlorite-rich band and a quartzo-feldspathic band which have some similarities to the layers evident in AP2 78.1m. The quartzo-feldspathic band is rich in quartz which show evidence of recrystallisation under moderate to relatively low strain conditions. The quartz grain boundaries are slightly sutured and there is ubiquitious strain extinction together with dimensional preferred orientation. A moderate cleavage is defined by subparallel aligned biotites and subordinate chlorite. Carbonate occurs in aggregates and partially replacing plagioclase porphyroblasts, as well as in veinlets cross-cutting the foliation.

There is a sharp contact with the chlorite-rich layer. It consists of abundant chlorite with a strong foliation enclosing tabular to slightly rounded plagioclase porphyroblasts (0.5 - 1.5 mm). These are either untwinned or display simple twinning and typically show partial replacement by carbonate around their grain boundaries and along cleavage planes. Elongate grains of magnetite (0.05 - 0.3 mm long) occur aligned with the chloritic matrix with disseminated aggregates of carbonate. A few small relict grains of epidote occur as inclusions in the plagioclase porphyroblasts.

The contact between the chloritic and quartz-rich layers displays an increased abundance of biotite and a small amount of biotite occurs within the mafic layer close to the contact. The lack of biotite in the chloritic layer would appear to be a compositional effect due to the lack of potassium.

Genetic interpretation: this sample is very similar to AP2 78.1m in containing the alternating mafic and quartzo-feldspathic layers which probably represent interbedded psammitic sediment and mafic volcaniclastic material.

As with the other samples, the carbonate appears to be introduced quite late and has not taken part in the pro-grade metamorphic reactions. The predominance of biotite over chlorite in the quartzo-feldspathic layer of this specimen compared with chlorite only in AP2 78.1 probably represent complete retrogression of biotite.

SAMPLE AP2 82m

Hand-specimen: compositionally banded mafic-psammitic schist.

Thin-section:

Mineral	Percentage abundance (%)
hornblende	30
chlorite	25
quartz	15
biotite	15
albite	10
magnetite	3
garnet	1
carbonate	1

Mineralogy: this specimen shows considerable heterogeneity in mineral assemblages ranging from a chlorite-rich band (similar to those in AP2 78.1 and AP2 81.5), to an amphibole-garnet-rich band, and an amphibole-biotite-quartz-rich zone.

The chlorite-rich band has essentially identical mineralogy and textures to the mafic layers described for the above two samples. In this sample, the distinction between the chloritic and adjacent bands is not clear-cut and there is a gradational transition to an amphibole-biotite-plagioclase-chlorite-magnetite assemblage (Fig. 14). Simple twinned xenoblastic porphyroblasts of plagioclase (0.3 - 1 mm) are set in a strongly foliated matrix of intergrown prismatic blue-green amphibole, platy biotite and chlorite (which encloses elongate crystals of magnetite). The plagioclase porphyroblasts have common oriented (but rotated) inclusions of amphibole, chlorite and biotite.

Several coarse-grained (0.3 - 2 mm) elongate pods of quartz are oriented parallel to the foliation. One relatively amphibole-rich band still contains plagioclase porphyroblasts and some fractured pale-pink porphyroblasts of garnet (0.3 - 0.7 mm). Some of the garnets exhibit chlorite rims and there is also clear evidence of retrogression of biotite to chlorite plus magnetite, and amphibole to very fine-grained chlorite plus magnetite aggregates.

Genetic interpretation: this sample exhibits the best examples of prograde and retrogressive assemblages. Peak metamorphic conditions appear to have produced a garnet amphibolite assemblage which has experienced minor to extensive retrogression to a chlorite-plagioclase (greenschist) assemblage. The more extensive retrogression may have occurred along very localised shear planes accounting for the considerable variability over short intervals of core and within the scale of this section, although the mineralogical differences may also partly reflect original compositional differences.

The precursor to this rock probably represents a mixed mafic tuff/psammitic sediment, although the former appears to be the dominant component in this sample.

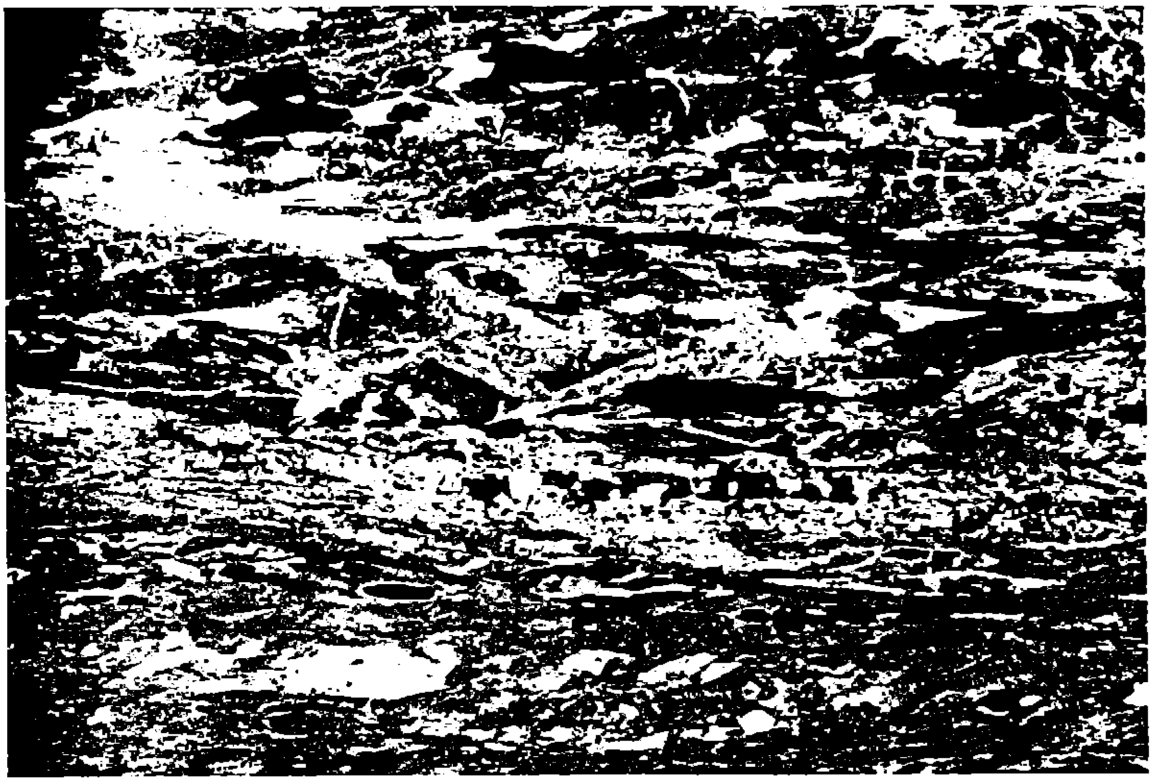

Fig. 14. Transition from chlorite-rich layer containing stringers of magnetite and plagioclase porphyroblasts, to a band rich in amphibole, biotite and magnetite. This same section also contains garnet, amphibole and plagioclase together with minor retrogressive chlorite. The chlorite-rich layer is interpreted as a thoroughly retrogressed equivalent of the amphibole-biotite-garnet assemblage. Sample AP2 82. Magnification x50, PPL.

Appendix III Geological core logs and magnetic susceptibility measurements: AP1 and AP2

W.Herrmann, 21/6/90

EL 56/89 - Corinna South ALPINE ANOMALY

Geological Core Logs: W.Herrmann, 21/6/90

Hole No: AP 1

0 - 30 No Core

30 - 36.8m Leached, Quartz-sericite-(clay) Schist

Pale creamy grey, strongly weathered and leached; with a fine silty-sandy relict quartz clastic fabric? and generally distinct foliation - appears to be a leached psammitic schist essentially similar to the psammitic units further downhole but here strongly oxidized. Core very broken and cruddy.
Minor disseminated pyrite specks below 33m, generally <0.5% but upto 2% at 36.5m

36.8 Base of Oxidation, (boundary quite sharp)

36.8- 46.2 Interlayered Graphitic/Pelitic and Psammitic Schists

A fairly thinly interlayered sequence of dark graphitic ? and paler grey psammitic schists, overall in approximately equal proportions but locally rather variable; individual layers generally from 20-100mm in thickness, probably relict bedding.
Comprised of:
Dark grey to black phyllite or fine grained pelitic mica schist, probably graphitic and derived from black shale; contains minor disseminated pyrite ~0.5% Py, mostly concentrated in thin sandy layers.
Pale grey fine grained silty to sandy meta siltstone with generally fairly well developed foliation defined by minor micas, chl-musc-biot? Contains trace disseminated pyrite generally <0.5%; possibly minor carbonate in matrix.
Primary schistosity parallels layering at somewhat variable angles but generally around 30-50 deg. to LAOC. Some evidence of crenulation cleavage and tight mesoscale folding with minor transposition of layering. Core is cut by numerous (20-50 /m of core) fine (<5mm) irregular veinlets of carbonate + quartz, generally without sulphides, possibly late stage and post foliation.

46.2- 49.0 Marly meta pelite/psammite

A thinly laminated / bedded unit of essentially similar character to above with interlayered black graphitic phyllite and grey metasiltstone beds but with the latter, particularly, having a uniform grey appearance and containing much carbonate; precursor was probably an impure marly sediment. Some zones are quite strongly brecciated or transposed with heavy infill of white-straw coloured carbonate (eg: 48.7m). Also abundant irregular veins and patches of barren quartz + carbonate. This unit is essentially devoid of pyrite.
Bedding is // to main foliation, generally 30-50 deg. to LAOC.

The lower contact is marked by an 0.3m zone of broken core, silicified and bleached greenish grey, possibly a fault.

49.0- 49.3 Bleached silicified fault ? zone.

49.3- 51.2 Graphitic Phyllite

Similar to the graphitic phyllite components of the interlayered unit above 46.2m. It contains conspicuous coarse semi-hedral grains or augen of pyrite lying sub // to foliation, possibly rotated framboids or porphyroblasts; estimated Py about 2-3% overall. The lower contact is also rather broken with some white-pink carbonate and clear quartz infill/ veining. Foliation is quite variable from 20-70 deg to LAOC.

51.2- 55.4 Psammitic quartz + mica +(carbonate) Schist

Pale grey, fine grained quartz + muscovite ? + carbonate schist, fairly well foliated and with very subordinate thin transposed laminae of black phyllite, minor carbonate in the matrix; probably a psammitic metasediment. There are occaisional scattered small lenses or cubes of pyrite averaging around 1% Py. Foliation mostly fairly acute at 20-40 deg to LAOC.

55.4- 62.0 Graphitic Phyllite

Similar to interval 49.3-51.2m. Locally with minor thin "interbeds" of grey psammitic metasiltstone with carbonate in matrix, carbonate is oxidised brownish, probably sideritic.

62.0- 81.6 Psammitic quartz + mica +(carbonate + albite ?) Schist

Predominantly a fairly massive uniformly pale grey rock, apparently consisting largely of micro-gneissic quartz, subordinate straw coloured carbonate and possibly some albite ? ; has a distinct foliation/cleavage defined by minor (<5%) sericite - muscovite. Some zones, notably 67.8-71.2m, contain upto 10-15% black graphitic ? phyllite as thin semi transposed laminae. The more massive sections also show some traces of banding suggestive of bedding; the precursor was very likely a psammitic sediment, essentially similar to psammitic components of units above. The upper contact is marked by about 1m of strong brecciation and white quartz-carbonate veining and semi pervasive silicification/carbonatization but not associated with significant sulphides; a similar zone occurs at 74.3-75.7m. Above 74.3m pyrite occurs (as elsewhere) as disseminated specks, generally at <0.5%, or in the phyllitic zone as conspicuous lensoidal blebs with Py upto about 2%. The late stage ? quartz+ carbonate veins are generally devoid of sulphide.

Below 75m there are fairly numerous "bands" of semi massive pyrite, possibly with some associated steely grey-translucent sphalerite ? The major zones are:

75.4m	30mm massive Py
76.6-76.9	foliation parrallel stringers of massive pyrite ranging 2-20mm thick constituting about 20% of volume.
77.4-77.6	as above.

77.9 30mm band, massive Py.
78.1-78.2 Stringers of massive Py, 2-20mm; 20% /vol.
79.5 60mm band of semi massive Py.

Although often broadly parallel to foliation the pyritic bands are associated with intense marginal shearing and seicitization and appear to cross cut ? the late stage> open space filling quartz+carbonate veins; (eg: specimen at 77.0m). The pyritic bands generally appear rather internally brecciated and often contain fragments and lenses of milky quartz +/- carbonate which resemble broken fragments of the quartz+carbonate veins.
The pyrite rich zone 76-82m is notably anomalous in zinc (0.1-0.4% Zn) and to lesser degree in copper (to 0.1% Cu) but there is no significant lead.

81.6- 81.9 Massive Pyrite

Essentially a thicker development of the pyrite bands described above; seems to consist of about 80% massive compact granular pyrite, locally internally brecciated with a grey siliceous (+carbonate ?) gangue. Magnetite and crosscutting quartz+carbonate veins are absent.

81.9- 83.7 Qtz + (musc + ser + carb + chl +/- alb) Schist.

A quartz rich schist similar to most of the psammitic units further up the hole, perhaps with slightly increased chlorite and carbonate content. It contains a few minor pyritic bands and is generally affected by narrow sericite altered shear zones - a form of retrograde mylonitic shear?

83.7- 84.3 Chloritic Psammitic Schist
This texturally resembles the psammites from above but has a darker greenish grey colour apparently reflecting chlorite alteration ? of the mica component. It retains a folded laminar structure and contains a few veins of quartz+carbonate +(pyrite, minor chalcopyrite) reflected in the anomalous 0.1% Cu.

84.3- 84.6 Laminar Quartz + carbonate + pyrite.

This is a quite well banded rock composed of thin 1-5mm alternate laminae of straw coloured carbonate and grey quartz + pyrite; there is slight hematitic staining near the lower contact. The rock is cross cut by fine, open space fracture fill type, veinlets of quartz carrying minor chalcopyrite.
The lower contact is irregular and appears to be a finely milled breccia of carbonate and interstitial pyrite, marked by a 50mm wide zone of milky quartz veining.

84.6- 85.3 Banded magnetite + pyrite Ironstone

A crudely banded ironstone composed of about 40% Mt, 40% Py and minor chalcopyrite with a sparse gangue of quartz and carbonate. There are some wispy lenses of dark chlorite or biotite associated with magnetite. The more massive pyritic zones or bands appear to have formed by replacement of magnetite and are sometimes associated with minor hematite and hematitic selvedges. Chalcopyrite is especially concentrated in

crosscutting veinlets and anastomosing networks but also occurs disseminated in the magnetite rich zones, possibly with spatial relationship to the margins of pyrite replacement zones.
This needs petrographic determination of whether the banding is relict sedimentary, replacive or tectonic/mylonitic ? Banding near the lower contact is broadly parallel to foliation in chloritic schist below but the actual contact is occupied by a 40mm band of massive pyrite + carbonate (similar to that at 84.3-84.6m) which is slightly irregular against the chlorite schist and transitional into the ironstone. Chalcopyrite bearing veinlets cut across this pyrite + carbonate margin.

85.3- 87.6 Chlorite + quartz + carbonate +/- albite Schist

A dense very fine grained dark green chloritic schist within 0.3m of the upper contact; becoming transitionally less chloritic below 85.6m to resemble that of the interval 83.7-84.3m. It is strongly foliated with plane of schistosity at about 40 deg. to LAOC. It becomes progressively less chloritic and more siliceous downwards and at the lower contact resembles a cherty mylonite ? The lower contact is parallel to foliation. it generally contains 1-3% pyrite as fine disseminations or as foliation parallel stringers.
This unit can be interpreted as representing the typical psammitic schist with intense chlorite alteration close to and waning away from the upper contact. Alternatively, and perhaps more likely, it could represent chloritic alteration of a variable pelitic/graphitic and psammitic sediment with the more chloritic upper part derived from alteration of phyllites similar to those seen further up the hole. The timing of alteration is not clear but would seem to predate dynamic metamorphism.

87.6- 92.7 Banded pyrite + magnetite Ironstone.

The upper contact is parallel to foliation in the unit above and is marked by a 100mm wide zone of pyrite + carbonate which is transitional downwards into Mt+Py+carbonate.
The ironstone is of rather variable character, consisting of three main assemblages:
1) banded magnetite + quartz + carbonate with little pyrite; typically contains at least 30% Mt and in some bands virtually massive magnetite. (eg: at 90.5m)
2) finely banded Mt + py with very subordinate quartz + carbonate gangue in which the pyrite seems to be replacing originally massive magnetite?; this type typically contains about 50% magnetite and upto about 30% pyrite. (eg: at 88.1m)
3) apparently brecciated originally massive magnetite ironstone with massive infill/replacement ? by carbonate + quartz + pyrite; this consists of upto about 40% pyrite. (eg: at 88.6m)

Below 91m the ironstone "lode" is fairly pyritic with fairly clear evidence of brecciation and veining of pre existing magnetite rich rock and replacement/infill by py + carb + qtz. This latter material appears to be of the same generation as the (zinc rich) pyritic bands above 82m and around the lower contact at 92.6-94m. There is some evidence for Py + quartz infilling of brecciated quartz + carbonate vein material.

the lower contact of the ironstone is considerably broken with much quartz + carbonate + pyrite veining, some of which is oxidised suggesting a permeable fault zone; there is considerable core loss in the interval 92.7-94m.

92.7-94.3 Fault brecca ?

Brecciated / silicified qtz-chl-alb?-carb schist with much qtz + carb + pyrite veining and breccia fill, partly oxidised; pyrite is one of the latest vein phases.

94.3-106.7 Graphitic Phyllite

Above 96.7m the core is strongly sheared (almost mylonitic ?) with associated strong silica-carbonate alteration and pervasive transposition of layering. Below 96.7m the phyllite is rather contorted but recognizably similar to the graphitic phyllite intervals in the upper part of the hole, with characteristic lenses and porphyroblasts of pyrite, averaging around 3% Py. Foliation in range 40-60 deg. to LAOC.

106.7m EOH.

Hole No: AP 2

0 - 55.5m No Core

55.5- 56.2 Banded magnetite + pyrite + quartz + carbonate Ironstone

Generally banded on a millimetric to centimetric scale with fairly massive bands of magnetite, or magnetite + minor quartz gangue, separated by bands rich in carbonate and pyrite. In places all phases are closely intermixed and there is some evidence for Py + carb replacement of massive Mt. The lower contact appears to be transitional/replacive with formerly fairly massive magnetite brecciated and intensely veined by a network of carbonate + pyrite + quartz veins which gradually coalesce to form massive carbonate+pyrite+quartz rock occupying the interval 56.1-56.2m.

56.2-58.6 Quartz + carbonate + albite "schist"

This is a rather oxidized lithology with mottled appearance and consisting of reddish brown specks or blotches in a mid greenish olive matrix. Purvis (CRAE, 1985) called it a serpentine skarn but I think the "serpentine" may be weathered sericite or albite? It generally has a fine granular to schistose fabric resembling that of the schists further down the hole but towards the lower contact it is porhyroblastic in pinkish brown carbonate or albite?

58.6-60.8 Ironstone, Py > Mt

This is a banded, "lacy" or blotchy mottled ironstone consisting of about 60-70% Py and ~20% Mt with a gangue of quartz + carbonate + chlorite. It includes a zone of chlorite + quartz schist with a kernel and stringers of carbonate + pyrite in the interval 58.9-59.1m. There is minor chalcopyrite associated with magnetite; I get the impression that the pyrite has replaced magnetite. The upper contact is broken and sheared.

60.8-64.6 Ironstone, Mt > Py

The upper contact is somewhat transitional but defined by the absence of blobby, massive (replacive ?) pyrite. The ironstone is generally finely banded and foliated in a lenticular fabric more suggestive of pervasive transposition or mylonitization rather than sedimentary laminae. Typically consists of 70% fine granular / massive magnetite in a base of cherty quartz, often stained reddish to jasper, with abundant fine foliation parallel stringers ? of pyrite (constituting about 20% / vol.) and some straw coloured carbonate (~10% /vol). Trace chalcopyrite occurs, usually in intimate association with pyrite.
The lower contact is quite sharp, parallel to foliation and appears to represent a strongly carbonatized/pyritized "annealed" sheared contact against the schist below.

64.6-66.7 Albite + quartz + chlorite + carbonate Schist

A variably pale grey to dark greenish grey banded rock of fine grained schistose to medium grained granoblastic/gneissic texture. The finer schistose layers are chlorite rich whilst the more granular layers appear to be albite, quartz and carbonate rich, these are locally weakly porphyroblastic in albite (?). Disseminated pyrite is present in the range about 0.5 - 2%. The distinct textural / compositional layeing suggests a sedimentary precursor and the fairly felsic-semi mafic composition suggests a volcaniclastic component; I suspect the original rock may have been a felsic to intermediate epiclastic but perhaps a selectively altered psammo-pelitic sediment cannot be ruled out.

66.7-68.2 Banded Ironstone, Mt > Py

Lithologically similar to ironstone in the interval 60.8-64.6m. The ironstone consists of at least 70% Mt as fractured augen and thin foliation parallel wisps and lenses of compact-massive magnetite with a subordinate gangue of quartz, jaspar, pyrite and carbonate. The texture suggests an origin involving cataclastic deformation of a massive magnetite ironstone with partial replacement or infill by pyrite, carbonate and quartz ?
The upper contact is quite sharp and semi parallel to cockade type magnetite/pyrite banding. The lower contact is also sharp but marked by an 80mm zone of milky quartz veining; despite this it could be essentially conformable to layering in the schist below.

68.2-69.8 Albite + quartz + chlorite + carbonate Schist

A well foliated and compositionally layered rock akin to that in the interval 64.6-66.7m; the layering is generally parallel to foliation (defined by alignment of micas) and appears to be axial to a tight, isoclinal ? fold hinge intersected at 68.4m. Elsewhere the rock is rather sheared and near the lower contact it is porphyroblastic in pink albite (or carbonate ?) and there resembles the (misnamed) "skarn" from 58.6m.

69.8-70.7 Ironstone, Py > Mt

The ironstone is locally banded just below the contact but is mostly of the blotchy type in which coarse masses of pyrite appear to have replaced a magnetite rich precursor; generally around 60% Py, 20% Mt with quartz + carbonate gangue.
The upper contact is sharp marked by a thin sericitized ? contact zone between the schist above and brecciated/massive carbonate + pyrite below. This carbonate + pyrite rock is about 100mm wide and is transitional over a short interval into the banded Mt + Py ironstone at 69.9m; the contact and the transitional zone are semi parallel to banding in the ironstone. The lower contact at 70.7m is very sharp against a 50mm wide zone of shearing and sericitization ? in the adjacent schist.

70.7-85.8 Albite + quartz + chlorite + carbonate Schist

This is a variably textured semi mafic schist varying from very fine grained and rather chloritic to medium grained granular of more felsic/ quartzose composition. It generally displays a fairly distinct textural/

compositional banding (at about 30-50 deg. to LACC) which is interpreted to represent relict sedimentary layering in a precursor of felsic-intermediate tuffaceous/epiclastic character. Some of the layers are tightly folded (eg: cherty band at 78.0m) and the mica defined foliation appears to be axial to these folds; it is likely that layering is locally transposed.
At 74.0-74.3 the core is strongly brecciated and veined with milky quartz; above this zone the rock appears to be pervasively altered, silicified ? with assemblage dominated by quartz, albite , carbonate and <5% chlorite; I'm uncertain whether this represents chlorite destructive alteration or a primary compositional variation.
A 20mm thick layer parrallel band of fine massive chlorite with feldspar ? porphyroblasts (or relict phenocrysts ?) at 81.5m may represent a mafic intrusive "dykelet".

85.8m EOH.

EL 56/89 - Corinna South; Alpine Anomaly

Drill Core Magnetic Susceptibility Measurements
CRAE Drillholes: AP1 and AP2 (1985)

Measured by: W.Herrmann 20/6/90
Instrument: Kappameter KT-5
Units: S.I./1000

Hole No: AP1

Depth (m)	Susceptibility min	Susceptibility max	Comments
30 - 31		0.1	NQ core, broken and weathered
31 - 32		0.1	"
32 - 33		0.1	"
33 - 34		0.1	"
34 - 35		0.1	"
35 - 36		0.1	"
36 - 37	0.1	0.7	"
37 - 38		0.1	"
38 - 39		0.1	NQ core, half sawn, short lengths
39 - 40	0.1	0.2	mostly <120mm;
40 - 41	0.1	0.2	measurement on flat sawn surface
41 - 42		0.1	out of tray.
42 - 43		0.1	"
43 - 44		0.1	"
44 - 45	0.1	0.2	"
45 - 46		0	"
46 - 47		0	"
47 - 48		0	"
48 - 49		0	"
49 - 50		0	"
50 - 51		0.1	"
51 - 52		0.1	"
52 - 53		0.2	"
53 - 54		0.2	"
54 - 55		0.2	"
55 - 56		0.2	"
56 - 57	0.2	0.3	"
57 - 58	0.2	0.3	"
58 - 59	0.3	0.4	"
59 - 60	0.3	0.4	"
60 - 61	0.4	0.6	"
61 - 62	0.5	0.6	"
62 - 63	0.3	0.5	"
63 - 64	"	"	"
64 - 65	"	"	"
65 - 66	"	"	"
66 - 67	"	"	"
67 - 68	"	"	"
68 - 69	"	"	"
69 - 70	"	"	"

0080

364163

Depth (m)	Susceptibility min	Susceptibility max	Comments
Hole No: AP1			
70 - 71	"	"	"
71 - 72	"	"	"
72 - 73	"	"	"
73 - 74	"	"	"
74 - 75	"	"	"
75 - 76	"	"	"
76 - 77	0.4	0.7	"
77 - 78	"	"	"
78 - 79	0.4	0.5	"
79 - 80	"	"	"
80 - 81	"	"	"
81 - 82	0.5	0.9	"
82 - 83	0.5	1.5	Massive Py: 1-1.5
83 - 84	0.5	1.0	
84 - 85	0.5	470	Mt rich zones: 400-470
85 - 86	0.7	300	Mt rich zones: 120-300
86 - 87	0.5	0.7	
87 - 88	0.5	360	Mt rich zones: 130-360
88 - 89	4.0	780	
89 - 90	2.0	300	NQ core, half sawn, short lengths
90 - 91	180	430	mostly <120mm;
91 - 92	70	270	measurement on flat sawn surface
92 - 93	0.5	400	out of tray.
93 - 94	0.2	#0.5	"
94 - 95		#0.2	"
95 - 96		0.1	"
96 - 97	0.1	0.3	"
97 - 98	0.1	0.3	"
98 - 99	0.1	0.1	"
99 - 100		0.2	"
100 - 101	0.1	0.2	"
101 - 102	0.1	0.2	"
102 - 103	0.1	0.2	"
103 - 104	0.1	0.1	"
104 - 105		0.1	"
105 - 106	0.1	0.1	"
106 - 106.7	0.1	0.1	"

Hole No: AF2

Depth (m)			Susceptibility min	max	Comments
55.5	-	56	280	340	NQ core, half sawn, short lengths mostly <120mm; measurement on flat sawn surface out of tray.
56	-	57	0.3	20.0	
57	-	58	0.2	0.7	
58	-	59	0.3	230	
59	-	60	170	440	"
60	-	61	150	350	"
61	-	62	340	480	"
62	-	63	370	680	"
63	-	64	540	640	
64	-	65	0.2	880	Ironstone: 430-880
65	-	66	0.2	0.8	
66	-	67	0.5	680	Ironstone: 75-680
67	-	68	700	900	
68	-	69	0.4	700	Ironstone: 600-700
69	-	70	0.2	270	Ironstone: 10-270
70	-	71	100	360	
71	-	72	0.2	0.4	
72	-	73	0.1	0.4	
73	-	74	0.1	0.7	
74	-	75	0.1	0.7	
75	-	76	0.5	0.7	
76	-	77	0.1	0.3	
77	-	78	0.1	0.2	
78	-	79	0.1	0.1	
79	-	80	0.1	0.7	
80	-	81	0.1	0.2	
81	-	82	0.2	1.3	
82	-	83	0.2	2.1	
83	-	84	0.1	0.3	
84	-	85.8	0.1	0.2	

Appendix IV List of thirteen ironstone samples and analytical data; AP1, AP2.

APPENDIX IV

List of AP1 and AP2 Ironstone analytical samples:

Sample No:	Hole	Depth (m)	Description
A104622	AP1	81.7-81.9	80% massive/granular pyrite, 10% carbonate, minor sp, cpy, gn; in 30cm band in psammitic schist.
104623	"	84.4-84.5	Laminar/banded straw coloured carbonate-quartz-pyrite, minor cpy.
104624	"	84.8-85.0	Banded/foliated magnetite-pyrite-(qtz-carb) ironstone; 40%Mt 40%Py; 2%Cpy partly in late tectonic zoned carb-qtz veins.
104625	"	87.9-88.1	Banded/foliated Mt-Qtz-Py-carbonate ironstone; 40%Mt 40%Qtz 20%Py 10%carb 1%Cpy disseminated throughout.
104626	"	88.6-88.8	Pyrite-carbonate rich ironstone; ~40%Py
104627	"	90.4-90.6	Low pyrite type banded magnetite-quartz-carbonate ironstone; 50%Qtz 25%carb 20%Mt 1%Py 2%Biotite; ferruginous-siliceous exhalative?
A104628	AP2	55.5-55.7	Banded magnetite-pyrite-quartz-carbonate ironstone.
104629	"	56.1-56.2	Carbonate-pyrite rich selvedge of Mt-Py-Qtz-Carb ironstone; 75%carb 20%Py, as pervasive replacement and veiny infilling of brecciated ironstone.
104630	"	59.8-60.0	Pyrite rich banded/blotchy/lacy ironstone; 60%Py 20%Mt
104631	"	61.3-61.5	Sub-mylonitic foliated/finely banded magnetite rich ironstone; ~40%Qtz 25%Mt 25%carb 5%Py
104632	"	64.3-64.4	Magnetite rich ironstone; 50%Mt
104633	"	67.6-67.8	Banded/foliated magnetite rich ironstone; 50%Mt 20%Qtz 20%carb 10%py; some minor evidence of pyrite and carbonate replacement of magnetite syn shearing but mostly these phases are in syn-tectonic equilibrium.
104634	"	70.0-70.2	Blotchy pyrite rich ironstone; 50%Py 30%carb 10%Mt 10%Qtz; evidence of partial carbonate-qtz alteration of pyrite.

0084

ANALABS

A division of MacDonald Hamilton & Co. Pty. Ltd.

Phone (09) 458 7999

52 Murray Road, Welshpool, W.A. 6106

Telex AA92560

FAX: 004 31 8890

ANALYTICAL REPORT No. 999.66.08.07205

THIS REPORT MUST BE READ IN CONJUNCTION WITH THE ACCOMPANYING ANALYTICAL DATA

Outokumpu Exploration Aust
Suite 2, Level 6
77 Pacific Highway
Sydney NSW 2060

ORDER No.	PROJECT
20231	EL 56/89

DATE RECEIVED	RESULTS REQUIRED
28/06/90	ASAP

No. OF PAGES OF RESULTS	DATE REPORTED	No. OF COPIES	TOTAL No. OF SAMPLES
1	24/07/90	1	13

SAMPLE NUMBERS	DRY	CRUSH / SPLIT / PULVERISE / SIEVE / OTHER SEE REMARKS / NONE	ANALYSIS (REFER TO ANALYSIS SECTION)	PREPARATION	METHOD
<A1046,22/34	SC	Prep: 006,010,011,012,013,016	Cu,Pb,Zn,Fe,Mg,Ca,Na,K/104		
<A1046,22/34	SC	Prep: 006,010,011,012,013,016	Cu,Pb,Zn,Fe,Mg,Ca,Na,K/104		
<A1046,22/34	SC		Ag,Bi,Co,Ni,Mn/140		
<A1046,22/34	SC		Ag,Bi,Co,Ni,Mn/140		
<A1046,22/34	SC		Au,AuChk/309		

RESULTS TO

W. Herrmann
RSD 1066
Devonport
Tasmania 7310

RESULTS TO

Outokumpu Exploration Aust
Suite 2, Level 6
77 Pacific Highway
Sydney NSW 2060

REMARKS

Alpine Cove Specimens
AP1, AP2

STATE OF SAMPLES

e core	WC
ore	SC
ng	CU
	Ro
	SO
	PU
	WA
e	TI
m sediment	SS
y mineral	HM

ANALYSIS — PREPARATION

perchloric acid	A1	cold acid	CA
hydrochloric acid	A2	specific sulphide	SS
nitric acid	A3	other mixed acids	Ma
aqua regia	A4	alkaline attack	AA
nitric-perchloric	A5	volatilization	VO
HF mixture	A6	ignition	IG
HF under pressure	A7	pressed powder (XRF)	PP
fusion	A8	glass fusion (XRF)	GF

ANALYSIS — METHOD

atomic absorbtion	AAS
x-ray fluorescence	XRF
spectrophotometry	SPEC
colorimetry	COL
chromatography	CHR
titration	TTN
other chemicals means	CHEM
miscellaneous	MISC
fluorescence	FLUOR
inductively coupled plasma	ICP

AUTHORISED OFFICER [signature]

ANALABS

A Division of Inchcape Inspection and Testing Services Australia Pty Ltd.

ANALYTICAL DATA

SAMPLE PREFIX	REPORT NUMBER	REPORT DATE	CLIENT ORDER No.	PAGE
	999.66.08.07205	24/07/90	20231	1 OF 1

TUBE No	SAMPLE No.	Cu	Pb	Zn	Fe	Mg	Ca	Na	K	Ag
1	A104622	950	400	16500	48.40	0.37	0.04	<0.01	0.08	3.0
2	A104623	775	50	300	44.90	1.21	0.23	<0.01	0.02	1.0
3	A104624	9700	<25	250	46.20	0.34	0.11	<0.01	<0.01	1.0
4	A104625	7500	<25	150	53.60	0.36	0.13	<0.01	<0.01	1.0
5	A104626	7750	<25	150	36.00	1.68	3.02	<0.01	<0.01	1.0
6	A104627	3050	<25	100	28.40	2.12	5.49	<0.01	0.02	<0.5
7	A104628	6500	25	225	40.10	1.01	0.28	<0.01	<0.01	1.0
8	A104629	3875	25	100	31.40	1.16	0.14	0.03	0.05	2.0
9	A104630	15100	<25	100	44.90	0.71	0.19	<0.01	<0.01	1.0
10	A104631	2550	<25	125	42.00	0.79	0.16	<0.01	<0.01	<0.5
11	A104632	2350	<25	150	56.80	0.43	0.09	<0.01	<0.01	1.0
12	A104633	3875	25	200	61.30	0.44	0.12	<0.01	<0.01	1.0
13	A104634	8400	25	175	47.00	0.80	0.18	<0.01	<0.01	1.0
14										
15										
16										
17										
18										
19										
20										
21										
22										
23	DETECTION	25	25	25	0.05	0.01	0.01	0.01	0.01	0.5
24	UNITS	ppm	ppm	ppm	%	%	%	%	%	ppm
25	METHOD	104	104	104	104	104	104	104	104	103

Results in ppm unless otherwise specified
T = element present; but concentration too low to measure
X = element concentration is below detection limit
— = element not determined

AUTHORISED OFFICER [signature]

ANALABS

A Division of Inchcape Inspection and Testing Services Australia Pty. Ltd.

ANALYTICAL DATA

SAMPLE PREFIX	REPORT NUMBER	REPORT DATE	CLIENT ORDER No.	PAGE
	999.66.08.07205	24/07/90	20231	1 OF 1

TUBE No.	SAMPLE No.	Bi	Co	Ni	Mn	Au	AuChk	As	As	Sb
1	A104622	<10	85	30	4000	0.081	–	230	>100	<3
2	A104623	<10	200	30	6600	0.105	–	–	50	<3
3	A104624	<10	305	15	1025	0.024	0.038	–	10	<3
4	A104625	<10	275	25	625	0.022	–	–	11	<3
5	A104626	<10	310	<10	3400	<0.008	–	–	15	<3
6	A104627	<10	115	25	1750	<0.008	–	–	6	<3
7	A104628	<10	270	45	2750	<0.008	–	–	8	<3
8	A104629	<10	190	10	3050	<0.008	–	–	53	<3
9	A104630	<10	650	40	1400	<0.008	–	–	4	<3
10	A104631	<10	210	50	2000	<0.008	–	–	5	<3
11	A104632	<10	245	10	710	<0.008	–	–	8	<3
12	A104633	<10	245	35	1400	<0.008	–	–	8	<3
13	A104634	<10	340	15	1375	0.026	–	–	4	<3
14										
15										
16										
17										
18										
19										
20										
21										
22										
23	DETECTION	10	5	10	5	0.008	0.008	100	1	3
24	UNITS	ppm	ppm	ppm	ppm	ppm	ppm	ppm	ppm	ppm
25	METHOD	103	103	103	103	309	309	101	114	401

Results in ppm unless otherwise specified
T = element present; but concentration too low to measure
X = element concentration is below detection limit
— = element not determined

AUTHORISED OFFICER Jenkins

ANALABS

A Division of Inchcape Inspection and Testing Services Australia Pty. Ltd.

ANALYTICAL DATA

SAMPLE PREFIX	REPORT NUMBER	REPORT DATE	CLIENT ORDER No.	PAGE
	999.66.08.07205	24/07/90	20231	1 OF 1

TUBE No.	SAMPLE No.	Sn	W	Mo	Ba	Zr	Y	La	Ti	Cr
1	A104622	<3	<20	<10	17	<5	1	<5	107	<10
2	A104623	5	<20	<10	16	<5	8	6	36	32
3	A104624	4	<20	<10	24	<5	2	<5	50	<10
4	A104625	6	<20	<10	14	<5	3	<5	45	32
5	A104626	<3	<20	<10	12	10	10	7	342	15
6	A104627	<3	<20	<10	53	<5	4	6	55	34
7	A104628	<3	<20	<10	18	<5	8	<5	76	29
8	A104629	<3	<20	15	28	<5	4	<5	129	17
9	A104630	<3	<20	<10	10	<5	5	<5	54	<10
10	A104631	4	<20	<10	19	<5	4	<5	44	41
11	A104632	<3	<20	<10	12	<5	4	<5	86	<10
12	A104633	<3	<20	<10	14	<5	8	<5	46	20
13	A104634	<3	<20	<10	7	<5	4	<5	31	<10
14										
15										
16										
17										
18										
19										
20										
21										
22										
23	DETECTION	3	20	10	5	5	1	5	10	10
24	UNITS	ppm	ppm	ppm	ppm	ppm	ppm	ppm	ppm	ppm
25	METHOD	401	201	201	201	201	201	201	201	201

Results in ppm unless otherwise specified
T = element present; but concentration too low to measure
X = element concentration is below detection limit
— = element not determined

AUTHORISED OFFICER Jenkins

Appendix V Drill core logs and drill sections: AP1 and AP2

G.Purvis / from CRAE Report No:13678
(Caithness, 1985; TCR 86-2538)

007

C.R.A EXPLORATION PTY. LIMITED
DRILL CORE LOG

SHEET No. 1
TENEMENT NAME EL 1/77 ROCKY CAPE No. ALPINE PROSPEC
LOGGED BY G. PURVIS

CO-ORDINATES 9100E, 9385N AZIMUTH 357° AMG (346° MAG) DRILLERS OVERLAND COMMENCED 22.1.85 DEPTH 106.7m HOLE No. PD85 AP1
RL COLLAR 192m INCLINATION -65° DRILL TYPE WARMAN 500 COMPLETED 30.1.85 CASING LEFT PVC to 4m DPO No(s) 31929

ASSAY VALUES (Analysed by ANALABS) — X = <0.008 ppm

Depth From (M)	Depth To (M)	Core Rec. (M)	Core Size	Graphic Log	Core Description	Special Features (Weath, Alteration, Fracturing, Veining, Mineralization)	Sample No.	From (M)	To (M)	Rec (M)	Cu	Pb	Zn	Ag	Au
PERCUSSION															
0	7			TERTIARY!	AMYGDALOIDAL MAFIC LAVA	5-7m, minor limonite stains, 1 thin qtz vein.	1154601	0	3		35	10	40	<.5	
					Pale yellow and grey.		1154602	3	5		70	10	25	<.5	+
					Soft, highly weathered and clayey.		1154603	5	7		90	<5	45	<.5	
					Fine gr, with 1-3mm amygdales filled with zeolite										
7	12				CEMENTED QUARTZ GRIT AND SILICEOUS 'GREY BILLY'	Highly limonite-stained.	1154604	7	9		90	<5	100	<.5	X
					An alluvial deposit cemented by silica.		1154605	9	11		80	<5	35	<.5	
					Yellow-brown. Hard.		1154606	11	13		65	<5	100	<.5	X
					Qtz grit with silica-limonite cement; qtz-pebble conglomerate with silica-limonite cement; and massive amorphous silica ('grey billy')										
12	18				Pale grey QUARTZ-MICA SCHIST,	Qtz veins to 25mm, generally <10mm	1154607	13	15		25	<5	40	<.5	
					Black GRAPHITIC SCHIST, and	1-5% dissem py. Some py in	1154608	15	17		25	<5	30	<.5	X
					soft, black CARBONACEOUS METASILTSTONE	qtz veins, and as thin beds (<1mm) in metasiltstone.	1154609	17	18		20	<5	20	<.5	
					Minor vesicular BASALT 13-15m c minor py.										
18	30				FAULT ZONE	Interval characterized by abundant	1154610	18	20		5	<5	100	<.5	X
					Pale green + white QTZ-SERICITE SCHIST	veins and irreg masses of vuggy	1154611	20	22		10	<5	65	<.5	
					Green, black + white QTZ-GRAPHITE-MICA SCHIST	xylling qtz.	1154612	22	24		5	5	50	<.5	X
						1-10% dissem py. Av 2-3%, strongest	1154613	24	26		5	<5	25	<.5	
					Minor, pale grey, finely laminated QTZ-MICA SCHIST.	20-24m. Poss arsenopy 22-24m	1154614	26	28		5	<5	20	0.5	X
						Hole making a lot of water commencing at 18m	1154615	28	30		5	<5	15	<.5	
					QUARTZITE PEBBLES coated with										

Detection limits noted above assay columns: 10, 20, 50, <.5

0041

SHEET No. 2

C.R.A EXPLORATION PTY. LIMITED
DRILL CORE LOG

TENEMENT NAME.................... No. ....

PLAN – MAP REFERENCE....................

CO-ORDINATES.................... AZIMUTH.................... DRILLERS.................... COMMENCED.................... DEPTH.................... HOLE No. PD85AP1

RL COLLAR.................... INCLINATION.................... DRILL TYPE.................... COMPLETED.................... CASING LEFT.................... DPO No(s). 31930

DEPTH From (M)	DEPTH To(M)	Core Rec. (M)	Core Size	Graphic Log	CORE DESCRIPTION	SPECIAL FEATURES Weath, Alteration, Fracturing, Veining, Mineralization	Sample No.	From (M)	To (M)	Rec (M)	Cu	Pb	Zn	Ag	Au	
					pyrite cement appear in samples	Caving ground 18-24m + 27-30m										
					below soft zone @ 19.5m											
					Rocks highly schistose and broken up											
					27 – 30m											
					COMMENCED NQ CORING AT 30m.											
30.00	36.80	4.7	NQ		QUARTZ-SERICITE SCHIST (SHEAR ZONE).	Highly broken, leached + clayey.	1154735	30	32	2.0	20	<5	20	3.0		
					Pale creamy-green.	Dissem py in rock + qtz veins, av	736	32	34	2.0	10	5	15	3.5		
					Abundant lining qtz veins and lenses	2%, locally 3-5%.	1154737	34	36.80	2.8	5	10	25	2.5		
					to 130mm, av ~10mm. Vuggy c ?throats											30.0 – 40.0 =
					of sericite.											10m @ 2.58 g/t
					Fe ?gr rock (prob after qtzose siltstone).											
					Schistosity 65°/LCA @ 32m.											
36.80	62.00	23.65	NQ		GRAPHITIC-MICA SCHIST and	Up to 10% dissem and veinlet py –	1154738	36.80	38	1.2	50	20	40	1.5		
					QUARTZ-MICA-CARBONATE SCHIST	best in graphitic zones. Some	739	38	40	2.0	30	10	45	2.0		
					After interbedded black shales and	bedded laminae of py-carb 1-2mm.	1154740	40	42		45	15	55	1.0		
					fine qtzose sandstones.	Augen of deformed coarsely xlline py	741	42	44		30	<5	40	1.5		
					Black and grey.	to 10mm in graphitic zones.	742	44	46		55	15	80	0.5		
					Badly broken and sheared in	Trace cp below 41m.	743	46	48		10	35	85	1.0		
					graphitic zones.	Details of py content:	744	48	50		20	10	30	0.5		
					Schistosity // bedding: 50°/LCA @ 37.5m;	36.8 – 46.1m: 3-5% py.	745	50	52		55	5	45	<0.5		
					42°/LCA @ 46.4m; 20°/LCA @ 50.1m;	46.1 – 49.3m: 1-2% py.	746	52	54		30	10	75	0.5		
					43°/LCA @ 60.7m.	49.3 – 51.3m: 3-5% py.	747	54	56		30	15	75	0.5		
					Strong shear // bedding, in graphitic zones,	51.3 – 55.5m: 1-2% py.	748	56	58		45	20	35	0.5		
					35°/LCA 45.7 – 46.1m.	55.5 – 62m: 5% py.	749	58	60		145	10	35	1.0		
					Impure beds of carb to 20mm 46.1 –		1154750	60	62		90	10	40	0.5		
					49.3m.											
					Irreg veins and laminae of qtz-carb to											
					35mm, av <5mm	[illegible] 70°/LCA										

ASSAY VALUES (Analysed by ANALABS)

C00

C.R.A EXPLORATION PTY. LIMITED
DRILL CORE LOG

SHEET No. 3
TENEMENT NAME .... No. ....
PLAN – MAP REFERENCE ....

CO-ORDINATES .... AZIMUTH .... DRILLERS .... COMMENCED .... DEPTH .... HOLE No. PD85AP1
RL COLLAR .... INCLINATION .... DRILL TYPE .... COMPLETED .... CASING LEFT .... DPO No(s) 31930

DEPTH From (M)	DEPTH To (M)	Core Rec. (M)	Core Size	Graphic Log	CORE DESCRIPTION	SPECIAL FEATURES Weath, Alteration, Fracturing, Veining, Mineralization	Sample No.	From (M)	To (M)	Rec (M)	Cu	Pb	Zn	As	Au	ASSAY VALUES (Analysed by ANALABS)
62·00	83·60	21·60	NQ		QUARTZ-MICA-CARBONATE SCHISTS	62–75·4m: 1-2% py, dissem + veinlets	1154751	62	64		35	15	35	<0,5		
					Inter variable sequence of finely	Rare trace cp. Trace cp-sp-gn in qtz	752	64	66		45	20	30	0,5		
					bedded sandstones, siltstones, grey	vein @ 64·3m.	753	66	68		30	15	55	0,5		
					and black shales. Minor graphitic	75·4–83·6m: 5-10% py, dissem +	754	68	70		35	45	150	0,5		
					sections	in veinlets, but mostly in massive	755	70	72		30	10	60	1,0		
					Pale grey to greenish-grey	and semi-massive bands // schistosity	756	72	74		30	20	55	1,0		
					Trace chlorite increasing below 82·1m	Best of these:	757	74	76		175	15	100	0,5		
					Highly micaceous 75–77·5m.	76·7m: 200mm, 45°/LCA.	758	76	78		290	70	1550	<0,5		76–84.2m =
					Diffuse irreg qtz-carb veins and	77·4m: 190mm, 45°/LCA.	759	78	80		970	40	1000	<0,5		8.2m @ 0.19% Cu
					patches up to 70mm, esp in silicified	78·1m: 100mm, 60°/LCA. Minor arsenopy	1154760	80	82		290	115	4150	0,5		
					zones 62–63·7m, 74·45–74·9m, 78·65	78·75m: 100mm, 45°/LCA.	761	82	84·20	2.2	1020	75	920	0,5		
					–79·9m.	79·3m: 40mm, 50°/LCA. Trace cp-arsenopy.										
					Minor breccia zones.	81·8–82·1m: 300mm, 60°/LCA. 5% sp-gn										
					Schistosity (after bedding): 48°/LCA	83·6m: 30mm, 55°/LCA. Minor cp-sp										82.0–94.75 =
					@ 70·2m, 53°/LCA @ 82·4m.	Minor arsenopy-cp-sp-gn, below 75m.										12.75m @ 0.24% Cu
					Basal contact 75°/LCA.											
83·60	84·20	0·60	NQ		QUARTZ-MICA-CHLORITE SCHIST	3% dissem + veinlet py. Minor cp.										
					Green.											
					Some irreg qtz veins											
84·20	85·15	0·95	NQ		SEMI-MASSIVE BANDED SULPHIDE		1154762	84·20	85·15	0.95	4600	30	85	0,5		
					Upper contact 65°/LCA, lower 30°/LCA.											
					Sulphide banding 45°/LCA											
					Bands and clots of py-magnetite-											
					-hematite in gangue of carb > qtz											
					> chlorite. 1-2% cp.											
					Intercalation of chlorite schist 84·5–84·6m.											
85·15	87·50	2·35	NQ		QUARTZ-CHLORITE SCHISTS	5% dissem py, locally 10%. Trace cp.	1154763	85·15	87·50	2.35	1000	15	65	0,5		

364172

C.R.A EXPLORATION PTY. LIMITED

DRILL CORE LOG

SHEET No. ......
TENEMENT NAME ...... No. ......
PLAN – MAP REFERENCE ......

CO-ORDINATES ...... AZIMUTH ...... DRILLERS ...... COMMENCED ...... DEPTH ...... HOLE No. PD85AP1

RL COLLAR ...... INCLINATION ...... DRILL TYPE ...... COMPLETED ...... CASING LEFT ...... DPO No(s) 31930

ASSAY VALUES (Analysed by ANALABS)

DEPTH From (M)	DEPTH To (M)	Core Rec. (M)	Core Size	Graphic Log	CORE DESCRIPTION	SPECIAL FEATURES Weath, Alteration, Fracturing, Veining, Mineralization	Sample No.	From (M)	To (M)	Rec (M)	Cu	Pb	Zn	Ag	Au
					Green and creamy-grey	Trace magnetite in upper 0.3m.									
					Minor carb and mica. Some diffuse										
					patches of xylline qtz-carb.										
87.50	92.85	5.30	NQ		BANDED SEMI-MASSIVE TO MASSIVE	Leaser hematite. 1% cp (locally 2%).	1154764	87.50	89.50	2.0	5000	20	50	1,0	
					PYRITE - MAGNETITE	Trace gn-sp. Some chalcocite and	765	89.50	91.50	2.0	990	20	40	0.5	
					Upper contact 38°/LCA.	bornite 91.5 – 92.85m.	766	91.50	92.85	1.35	3100	25	65	<0.5	
					Sulph + mag gen more-massive towards										
					upper + lower margins of zone.										
					Qtz > carb gangue. Very hard										
					Minor chlorite. Poss bornite @ 90.5m										
					Banding in sulph: 43°/LCA @ 88.1m,										
					52°/LCA @ 92m.										
					Basal contact a shear 65°/LCA.										
92.85	93.75	0.35	NQ		SHEAR ZONE IN QUARTZ - CHLORITE -	7-10% dissem py. Minor cp.									
					CARBONATE SCHIST 60°/LCA.	Highly broken and clayey.									
					Minor mica and dark magnesian chlorite										
93.75	96.75	2.55	NQ		QUARTZ-MICA SCHIST	3-5% py, minor persistent cp.	1154767	92.85	94.75	1,9	2600	10	75	<0,5	
					After finely bedded qtzose sandstones,		768	94.75	96.75		175	5	40	1,0	
					siltstones and black shales.										
					Minor graphitic zones. Minor chlorite + carb										
					Main shear continues to 94.3m - highly										
					broken, with irreg qtz veins to 80mm.										
					Below this, some sheared micaceous zones										
					and brecciated qtzose zones.										
					Schistosity (after bedding) 50°/LCA @ 95.8m.										
96.75	106.70	8.70	NQ		GRAPHITIC SCHIST	7-10% dissem py. Some as clots after	1154769	96.75	99		70	5	60	1,0	

364173

011

C.R.A EXPLORATION PTY. LIMITED
DRILL CORE LOG

SHEET No. 5

TENEMENT NAME .... No. ....

PLAN – MAP REFERENCE ....

CO-ORDINATES .... AZIMUTH .... DRILLERS .... COMMENCED .... DEPTH .... HOLE No. PD85AP 1

RL COLLAR .... INCLINATION .... DRILL TYPE .... COMPLETED .... CASING LEFT .... DPO No(s) 31930

DEPTH From (M)	DEPTH To (M)	Core Rec. (M)	Core Size	Graphic Log	CORE DESCRIPTION	SPECIAL FEATURES Weath, Alteration, Fracturing, Veining, Mineralization	Sample No.	From (M)	To (M)	Rec (M)	ASSAY VALUES (Analysed by ANALABS) Cu	Pb	Zn	Ag	Au
					A qtz-graphite-mica ± chlorite rock.	15mm. Tiny (<<1mm) threads of py	1154771	101	103		70	10	80	1.0	
					Black ē pale grey qtose bands.	// schistosity.	772	103	105		60	15	100	1.5	
					Highly Schistose, crenulated in places.	Irreg qtz ± carb ± chlor veins to 100mm	773	105	106.70		60	5	45	1.0	
					Gen badly broken. 100mm puggy	ē rare trace py.									
					clay zone @ 99.8m.										
					Schistosity 63°/LCA @ 98.5m, 50°/LCA										
					@ 103m.										
					END OF HOLE										

1609

364174

C.R.A EXPLORATION PTY. LIMITED
DRILL CORE LOG

SHEET No. 1
TENEMENT NAME ROCKY CAPE - ALPINE PROSPECT No. EL 1/7
LOGGED BY: G. PURVIS

CO-ORDINATES 8700 SE 9094 N AZIMUTH 357° AMG (346° MAG) DRILLERS OVERLAND COMMENCED 30.1.85 DEPTH 85.80m HOLE No. PD85AP2

RL COLLAR 189m INCLINATION -68° DRILL TYPE WARMAN 500 COMPLETED 2.2.85 CASING LEFT PVC TO 85m DPO No(s) 31928

Depth From (M)	Depth To (M)	Core Rec. (M)	Core Size	Graphic Log	CORE DESCRIPTION	SPECIAL FEATURES Weath, Alteration, Fracturing, Veining, Mineralization	Sample No.	From (M)	To (M)	Rec (M)	Cu	Pb	Zn	Ag	Au
	PERCUSSION														
0	4				MAFIC VOLCANIC		1154616	0	2		45	5	10	<.5	x
					Pale yellow and grey		1154617	2	4		110	5	5	<.5	
					Highly weathered, clayey, soft.										
					Fi-grained gr. Small (1mm) amygdales										
4	14				CHERT	1-5% py dissem. Some thin zones	1154618	4	6		70	<5	25	<.5	x
					A capping?	or bands of semi-massive py.	619	6	8		30	<5	30	<.5	
					V hard, fi gr. Dark bluish-grey c	Limonite stains	620	8	10		35	<5	45	<.5	x
					characteristic white exterior surface		621	10	12		60	10	55	<.5	
					to fragments. Dog tooth qtz xyls on		622	12	14		50	5	70	<.5	x
					exterior surfaces.										
					Rock composed of xylline qtz and										
					bluish chalcedonic qtz - some c agate										
					banding. Minor fine mica and										
					minor qtz-mica schist, variably silicified.										
14	14.50				SEMI-MASSIVE PYRITE		1154623	14	16		30	10	270	0.5	
					In quartz gangue										
14.50	19.50				QUARTZ-MICA SCHIST	1-3% dissem py.	1154624	16	18		45	5	270	<.5	x
					Pale grey, finely laminated.		625	18	20		50	35	600	1	
					Numerous barren qtz veins										
					Minor chlorite where more qtzose.										
19.50	45				QUARTZ-MICA-CHLORITE SCHIST	1-10% py, av 3%. Dissem, but	1154626	20	22		90	90	1600	<.5	x
					Greenish-grey. Finely laminated	also in massive and semi-massive	627	22	24		60	30	370	0.5	
					with intercalations of more-micaceous	laminae up to 15mm with minor	628	24	26		65	30	770	<.5	x
					and chloritic schist	hematite. Rare trace cp below 32m.	629	26	28		50	20	290	0.5	

x = <0.008 ppm

C.R.A EXPLORATION PTY. LIMITED

DRILL CORE LOG

SHEET No. 2

TENEMENT NAME .... No. ....

PLAN – MAP REFERENCE ....

CO-ORDINATES .... AZIMUTH .... DRILLERS .... COMMENCED .... DEPTH .... HOLE No. PD85AP 10

RL COLLAR .... INCLINATION .... DRILL TYPE .... COMPLETED .... CASING LEFT .... DPO No(s) 31930;

Depth From (M)	Depth To (M)	Core Rec. (M)	Core Size	Graphic Log	Core Description	Special Features (Weath, Alteration, Fracturing, Veining, Mineralization)	Sample No.	From (M)	To (M)	Rec (M)	Cu	Pb	Zn	Ag	Au	Assay Values (Analysed by ANALABS)
						-chlorite-qtz schist zone	1154631	30	32		55	15	180	<.5		
							632	32	34		275	90	650	1	x	
45	46				SEMI-MASSIVE PYRITE		633	34	36		45	10	180	0.5		
					In quartz gangue. Rare hematite.		634	36	38		35	10	140	0.5	x	
							635	38	40		55	20	135	0.5		
46	53				QUARTZ-MICA SCHIST	46-48m: 15% dissem py; conc in	636	40	42		55	5	155	0.5	x	
					Grey.	highly siliceous schist zones c̄ minor	637	42	44		185	10	1400	0.5		
					Finely laminated	hematite staining. Minor cp.	638	44	46	2.0	7650	30	290	1.5	0,03	
					Minor chlorite. Minor barren qtz	48-53m: 5-10% py. 1% cp 48-50m	639	46	48	2.0	5250	30	105	1.0		44 – 56,2m =
					veins.	Minor sp-gn-cp.	640	48	50	2.0	4900	15	160	0.5	x	12,2m → 0,629 %Cu
							641	50	52	2.0	3500 (3550)	30 (35)	170 (190)	<.5 (<.5)		
53	55.5				SEMI-MASSIVE HEMATITE-PYRITE-	Minor cp to 54m, then 3-5% cp.	642	52	54	2.0	1.30%	60	245	<.5	x	
					MAGNETITE	Note: Much contamination of sample	643	54	55.5	1.5	3500	25	410	<.5		
					In siliceous (cherty) gangue, some carbonate	1154643 by cave-in qtz-mica-										
					Reddish-purple colour.	chlorite schist from higher in hole.										
					Some fine banding.											
CORING																
55.5	56.20	0.70	NQ		SEMI-MASSIVE PYRITE-MAGNETITE	1% cp > bornite	1154774	55.50	56.20	0,7	4150	30	75	1.0		
					In qtz-carbonate (dolomite)-gangue.	Minor hematite.										
					V. hard. Some possible wollastonite.											
					Creamy-black in colour.											
					Finely banded 70°/LCA											
56.20	58.60	2.40	"		QTZ-CARBONATE-SERPENTINE SKARN	Minor py and cp.	1154775	56.20	58.60		870	<5	80	<0.5		
					Pale yellowish-green. Mod hard.											
					Prob after altered carbonate unit.											
					Small aggregates of fawn dolomite xyls											
					to 3mm, with minor talc, in matrix											
					of qtz >> serpentine.											
					Indistinctly banded 50°/LCA.											
					Shear at base											

3641 76

C.R.A EXPLORATION PTY. LIMITED

DRILL CORE LOG

SHEET No. 3

TENEMENT NAME.......................... No. ....

PLAN – MAP REFERENCE..........................

CO-ORDINATES.................... AZIMUTH.................... DRILLERS.................... COMMENCED.................... DEPTH.................... HOLE No. PD 85 AP 2

RL COLLAR.................... INCLINATION.................... DRILL TYPE.................... COMPLETED.................... CASING LEFT.................... DPO No(s) 31930

Depth From (M)	Depth To (M)	Core Rec. (M)	Core Size	Graphic Log	Core Description	Special Features (Weath, Alteration, Fracturing, Veining, Mineralization)	Sample No.	From (M)	To (M)	Rec (M)	Cu	Pb	Zn	Ag	Au			
8.60	64.80	6.20	NQ		MASSIVE PYRITE-MAGNETITE-HEMATITE	Up to 1% cp. Trace bornite.	1154776	59.60	60.60	2.0	1,25[illegible]	20	65	<0.5		]		
					Above 60.7m mostly pyrite c̄ indistinct		777	60.60	62.60	2.0	7100	20	60	<0.5			58.6–	66.65m
					banding. Below 60.7m mostly		778	62.60	64.80	2.2	4400	20	55	<0.5			= 8.05m	@ 0.72%
					magnetite > hem > py c̄ fine banding													
					(38°/LCA @ 61.3m).													
					Minor qtz-carb-chlor gangue.													
											4800							
4.80	66.65	1.85	NQ		CHLORITE-QUARTZ-CARBONATE SCHIST	1% py, minor cp.	1154779	64.80	66.65	1.85	[illegible]	30	50	<0.5		]		
					After altered mafic volc tuffs?	Minor qtz-carb veining.												
					Green, med gr.													
					Vague 1° layering 25°/LCA.													
.65	68.30	1.65	NQ		MASSIVE PYRITE-MAGNETITE-HEMATITE	Up to 1% cp. Minor bornite.	1154780	66.65	68.30		590	<5	45	<0.5				
					Hard. Minor qtz-carb gangue.													
					Banding 50°/LCA @ 68m.													
					Conformable basal contact 73°/LCA													
3.30	69.65	1.35	NQ		CHLORITE-CARBONATE-QUARTZ SCHIST	1-2% py, minor cp. Dissem + in	1154781	68.30	69.65		295	10	65	0.5				
					After altered mafic volc tuffs?	veinlets.												
					Pale green, med gr.													
					Banding (schistosity) 56°/LCA @ 68.7m.													
					Dolomite xyls to 3mm av < 1mm, in													
					matrix of chlorite, qtz and minor													
					serpentine.													
9.65	[illegible].80		NQ		MASSIVE PYRITE – MAGNETITE	Minor hematite, cp, bornite.	1154782	69.65	70.45	0.8	[illegible]	20	80	<0.5		]	69.65–	71.4m
					Minor qtz-carb gangue, trace chlorite.												= 1.75m	@ 0.44%
					Banded 45°/LCA													
	[illegible]				CHLORITE – QTZ – CARBONATE SCHIST	70.45–71m: 2% cp + bn, 1-2% py.	1154783	70.45	71.40	0.95	3050	5	30	<0.5		]		
					Green, med gr.	71–72.2m: 3% py, minor cp.												

3641[illegible]

C.R.A EXPLORATION PTY. LIMITED

DRILL CORE LOG

SHEET No. 4

TENEMENT NAME .... No. ....

PLAN – MAP REFERENCE ....

CO-ORDINATES .... AZIMUTH .... DRILLERS .... COMMENCED .... DEPTH .... HOLE No. PD85AP2

RL COLLAR .... INCLINATION .... DRILL TYPE .... COMPLETED .... CASING LEFT .... DPO No(s) 31931

DEPTH From (M)	DEPTH To (M)	Core Rec. (M)	Core Size	Graphic Log	CORE DESCRIPTION	SPECIAL FEATURES Weath, Alteration, Fracturing, Veining, Mineralization	Sample No.	From (M)	To (M)	Rec (M)	Cu	Pb	Zn	Ag	Au	Ba
					Carb mainly dolomite to 75m then calcite	72.2 – 84.4m: 1% py. Trace cp + bn.	1154730*	71.4	74.4		640	<5	80	<.5	<0.008	110
					– often partially leached.	84.4 – 85.8m: 2–3% py. Trace cp + bn.	731	74.4	77.4		180	<5	65	<.5		
					Minor irreg veins of qtz and/or carb,	Sulphides dissem + in 1-2mm veinlets	732	77.4	80.4		175	<5	50	<.5	<0.008	60
					often partly leached.		733	80.4	83.4		220	<5	75	<.5		
					Above 77m some highly siliceous zones	Cavity 75.75 – 76.3m – core loss.	734	83.4	85.8		195	<5	60	<.5	<0.008	20
					Some mineral banding prob after 1°											
					lineation (50° LCA @ 81.6m) – folding											
					evident.											
					END OF HOLE											

ASSAY VALUES (Analysed by ANALABS)

* 1154730 – 734 are grind samples.

364178

0097

364179

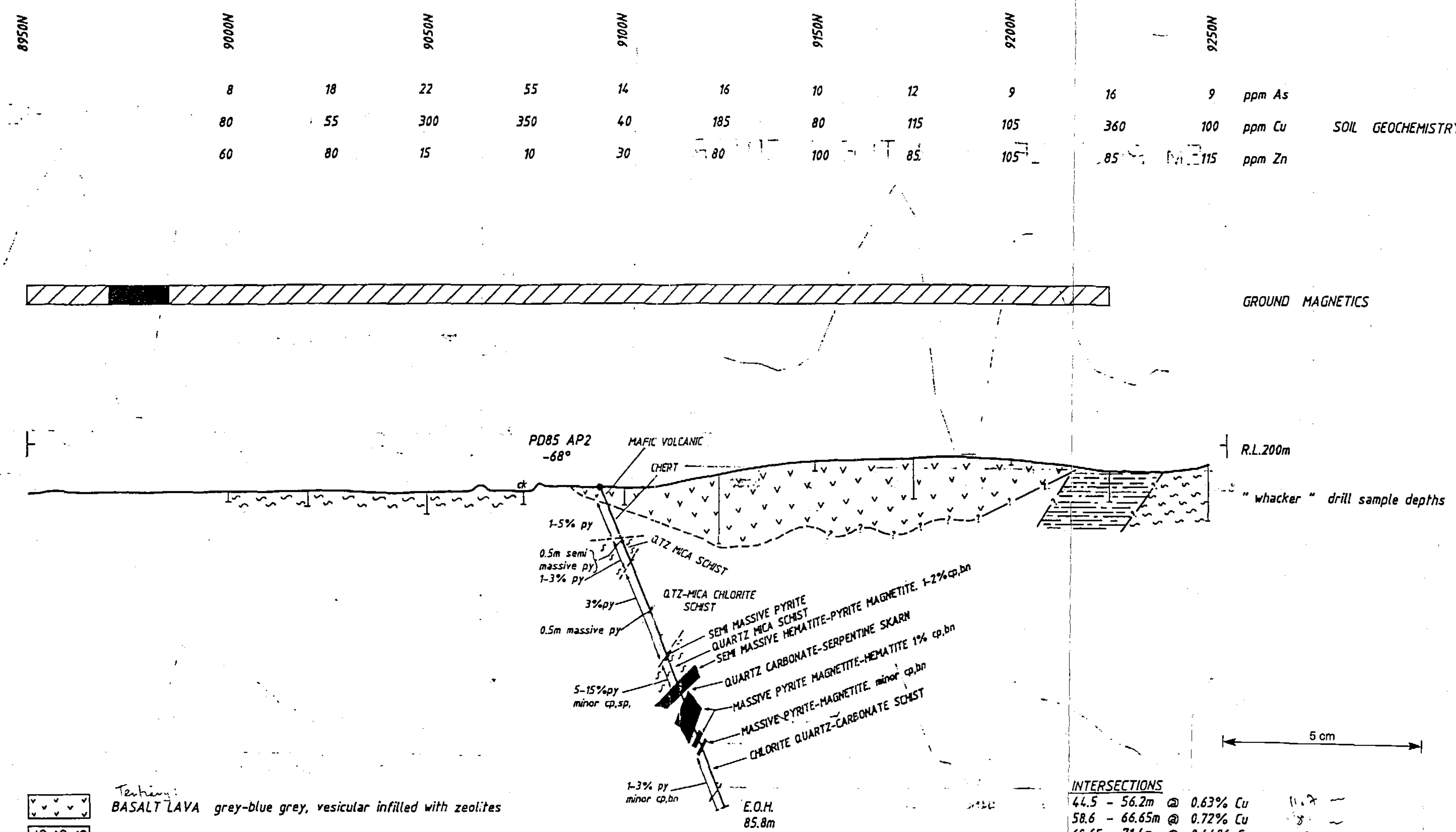

Tertiary:

BASALT LAVA grey-blue grey, vesicular infilled with zeolites

QUARTZ MICA SCHIST chloritic in part, grades? into a micaceous sandstone.

SILTSTONE blue-grey, slightly chloritic interpreted as possible black shale

------- GEOLOGICAL CONTACT

SCHISTOSITY

INTERSECTIONS

44.5 – 56.2m @ 0.63% Cu
58.6 – 66.65m @ 0.72% Cu
69.65 – 71.4m @ 0.44% Cu

E.M. Conductor at 9125N Dip 55° to south. Depth to top 15m. Approximately Approx 10m thick. Hole designed to intersect at 40m vertical depth.

PD85 AP2 DRILL SECTION LOOKING WEST
COLLAR CO-ORDINATES 8700E. 9094N.
DIP -68°, BEARING 346° MAGNETIC

CRA EXPLORATION PTY. LIMITED

ROCKY CAPE E.L. 1/77
ALPINE ANOMALY LINE 8700E
PD85 AP2 DRILL SECTION
LOOKING WEST

270

REF.	SKSS - 3		
SCALE	1 : 1000	DRAWN	R.T.
AUTHOR	J.W. & G.P.	REPORT No.	
DATE	14 - 3 - 1985	PLAN No	TASh 2549

364180

SOIL GEOCHEMISTRY

	9300N	9350N		9400N		9450N		9500N		9550N	9600N
ppm As	12	18	16	8	450	14	20	38	20	22	12
ppm Zn	35	80	140	105	40	940	195	540	800 800	40	350
ppm Cu	40	65	85	220	380	90	55	40	75	85	165

GROUND MAGNETICS

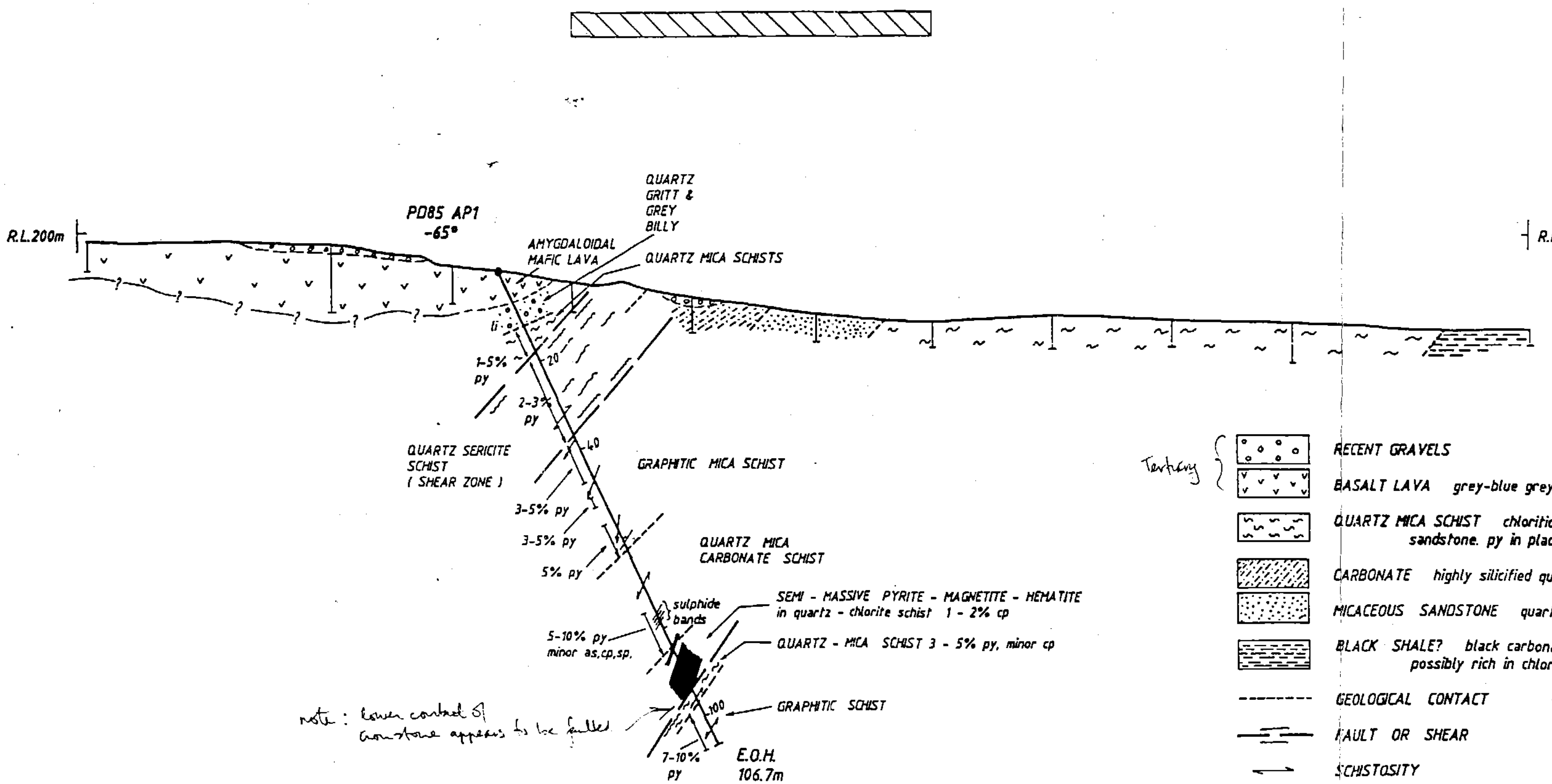

Tertiary
- RECENT GRAVELS
- BASALT LAVA grey-blue grey,vesicular infilled with zeolites
- QUARTZ MICA SCHIST chloritic in part, grades? into a micaceous sandstone. py in places.
- CARBONATE highly silicified quartz rich carbonate 10 - 20% py in pla
- MICACEOUS SANDSTONE quartz rich version of the schist
- BLACK SHALE? black carbonaceous / graphitic rock possibly rich in chlorite.
- GEOLOGICAL CONTACT
- FAULT OR SHEAR
- SCHISTOSITY
- BEDDING
- li LIMONITE
- py PYRITE

INTERSECTIONS

30.0 - 40.0m = 10m a 2.5 g/t Ag
76.0 - 84.2m = 8.2m a 0.19% Zn 8.2
82.0 - 94.75 = 12.75m a 0.24% Cu 12.75

5 cm

PD85 AP1 DRILL SECTION LOOKING WEST
COLLAR CO-ORDINATES 9100E. 9385N.
DIP -65°, BEARING 346° MAGNETIC.

E.M. Conductor at 9425N Dip 45° to south, Approx 15m thick. Depth to top 20m. Hole designed to intersect at 50m vertical depth.

CRA EXPLORATION PTY. LIMITED

ROCKY CAPE E.L. 1/77
ALPINE ANOMALY LINE 9100E
PD85 AP1 DRILL SECTION
LOOKING WEST

273

REF.	SK55 - 3		
SCALE	1 : 1000	DRAWN	R.T.
AUTHOR	J.W. & G.P.	REPORT No.	
DATE	14 - 3 - 1985	PLAN No. TASh	2548